UNIVERSITY OF SOUTHAMPTON

FACULTY OF MEDICINE

Clinical Experimental Sciences

Characterisation of Bacterial Profiles in Chronic Rhinosinusitis

by

Stephen MA Hayes

Thesis for the degree of Doctor of Philosophy

March 2018

ABSTRACT

UNIVERSITY OF SOUTHAMPTON

FACULTY OF MEDICINE, CLINICAL EXPERIMENTAL SCIENCES

Doctor of Philosophy

CHARACTERISATION OF BACTERIAL PROFILES IN CHRONIC RHINOSINUSITIS

By Stephen Michael Andrew Hayes

Chronic rhinosinusitis (CRS) with or without nasal polyps (NP) affects up to 15% of the UK population significantly affecting quality of life and impacting heavily on health care resources. Despite millions of pounds spent on research each year, the underlying cause of CRS remains unknown. Bacteria have been implicated in playing a role in mediating the ongoing inflammation in CRS. Bacteria possess the ability to quickly adapt to environmental changes, readily interchanging between planktonic, biofilm and intracellular profiles. Emerging evidence suggests that CRS is the result of a locally dysregulated innate immune system caused by changes in bacterial profiles in a bid for survival. The work presented in this thesis aimed to clarify this proposed theory through characterisation of bacterial profiles in CRS and analysis of the effect on the local innate immune system at a cellular level.

A prospective study was performed using *ex-vivo* sinonasal mucosal and NP tissue from CRS patients, and sinonasal mucosa from non-CRS patients undergoing trans-sphenoidal pituitary surgery as a control. Tissue was analysed using the LIVE/DEAD® BacLight™ viability kit, fluorescent *in situ* hybridisation, scanning electron microscopy, transmission electron microscopy, confocal laser scanning microscopy and immunohistochemistry. An explant tissue model was developed to explore histological changes at the host-environment interface after addition of exogenous *Staphylococcus aureus* (*S aureus*) and *Staphylococcus* enterotoxin B (SEB). An *in vitro* cell culture model was developed to investigate cellular changes resulting from mast cell-*S aureus* interactions.

Surface-related biofilms were identified on CRS sinonasal mucosa. *S aureus* was the commonest microbe identified. Sodium nitroprusside appeared to have little or no effect on dispersal of surface-related CRS biofilms. In NP, bacteria were sub-epithelial and within mast cells (intracellular). This is the first reported study to observe intracellular *S aureus* within mast cells in NP. The presence of SEB significantly increased the internalisation of *S aureus* into mast cells. *S aureus* entered mast cells through phagocytosis and via extracellular traps. Proliferating intracellular *S aureus* led to mast cell expansion and eventual rupture, seeding viable *S aureus* and pro-inflammatory mediators into the extracellular space.

These findings demonstrate the ability of *S aureus* in CRS to manipulate the host's innate immune system in order to facilitate survival. Adaptation of bacteria into different profiles results in different pathophysiological effects. The intermittent dispersal of active planktonic bacteria from surface-related bacterial biofilms on non-polypoidal mucosa mediates the ongoing chronic inflammation and symptom relapse in CRS. Intracellular *S aureus* within mast cells could act as a reservoir for bacteria constantly seeding into the extracellular environment leading to the build-up of pro-inflammatory cytokines and mediators, thus promoting tissue oedema and potentially nasal polyp growth. These findings suggest that NP formation may be an indirect consequence of a *S aureus* survival strategy to evade host defences.

Contents

List of Figures

List of Tables

Academic Thesis: Declaration Of Authorship

I, Stephen Michael Andrew Hayes

declare that this thesis and the work presented in it are my own and has been generated by me as the result of my own original research.

Characterisation of Bacterial Profiles in Chronic Rhinosinusitis

I confirm that:

1. This work was done wholly or mainly while in candidature for a research degree at this University;
2. Where any part of this thesis has previously been submitted for a degree or any other qualification at this University or any other institution, this has been clearly stated;
3. Where I have consulted the published work of others, this is always clearly attributed;
4. Where I have quoted from the work of others, the source is always given. With the exception of such quotations, this thesis is entirely my own work;
5. I have acknowledged all main sources of help;
6. Where the thesis is based on work done by myself jointly with others, I have made clear exactly what was done by others and what I have contributed myself;
7. Parts of this work have been published as:

   Hayes SM, Howlin R, Johnston DA, Webb JS, Clarke SC, Stoodley P, Harries PG, Wilson SJ, Pender SL, Faust SN, Hall-Stoodley L, Salib RJ. Intracellular residency of *Staphylococcus aureus* within mast cells in nasal polyps: A novel observation. J Allergy Clin immunol. 2015;135(6):1648-51

Signed: .....

Date: .....

Acknowledgements

I would like to firstly thank my main supervisor Mr Rami Salib. Without your support, guidance and belief in me, I would not have achieved so much with this project. It has been a pleasure working for you and I look forward to working on new projects with you in the future. You have been an inspiration to me and a fantastic mentor, both academically and clinically.

I would also like to thank my scientific supervisor Dr Sylvia Pender for her support and guidance throughout. Your passion and enthusiasm for this project has been fantastic and you have helped me 'tell a story!'

I would like to thank all the members of the Biofilm Group and Wellcome Trust Clinical Research Facility for your support and expertise throughout my project. In particular, I would like to thank Professor Saul Faust, Dr Robert Howlin, Dr Ray Allan, Dr Luanne Hall-Stoodley, Dr Stuart Clarke and Professor Jeremy Webb.

I am also indebted to the Biomedical Imaging Unit for your constant help and support. Without your expertise, patience and advice I would not have managed to produce such good images, which were pivotal to my project. I would specifically like to thank Dr Anton Page, Dr David Johnston and Dr Elizabeth Angus.

I would also like to thank the Histochemistry Research Unit for your help, guidance and patience. Specifically, I would like to thank Dr Susan Wilson, Mr Jon Ward and Miss Helen Rigden.

Above all, I would like to thank my wife, Gemma and children, Henry and Matilda. Without your constant support and understanding over the last five years, this degree would simply not have been possible.

Definitions and Abbreviations

AEC	3-amino-9-ethylcarbazole
AERD	Aspirin Exacerbated Airway Disease
APC	Antigen Presenting Cells
BHI	Brain-heart infusion medium
BDR	Biofilm Detection Rate
CFC	Cetrimide, Fucidin, Cephalosporin
CI	Confidence intervals
CLSM	Confocal Laser Scanning Microscopy
CRS	Chronic rhinosinusitis
CRSsNP	Chronic rhinosinusitis without nasal polyps
CRSwNP	Chronic rhinosinusitis with nasal polyps
CF	Cystic Fibrosis
CFU	Colony Forming Unit
CNS	Coagulase negative *Staphylococcus*
COX-1	Cyclooxygenase 1
CT	Computed Tomography
DAB	3,3'-Diaminobenzidine
DAMPs	Damage-associated molecular patterns
DAPI	4',6'-diamidino-2-phenylindole
ECA	External carotid artery
EPOS	European Position Paper on Rhinosinusitis and nasal polyps
EPS	Extracellular Polymeric Substance
EUB	Eubacterial FISH probe
FACS	Fluorescence-activated cell sorting
FBS	Foetal Bovine Serum
FESS	Functional Endoscopic Sinus Surgery
FISH	Fluorescence *in situ* hybridisation
GMA	Glycol methacrylate
HBSS	Hank's Balanced Salt Solution
H influenzae	*Haemophilus influenzae*
HMC-1	Human mast cell culture line 1
IB	Intracellular bacteria
IBDR	Intracellular bacteria detection rate

ICA	Internal carotid artery
IFNγ	Interferon Gamma
IgE	Immunoglobulin E
IL	Interleukin
LMS	Lund-Mackay Score
MHC-II	Major Histocompatability Complex Class II
MRSA	Methicillin-resistant Staphylococcus aureus
MMP-9	Matrix Metalloproteinase 9
NO	Nitric oxide
NO_2	Nitrite
NO_3	Nitrate
NOS	Nitric Oxide Synthase
NP	Nasal polyps
ONOO	Peroxynitrite
P aeruginosa	*Pseudomonas aeruginosa*
PAMPs	Pathogen-associated molecular patterns
PBS	Phosphate Buffered Saline
PCD	Primary Ciliary Dyskinesia
PCR	Polymerase Chain Reaction
PI	Propidium Iodide
PIPES	Piperazine-N,N′ -bis
PLUNC	Palate lung nasal epithelial clone
PRRs	Pattern recognition receptors
RANTES	Regulated on Activation, Normal T Cell Expressed and Secreted
RPMI	Roswell Park Memorial Institute medium
S aureus	*Staphylococcus aureus*
SB	Surface biofilms
SEM	Scanning Electron Microscopy
SNOT 22	Sinonasal outcome Test
SNP	Sodium Nitroprusside
SPT	Skin Prick Test
SBDR	Surface-related biofilm detection rate
SPA	Sphenopalatine artery
SYTO 9	Fluorescent nucleic acid stain
TEM	Transmission Electron Microscopy
TGFβ	Transforming Growth Factor Beta

T_H1	T helper 1
T_H2	T helper 2
TLR	Toll-like receptor
TNFα	Tumour Necrosis Factor Alpha
TNFβ	Tumour Necrosis Factor Beta
Treg	Regulatory T Cells
T-RFLP	Terminal Restriction Fragment Length Polymorphism
VAS	Visual Analogue Scale
WHO	World Health Organisation

1 Introduction

1.1 Upper Airways - Anatomy and physiology

1.1.1 Nasal cavity

The internal nose comprises of two nasal cavities which extend from the nares anteriorly to the choanae posteriorly, separated by the nasal septum. The nares open into the vestibule, the skin-lined part of the nasal cavity containing nasal hairs, follicles and sebaceous glands. The skin meets mucosa at the narrowest part of the nasal cavity, the nasal valve. Mucosa lines the rest of the sinonasal cavities.

The floor of the nasal cavity is formed by the palatine process of the maxilla and the horizontal plate of the palatine bone and extends posteriorly 4.5cm to the soft palate. The floor extends medially to the nasal septum and laterally to the inferior meatus.

The roof of the nasal cavity is divided into three- the frontonasal, ethmoidal and sphenoidal sections, which form the base of the skull and floor of the anterior cranial fossa. The frontonasal portion is formed by the nasal bones and the nasal spine of the frontal bone. The ethmoidal section is formed by the cribiform plate of the ethmoidal bone and is named the olfactory area. The sphenoidal section is formed by the anterior wall of the sphenoid sinus and contains the sphenoethmoidal recess. It is into the sphenoethmoidal recess that the sphenoid sinus drains via the sphenoid ostium. The nasal cavity terminates at the junction where the vertical anterior wall of sphenoid meets the horizontal floor of the sphenoid sinus and is called the choana.

The medial wall comprises of the nasal septum, which is composed of septal cartilage, the perpendicular plate of the ethmoid bone and the vomer. The perpendicular plate of the ethmoid bone forms the superior part of the septum, where it ascends superiorly to form the cribiform plate and crista gali. The vomer forms the posteroinferior section of the nasal septum with contribution from the nasal crests of the maxillary and palatine bones.

The lateral wall of the nasal cavity is comprised of three pairs of shelf-like conchae termed the superior, middle and inferior turbinates (Figure 1.1A). These three turbinates divide the nasal cavity into three spaces, the superior,

middle and inferior meatus (Figure 1.1B). The superior meatus forms the space between the superior and middle turbinates and contains the opening to the posterior ethmoid sinuses. The middle meatus forms the space between the inferior and middle turbinates and receives drainage from the maxillary, anterior ethmoidal, the agger nasi and frontal sinus forming a complex drainage unit called the osteomeatal complex. Anterosuperiorly to the middle meatus the ethmoidal infundibulum leads to the frontal sinus ostium via the frontonasal duct. The frontal sinus ostium opens into a semicircular groove called the semilunar hiatus. Superiorly to the semilunar hiatus is the ethmoid bulla (Figure 1.2A), a rounded elevation formed by cells from the ethmoid sinuses. Inferiorly to the semilunar hiatus is the uncinate process (Figure 1.2A) of the ethmoid bone and posteriorly, the maxillary sinus ostium (Figure 1.2B). The inferior meatus lies inferolateral to the inferior turbinate and contains the opening of the nasolacrimal duct anteriorly, which drains tears from the lacrimal sac.

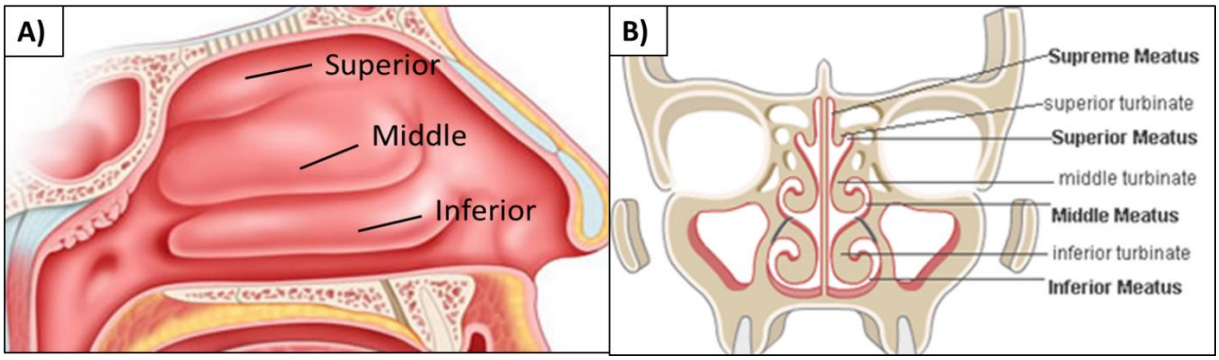

Figure 1.1 Anatomy of the nasal cavity and turbinates. (A) Sagittal image of superior, middle and inferior turbinates on the lateral wall of the nasal cavity (1). (B) Coronal image of turbinates and associated meatus (2).

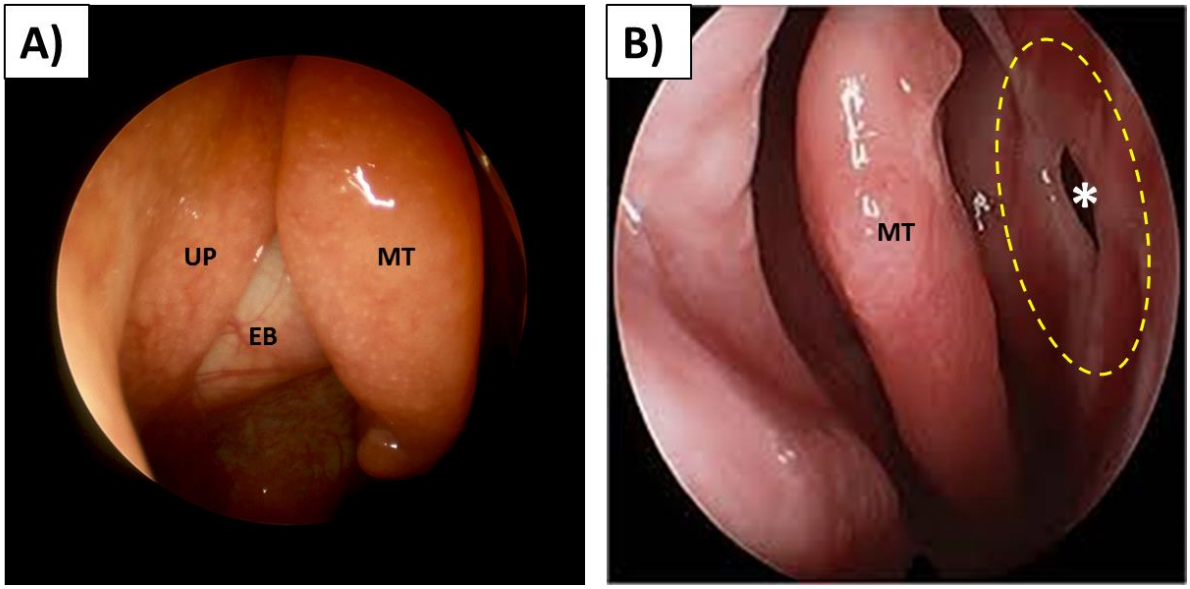

Figure 1.2 Endoscopic appearance of nasal cavity. (A) Endoscopic images of right sided nasal cavity showing the ethmoid bulla **EB** and uncinate process **UP** and middle turbinate **MT**. (B) Endoscopic images of left sided nasal cavity showing the middle turbinate **MT** and middle meatus (yellow dotted circle) after removal of the **UP**. The maxillary sinus ostium (white asterisk) can be clearly observed within the middle meatus. (1)

1.1.2 Paranasal sinuses

The paranasal sinuses are comprised of 4 paired air-filled extensions of the respiratory part of the nasal cavity. They develop within the bones of the face and base of the skull. They include the frontal, maxillary, ethmoid (anterior and posterior) and the sphenoid sinuses. The frontal sinuses form between the anterior and posterior tables of the frontal bone and usually start to develop from 8 years of age. Each frontal ostium opens into the frontonasal duct and drains into the semilunar hiatus of the middle meatus. The maxillary sinuses are the largest pair of paranasal sinuses. Each maxillary sinus drains through natural and often accessory ostia through the middle meatus and into the nasal cavity. The ethmoidal sinuses are composed of multiple cavities or cells that develop between the nasal cavity and the orbit. The most anterior ethmoidal cells are called the agger nasi. The ethmoid sinuses are divided into the

anterior and posterior sinuses. The anterior ethmoidal cells drain into the middle meatus via the infundibulum. The posterior ethmoidal cells open into the superior meatus. The sphenoid sinuses are paired asymmetrical cavities within the body of the sphenoid bone and drain into the sphenoethmoidal recess through the sphenoid ostium.

1.1.3 Vasculature and innervation

The sinonasal cavity receives its blood supply from branches of the internal carotid artery (ICA) and external carotid artery (ECA) (Figure 1.3). The anterior and posterior ethmoidal arteries branch from the ophthalmic artery, which in turn is a branch of the ICA. The anterior ethmoidal artery accompanies the nasociliary nerve through the anterior ethmoidal canal to supply the anterior ethmoidal and frontal sinuses as well as the anterosuperior aspect of the nasal cavity. The sphenopalatine artery (SPA) is a branch of the maxillary sinus, which in turn is a branch of the ECA. From the maxillary artery it passes through the sphenopalatine foramen into the superior meatus of the nasal cavity. Here it terminates at the nasal septum with the posterior septal artery and anastomoses with the greater palatine artery.

The descending palatine artery branches off the maxillary sinus in the pterygopalatine fossa and passes through the greater palatine canal and foramen emerging as the greater palatine artery. Here the artery passes through the incisive canal and anastomoses with the SPA to supply the nasal septum. The superior labial artery and lateral nasal branches of the facial artery also contribute to the blood supply of the sinonasal cavity. Terminal branches of all arteries supplying the nasal cavity anastomose on the anterior nasal septum, forming a rich network of capillaries called Little's area (or Kiesselbach's area) (Figure 1.3).

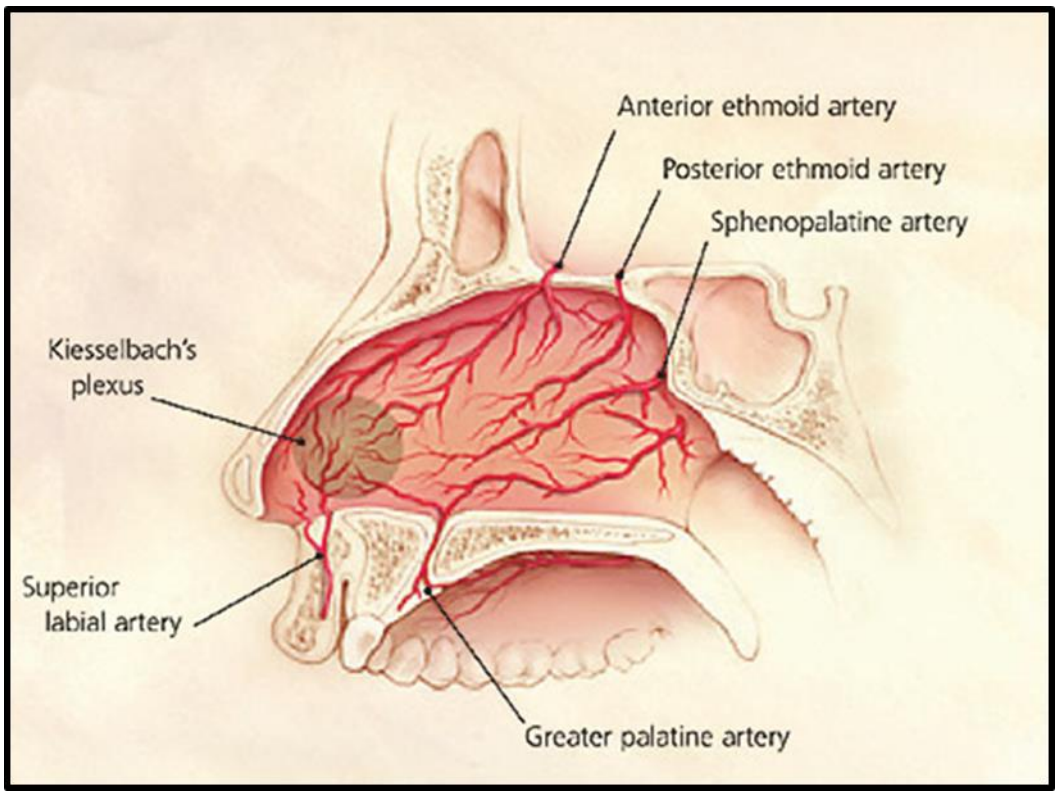

Figure 1.3 Arterial blood supply to sinonasal cavity (1)

A plexus of veins deep within the sinonasal mucosa drain into the sphenopalatine, facial and ophthalmic veins. This plexus is a crucial part of the nasal thermoregulatory system, warming and humidifying air before it enters the lower respiratory tract.

The maxillary and nasopalatine nerves provide innervation to the majority of the sinonasal mucosa. The remaining nerve supply comes from the posterior lateral branches of the greater palatine nerve, which supply the lateral wall of the nasal cavity and the anterior and superior ethmoidal nerves. The sense of smell is detected exclusively through the olfactory fibres embedded within the epithelium lining the anterosuperior aspect of the base of skull. These fibres penetrate the cribiform plate, forming the olfactory nerve and eventually the olfactory bulb.

1.1.4 Physiology and Histopathology

Despite many proposed theories, the actual role of the sinuses remains unknown. Initial structural theories suggested that pneumatised sinuses reduced the weight of the cranium, therefore reducing strain on the musculature of the neck. This theory was disproved after ossification of the sinuses was demonstrated to increase the overall weight of the head by only 1%. Evolutionary theories include improving the floatation of the head when swimming, thus protecting the airway and also as shock-absorbing pockets protecting the brain after facial trauma. Functional theories propose sinuses are crucial for vocal resonance. Despite controversy regarding the true evolutionary origin of the sinuses, the sinonasal cavity is the doorway to the upper airway and as such, provides important functions in filtering and conditioning air before it enters the lower airways, as well as defence against inhaled environmental pathogens.

The sinonasal mucosa is lined by respiratory epithelium with small areas of neuroendocrine olfactory epithelium within the superior cavity adjacent to the cribiform plate. Respiratory epithelium is composed of ciliated and non-ciliated pseudostratified columnar cells, basal pluripotential stem cells and goblet cells. The epithelium is separated from the underlying layer of connective tissue by the lamina propria and contains seromucinous glands and vascular networks. However, throughout the sinonasal cavity, these histological components and layers differ slightly to facilitate different physiological requirements.

For the first 1-2cm, the nasal vestibule is lined by keratinised stratified squamous epithelium, transitioning at the mucocutaneous junction (limen nasi) into pseudostratified columnar and ciliated epithelium, which cover the remaining nasal cavity. On the nasal septum, the number of goblet cells increase from anterior to posterior and from superior to inferior **(Figure 1.4A).** In contrast, the seromucinous glands decrease from anterior to posterior and from superior to inferior. The pseudostratified epithelium of the superior nasal septum merges with olfactory epithelium superiorly, which contains sensory receptor cells, supporting cells with microvilli, basal stem cells and Bowman's glands.

As the mucosa passes over the turbinates (particularly the middle and inferior) the lamina propria increases in thickness containing both superficial and deep glandular layers with a large vascular network of vessels capable of marked variation in luminal capacity (nasal pseudo-erectile tissue) **(Figure 1.4B).**

Within the sinuses, the mucosa becomes thinner, losing the deep and superficial glandular layers, with only a thin submucous fibrous layer adjacent to the underlying periosteum **(Figure 1.4C)**. Unlike turbinate mucosa, there is no prominent vascular layer.

Ciliated pseudostratified epithelium extends from the nasopharynx to the middle ear via the Eustachian orifice. The lamina propria is thick and contains a rich supply of capillaries and glands, which open into the lumen of the tube. A mixture of pseudostratified columnar and ciliated epithelium with goblet cells continues into and lines the middle ear cavity. Here the underlying lamina propria thins and strongly adheres to the underlying periosteum.

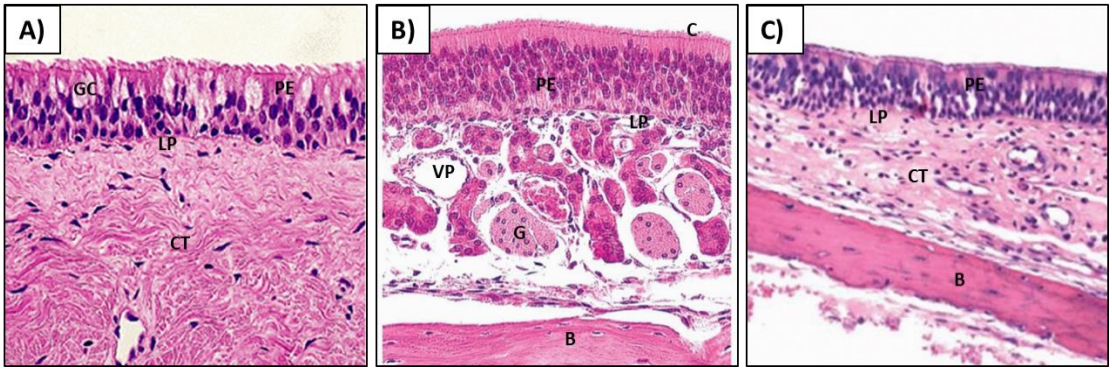

Figure 1.4 Histology of sinonasal mucosa. Photomicrographs of hemotoxylin and eosin stained sections of nasal septal mucosa (A), Inferior turbinate mucosa (B) and sinus mucosa. **C**, cilia; **PE**, pseudostratified epithelium; **GC**, goblet cells; **LP**, lamina propria; **CT**, connective tissue; **G**, glandular tissue; **VP**, vascular plexus; **B,** bone. (A) x10 magnification. (B) x60 magnification (1).

1.1.4.1 The conditioning of inspired air

The sinonasal mucosa functions to warm and humidify air entering the nasal cavity before it reaches the lower airways. The turbinates help to increase the surface area of sinonasal mucosa within the sinonasal cavity to approximately 180cm^2. Within the underlying connective tissue, a rich vascular plexus consisting of sinusoids, distensible veins, arteriovenous anastomosies, arterioles and venules acts to engorge the nasal mucosa with blood, creating a heat exchange system allowing humidification of air entering the nasal cavity. Engorgement of the sinonasal mucosa warms the inspired air, whereas constriction leads to cooling of the inspired air.

1.1.4.2 Mucociliary clearance

Ciliated cells are tall columnar cells with cilia that project through the full thickness of the epithelial layer into the mucus covering the surface and work as a protective mechanism to remove pathogens and environmental particles. Each cell contains approximately 250 cilia that work in a coordinated sweeping motion moving the mucus coat from the sinuses into the nasal cavity, ready to be excreted or ingested.

Goblet cells are located throughout the epithelium, interspersed among the ciliary epithelial cells. Goblet cells are more abundant in regions within the nasal cavity where air irritation is greatest. Goblet cells function to synthesise and secrete mucus into the sinonasal cavity. Mucus contains several properties that help protect the sinonasal cavity. The thick, viscous nature of mucus creates a physical barrier and helps to trap dust, pollutants, pathogens and any other particles that could irritate the lower respiratory system. Mucus consists of water (95%), glycoprotein (2.5%) electrolytes (2%). lysozyme enzymes and IgA (0.5%). The efficacy of the mucociliary clearance system depends on the integrity of the ciliated cells, goblet cells and mucus.

1.2 Chronic Rhinosinusitis

1.2.1 Background

Chronic rhinosinusitis (CRS) is a disease characterised by inflammation of the mucosa lining the nose and paranasal sinuses (3). It represents one of the commonest conditions encountered in medicine, affecting up to 15% of the population in the United Kingdom (UK) (4) and 16% of the population in the United States of America (USA) (5). CRS presents to a wide range of clinicians, from primary and emergency care to respiratory, allergy, otorhinolaryngology and even critical care and neurosurgery when complications occur (3). It is not surprising, therefore, that CRS impacts enormously on the healthcare economy (6). In the UK alone, CRS is estimated to cost the economy £100 million per year (7). In the USA, CRS accounts for more than thirteen million physician visits per year (5, 8), is ranked as the second most prevalent chronic disease in society (8) and is estimated to cost the US economy over $5.8 billion per year (9).

As well as representing a huge economic burden on society, CRS is also associated with a significant impact on quality of life (QOL). A study by Gliklich and Metson, in 1995, showed that patients with CRS had a QOL comparable with other chronic medical conditions, such as congestive heart failure, angina, chronic obstructive pulmonary disease and chronic back pain (10). A recent study by Stankiewicz *et al*, in 2011, also showed that CRS has a negative effect at work by significantly reducing the productivity and mental activity of each patient (11).

CRS also impacts heavily on antimicrobial resistance due to the requirement for repeated courses of short and long-term antimicrobial therapy. Concerns have been raised regarding the increasing prevalence of Methicillin-resistant *Staphylococcus* aureus (MRSA) within the sinonasal cavities and the increased resistance of CRS microbes to current macrolide therapy (12). The World Health Organisation (WHO) has recently reported that antimicrobial resistance is a global problem and threatens the effective prevention and treatment of an ever-increasing range of infections (13). It is therefore important to develop

more specific microbial detection methods and novel therapies with the goal of minimising antimicrobial resistance in the future.

1.2.2 Definition

1.2.2.1 Chronic Rhinosinusitis

CRS is a disease of the mucosa lining the sinonasal cavity characterised by recurrent episodes of inflammation resulting in chronic symptoms, such as nasal obstruction, facial pain, rhinorrhoea and a reduction in sense of smell (3, 6). Rhinitis and sinusitis usually co-exist and are concurrent in most patients suffering with CRS (3, 6). Therefore, the most accepted terminology is now rhinosinusitis. For many years there was little guidance on definition and diagnostic criteria. With the emergence of evidence-base medicine and increasing research into the pathophysiology of CRS, the development of structured guidelines and diagnostic criteria have become essential. Several documents containing guidelines have now been published (3, 6, 14-16). The most recent and universally adopted clinical definition of CRS was published in the *European Position Paper on Rhinosinusitis and Nasal Polyps* (EPOS) in 2007 and recently updated in 2012 (3, 6). The defining criteria are displayed in Table 1.1. Chronicity was defined as un-resolving symptoms for more than twelve weeks' duration.

SYMPTOMS	• Inflammation of the nose and the paranasal sinuses characterised by two or more symptoms, one of which should be either nasal blockage/ obstruction/congestion or nasal discharge (anterior/posterior nasal drip) • +/- Facial pain or Facial Pressure
ENDOSCOPY	**And endoscopic signs of:** • polyps and/or • mucopurulent discharge from the middle meatus
RADIOLOGY	**And/or:** • CT changes – mucosal changes within the ostiomeatal complex and/or sinuses
TIME	• Symptoms for more than twelve weeks without complete resolution of symptoms

Table 1.1 Definition and diagnostic criteria for CRS (3)

1.2.2.2 Chronic rhinosinusitis with and without nasal polyps

CRS is subdivided into CRS with and without nasal polyps (NP) (CRSwNP and CRSsNP respectively) (Figures 1.5 A & B). In 20% of CRS patients, the chronically inflamed mucosa develops into non-sensile (grape-like) out-pouches called NP, comprising of a thin layer of ciliated pseudostratified epithelium surrounding a loose stroma of oedema, cytokines and inflammatory cells (6). Although generally benign, NP can physically obstruct the sinus ostia and nasal airways, preventing sinus drainage and ventilation, leading to infection (3, 17, 18). This can be seen on a CT of the sinuses (Figures C & D). Evidence suggests that when present, NP create a greater burden of symptoms, a higher radiological severity score and require more revision surgery and medical treatment (17). The clinical differentiation between CRSwNP and CRSsNP is based on endoscopy (3).

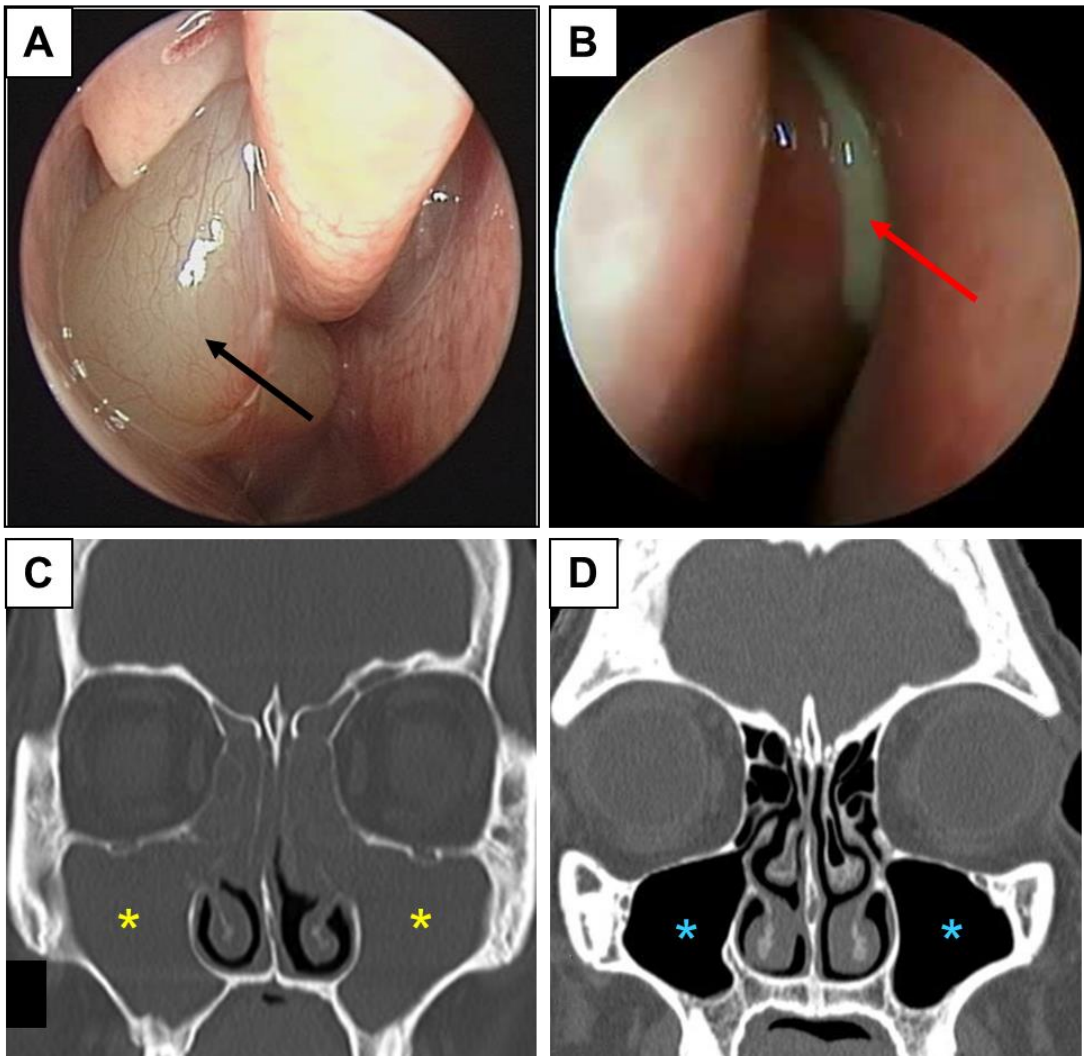

Figure 1.5 Endoscopic and CT appearance of patients with CRSwNP and CRSsNP. (A) Endoscopic appearance of nasal polyp (black arrow) from patient with CRSwNP. (B) In the sinonasal cavities of patients with CRSsNP there are no nasal polyps, but chronically infected mucopus (red arrow) is often observed coming from the middle meatus (1). (C) CT sinuses (coronal view) showing bilateral opacified maxillary (yellow stars) and ethmoidal sinuses in a patient with CRSwNP. (D) Normal CT sinuses (coronal view) showing bilateral pneumatised maxillary (blue stars) and ethmoidal sinuses.

1.2.3 Epidemiology

Due to the heterogeneity of CRS and the lack of accepted diagnostic criteria, there is a relative paucity of high quality CRS-related epidemiological data (3). A summary of the prevalence data for CRS and NP is displayed in Table 1.2. In a survey of the prevalence of CRS in the US population between 1990 and 1992, 15.5% of the total population suffered with an episode of sinusitis lasting for more than three months (8). This study also demonstrated CRS to be the second most prevalent chronic disease in the USA (8). A follow-up study in 1997, using the same criteria, confirmed the prevalence of CRS as 16% of the US population (5). However, these values are thought to represent an over-estimation as strict diagnostic criteria were not followed and the majority of General Practitioners did not have either the skills or facilities to perform confirmatory nasal endoscopy (19). A further study, using ICD-9 diagnostic codes, demonstrated a prevalence of 2%, which was thought to be an underestimation for the USA population (20). More recently, the Global Allergy and Asthma Network of Excellence (GA2LEN) study, involving nineteen centres across Europe and using the EPOS diagnostic criteria (Table 1.1), demonstrated a CRS European prevalence of 10.9% (range 6.9-27.1) (4). Other studies demonstrate geographical variation with a prevalence of 1.01% identified in Korea, 5.5% in Brazil, 6% in Belgium, 9.6% in Scotland and 9.3% in the Caribbean (21-24).

In the USA, the prevalence of CRS was demonstrated to be higher in females, with a ratio of 3:2 (8). Similar findings were shown in Canada, with a prevalence of 5.7% in females and 3.4% in males (25). Despite CRS affecting patients of all ages, the prevalence appears to increase with age, from a mean of 2.7%, in the 20-29 age group, up to a mean of 6.6% in the 50-59 age group (25). After 60 years of age, the prevalence of disease drops to 4.7% (25).

Approximately 20% of patients suffering with CRS develop NP (3). Accurate epidemiological data for the prevalence of NP in CRS is difficult due to the complexities of diagnosis. It may be possible to diagnose severe nasal polyposis using anterior rhinoscopy, but most cases need verification with nasal endoscopy (3). The prevalence exhibits a geographical variation. The prevalence of NP in Sweden is reported as 2.7% of the total population (26). In

Korea, the prevalence is reported as 0.5% (27). Finland has a prevalence of 4.3%, France 2.1% and the USA 4.2% (28-31). Differing from CRSsNP, NP develop more commonly in males compared to females (2.2:1). However, CRS prevalence appears to increase with age in all races (29, 32, 33). NP are rarely found in patients under twenty years of age, but develop in 5% of all those over 60 years (30). The average age of onset is approximately forty-seven years (34, 35).

The prevalence of NP significantly increases in patients who suffer with asthma and aspirin sensitivity (36, 37). Between 40% and 80% of patients with aspirin sensitivity suffer with nasal polyps and 15% of patients with NP have aspirin sensitivity (38). The presence of hypersensitivity to aspirin or any non-steroidal inflammatory drug (NSAIDs) in patients suffering with asthma and CRS is associated with a particularly aggressive and treatment-resistant form of the disease (39). Ingestion of aspirin or NSAIDs inhibits the production of cyclooxygenase (COX-1) enzymes with subsequent activation of both lipid and non-lipid mediators, causing an acute exacerbation of underlying upper and lower airway inflammation (40, 41). This syndrome was originally known as Samter's Triad, but has more recently been termed Aspirin Exacerbated Respiratory Disease (AERD) (42, 43). AERD affects between 0.3% and 0.9% of the total population in Europe with the prevalence of nasal polyposis between 60% to 70% (30, 44).

STUDY	YEAR	COUNTRY	PREVALENCE (%)
Chronic Rhinosinusitis			
Collins (8)	1997	USA	15.5% (Survey period 1990-92)
Gordts & Clement (23)	1997	Belgium	6%
Blackwell *et al* (5)	2002	USA	16% (Survey period 1997)
Ahsan *et al* (24)	2004	Scotland	9.6% (Scotland), 9.3% (Caribbean)
Shashy *et al* (20)	2004	USA	2% (ICD-9 diagnostic coding)
Hastan *et al* (4)	2011	Europe	10.9% (GA2LEN study -19 centres across Europe. EPOS diagnostic criteria)
Pilan *et al* (22)	2012	Brazil	5.5%
Nasal Polyps			
Settipane (30)	1996	USA	4.2%
Hedman *et al* (28)	1999	Finland	4.3%
Johansson *et al* (26)	2003	Sweden	2.7%
Klossek *et al* (29)	2005	France	2.1%
Kim *et al* (27)	2011	Korea	0.5%

Table 1.2 Summary of the prevalence data for chronic rhinosinusitis and nasal polyps

1.3 Pathophysiology of chronic rhinosinusitis

Recent guidelines propose the classification of CRS into two distinctive pathological entities (CRSwNP and CRSsNP), primarily based on differences in inflammatory cytokine profiles (3). A CRSwNP T-helper 2 (T_H2)-mediated profile is characterized as eosinophilic, with elevated IL-5, immunoglobulin E, Regulated on Activation Normal T Cell Expressed and Secreted (RANTES) and eotaxin (3, 45-47). CRSsNP T-helper 1 (T_H1)-mediated profile is characterised as neutrophilic, with elevated Tumour Necrosis Factor Alpha (TNF-α), IL-8, Transforming Growth Factor Beta (TGF-β), and Interferon Gamma (IFN-γ) (3, 48). However, there still exists a significant amount of overlap in the pathophysiological mechanisms between both subtypes and, as such, the classification is not universally accepted (49, 50).

To date, the aetiology and pathophysiology of CRSwNP and CRSsNP remain unclear, with many factors implicated in the aetiopathogenesis of the disease lacking substantial evidence. Factors thought to contribute to the disease are discussed below.

1.3.1 Mucociliary impairment

Mucociliary function of the mucosa lining the sinonasal cavities plays a crucial role in clearing allergens and pathogens from the upper airway tract. Conditions which impair the mucociliary function, such as primary ciliary dyskinesia (PCD) or cystic fibrosis (CF), can therefore lead to accumulations of allergens and pathogens, resulting in chronic inflammation (6).

Cystic fibrosis is an autosomal recessive exocrinopathy caused by defective cystic fibrosis transport regulator gene function, encoded on the q31 region of the long arm of chromosome 7 (51, 52). The prevalence of NP in CF is quoted as between 18.2% and 44.8%, primarily affecting adolescents (53, 54).

Several associated factors have been reported in the possible development NP in CF, but no single factor has been identified (54). These possible associations include long-term pulmonary colonisation with *Pseudomonas aeruginosa* (*P.*

aeruginosa) (55) and allergy to *Aspergillus fumigatus* (56). However, it is fully accepted that the underlying pathophysiology is impaired mucociliary function caused by a defective epithelial ion transport system, which leads to the production of less hydrated fluids with increased viscoelasticity (57). This differs from non-CF NP at both a histological and biochemical level (58, 59). Histopathological analysis demonstrated significant duct dilatation and mucous gland proliferation in CF NP, when compared to non-CF NP (58). The vascular network remained identical between the two tissue groups (60). The CF NP were found to contain higher levels of neutrophils, IL-8 and IL-1β compared to the non-CF NP, which contained higher levels of eosinophils, consistent with the literature (59). The impaired mucociliary function in CF leads to increased pathogen colonisation and mucosal inflammation driven by a neutrophil-dominated host reaction (54). This leads to sinus ostia occlusion and further impairment of mucociliary function (54).

CF NP and non-CF NP represent two separate underlying pathophysiological processes resulting in the same outcome of NP formation. Although not primarily an aetiological factor in CRS, impaired mucociliary function results as a consequence of chronically inflamed sinonasal mucosa and can contribute to sinus ostia occlusion and mucociliary stasis.

1.3.2 Allergy

Allergy has also been associated with CRS. Inflammation of the sinonasal mucosa caused by allergens is thought to lead to increased mucus production, increased nasal obstruction and blockage of the sinus ostia, leading to symptoms of CRS (61). Benninger showed that 54% of CRS patients had positive skin prick tests (SPT) (62). However, the role of allergy remains unclear, as other studies have shown no increase in CRS prevalence over the high pollen count months (62). On examination of NP fluid, no increase in concentration of either IgE or histamine was seen in patients with clinical hypersensitivity compared to non-allergic patients, suggesting allergy is unlikely to play a central role in the pathogenesis of CRSwNP (63, 64).

1.3.3 Asthma

Asthma has been implicated as a co-morbidity with CRS. The link between the upper and lower airways is now well established and has led to the publication of the Allergic Rhinitis and its Impact on Asthma (ARIA) position paper in 2001 (65) and revision in 2010 (66). This provided evidence that inflammation within the lower and upper airways co-exists and led to the concept of 'one airway, one disease' (38). Allergic rhinitis has been identified as a risk factor for the development of asthma and therefore, early recognition and control of allergic rhinitis is now recommended (65). Evidence suggests that up to 80% of asthmatics also suffer with CRS or allergic rhinitis and 50% of patients with CRS also have co-existing asthma (38). Upper airway infections have also been linked to asthma exacerbations (67). The identification of similar mediators of inflammation in both the upper and lower airways has led to the conclusion that asthma and rhinitis are not diseases of a single organ, but in fact involve the whole respiratory tract which has been termed the 'United Airway'.

The concept of the 'United Airway Disease' also applies to NP with a strong correlation demonstrated between asthma and NP (3). Patients with asthma have a 7% chance of developing NP compared to 4% of the normal population (3, 31,66). This rises dramatically to 15-26% in patients with late onset asthma (62). On the other side, 45% of patients with NP will go on to develop asthma, which rises to 60% in those with late onset NP (68). Asthmatics with NP also have more severe upper and lower airway disease (62). Both conditions share similar histopathological changes, such as mucosa remodelling, eosinophilic infiltration, T-helper cell involvement and increased synthesis of IL-5, suggesting similar underlying mechanistic processes (68). However, despite huge advances in this field, there remains a lack of consistent evidence to explain the link between asthma and NP.

It is also unknown why the association is significantly stronger, with worse clinical outcomes if either condition develops later on in life (68). Earlier onset of NP more commonly affects males, but late onset NP are more common in females (3, 68). This may suggest a hormonal contribution in late onset disease. More sever inflammation, remodelling and increased levels of inflammatory cytokines will lead to a reduction in mucociliary clearance and a

better environment for opportunistic bacterial and fungal biofilms to form. This may explain why these patients have worse clinical outcomes.

1.3.4 Aspirin exacerbated airway disease

Hypersensitivity to aspirin (or other NSAIDs) together with coexisting asthma in patients suffering with CRSwNP or CRSsNP is known as aspirin exacerbated airway disease (AERD) or Samter's Triad (39) and is associated with a particularly persistent and recalcitrant form of the disease (39). These patients have chronic underlying upper and lower airway inflammation, which is exacerbated by the intake of aspirin (or NSAIDs). AERD is associated with a severe upper airway disease reflected in the high recurrence rates of NP (60% to 70%) (30, 44, 69). On computer tomography (CT) scans, patients with AERD have been shown to have significantly thicker nasal mucosa compared to CRS patients with no aspirin hypersensitivity (3). In AERD patients, the intake of aspirin inhibits the enzyme cyclooxygenase-1 (COX-1), leading to the activation of inflammatory cells, such as mast cells and eosinophils (40, 41, 70-72). AERD is associated with a marked eosinophilia, resulting in the release of large quantities of IL-5, RANTES and eotaxin (73, 74). AERD patients require extensive medical therapy including regular oral corticosteroid treatments as well as increased frequency of endoscopic sinus surgery.

Patients with AERD have been shown to benefit clinically in terms of asthma and nasal polyp symptoms, after aspirin desensitisation. The mechanism underlying this involves suppression of IL-4 and the downregulation of proinflammatory matrix metalloproteinase 9 (MMP-9) (75). These benefits were not seen as readily in non-AERD patients and therefore, EPOS has not recommended aspirin desensitisation in non-AERD patients (3).

1.3.5 Hormones

There is evidence to suggest that hormones play a role in CRS. It has been shown that during pregnancy, one in five women develop symptoms and signs

of CRS (76). The hormones proposed include oestrogen, progesterone and placental growth hormone (76). However, the mechanisms underlying this remain unknown.

1.3.6 Anatomical variations

Anatomical variations, such as deviation of the nasal septum, enlarged inferior turbinates, concha bullosa and displacement of the uncinate process have all been proposed as increasing the risk of developing CRS (77). However, several more recent studies have provided conclusive evidence that no such correlation exists (78, 79). Anatomical variations probably exacerbate pre-existing CRS, rather than cause the disease.

1.3.7 Osteitis

Chronically inflamed bones surrounding the sinuses have been proposed as mediating the chronically inflamed mucosa in CRS. These changes are commonly seen on CT scans of the paranasal sinuses in patients with recalcitrant CRS (72). However, it is possible that these osteitic changes are secondary to chronically inflamed mucosa, rather than the actual cause.

1.3.8 Fungi

Airborne fungal antigens have been thought to play a role in the pathophysiology of CRS for many years. They are regularly cultured from the sinuses of patients undergoing endoscopic sinus surgery and in some cases they can form benign fungal balls and invasive fungal sinusitis. Studies have shown clear evidence of fungus in CRS, but have also found the same levels of fungus in control samples (81, 82). Therefore, the role of fungus in CRS is still unclear.

1.3.9 Epithelial integrity and defects

It is well established that epithelium plays a crucial role in initiating, regulating and maintaining the innate and adaptive immune system (83). It also provides an important barrier against environmental allergens and pathogens to the mucosa (83, 84). Defective epithelial layers have been shown to contribute to a number of chronic diseases, such as inflammatory intestinal disease (7), atopic dermatitis (85), psoriasis (86) and asthma (87).

Recent studies within the literature have proposed that disrupted epithelial barriers may lead to a breakdown in the innate and adaptive immune system within sinonasal mucosa, leading to chronic inflammation and the development of NP (84). This research has focused mainly on tight junction proteins, such as the epithelial protein LEKT1 (88). These proteins form apical intercellular junctions between epithelial cells and are responsible for a number of important functions, such as prevention of environmental allergens or pathogens entering into the sub-epithelial layer and regulation of the accumulation or excretion of inflammatory cells and tissue oedema (84).

Epithelial defects as aetiological agents in CRS is an interesting concept, but there is still a lack of evidence directly linking the defects to the development of CRS or NP. It is more likely to be the result of another aetiological factor, with the ability to damage or down regulate tight junction proteins in a strategy to manipulate the innate and adaptive immune system.

1.3.10 Bacteria

The role of bacteria in CRS remains unclear. Intraoperative bacterial cultures taken from the middle meatus of the sinonasal cavity are often sterile. Culturing of planktonic bacteria from the sinuses identified *Staphylococcus aureus (S aureus)* as the commonest microbe present (36%) (89). Other microbes cultured included Coagulase negative *Staphylococcus* (*CNS)* (20%) and *Streptococcus pneumonae* (17%) (89). Other studies confirmed *S aureus* as the commonest planktonic bacteria to colonise the nasal cavity, with rates of 27% in patients with CRSsNP, 60% in patients with CRSwNP and in 33% of

control patients (36). In patients with AERD, levels of *S aureus* colonising the nasal cavity have been found to be as high as 87% (36, 90).

The findings of colonised *S aureus* in one third of control patients raises the question of the relevance of planktonic bacteria within the sinonasal cavities, but the large proportions within CRSwNP and AERD suggest that *S aureus* may play some role in the pathophysiology of NP. On closer inspection of *S aureus* within the sinonasal cavities, Clement *et al,* in 2005, described the appearance of *S aureus* on CRS sinonasal mucosa as being in reservoirs, which differed in appearance to planktonic bacteria on control tissue (91). Further studies showed that within these *S aureus* reservoirs, some bacteria appeared to have passed through the epithelial surface of the sinonasal mucosa and in some areas, adopted intracellular residency (92-94). This was mostly observed in the sinonasal mucosa of patients with AERD. These reservoirs could represent bacterial biofilms and could, therefore, be contributing to the growing evidence implicating bacterial biofilms in the pathophysiology of CRS, discussed later in *Section 1.6.*

1.3.11 *Staphylococcus aureus* superantigens

S aureus is frequently identified as the commonest microbe within the sinonasal cavity of CRS patients (95). Depending on specific accessory gene regulator (agr) loci, *S aureus* has the ability to produce exotoxins which are potent virulence factors called superantigens (SAgs) (96). SAgs have been demonstrated to exert effects on both host cells and cytokines associated with local innate immunity (97). Host cells stimulated by the secretion of SAgs include epithelial cells, B and T cells, eosinophils, fibroblasts, dendritic cells and mast cells (98-100). SAgs upregulate IL-4, IL-5 and prostaglandin E2 and downregulate Regulatory T Cells (Treg), Transforming Growth Factor beta (TGF-β) and Interleukin-10 (IL-10) (101-103). Other effects reported include manipulation of eicosanoid metabolism (104-105), granulocyte augmentation (106) and the induction of glucocorticoid insufficiency (107). The net effect results in tissue damage, remodelling, a T_H2 skewed cytokine profile, generation of polyclonal IgE, an eosinophilia and mast cell degranulation

(Figure 1.5). It is due to this manipulation of the innate immune system that SAgs have been proposed as potential mediators of NP formation.

High levels of IgE antibodies to the SAgs *S aureus* enterotoxin A (SEA) and *S aureus* enterotoxin B (SEB) have been identified within NP, providing further evidence of a potential role in their pathogenesis (99, 108). Levels of IgE antibodies to SEA and SEB were particularly high in patients suffering with AERD (108-109). Despite this strong evidence, SAgs appear to be involved in only 50% of CRSwNP patients (110) and therefore, currently SAgs are considered more to be disease modifiers than direct aetiological agents in NP formation (3).

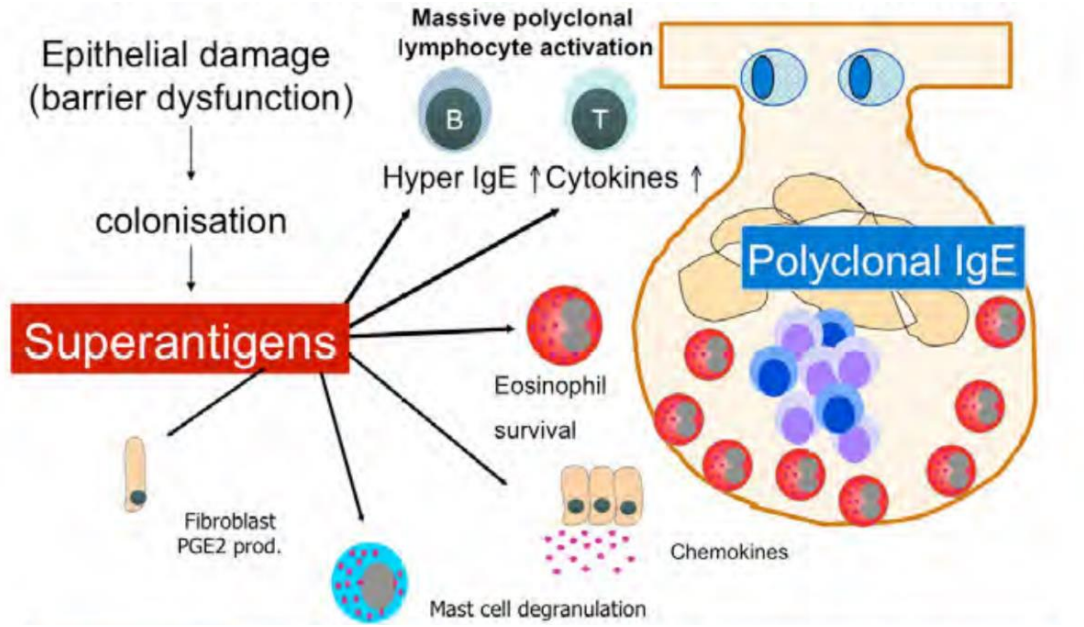

Figure 1.6 Superantigen (SAg) hypothesis in CRS. Mechanistic diagram taken from Bachert et al, 2007 (100).

1.4 Treatment of chronic rhinosinusitis with and without nasal polyps

Guidance for the treatment of CRS is provided by the EPOS guidelines (2012) (3). Treatment pathways for both CRSsNP and CRSwNP are displayed in Figures 1.7 and 1.8 respectively.

1.4.1 Medical treatment

The initial medical treatment regimen in CRS has been termed 'maximal medical therapy' (3). This includes a combination of an 8-week course of a topical corticosteroid, a sinus douche and a low-dose antibiotic (3). In CRSsNP, the antibiotic recommended is the macrolide, clarithromycin. In CRSwNP, the antibacterial therapy recommended is doxycycline (3). A short course of oral corticosteroids may be required in severe nasal polyposis. Further adjuvant medical therapies can be considered in the presence of certain associated co-morbidities. Individual medical therapies are described in detail below (3).

1.4.1.1 Corticosteroids

Glucocorticoids reduce airway eosinophil infiltration through activation of the intracellular glucocorticoid receptors GRα and GRβ (111-115). GRα receptor activation causes an anti-inflammatory effect and represses pro-inflammatory gene transcription (115). Levels of expression of these receptors will determine the clinical effectiveness of topical corticosteroids (115- 116). In CRSsNP, significant improvements have been demonstrated in maxillary ostial patency, nasal resistance, mucocilary clearance and a reduction in the levels of T-cells, eosinophils, IL-4 and IL-5 (117-121). The evidence for clinical efficacy of topical corticosteroids in CRSwNP is even more striking. Significant improvements have been demonstrated in nasal blockage, sneezing, rhinorrhoea, sense of smell, rhinitis, postnasal drip and quality of life (122-126).

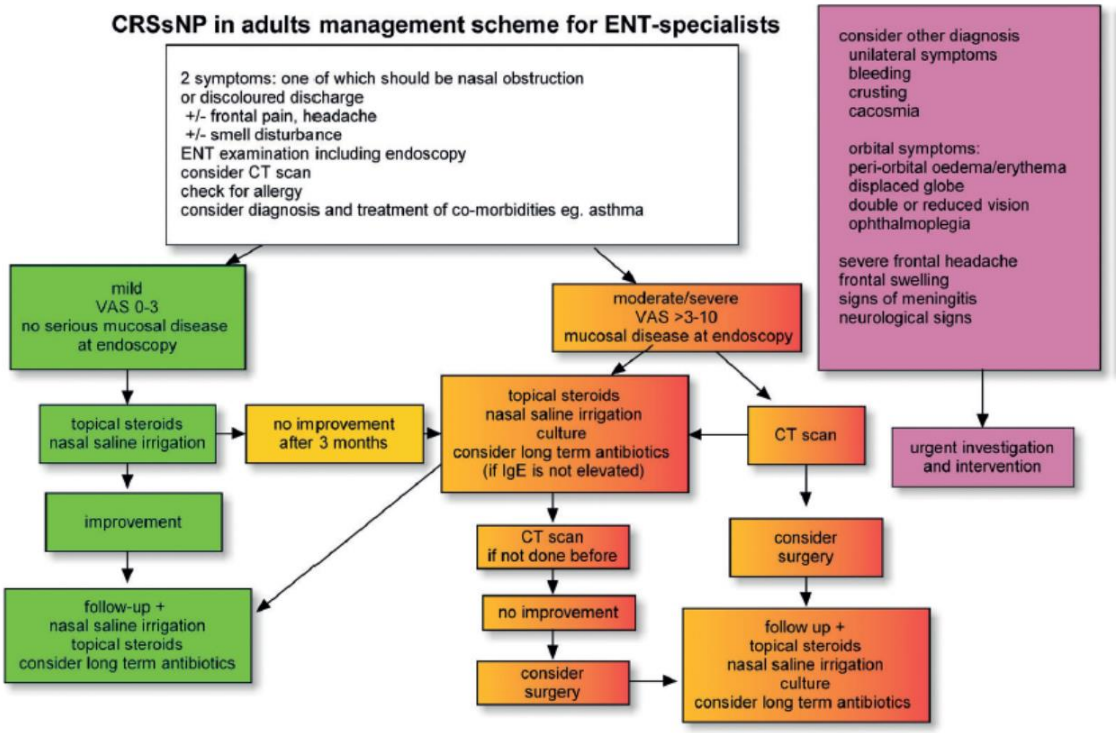

Figure 1.7 EPOS treatment pathway for CRSsNP

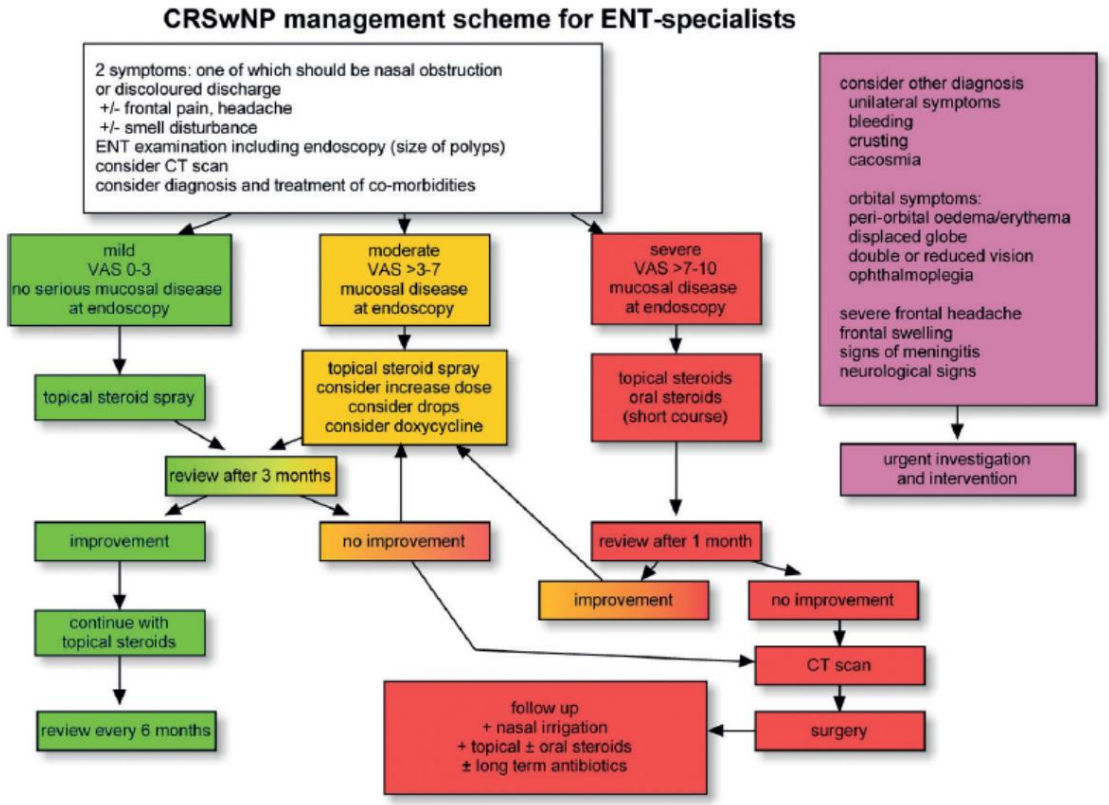

Figure 1.8 EPOS treatment pathway for CRSwNP

There is no evidence within the literature demonstrating efficacy of oral corticosteroids in CRSsNP (3). However, in CRSwNP the use of systemic steroids appears to be most beneficial. Several studies have demonstrated significant reduction in NP size (in up to 72% of the population), improvement in nasal symptoms (nasal obstruction, secretion, sneezing and sense of smell), nasal expiratory peak flow and improvement in endoscopic and radiological appearances after only a short course of systemic steroids (126-134).

In addition to the anti-inflammatory effects, corticosteroids produce collateral metabolic effects, resulting in possible unwanted side effects, such as changes in bone mineral density, fat metabolism, catabolic muscle effects, appetite, glucose intolerance, risk of cataract formation and pituitary-hypothalamic axis suppression (3). Although precautions are taken to minimise these side-effects, long-term oral steroids are occasionally needed in long-term management of the most resistant cases and individual risk versus benefit assessments need to be made. In general, a combination of an initial short course of oral steroids followed by long-term intranasal topical corticosteroids has become the preferred protocol demonstrating significant NP reduction, improved anterior rhinomanometry and improved CT findings after a twelve-week regimen (135).

1.4.1.2 Antibiotics

In patients suffering with CRSsNP there is little evidence to support the effective use of short-term antibiotics (3). A study investigating the efficacy of a two week course of either amoxicillin/clavulanic acid (co-amoxiclav) or cefuroxime in patients with CRSsNP demonstrated a bacteriological cure rate of only 65% and 68% respectively (136). In a study looking at the efficacy of low-dose, long-term macrolide treatment (twelve-week regimen) in patients with panbronchitis and CRS, the ten-year survival rate increased from 25% to 90% and the associated CRS was controlled (137). Therefore, short-term antibiotic therapy has been superseded by a longer low-dose course (8-12 weeks) of macrolides (3). As macrolides also possess an anti-inflammatory effect, they are both immuno-modulatory and antibacterial (3). As well as increased bacterial eradication, long-term macrolide therapy has

demonstrated a reduction in inflammatory markers, increased ciliary beat frequency, improved Sino-Nasal Outcome Test 20 (SNOT-20) scores, improved nasal endoscopy appearances and reduced levels of IL-8 (138). Evidence suggests that macrolide therapy is less effective in patients with high levels of serum IgE, such as those suffering with CRSwNP (139).

As discussed in *Section 1.3.11*, *Staphylococcus* superantigens have been implicated as modulators of disease in CRSwNP and may play a role in NP formation (140, 141). Significant levels of superantigens have been demonstrated in NP tissue, particularly in patients suffering with severe asthma (140). In contrast to CRSsNP, CRSwNP appears to have both an inflammatory and antibacterial element to the disease process. Doxycycline has therefore, been proposed for use in CRSwNP due to its dual anti-inflammatory and antimicrobial properties (134). Subsequent studies have demonstrated a reduction in nasal polyp size, nasal symptoms and mucosal and systemic markers of inflammatory after treatment with doxycycline (126, 142- 143). Doxycycline has therefore, been recommended by EPOS for use in patients with CRSwNP (3).

1.4.1.3 Sinonasal irrigation

Isotonic and hypertonic sinonasal irrigation, or sinus douching, represents an essential treatment modality in both CRSsNP and CRSwNP (3). When delivered as a high volume, low-pressure douche this was demonstrated to be more effective at irrigating the sinuses than the low volume, high-pressure nasal sprays (144-145). In a Cochrane report, nasal irrigation was demonstrated to be beneficial in both CRSsNP and CRSwNP (146). Post-operative douching was shown to reduce discharge and oedema at three weeks but had no effect on adhesions, NP or crusting. At three months, no significant difference was observed between douched cavities and non-douched cavities (147).

Regular irrigation of the sinuses using a high volume low-pressure douche is a recommended treatment for CRSsNP and CRSwNP, when the patency of the nasal cavities permits and in patients after endoscopic sinus surgery (3).

1.4.2 Adjuvant medical treatments

1.4.2.1 Leukotriene antagonists

Leukotriene antagonists, such as Montelukast, are useful in patients suffering with CRSwNP in association with asthma and as an adjuvant therapy to intranasal and inhaled corticosteroids. In the majority of patients studied fitting this criteria, Montelukast significantly improved clinical symptoms, acoustic rhinometry and peak nasal inspiratory flow (148). In another study looking at postoperative patients with CRSwNP commenced on Montelukast, improvements in nasal blockage, rhinorrhoea, nasal itching and sense of smell were demonstrated and less proinflammatory biomarkers were identified in nasal lavage washings (149).

1.4.2.2 Antihistamines

Antihistamines have been demonstrated to have no effect on reducing the number or size of NP in CRSwNP and are therefore not a recommended treatment (150). However, in CRS patients with positive skin prick allergy test, antihistamines may be beneficial (3).

1.4.2.3 Anti-IL-5

IL-5 is a powerful activator of eosinophils, which have been demonstrated to be in high levels in NP. The development of an anti-IL-5 medication (Mepolizumab and Reslizumab) was aimed at reducing eosinophilia and NP size (3). Although initial Phase I/II trials demonstrated improved NP scores and reduced opacification on CT scans, adverse effects including nasopharyngitis, fatigue and pharyngolaryngeal pain were commonly reported and therefore use is not recommended routinely in CRS patients (3).

1.4.3 Surgical treatment

If medical treatment fails to improve the patient's symptoms to an acceptable level and the patient is well enough to undergo a general anaesthetic, surgery may be offered in the form of functional endoscopic sinus surgery (FESS). Through the removal of chronically inflamed or polypoidal mucosa and through widening of the sinus ostia, FESS surgery aims to improve the ventilation and drainage of the sinonasal cavities, which helps to restore normal mucociliary clearance (3).

In both CRSsNP and CRSwNP patients, FESS results in a significant improvement in symptom scores, with the biggest improvements seen in nasal obstruction, facial pain and postnasal discharge. However, FESS appeared to only have a small effect on headaches and hyposmia (151). In the few studies distinguishing between the two groups, a significant improvement in SNOT-22 scores was demonstrated at three, twelve and thirty-six months post-operatively in patients with CRSwNP when compared to CRSsNP (152). However, these patients demonstrated a higher rate of recurrence and need for revision surgery (153). FESS is, therefore, not a cure for CRS and the long-term control of the disease process is highly dependent on the continuing use of anti-inflammatory medical therapies in the post-operative period (3).

1.5 Host inflammatory pathways in chronic rhinosinusitis

The sinonasal mucosa represents the host-environment interface where a combination of mucocilary clearance and the innate and the adaptive immune systems form a barrier against environmental agents, such as pathogens, irritants and aero-allergens (3). It is the manipulation and alteration of the innate and adaptive immune system that is thought to be key in the pathogenesis of CRS. However, there remains little evidence of a single exogenous agent leading to these changes and it is thought more likely to be multifactorial.

1.5.1 Mechanical barrier

The first port of defence encountered by environmental agents is the epithelial barrier. This consists of a thick layer of mucus, sitting on top of motile cilia attached to respiratory epithelial cells (3). Mucus, together with motile cilia, forms the mucociliary transport system, which traps exogenous agents and transports them through the nasal cavities to the postnasal space, where they are swallowed (3). Mucus consists of secretions from submucosal glands, goblet cells, epithelial cells, lacrimal glands and vascular transudate and is primarily composed of mucin glycoproteins (3). Glycoproteins combine the secretions together, creating the thick, sticky blanket of mucus (3). Mucins have the ability to alter the surface proteins of invading pathogens, preventing progression towards the epithelial layer (154). The glycoproteins are arranged as such to produce a gel-like outer layer, with a low viscosity inner layer, allowing the mucus, with the help of the cilia, to transport foreign particles out of the nose and sinuses (3). Alterations in the consistency of mucus, leading to increased viscosity, have been associated with increased disease severity in CRS (155).

1.5.2 Epithelial cells

Epithelial cells are held tightly together by intercellular apical adhesion complexes. These include tight junctions, desmosomes and hemi-desmosomes. Alterations in these junction proteins lead to barrier defects and reduced epithelial integrity, leading to increased vulnerability to mucosal penetration by pathogenic organisms. In CRSwNP, studies have demonstrated a reduction in desmosomal proteins (DSG2 and DSG3) (156), tight junction proteins (claudin and occuldin) (157) and epithelial proteins (LEKT1) (158). LEKT1 is encoded by the SPINK5 gene and is a protease inhibitor regulating tight junctions (158). A reduction in LEKT1 leaves the epithelial barrier vulnerable to exogenous agents with significant protease activity (158).

The epithelial cells play a crucial role in regulating both the innate and adaptive immune system (83, 159). The innate immune system provides an immediate, but non-specific response to pathogenic organisms that rely on cytokines and phagocytic cells that activate immediately upon recognition of generic features of invading pathogens. In contrast, the adaptive immune system is slower to activate on first exposure to a new pathogen, but through the synthesis and proliferation of specific B and T cells, it possesses the ability to recognise specific pathogens and destroys them immediately on repeated contact.

Through the use of cytoplasmic pattern recognition receptors (PRRs), epithelial cells possess the ability to recognise pathogen-associated molecular patterns (PAMPs) expressed on all environmental organisms (160-164). Activation of PRRs leads to the release of chemokines and cytokines, which stimulate innate immune cells, such as macrophages, neutrophils and mast cells (3). Epithelial cells can also detect damaged cells via damage-associated molecular patterns (DAMPs) and together with stimulations of PRRs, activate the adaptive immune system (161, 165-156).

The majority of PRRs are composed of Toll-Like Receptors (TLR), which form a family of ten membrane glycoproteins that recognise PAMPs (3). TLR2, TLR3, TLR4 and TLR9 are expressed on epithelial cells in sinonasal mucosa (167). It is hypothesised that these cells are crucial in mediating inflammation and therefore, an alteration in these proteins could lead to chronic inflammation

(167). Decreases in TLR2 and TLR9 mRNA, which are associated with bacteria recognition, have been identified in CRSwNP (163, 168).

A further antimicrobial property of epithelial cells includes the release of antimicrobial compounds, such as enzymes, opsonins, permeating proteins, collectins and binding proteins (169-170). The majority of studies within the literature have demonstrated no change in the level of these compounds in CRS compared to controls. However, the one exception includes the palate lung nasal epithelial clone (PLUNC) protein, which is downregulated in CRSwNP (171). This may be relevant as PLUNC proteins contain potent anti-biofilm properties (171).

There is also evidence demonstrating that T_H2 cytokines cause epithelial cells to downregulate the production of innate immune compounds, such as IL-22, human beta-defensin 2, surfactant protein A and the transcription factor STAT 3 (172-175). These molecules are involved in mucosal host defence and epithelial layer repair and have been shown to be downregulated in CRS (176) (177).

Epithelial cells possess the ability to produce nitric oxide synthase (NOS). NOS produces nitric oxide (NO), an intracellular messenger and neurotransmitter crucial in many biological processes, including mediation of inflammation, defence against pathogens and cell apoptosis. NO is produced in large amounts within the normal sinonasal cavities and is thought to prevent bacterial colonisation through upregulation of specific chemokines, cytokines, allergens and bacterial toxins within the epithelial layer (178). This hypothesis is strengthened by studies demonstrating reduced levels of NO in the sinonasal cavities of patients with CRSsNP and CRSwNP and with increasing levels of NO after commencement of maximal medical treatment (179-181).

1.5.3 Macrophages

Macrophages play a crucial role in the innate immune response to pathogens within sinonasal mucosa (3). Macrophages are classified into pro-inflammatory M1 cells associated with the T_H1 response, or immunosuppressive M2 cells, which are associated with the T_H2 pathway and have been shown to have

reduced phagocytic properties (182, 183). This M2 pathway is important in providing defence against helminths and repairing damaged tissue (184). M2 macrophages have been shown to be present in larger amounts in CRSwNP, compared to CRSsNP and controls (185). A recent study has shown that NP-derived M2 macrophages have an impaired ability to phagocytose *S aureus*, allowing bacteria to survive intracellularly (186). This may be relevant in the pathogenesis of NP. A transmission electron microscopy (TEM) image of a macrophage within a NP is displayed in Figure 1.9.

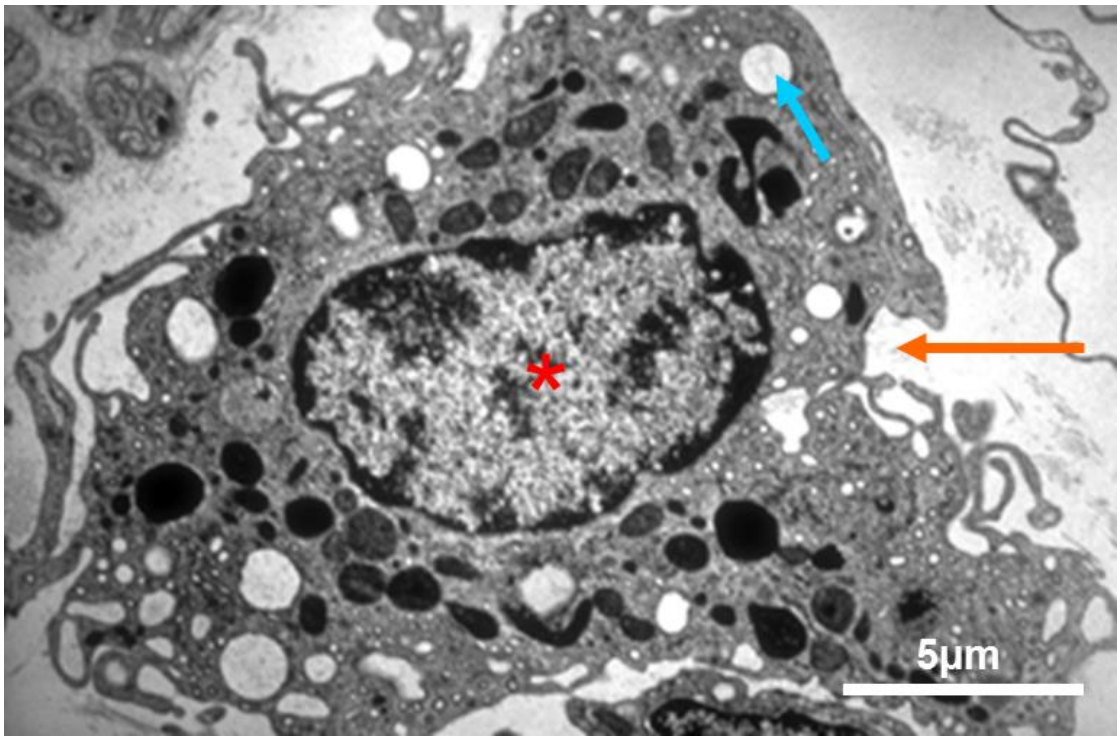

Figure 1.9 TEM image of a macrophage within a NP. Representative TEM image demonstrates the macrophage nucleus (red star), cytoplasmic infoldings (orange arrow) and vacuoles (blue arrow)

1.5.4 Eosinophils

Eosinophils are white blood cell granulocytes involved in the innate immune response and tissue remodelling and repair and are closely associated with allergic rhinitis and asthma (3, 187). Pre-formed granules located within the

cell cytoplasm are filled with histamines, proteins, eosinophil peroxidase, ribonuclease, deoxyribonucleases, lipase, plasminogen and major basic protein (Figure 1.10).

Initially, eosinophils were considered crucial in the pathophysiology of CRS, whereby, in response to fungal colonisation, the release of toxic mediators through degranulation was thought to drive ongoing inflammation (81, 188). However, both the levels of fungal colonisation and tissue eosinophilia varied significantly amongst CRS patients and, therefore, the hypothesis lost some credibility (3). Tissue eosinophilia was shown to be higher in Caucasian patients with CRSwNP compared to those with CRSsNP (189-190). However, this association was not demonstrated in non-Caucasian populations where the majority of NP were shown to be non-eosinophilic (191-192). Due to the geographical variation in NP eosinophil levels, eosinophils are not considered aetiological factors in either the pathogenesis or pathophysiology of NP (3). Despite this, eosinophils are found in high levels in NP and appear to be an important biomarker for recalcitrant disease (3). Eosinophil recruitment into the tissue appears to be the result of a switch from a T_H1 to T_H2 cytokine pathway, regulated by the chemokines RANTES, eotaxin and IL-5 (193-194). The cause of the switch to a T_H2 pathway remains unknown, but appears to be driven by T-helper cells (195, 196).

1.5.5 Neutrophils

Neutrophils are immune effector cells capable of phagocytosing invading organisms and are recruited through cytokine release after pathogenic stimulation of PRRs (3). The relevance of neutrophils in CRS remains unclear. However, levels of neutrophils are elevated in both CRSwNP and CRSsNP, compared to controls (3). IL-8 has been linked to neutrophil stimulation and is upregulated in CRSwNP and CRSsNP (197-198). Neutrophilic infiltration dominates within a T_H1 cytokine pathway, which is associated with CRSsNP, whereas an eosinophilic infiltration dominates within a T_H2 cytokine pathway (3). Epidemiologically, tissue from Asian patients with CRS demonstrated less neutrophilic infiltration than tissue from Caucasian patients (191, 199).

Despite this, they still demonstrated a neutrophilia compared with control tissue, which was higher in patients with CRSsNP than CRSwNP (195).

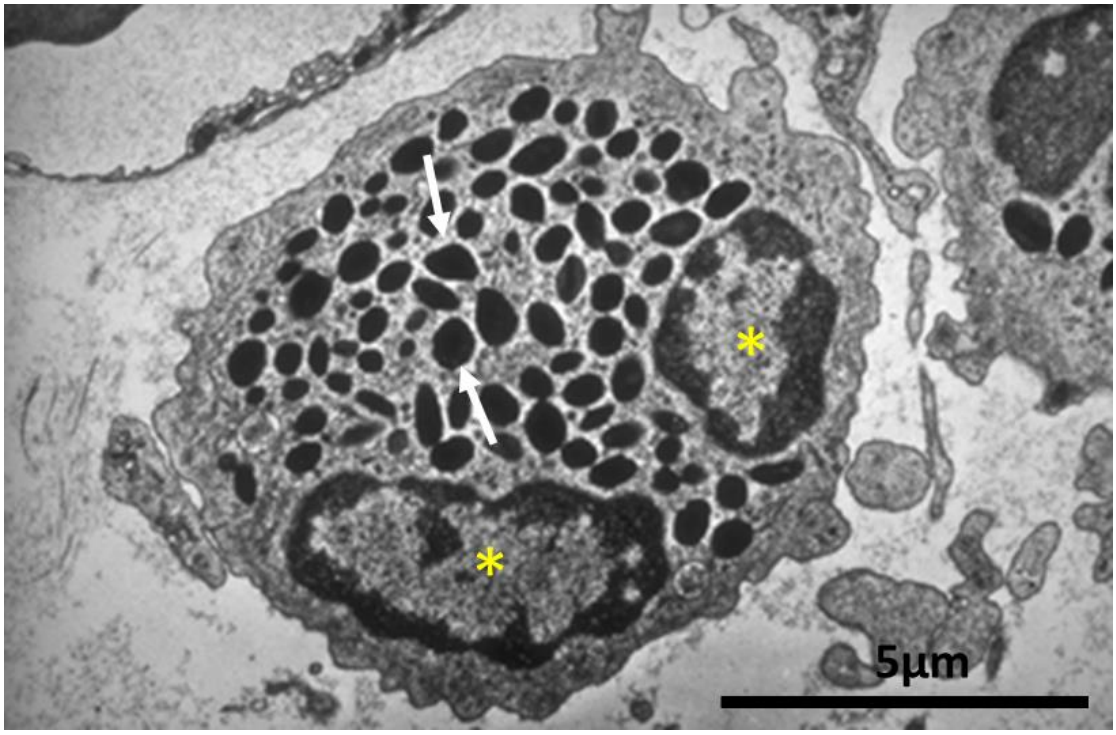

Figure 1.10 TEM image of an eosinophil within a NP. Representative TEM image demonstrates the bi-lobed nucleus (yellow stars) and multiple granules (white arrows) of a NP eosinophil

1.5.6 Mast cells

Mast cells (**Figure 1.11**), like basophils, are white blood cell granulocytes which originated from bone marrow as haematopoietic progenitor cells, specifically from CD34+ cells (200). Unlike basophils, mast cells leave the bone marrow as immature cells and do not usually circulate within the blood stream, but typically complete their differentiation into mature end cells in peripheral vascularised tissue (200). This accounts for their difference in life span with basophils surviving from 4 hours to 5 days and mast cells living up to 300 days. Mast cells usually reside along vascular structures or beneath the epithelial layer along the host-environment interface, such as within the sinonasal cavity, respiratory tract and gastrointestinal tract (200).

On reaching their final destination, mast cells differentiate into mature end cells and their ultimate function is dependent on the requirements of the specific tissue. This differentiation is regulated by stem cell factor, IL-3, IL-4, IL-9, IL-10 and nerve growth factor (200). During maturation mast cells begin to express high affinity receptors for IgE (FcεRI) on the cell surface (200). This is a tetrameric receptor complex that binds the Fc portion of the heavy chain of IgE. Activation of this complex leads to degranulation where the contents of cytoplasmic granules inside the mast cell are released in varying speeds and concentrations. Cytoplasmic granules contain proteoglycans (chondroitin sulphates and heparin), histamine, serine proteases (tryptase and chymase), lipid mediators (prostaglandin D2 and leukotriene C4), serotonin, adenosine triphosphate, lysosomal enzymes and cytokines (IL-4 and TNF-α) (200). The rate of action for each mediator and cytokine released varies. For example, histamine dissociates very rapidly, whereas serine proteases are released slower (200). Released mediators have the ability to interact and activate other cells, such as epithelial cells, eosinophils, B and T cells, neutrophils and macrophages. These mediators are transitory and only last long enough to initiate further cellular functions. This complex chemical communication system makes the mast cell a key player in both the innate and adaptive immune system and explains why they are situated at the host environmental interface.

Within the sinuses, mast cells play an important role in promoting innate immunity against microbial pathogens (201-202). Known as the sentinel cells, mast cells are usually the first innate effector cells pathogens come into contact with once the epithelial layer is breeched (203). Through activation of $CD8^+$ T cells, mast cells possess the ability to regulate both the T_H1 and T_H2 cytokine pathways and can therefore adopt both immunosuppressive and immunostimulatory properties (201). Recently, mast cells have been demonstrated to exert phagocytosis-independent antimicrobial activity against *S aureus*, mediated through extracellular traps and the release of antibacterial enzymes (203). Mast cell activation can occur through stimulation of PRRs (202). Once activated, mast cells degranulate, releasing the contents of their granules (3). *S aureus* surface protein A (SpA) has been demonstrated to stimulate mast cell degranulation (101).

It is well established that mast cell degranulation within the sinuses is associated with allergic rhinitis through antigen driven IgE cross-linking (3). Mast cells also have the ability to mediate eosinophilic infiltration through IgE-dependent and independent processes (204-205). Other studies have shown mast cell prostaglandins capable of activating T_H2-lymphocytes, independent of T-cell activation, leading to the secretion of T_H2 cytokines (102, 206). This raises the possibility of mast cells playing a role in NP pathogenesis through the induction of a T_H2 cytokine pathway and the stimulation of an eosinophilic infiltrate. Despite this theory, the role of mast cells in NP remains unclear.

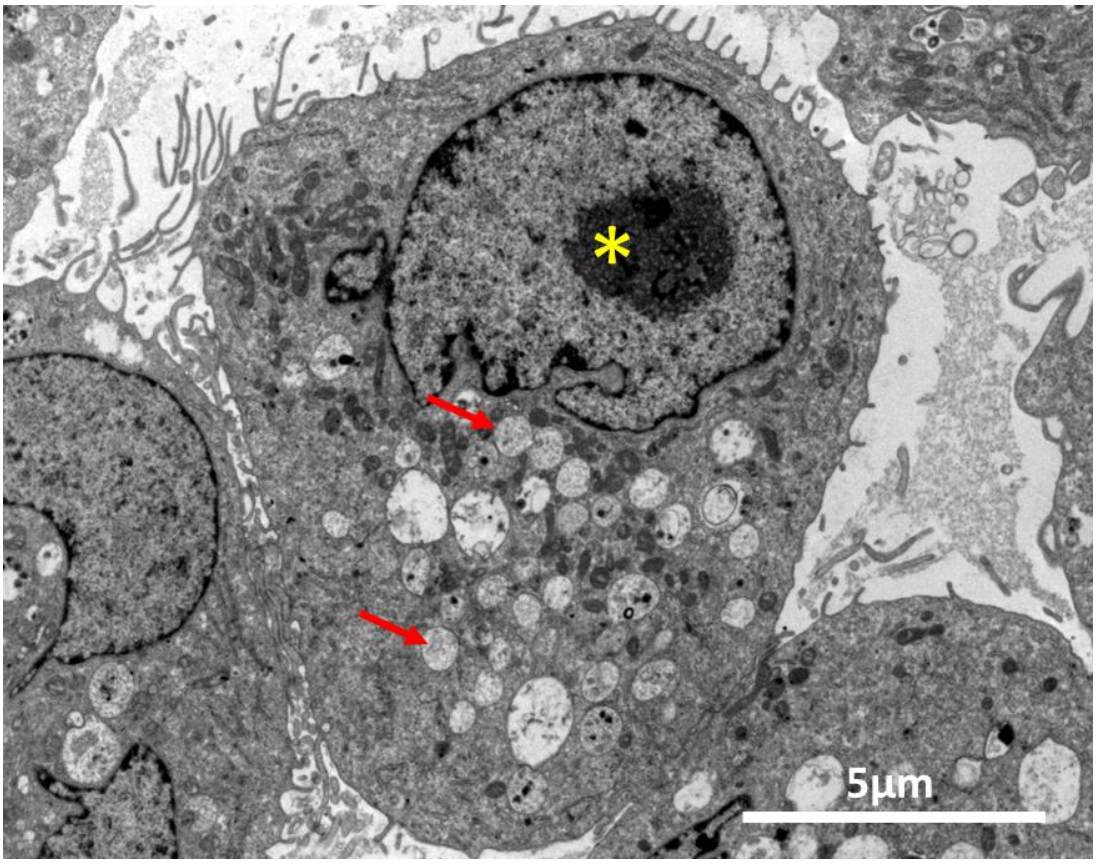

Figure 1.11 TEM image of a mast cell within a NP. Representative TEM image demonstrating a mast cell within NP tissue. Image demonstrates an intact mast cell nucleus (yellow star) and pre-formed granules (red arrows) (Image taken by author)

1.6 Surface-related bacterial biofilms

Bacterial biofilms are defined as an aggregation of complex, structural and antibiotic-tolerant communicating microorganisms encased within a self-produced hydrated polysaccharide matrix, allowing adherence to both biotic and abiotic surfaces (9, 207).

The polysaccharide matrix, or extracellular polymeric substance (EPS), makes up at least 90% of the biofilm mass (208) and provides a number of critical functions to ensure the survival of the embedded bacteria. Firstly, through mediation of surface proteins and formation of anchoring cells, the EPS can form irreversible electrostatic adherence to both living and inert surfaces (209). Secondly, the EPS appears to protect the biofilm from environmental pathogens and antimicrobial therapy. One theory suggests that the EPS prevents penetration of antibiotics into the biofilms (9). However, Palmer et al (2005) showed antibiotics diffusing readily throughout the biofilm (210). Another theory suggested that the negatively charged polymers within the EPS interact with the positively charged polymers of the antibiotics, deactivating or neutralising the antimicrobial therapy (9). A popular theory is that once the biofilm phenotype is formed, the EPS can cause the embedded bacteria to mutate in response to the commencement of antibacterial therapy, resulting in a downregulation in metabolic activity and growth rate (211), leading to a dormant persister-cell phenotype (212). Antibiotics usually target metabolically active cells and therefore this dormant layer of bacteria within the biofilm could confer relative antibacterial resistance (9, 211-212). It is also thought that due to the close relationship to each other within the biofilm, bacterial cells are able to share genetic material, increasing the transmission of resistant genes (213). Metabolic activity and growth are thought to resume once the antimicrobial therapy has ended.

Bacterial biofilms attach, mature, disperse and re-colonise in a biofilm life-cycle (Figure 1.12). Attachment to a surface forms the first stage of biofilm development (214). The second stage is growth and maturation (214). The EPS allows the biofilm to grow and mature by providing an environment safe from unfavourable host defences and antimicrobial therapy, whilst at the same time providing essential nutrients and removing toxic waste via the formation of

water channels (207, 215-216). Once the biofilm reaches a critical size, various dispersal mechanisms are orchestrated leading to the final stage of dispersal (214). Bacteria is released in its most basic phenotype, as planktonic (or free-floating) bacteria and results in colonisation of new anatomical locations (9). The planktonic bacterial phenotype, however, differs significantly from the biofilm one. Bacteria within biofilms are between 500-1000 times more resistant to antimicrobial therapy compared to bacteria in its planktonic state due to the lack of EPS (217).

The release of planktonic bacteria from the biofilm initiates an acute inflammatory reaction resulting in the host's immune system eradicating the majority of bacteria. However, any remaining bacteria usually aggregate to restart the biofilm life-cycle, often in different regions allowing spread of bacteria.

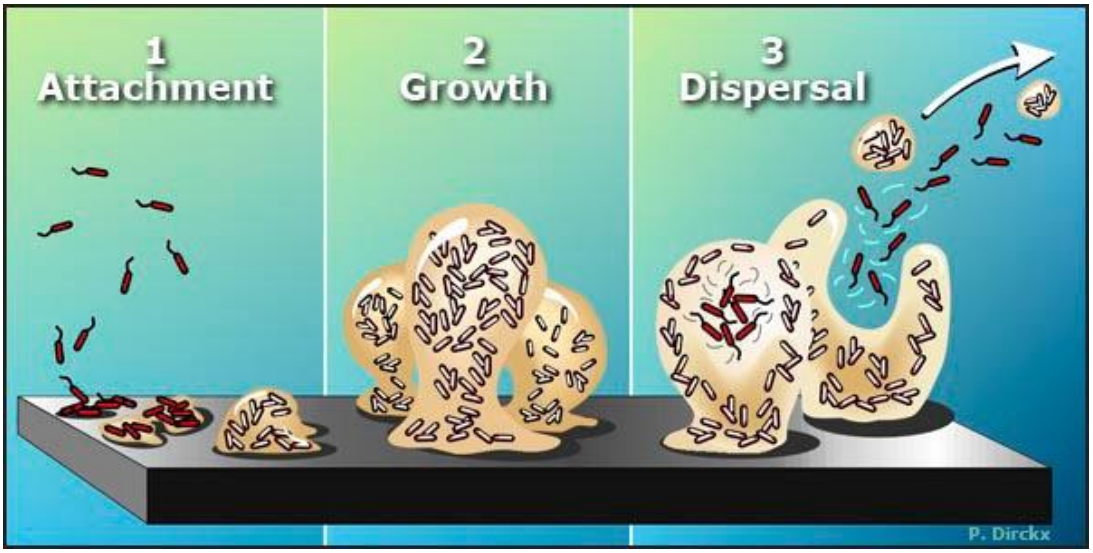

Figure 1.12 Bacterial biofilm life-cycle *(218)*

1.6.1 Biofilm-mediated disease

The ability to survive and re-populate new colonies despite local host immune defences and an inherent resistance to antimicrobial therapy has led to biofilms being implicated in many human chronic infections. In fact, the Centre for Disease Control in the USA has estimated that biofilms account for 65% of all human bacterial infections (219).

Biofilms in human disease are not a new entity. In the Seventeenth Century, Anton van Leeuwenhoek scraped the plaque from his teeth and looking under his light microscope, commented on organised microbial communities (207). However, it is only since the 1970s that the complexity of these communities has been appreciated in the environmental setting and only over the last ten to fifteen years that biofilm formation has been recognised as causing or exacerbating chronic infections in humans (220). Some of these chronic infections that have shown to have biofilm involvement in their pathophysiology include periodontitis (207), otitis media with effusion (221), recurrent tonsillitis (215), CF pneumonia (222), chronic adenoid infections (223-225), urinary tract infections (226), cholesteatomas (227), chronic wound infections (228), central venous catheters) (229), cochlear implants (230), tympanostomy tubes (231), urinary catheters (229), orthopaedic devices (207) and, more recently, CRS (232).

Due to advances in microbial detection methods, bacterial biofilms have only recently been demonstrated in chronic diseases where conventional cultures have been negative, raising questions of their possible importance in the pathophysiology of these conditions.

1.6.2 Sinogenic bacterial biofilms in cystic fibrosis

Sinogenic bacterial biofilms have also been demonstrated to play a role in mediating pulmonary disease in up to 50% of CF population (233). The commonest bacterial biofilms isolated in the sinuses of CF patients are reported as *P aeruginosa* and *S aureus* (234-235). Godoy et al (2011), demonstrated a significant associated between sinus and pulmonary cultures

within patients with CF (236). Walter et al (1997), demonstrated identical *P aeruginosa* isolates colonising the lungs of pre and post lung-transplant CF patients (237). Mainz et al (2009), demonstrated identical upper and lower *S aureus* and *P aeruginosa* genotypes in CF patients (235). In regards to fungal biofilms, Aspergillus fumigatus and candida species were regularly isolated and genotyped, but were mainly identified colonising the lower airway with no association with the upper airways (235). The increase in fungal colonisation of the lower airways in CF is thought to be due to the increased use of inhaled corticosteroids and better microbial detection technology (234).

These studies suggest that the sinuses play a role in harbouring bacterial biofilms which can colonise, recolonise and seed the lower airways (237). This led to many lung-transplant CF patients undergoing pre-transplant sinus surgery in an attempt to eradicated these biofilms and reduce re-colonisation of the new lung allografts.

The behaviour of the upper and lower airway bacteria and biofilms in the CF population provides further evidence for a united airway and raises the possibility of sinogenic bacterial seeding of the lower airways in other non-CF chronic conditions, such as asthma and chronic obstructive pulmonary disease.

1.6.3 Bacterial biofilms in chronic rhinosinusitis

Due to the recalcitrant nature of CRS, emerging evidence has implicated bacterial biofilms in the pathogenesis of this inflammatory disease. A summary of this evidence is presented in Table 1.3.

Perloff and Palmer, in 2004, first associated bacterial biofilms with CRS when frontal sinus stents, taken from patients with CRS, were imaged with scanning electron microscopy (SEM) and found in all cases to contain surface-related aggregates of bacteria (238). In a further study, they validated their initial findings using a rabbit-biofilm model (239). No biofilms were observed on any control tissue (239). Using SEM, Cryer *et al*, in 2004, was the first to identify bacterial biofilms on human sinonasal mucosa, taken from patients suffering

with CRS (237). Following this breakthrough observation, several further studies successfully identified bacterial biofilms on the sinonasal mucosa of CRS patients, using a mixture of SEM or TEM, with varying success (240-242) (Table 1.2).

As the evidence for biofilms in CRS strengthened, the limitations of SEM and TEM became more evident as the need to identify species-specific biofilms was required in order to attempt to understand their pathophysiological relevance. Sanderson *et al*, in 2006, were the first to successfully evaluate CRS mucosa and control tissue using a combination of fluorescence *In Situ* hybridisation (FISH) and confocal laser scanning microscopy (CLSM) (243-244). Further studies followed, successfully identifying bacterial biofilms on CRS mucosa using combinations of either FISH with CLSM or LIVE/DEAD® BacLight™ viability stains with CLSM (216, 244-249) (Table 1.3).

The commonest biofilm-forming microbe in CRS was found to be *S aureus* (216, 243, 250-251). Other biofilm-forming bacteria identified included *H influenzae*, *P aeruginosa*, CNS and *S pneumoniae* (243, 250-251). The presence of bacterial biofilms on sinonasal mucosa was associated with worse preoperative radiological scores, worse pre and postoperative quality-of-life scores and a worse mucosal appearance (245-246). These patients were also found to have significantly more postoperative appointments and courses of antibiotics (247, 248).

	STUDY	YEAR	SLAMPE	TECHNIQUE	EVIDENCE / SUMMARY FOR BIOFILMS IN CRS
1	Perloff & Palmer (233)	2004	Stents n=6	SEM/Culture	Frontal stents. Biofilms identified in 100% stents. *S aureus* cultured in 83% of stents.
2	Cryer *et al* (232)	2004	CRS=16	SEM	Morphological evidence of biofilms seen on 25% of CRS samples
3	Ramadam *et al* (239)	2005	CRS n=5	SEM	Bacterial biofilm in all CRS samples
4	Perloff & Palmer (238)	2005	Rabbits n=22 Control n=22	SEM/Culture	Biofilms identified in all 22 diseased samples. No biofilms seen in controls.
5	Sanclement *et al* (240)	2005	CRS n=30 Control n=4	SEM/TEM	Morphological evidence of biofilms in 80% CRS samples. No biofilms seen in controls.
6	Ferguson *et al* (241)	2005	CRS n=4	TEM	Morphological evidence of biofilms in 50% samples
7	Sanderson *et al* (242)	2006	CRS n=18 Control n=5	FISH & CLSM	Biofilms identified in 78% CRS samples. Biofilms identified in 40% controls. *S aureus* & *H influenzae* identified.
8	Psaltis *et al* (244)	2007	CRS n=38 Control n=9	LIVE/DEAD & CLSM	Biofilms identified in 45 CRS samples. No biofilms seen in controls. Biofilm-positive patients had higher disease recurrence rate
9	Healy *et al* (243)	2008	CRS n=11 Control n=3	FISH & epi-fluorescence	Bacterial biofilms identified in 45% CRS samples. Fungal biofilms identified in 64% of CRS samples
10	Psaltis *et al* (244)	2008	CRS n=40	CLSM	Biofilms identified in 50% CRS samples. Biofilms positive patients had higher LMS.
11	Foreman *et al* (211)	2009	CRS n=50 Control n=10	FISH & CLSM	Biofilms detected in 72% of CRS samples. No biofilms seen in controls. *S aureus* commonest organism identified
12	Bendouah *et al* (250)	2006	CRS n=31	Culture	*S aureus*, CNS and *P aeruginosa* isolated from CRS tissue. 71% isolates grew biofilms *in vitro*. These included 80% *S aureus*, 60% *P aeruginosa* and 80% CNS.
13	Psaltis *et al* (245)	2008	CRS n = 41 Control n =21	LIVE/DEAD & CLSM SEM	SEM identified biofilms in 35% of CRS samples. LIVE/DEAD with CLSM identified biofilms 100% of samples. No biofilms seen in controls.
14	Singhal *et al* (246)	2010	CRS n=51	LIVE/DEAD & CLSM	Biofilms detected in 71% of CRS samples. Biofilm-positive patients had worse preoperative LMS and endoscopic appearances. Higher disease recurrence in biofilms-positive patients
15	Foreman & Wormold (249)	2010	CRS n= 24	FISH	37 biofilms identified in 24 samples. In 45% of samples biofilms were polymicrobial. These groups had higher LMS. *H influenzae* most commonly identified as single organism and had lowest LMS. *S aureus* commonest microbe forming biofilms. *S aureus* associated with worse symptoms.
16	Foreman *et al* (247)	2010	CRS n=20	LIVE/DEAD & CLSM FISH & CLSM	LIVE/DEAD & CLSM detected biofilms in 65% samples. FISH & CLSM detected biofilms in 70% of samples. Combined methods detected biofilms in 90% of CRS samples
17	Chen *et al* (251)	2012	CRS n=24 Controls	SEM	Biofilms detected in 54.2% CRS patients and 8.3% controls
18	Sun *et al* (252)	2012	CRSwNP n=19 Controls n=12	SEM	Biofilms detected in 68.4% CRS patients. No biofilms seen in controls
19	Wang *et al* (253)	2014	CRSwNP n=19 CRSsNP n=15 Controls n=13	SEM	Biofilms detected in 73.7% of CRSwNP & 73.3% CRSsNP. No biofilms seen in controls
20	Jung *et al* (254)	2015	CRS n=26 Control n=7	SEM	Biofilms detected in 50% CRS samples & 14.3% controls. Higher LMS in patients with detected biofilms
21	Arild Danielsen *et al* (255)	2016	CRSsNP n=34 CRSwNP n=27 Controls n=25	LIVE/DEAD & CLSM	Biofilms identified in 97% CRSwNP, 82% CRSsNP. Biofilms identified on 80% ethmoid bulla and 71% uncinated process

Table 1.3 Summary of literature for bacterial biofilms in CRS

Over the last ten years, biofilm detection methods have improved enormously, but they continue to have limitations. A recent systematic review concluded that at present, a combination of FISH and CLSM was the gold standard technique for detecting biofilms in CRS tissue (214). However, FISH is limited in its ability to quantify bacterial biofilms and can only detect the bacteria that are specifically targeted. There is also variation between studies in sample sizes (256). Tissue samples have also been taken from different regions of the sinonasal cavities, such as the middle meatus, the inferior turbinates, the uncinate processes, and the ethmoidal sinuses. Recently, a tissue sampling study has been performed in CRS patients, to identify the anatomical sites within the sinonasal cavity that contain the highest concentration of surface-related bacterial biofilms. Using the LIVE/DEAD® BacLight™ Viability Kit, Arild Danielsen *et al*, in 2016, identified the ethmoid bulla and the uncinate process as the structures containing the highest concentrations of surface-related bacterial biofilms within the sinus cavities of CRS patients (80% and 71% respectively) (255).

1.6.4 Polymicrobial biofilms in chronic rhinosinusitis

With the advancement of microbial detection methods, it has become evident that sinogenic biolfilms are often composed of more than one organism and commonly contain a mixture of bacterial and fungal colonies. Foreman and Wormold (2010), used FISH and CLSM to identified polymicrobial biofilms in 46% of samples taken from the sinuses of patients suffering with CRS (249). Organisms identified included *S aureus, H influenza, P aeruginosa* and fungal species (249). *H influenza* was the commonest single-species biofilm identified and represented the least severe disease (249). *S aureus* was the most commonly identified microbe and when part of a polymicrobial biofilm, represented the most severe disease (249). Disease severity increased with the number of organisms within a polymicrobial biofilm. The presence of fungal colonies within a polymicrobial biofilm appeared to not affect disease severity (249).

The ability of bacterial and fungal species to form polymicrobial biofilms is evident with improving microbial detection methods, but their relevance and relationships with each other remains unknown. Species, such as *S aureus,* appear to thrive within a polymicrobial biofilm forming symbiotic relationships with other species, such as fungi (247). Cooperative relationships lead to biofilm augmentation through enhanced transfer of antimicrobial resistance data, strengthening of surface adherence and the formation of a larger EPS (247). *H influenzae* appears to be competitive, resistant to form polymicrobial biofilms. Other bacterial species may be within the biofilms coincidently and form no relationships with other microbes.

Polymicrobial biofilms are complex and many aspects of their pathophysiology remains unknown making their eradication extremely challenging.

1.6.5 Eradication of bacterial biofilms

Increasingly, there is a focus on developing novel methods and technologies to target and eradicate bacterial biofilms. The medical community has been successfully eradicating bacterial biofilms through physical removal long before their formal identification. For example, the physical removal of dental plaque, the removal of infected joint replacements and the removal of tonsils and adenoids to name but a few. To a certain degree, functional endoscopic sinus surgery (FESS) physically disrupts bacterial biofilms and provides symptomatic relief in the majority of patients suffering with CRS (240). However, evidence has shown that surgery alone does not eliminate bacterial biofilms from the sinuses entirely (257) and there remains a group of patients resistant to both maximal medical and surgical therapy, who may benefit from novel adjuvant treatments (258).

Studies have attempted to disrupt bacterial biofilms with varying success by targeting different stages of the biofilm life-cycle (256). Studies focusing on the prevention of biofilm formation have had varying success in targeting antibodies against bacterial chemicals that facilitate accumulation and adhesion of planktonic bacteria into a biofilm (259-260). Others have attempted to disrupt extracellular pili, leading to a reduction in biofilm

formation (261). Other studies have focused on the destruction of the biofilm, by using silver in chronic wound biofilms (262-263), using enzymes, such as DNase to disrupt the stabilising DNA in *P aeruginosa* biofilms in the infected lungs of patients with CF (264) and the use of electric currents which have been shown to have anti-biofilm effects (265). Studies have also attempted to weaken biofilms through inhibition of quorum-sensing (266) and of the Type III Secretion System (267), leading to interference with communication and the exchange of genetic material.

There have been a number of studies reporting novel anti-biofilm therapies with varying success. Bartley *et al*, in 2009, initially advocated the idea of using ultrasonic pulsations within the sinuses to disrupt bacterial biofilm formation on the sinus mucosa (268). Young *et al*, in 2010, performed a study looking at twenty-two patients with recalcitrant CRS, each undergoing a 6 session course of pulsed ultrasonic therapy and showed that 18/22 had improvements in their nasal mucosa and their CRS symptoms (269). However, there was no evidence provided on the effect that the ultrasonic pulsations had on bacterial biofilms.

The remaining anti-biofilm therapies include topically delivered techniques. Desrosiers *et al*, in 2007, showed that the addition of a citric acid/zwitterionic surfactant to *in vitro* CRS biofilms caused a reduction in colony forming unit (CFU) counts and also a reduction in biofilm mass on CLSM (244). Valentine *et al*, in 2011, delivered this citric acid/zwitterionic surfactant to the frontal sinuses of forty-two sheep inoculated with *S aureus*, but this resulted in adverse effects on the sinus cilia morphology (270). Uren *et al*, in 2008, used the topical antibacterial therapy Mupirocin, at a concentration of 0.05%, in a nasal douche delivered to the sinuses of sixteen patients with surgically recalcitrant CRS over a period of three weeks (271). Although 15/16 patients showed an improvement in the appearance of their nasal mucosal and 12/16 in their symptoms, the study once again provided no evidence of Mupirocin's effect on established CRS biofilms (271). Chiu, *et al*, in 2008, performed a clinical trial using 1% baby shampoo in a nasal douche delivered to the sinuses of eighteen patients with recalcitrant CRS (272). Only 8/18 patients experienced an improvement in their symptoms and *in vitro* experiments showed that 1% baby shampoo had no effect on CRS *P aeruginosa* biofilms

(272). In a similar study on a rabbit sinusitis model, Chiu *et al*, in 2007, showed that the antibiotic tobramycin delivered as a nasal douche at varying concentrations also had no effect on disrupting *P aeruginosa* biofilms (273).

A topical treatment showing very promising results in treating CRS biofilms is Manuka honey. This natural remedy has been used through the ages for its antibacterial therapy, but has recently resurfaced as a possible therapy for treating CRS-related biofilms. Manuka honey has been found to contain an active antibacterial chemical called methylglyoxal which separates it from other honeys in its potent bactericidal ability (274-276). Alendejani *et al*, in 2009, showed Manuka honey to be 100% effective in killing *S aureus* planktonic bacteria, 73% effective at destroying MRSA biofilms and 91% effective at killing a *P aeruginosa* biofilm (277). The capability of Manuka honey to breakdown bacterial biofilms lies in its ability to inhibit bacterial adhesion to surfaces (278), to inhibit fibronectin binding (279) and to interfere with genes controlling quorum sensing and virulence (280). Kilty *et al*, in 2010, have recently used a rabbit animal model to test the toxicity of Manuka honey on respiratory mucosa and found no histological evidence of epithelial injury (281). Other bee products, such as propolis and royal jelly, have also been shown to have strong antibiotic and anti-biofilm activity, but have yet to be studied in the context of CRS biofilms.

Due to the rise in antimicrobial tolerance, there is a need to develop novel adjunctive biofilm-targeted therapies in order to reduce the use of antibiotics as well as the need for multiple operations on people with CRS. Currently, within our research group (Upper Airway Research Group,) we are testing a novel biofilm-targeted therapy called Surgihoney™ on CRS-related biofilms. This is a novel, topical engineered honey, which releases hydrogen peroxide in contact with fluid. The initial *in vitro* data shows a very impressive antimicrobial profile against *S aureus*, both in the planktonic and biofilm states. We are hoping to test this in the clinical setting by undertaking a small clinical trial to test its efficacy in CRS patients after FESS.

1.7 Nitric oxide

Nitric oxide (NO) is an important inflammatory marker and potent vasodilator (282-283). It is also an important mediator possessing antibacterial, antifungal and antiviral properties (184, 282, 284). The role it plays in the pathophysiology of the sinuses has been debated over the last two decades. Gustafsson *et al*, in 1991, were the first to identify the presence of NO in exhaled air from the nasal cavity (285). NO is synthesised from the amino acid L-arginine and oxygen by the action of the enzyme NO synthase (NOS) (286). Lundberg *et al*, in 1994, identified that NOS was situated within the mucosal lining of the sinuses and upper airway and this accounted for the high levels of NO in the sinonasal cavity (284). They also showed that the levels NOS were increased in areas of inflamed or infected mucosa (287). This would make sense, as increased production of NO is known to enhance local defences within the upper airways by stimulating mucociliary function and inhibiting growth of pathological organisms (288-289). Lindberg *et al*, in 1997, showed that a decrease in the production of NO led to an impaired mucociliary function and therefore an increase in susceptibility to pathogens (288). The results from a genetic study by Zhang *et al*, in 2011, further highlight the importance of NO in the sinuses by suggesting that polymorphisms in the gene responsible for the synthesis of NOS may increase the susceptibility of developing CRS (286).

The concentration of NO within the sinuses has been shown to fluctuate with different conditions. The concentration is increased in asthma (290), allergic rhinitis (291) and upper respiratory tract infections (292) and decreased in acute (293) and chronic rhinosinusitis (180). This can be explained by the biochemistry of NO. Within the sinonasal cavity, NO is converted to the more stable metabolites nitrite (NO_2) and nitrate (NO_3) before being oxidised to peroxynitrite (ONOO) (294). In the presence of pus, caused by acute or chronic sinusitis, the environment becomes acidic and peroxynitrite is protonated to peroxynitrous acid, producing the cytotoxic metabolites hydroxyl and nitric dioxide (294). In a rabbit animal model with chronically infected sinuses, Schlosser *et al*, in 2000, showed a reduction in sinus NO concentration and an increase in NO metabolites (295). These levels returned to normal with treatment as the sinuses recovered (295). This was validated by Naraghi *et al*,

in 2007, who conducted this work in patients with recalcitrant CRSwNP and CRSsNP and showed reduced sinus NO and increased NO metabolites when compared to controls (296).

There is evidence that NO also possesses anti-biofilm properties by causing bacterial biofilms to disperse in the final stage of their life-cycle (297). Once the biofilm has matured and reached an optimal size, there is an orchestrated dispersal where the biofilm transforms from its sessile form into more vulnerable planktonic bacteria (298). This facilitates re-colonisation and the formation of new biofilms in different locations (9).

Barraud *et al*, in 2006, showed that by using low, non-toxic concentrations of NO *in vitro*, in the form of sodium nitroprusside (SNP), it was possible to trigger dispersal of *P aeruginosa* biofilms (297). They also showed that by using NO as an adjuvant therapy with antibiotics, biofilm eradication was even more extensive (297, 299). At low doses, it appears that NO stimulates the activity of the degradation enzyme phosphodiesterase in *P aeruginosa,* reducing the levels of intracellular cyclic-di-GMP and thereby inducing dispersion (300). In a later study, Barraud *et al*, in 2009, using varying concentrations of NO in the form of SNP, demonstrated dispersal of the single-organism biofilms *Serratia marcescens*, *Vibrio cholerae, Escherichia coli*, *Bacillus licheniformis*, *Staphylococcus epidermidis* and the yeast *Candida albicans* (299).

The ability of NO to induce dispersal of *P aeruginosa* biofilms into the planktonic state has formed the basis of a clinical trial within our Biofilm Group, looking at NO as a novel adjuvant therapy in the treatment of chronic *P aeruginosa* lung infections in CF patients (Reducing Antibiotic Tolerance using Nitric Oxide). It is thought that by administering NO to CF lungs, the carriage of *P aeruginosa* will be reduced by inducing biofilm dispersal, therefore subverting antibiotic resistance mechanisms associated with biofilm structure and increasing bacterial antibiotic sensitivity. We have extended these findings by investigating the role of NO on CRS-related biofilms. This is novel as there have been no previous studies looking at the effects of NO on CRS biofilms.

1.8 Study Aims & Objectives

Chapter 2

- Materials and Methods

Chapter 3

- **Aims:** To evaluate the presence, species and biology of surface-related bacterial biofilms on *ex vivo* sinonasal mucosa obtained from adults with CRSwNP and CRSsNP
- **Objectives:**
    1. To evaluate the presence of surface-related bacterial biofilms on CRS sinonasal mucosa and control mucosa
    2. To characterise the specific bacteria forming biofilms on CRS sinonasal mucosa

Chapter 4

- **Aims:** This chapter investigates the effects of low-dose NO on CRS-related bacterial biofilms
- **Objectives:**
    1. To evaluate the effect of NO on bacteria in biofilms
    2. To quantify the ability of NO to enhance the efficacy of antibiotics conventionally used to treat CRS

Chapter 5

- **Aims:** The primary aim of this chapter is to characterise bacterial profiles in NP and compare them with non-polypoidal mucosa from the same patient
- **Objectives:**
    1. To characterise bacterial profiles in NP
    2. To compare the bacterial profiles in NP with those on adjacent non-polypoidal sinonasal mucosa from the same patients

Chapter 6

- **Aims:** To investigate the mechanistic processes behind the internalisation of *S aureus* into mast cells and its relevance to the pathogenesis of NP
- **Objectives:**
    1. To develop an explant model using non-polypoidal mucosal tissue from patients with CRSwNP
    2. To determine the effects of treatment with different combinations of exogenous agents on the epithelial and sub-epithelial host cells using this explant model

Chapter 7

- **Aims:** To determine the *in vitro* morphological and proliferative effects of *S aureus* and exogenous SEB on the HMC-1 cell line
- **Objectives:**
    1. To develop a working mast cell co-culture model to investigate *S aureus*-mast cell interactions
    2. To investigate the effects of *S aureus* and exogenous SEB on mast cell proliferation rates
    3. To assess the morphological sequelae in mast cells after exposure to *S aureus* and exogenous SEB
    4. To clarify the mechanisms underlying *S aureus* internalisation

2 Materials & Methods

2.1 Ethical considerations

Ethical approval for this study was obtained from the Southampton and South West Hampshire Research Ethics Committee (Ethics Reference Code: REC 09/H0501/74). Formal written consent (**Appendix I**) was obtained from each study participant and original copies were stored in the project site file. A formal discussion regarding the research project was carried out with each participant and appropriate written information was provided at the time (**Appendix II**).

2.2 Subjects and control samples

Patients with chronic rhinosinusitis with and without nasal polyps (CRSwNP and CRSsNP) who met the diagnostic criteria defined in the EPOS guidelines (3) were recruited into the project. These patients, who had previously failed an eight week trial of maximal medical therepy with antibiotics, topical steroids and nasal douches, underwent functional endoscopic sinus surgery (FESS) at University Hopsital Southampton NHS Foundation Trust (UHSNFT) by Consultant Ear, Nose and Throat Surgeons Mr Rami Salib and Mr Philip Harries. None of the patients were using either topical or systemic corticosteroid, antibacterial or antihistamine therapies in the eight weeks prior to surgery. Exclusion criteria included age under eighteen years and patients suffering from cystic fibrosis (CF), primary ciliary dyskinesia (PCD) and immunocompromised patients.

Tissue was obtained from a total of 46 patients with CRS. Each patent was allocated a specific study number and these are displayed in Table 2.1.

STUDY NUMBER	NP	CHAPTER 3			CHAPTER 4		CHAPTER 5						CHAPTER 6
		LIVE/DEAD	SEM (NON-POLYP)	FISH (NON-POLYP)	Nitric Oxide (PILOT)	Nitric Oxide	SEM (NP)	FISH (NP)	IHC	TEM	LIVE/DEAD	VIABILITY ASSAY	IHC
CRS 1	N	Y	N	N	N	N	N	N	N	N	N	N	N
CRS 2	N	Y	N	N	N	N	N	N	N	N	N	N	N
CRS 3	N	Y	Y	N	N	N	N	N	N	N	N	N	N
CRS 4	Y	Y	N	N	N	N	N	N	N	N	N	N	N
CRS 5	Y	Y	Y	N	N	N	N	N	N	N	N	N	N
CRS 6	N	Y	Y	N	N	N	N	N	N	N	N	N	N
CRS 7	Y	Y	Y	Y	N	N	Y	Y	N	N	N	N	N
CRS 8	Y	Y	N	Y	N	N	Y	Y	N	N	N	N	N
CRS 9	N	Y	Y	Y	N	N	N	N	N	N	N	N	N
CRS 10	Y	Y	Y	Y	N	N	Y	Y	N	N	N	N	N
CRS 11	Y	Y	N	Y	N	N	Y	Y	N	N	N	N	N
CRS 12	Y	Y	N	Y	N	N	Y	Y	N	N	N	N	N
CRS 13	Y	Y	Y	Y	N	N	Y	Y	N	N	N	N	N
CRS 14	Y	N	Y	Y	N	N	Y	Y	N	N	N	N	N
CRS 15	Y	N	Y	Y	N	N	Y	Y	N	N	N	N	N
CRS 16	Y	N	N	Y	N	N	Y	Y	N	N	N	N	N
CRS 17	Y	N	N	N	Y	N	N	N	N	N	N	N	N
CRS 18	N	N	N	N	Y	N	N	N	N	N	N	N	N
CRS 19	Y	N	N	N	Y	N	N	N	N	N	N	N	N
CRS 20	N	N	N	N	Y	N	N	N	N	N	N	N	N
CRS 21	Y	N	N	N	N	Y	N	N	N	N	N	N	N
CRS 22	Y	N	N	N	N	Y	N	N	N	N	N	N	N
CRS 23	N	N	N	N	N	Y	N	N	N	N	N	N	N
CRS 24	N	N	N	N	N	Y	N	N	N	N	N	N	N

STUDY NUMBER	NP	CHAPTER 3			CHAPTER 4		CHAPTER 5						CHAPTER 6
		LIVE/DEAD	SEM (NON-POLYP)	FISH (NON-POLYP)	Nitric Oxide (PILOT)	Nitric Oxide	SEM (NP)	FISH (NP)	IHC	TEM	LIVE/DEAD	VIABILITY ASSAY	IHC
CRS 25	Y	N	N	N	N	N	N	N	Y	N	N	N	N
CRS 26	Y	N	N	N	N	N	N	N	Y	N	N	N	N
CRS 27	Y	N	N	N	N	N	N	N	Y	N	N	N	N
CRS 28	Y	N	N	N	N	N	N	N	Y	N	N	N	N
CRS 29	Y	N	N	N	N	N	N	N	Y	N	N	N	N
CRS 30	Y	N	N	N	N	N	N	N	Y	Y	N	N	N
CRS 31	Y	N	N	N	N	N	N	N	Y	Y	N	N	N
CRS 32	Y	N	N	N	N	N	N	N	Y	Y	N	N	N
CRS 33	Y	N	N	N	N	N	N	N	Y	Y	N	N	N
CRS 34	Y	N	N	N	N	N	N	N	Y	Y	N	N	N
CRS 35	Y	N	N	N	N	N	N	N	N	N	Y	Y	N
CRS 36	Y	N	N	N	N	N	N	N	N	N	Y	Y	N
CRS 37	Y	N	N	N	N	N	N	N	N	N	Y	Y	N
CRS 38	Y	N	N	N	N	N	N	N	N	N	Y	Y	N
CRS 39	Y	N	N	N	N	N	N	N	N	N	Y	Y	N
CRS 40	Y	N	N	N	N	N	N	N	N	N	N	N	Y
CRS 41	Y	N	N	N	N	N	N	N	N	N	N	N	Y
CRS 42	Y	N	N	N	N	N	N	N	N	N	N	N	Y
CRS 43	Y	N	N	N	N	N	N	N	N	N	N	N	Y
CRS 44	Y	N	N	N	N	N	N	N	N	N	N	N	Y
CRS 45	Y	N	N	N	N	N	N	N	N	N	N	N	Y
CRS 46	Y	N	N	N	N	N	N	N	N	N	N	N	Y
Total		13	9	10	4	4	9	9	10	5	5	5	7

Table 2.1 CRS Study numbers with allocated experiments

Control tissue was obtained from non-CRS patients with no clinical history or radiological evidence of CRS, undergoing endoscopic trans-sphenoidal pituitary surgery at the Wessex Neurological Centre, University Hospital Southampton NHS Foundation Trust (UHSNFT), by Mr Salil Nair (Consultant Rhinologist & Anterior Skull Surgeon), Mr Ashok Rokade (Consultant Rhinologist & Anterior Skull Surgeon) and Mr Nijaguna Mathad (Consultant Neurosurgeon). Control patients were excluded from the study if they had used either topical or systemic corticosteroids, antibacterial or antihistamine therapies in the eight weeks prior to surgery. All patients selected had serum cortisol levels within normal limits.

Tissue was obtained from a total of 13 control patients. Each patent was allocated a specific study number and these are displayed in Table 2.2.

STUDY NUMBER	CHAPTER 3			CHAPTER 4	CHAPTER 5			
	LIVE/DEAD	SEM	FISH	Nitric Oxide	SEM	FISH	IHC	TEM
CT 1	Y	Y	Y	N	N	N	N	N
CT 2	Y	Y	Y	N	N	N	N	N
CT 3	Y	Y	Y	N	N	N	N	N
CT 4	Y	Y	Y	N	N	N	N	N
CT 5	Y	Y	Y	N	N	N	N	N
CRS 6	N	N	N	Y	N	N	N	N
CRS 7	N	N	N	N	Y	Y	Y	Y
CRS 8	N	N	N	N	Y	Y	Y	Y
CRS 9	N	N	N	N	Y	Y	Y	Y
CRS 10	N	N	N	N	Y	Y	Y	Y
CRS 11	N	N	N	N	Y	Y	Y	Y
CRS 12	N	N	N	N	Y	Y	Y	Y
CRS 13	N	N	N	N	Y	Y	Y	Y
TOTAL	5	5	5	1	7	7	7	7

Table 2.2 Control study numbers with respective studies

2.3 Data collection

All subjects were skin-prick allergy tested (SPT) to a standard battery of common aero-allergens (Histamine (control), house dust mite, tree pollen, grass pollen, indoor mould, outdoor mould, feather, cat pelt and dog dander (ALK-Abello, Reading, Berkshire, UK) prior to surgery.

Radiological severity of sinus disease was graded on a CT scan of the sinuses using the Lund-Mackay (LM) scoring system (301). The LM score is a simple objective assessment tool for assessing the severity of CRS on a CT scan (302). Each sinus is assessed as no opacification (0 points), partial opacification (1 point) or total opacification (2 points). The ostiomeatal complex (OMC) is assessed as patent (0 points) or obstructed (2 points). With 5 paired sinuses and 2 OMC the LM score ranges from 0 to 24. As a result of its simplicity and there being no requirement for radiological training, the assessment tool has a high level of user reliability and as such, has been recommended by the Task Force on Rhinosinusitis for use in outcome research (302). We have therefore included the LM score in this study. However, a limitation of the LM scoring system is that the normal non-CRS population can have a radiological Lund-Mackay (LM) score of 0-5 (303). To overcome this limitation and to reduce error (the chances of including patients with sub-clinical CRS), only control patients with a LM score of 0 out of 24 were included in the study.

Pre-operative demographical data were collected including age, gender, atopic status, previous sinonasal surgery, past medical history, history of asthma, history of aspirin sensitivity and smoking habits. The perioperative endoscopic appearance of the sinonasal cavities, such as the presence or absence of pus, nasal polyps (NP) or allergic mucin was noted.

Each sample was allocated a reference number and sent anonymously for histopathological evaluation in each case. Pus swabs were taken from the middle meatus and sent for microbiological culture and sensitivity.

2.4 Tissue sampling

Intra-operative tissue samples were obtained from regions within the sinonasal cavity which were being removed as part of the planned surgery and therefore represented waste material. Initially, samples were obtained from different regions of the sinonasal cavity and evaluated for biofilm consistency. These regions included the middle meatus, the uncinate process and the ethmoid bulla. Analysis of these different anatomical regions demonstrated more consistent bacterial biofilms on the uncinate process and ethmoid bulla. This is in keeping with recent literature (255). Tissue biopsies from CRS patients were, therefore, obtained from the uncinate process when present and the ethmoid bulla when the uncinate process had been previously removed. All biopsies were stored initially in Hank's Balanced Salt Solution (HBSS) and placed on ice for immediate transfer to the Wellcome Trust Clinical Research Facility (WTCRF) for processing.

2.5 Tissue and biofilm viability

Tissue and microbial viability were assessed using the LIVE/DEAD® BacLight™ Viability Kit. This kit includes the two nucleic acid stains SYTO™ 9 and propidium iodide (PI). The SYTO™ 9 nucleic acid stain fluoresces both viable and non-viable cells green when viewed under confocal laser scanning microscopy (CLSM). Propidium iodide (PI) nucleic acid stain only penetrates non-viable cells and when used in combination with SYTO™ 9, reduces the fluorescence giving a red appearance. Therefore, using this viability kit, all viable cells fluoresced green and all non-viable cells fluoresced red. Each tissue biopsy was analysed with the LIVE/DEAD® BacLight™ Viability Kit according to the manufacturer's instructions (Thermofisher, Loughborough, UK). In brief, biopsy samples were treated with 20µl of each nucleic acid stain and left to stand for twenty minutes at room temperature. All samples were then assessed using CLSM.

2.6 Isolation of bacteria from chronic rhinosinusitis tissue

Isolation of *S aureus* from CRS tissue was performed using the standard Biomedical Sciences standard operating protocol (**Appendix III**). Fresh tissue samples were placed in HBSS and transferred on ice to the WTCRF. Tissue samples were added to DNase, blood and Baird-Parker agar plates and incubated at 37°C for 18-24 hours. Colony morphology was then analysed, showing creamy gold colonies on DNase and blood agar plates and grey-black, shiny colonies surrounded by a zone of clearing on Baird-Parker agar plates. Further tests performed to confirm *S aureus* isolates included a DNase test, a coagulase test, a catalase test and Polymerase Chain Reaction (PCR).

2.7 Surface-related biofilm detection rates

For each patient and tissue type, five specimens were imaged with CLSM to detect biofilms. The patient was deemed to have surface-related bacterial biofilms on their sinonasal mucosa if the bacteria observed met the biofilm definition criteria (*Section 2.9*) on one or more of the five samples analysed. A surface-related biofilm detection rate (SBDR) was calculated by dividing the number of biofilm positive samples by five.

2.7.1 Surface-related biofilm detection rate classification

(0 out of 5) (No biofilms) SBDR = 0.0

(1 out of 5) (Minimal) SBDR = 0.2

(2 out of 5) (Mild) SBDR = 0.4

(3 out of 5) (Moderate) SBDR = 0.6

(4 out of 5) (Severe) SBDR = 0.8

(5 out of 5) (Extensive) SBDR = 1.0

2.8 Intracellular bacteria detection rates

For each patient and tissue type, five specimens were imaged with CLSM to detect intracellular bacteria. The patient was deemed to have intracellular bacterial if identified on one or more of the five samples analysed. An intracellular bacteria detection rate (IBDR) was calculated by dividing the number of intracellular bacteria positive samples by five.

2.8.1 IBDR Intracellular bacteria detection rate classification

(0 out of 5)	(No biofilms)	IBDR = 0.0
(1 out of 5)	(Minimal)	IBDR = 0.2
(2 out of 5)	(Mild)	IBDR = 0.4
(3 out of 5)	(Moderate)	IBDR = 0.6
(4 out of 5)	(Severe)	IBDR = 0.8
(5 out of 5)	(Extensive)	IBDR = 1.0

2.9 Biofilm analysis diagnostic criteria

Diagnostic criteria for biofilm detection were based on the Parsek and Singh criteria (304), in which they state that biofilms should be:

1. Associated with a surface
2. Aggregated in clusters encased in a matrix

2.10 Confocal laser scanning microscopy

All tissue requiring analysis with confocal laser scanning microscopy (CLSM) was transported to the Biomedical Imaging Unit (BIU) at the UHSNFT. All tissues

were mounted within chamber slides with cover-slip bottoms and imaged with a Leica TCS SP5 inverted confocal system (Leica Microsystems, Milton Keynes, UK) using a 63x oil immersion lens. Sequential scanning was used to further eliminate cross talk interference from multiple fluorophores. Images were collected and analysed using Leica LAS-AF software. CLSM was applied to various techniques including fluorescence *in situ* hybridisation (FISH), LIVE/DEAD viability assay, intracellular bacteria viability assay and co-cultivation cell line culture. The CLSM was facilitated by the BIU.

2.11 Fluorescence *in situ* hybridisation

The protocol was adopted from Nistico *et al*, in 2011(305) and optimised for use on CRS tissue.

2.11.1 Optimisation for fluorescence *in situ* hybridisation on chronic rhinosinusitis tissue

The lysozyme and formamide concentrations were optimised *in vitro* using a CRS strain of *S aureus* (strain ATCC25923). A standard growth curve was performed and a mid-log phase of 150 minutes was achieved. Poly-L-Lysin slides were prepared with the *S aureus* strain.

The concentrations of lysozyme used were 0.25mg, 0.5mg, 1mg, 2.5mg, 5mg and 10mg (lysozyme concentration calculations can be seen in Appendix IV. The concentration of formamide used included 20%, 30% and 40%. The 16S rRNA FISH probes used in this optimisation experiment included the Eubacterial consensus probe (Eub338, 16S sequence GCTGCCTCCCGTAGGAGT), the *Staphylococcus* genus probe (Sta, 16S sequence TCCTCCATATCTCTGCGC) and the *S aureus* probe (S.au, 16S sequence GAAGCAAGCTTCTCGTCCG). The fluorescence intensity was measured by the Leica software of the TCS SP5 confocal microscope. This experiment was repeated 3 times and average intensities can be viewed in Table 2.3. Analysis of results showed that the strongest fluorescence intensities were seen with lysozyme concentrations between 0.25mg-0.5mg

and formamide concentrations at 20%. Therefore, when performing FISH on CRS and control tissue, 0.5mg of lysozyme with 20% formamide was used.

Lysozyme conc. (mg)	Formamide concentration (%)								
	20%			30%			40%		
	Sta	S.au	EuB	Sta	S.au	EuB	Sta	S.au	EUB
0.25	250	200	205	235	145	95	230	75	95
0.5	250	220	190	220	70	90	220	125	95
1	240	220	130	125	135	60	170	55	65
2.5	240	230	115	150	75	60	225	80	75
5	240	170	130	200	190	170	210	90	80
10	240	160	125	205	100	95	220	105	120

Table 2.3 The variation of fluorescence intensity of three 16s rRNA FISH probes.16s rRNA FISH probes: Sta, *Staphylococcus* genus; S.au, *Staphylococcus aureus*; EuB, Eubacterial consensus sequence probe.

2.11.2 Fluorescence *in situ* hybridisation protocol

Specimens were fixed in 4% Paraformaldehyde followed by serial washes with phosphate buffered saline (PBS) and finally stored at -20°C in PBS-Ethanol (1:1). The 16S rRNA FISH probes utilised were: *S aureus (S.au)*, *Staphylococcus genus (Sta)*, *H influenzae (Hinf), P aeruginosa (PaerA),* and the universal *eubacterial consensus sequence* probe (Eub338). A maximum of 3 probes were used on each specimen to limit cross-interference with the 3 labelled fluorescent dyes, Cy3, Cy5 and 6-FAM.

Samples were each treated with 20µl of 0.5mg/ml of lysozyme (Sigma-Aldridge) and incubated within a hydration chamber (a 50ml centrifuge tube containing tissue dampened with sterile water, see Figure 2.1), at 37°C/5% CO_2 for 3 hours. This was followed by incubation with 4µl of either the *S aureus* (1.33µl Sta, 1.33µl S.au and 1.33µl Eub) or *P aeruginosa* and *H influenzae* (1.33µl Hinf, 1.33µl PaerA and 1.33µl Eub338) FISH probes combined with 16µl of hybridisation buffer (360µl 5M NaCl, 40µl TrisHCL (pH 8), 400µl of 20% formamide, sterile water and 2µl of 10% Sodium Dodosyl Sulphate (SDS)), for 2 hours at 48°C. Finally, samples were submerged in wash buffer (1µl TrisHCL, 2150µl of 5M NaCl, 500µl 0.5M ETDA, sterile water and 50µl of 10% SDS), at 46°C for 15 minutes followed by immersion in PBS and visualised using CLSM.

The serial dehydration steps used in the original protocol were found to dehydrate the tissue and damage the surface architecture. The serial dehydration steps were therefore not used in this adapted protocol.

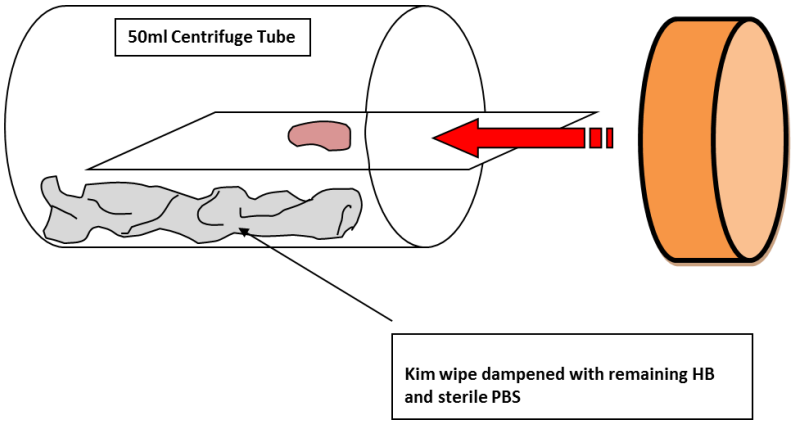

Figure 2.1 Hydration chamber. Chamber created to keep tissue sample hydrated. Tissue sample placed on slide and inserted into 50ml centrifuge tube. Kim wipes soaked in hydration buffer (HB) and sterile phosphate buffered saline (PBS) and inserted within the chamber to prevent dehydration.

2.12 Scanning electron microscopy

Imaging was performed at the UHSNFT BIU. Specimens were fixed in 3% glutaraldehyde in cacodylate sucrose buffer with 0.15% alcian blue for 24 hours to retain biofilm matrix (306). Samples were rinsed in 0.1M Na-Cacodylate and post fixed in 1% osmium tetroxide for 1 hour. Specimens were then serially dehydrated (for 10 minutes at 30%, 50%, 70%, 95%, 100%, 100% ethanol) critical point dried, mounted on aluminium stubs, coated with gold-palladium and imaged on an FEI Quanta 200 scanning electron microscope. The CLSM was facilitated by the BIU.

2.13 Transmission electron microscopy

Transmission electron microscopy (TEM) was performed at the UHSNFT BIU. Specimens were fixed in 3% glutaraldehyde and 4% formaldehyde in 0.1M PIPES (piperazine-N,N′-bis) for 24 hours. Specimens were rinsed in 0.1M PIPES and post fixed in 1% osmium tetroxide in 0.1M PIPES for 1 hour. After further rinsing in 0.1M PIPES, uranyl acetate was added to the specimens. Specimens were then serially dehydrated in ethanol (30%, 50%, 70%, 95%, 100%, 100%), and then placed in acetonitrile. Specimens were then subjected to acetonitrile:resin (50:50) for 1 hour, then infiltrated in resin overnight. After 16 hours, specimens were embedded in new epoxy resin and polymerised at 60°C. Tissue sections were each cut with an Ultra Cut E Ultramicrotome. Sections were finally imaged using a Hitachi H7000 TEM. TEM was facilitated by the BIU.

2.14 Dispersal of bacterial biofilms with nitric oxide

2.14.1 Nitric oxide donor

In this study, sodium nitroprusside (SNP) was used as the nitric oxide (NO) donor *in vitro* on *ex vivo* mucosal samples at a concentration of 1mM. SNP is an inorganic compound comprised of a ferrous centre surrounded by 5 cynanide ligands and 1 linear NO ligand ($Na_2[Fe(CN)_5NO]\cdot 2H_2O$). SNP is a potent

vasodilator and is used clinically in the intensive care setting for acute hypertensive emergencies. NO is released and works by increasing intracellular production of cyclic-di-GMP which stimulates calcium to move from the cytoplasm to the endoplasmic reticulum, reducing the amount available for smooth muscle contraction. Therefore, smooth muscle relaxes, allowing vascular dilatation.

2.14.2 Antibiotic therapy

Amoxicillin/clavulanic acid (co-amoxiclav) was used as it represents one of the antibiotics used to treat CRS.

2.14.3 Dispersal of bacterial biofilms using nitric oxide

This protocol was adapted from Barraud *et al*, 2009 (297), and optimised for this study using CRS tissue samples. Tissue samples were obtained from patients with CRS and control subjects as described previously. A 5x5mm specimen of tissue was treated in each of the treatment groups at 37°C/5% CO_2, for 3 hours. Four separate treatment groups were setup, as shown in Table 2.4. Each treatment group contained 10% foetal bovin serum (FBS) in Hanks' Balanced Salt Solution (HBSS). Group 1 (control group) contained no additional co-amoxiclav (antibiotic) or SNP (NO donor). Co-amoxiclav only was used to treat tissue in Group 2 (Antibiotic Group). SNP only was used to treat tissue in Group 3 (SNP Group). Co-amoxiclav and SNP were used to treat tissue in Group 4 (Antibiotic/SNP Group).

	Group	Co-amoxiclav	SNP	FBS/HBSS
1	Control	-	-	1ml/9mls
2	Antibiotic	6µl	_	1ml/9mls
3	SNP	-	100µl	1ml/9mls
4	Antibiotic/SNP	6µl	100µl	1ml/9mls

Table 2.4 Treatment groups for nitric oxide pilot study

After 3 hours' incubation, the tissue specimens were rinsed 3 times with sterile PBS followed by maceration through a filter mesh to form 4 homogenates representing each treatment group. Each homogenate was serially diluted to $1x10^7$. The diluted homogenates were then plated to 3 different agar plates: blood agar, chocolate agar and CFC (cetrimide, fucidin, cephalosporin) *Pseudomonal* agar. These agar plates were chosen to facilitate the growth of common CRS pathogens (*S aureus, H influenzae* and *P aeruginosa*). These agar plates were then incubated at 37°C/5% CO_2 and analysed at 24 and 48 hours. Colony forming unit (CFU) counts were documented for each agar plate.

2.14.3.1 Bacterial identification

The bacteria from each agar plate were isolated and sent to the Health Protection Agency (HPA) Microbiological Laboratories at University Hospital Southampton NHS Foundation Trust (UHSFT) for microbial species identification.

2.15 Immunohistochemistry

2.15.1 Fixing and tissue preparation for glycolmethacrylate

Biopsy specimens were fixed in ice-cold acetone and stored at -20°C overnight. Specimens were then embedded in water-soluble resin glycolmethacrylate (GMA) (Park Scientific, Northampton, UK) as previously described (307).

2.15.2 Immunohistochemistry

GMA embedded sections were cut at a thickness of 2µm and mounted on glass slides. Sections were treated with 0.1% sodium azide with 3% hydrogen peroxide to inhibit endogenous peroxidases for 30 minutes, followed by application of a Dulbecco's Modified Eagles Medium for 2 hours. Primary antibodies were applied for 24 hours at room temperature at previously

titrated optimal dilutions (Table 2.5). Biotinylated secondary antibodies were applied for 2 hours followed by avidin biotin-peroxidase complexes. Depending on specimen analysis, either 3-amino-9-ethylcarbazole (AEC) or 3, 3'-Diaminobenzidine (DAB) substrate were applied and counterstained with Mayer haematoxylin. All experiments included a negative control slide without primary antibodies applied and an isotype-matched antibody control.

Primary antibody	Clone	Source	Host species	Working dilution
Mast cell tryptase	AA1	Abcam, Cambridge, UK	Mouse	1:20000
Neutrophils	NOE	Dako, Ely, UK	Mouse	1:1000
Eosinophils	EG2	Life Technologies, Paisely, UK	Mouse	1:2000
Macrophages	CD68 PGMI	Dako, Ely, UK	Mouse	1:100
Lymphocytes	CD3	AbD Serotec, Oxford, UK	Mouse	1:700
B Lymphocytes	CD20	Dako, Ely, UK	Mouse	1:2000
Epithelial cells	PanCK	Sigma-Aldrich, St Louis, USA	Mouse	1:4000
S aureus	SA	Abcam, Cambridge, UK	Mouse	1:100

Table 2.5 Monoclonal antibodies used in GMA immunohistochemistry and associated dilutions

2.15.3 Validation of *Staphylococcus aureus* primary monoclonal antibody

A mouse anti-*S aureus* primary antibody was obtained from Abcam (Milton, Cambridge, UK) to identify *S aureus* in sinonasal specimens. A positive control was developed to optimise concentrations and assess the sensitivity of this *S aureus* antibody. The *S aureus* strain (ATCC25923) was previously isolated from CRS tissue and used for this validation. After performing a standard growth curve, the mid-log phase was found to be between 120-180 minutes.

Previous tissue viability experiments showed that CRS tissue remained viable at 18 hours in Roswell Park Memorial Institute medium (RPMI). RPMI, therefore, was used as a culture medium. A *S aureus* broth was created by adding *S aureus* to 50mls of RPMI and incubated at 36^0C/5% CO_2. After 150 minutes (mid-log phase selected) CRS sinonasal mucosa and NP tissue was added to the *S aureus* broth and returned to the incubating oven at 36^0C/5% CO_2 for 18 hours. Specimens were removed and placed in acetone before being embedded in GMA for IHC. Serial dilutions of the anti-*S aureus* antibody were used to detect the *S aureus* on the GMA embedded samples. It was determined using dilutions 1:25, 1:50, 1:100, 1:200 and 1:400 to obtain the best detection.

2.15.4 Cell count

Cells were counted manually for each tissue section. The epithelial length and sub-epithelial area were measured with the assistance of computerised image analysis (KS400 software with a Zeiss Axioskop 2 microscope and Axiocam, Zeiss, Bicester, UK).

Epithelial cell rates were calculated using the equation:

$$\textbf{Epithelial cell rate (cells mm}^{-1}\textbf{)} = \frac{\textbf{Total number of cells}}{\textbf{Epithelial length (mm)}}$$

Sub-epithelial cell rates were calculated using:

$$\textbf{Sup-epithelial cell rate (cells mm}^{-2}\textbf{)} = \frac{\textbf{Total number of cells}}{\textbf{Sub-epithelial area (mm}^2\textbf{)}}$$

2.15.5 Cell accumulation measurements

A 10 x 10 grid was used to measure cell accumulation on IHC sections, with each individual square measuring 25µm x 25µm (at x40 magnification). The cell rate was calculated at intervals of 100µm deep into the loose stroma from the epithelial basement membrane. The area of each 100µm depth interval was calculated at 25000µm^2 (250µm X 100µm). A conversion factor of 40 was used to convert the rate of cells per 25000µm^2 to rate of cells per mm^2.

2.16 Proliferation assay

The Click-iT® EdU proliferation assay (Thermofisher, Loughborough, UK) was used to detect DNA synthesis and provides an accurate method of assessing cell proliferation. The Edu (5-ethynyl-2´-deoxyuridine) is a nucleoside analogue to thymidine and incorporates into DNA during active DNA synthesis. Detection is based on a click reaction, a copper catalyzed covalent reaction between picolyl azide (Alexa Fluor®488 dye) and an alkyne EdU (Figure 2.2).

2.16.1 Click-iT® EdU proliferation assay on sinonasal tissue

The method for using the Click-iT® EdU proliferation assay in sinonasal tissue was performed according to the manufacturer's product protocol. Briefly, CRS tissue was prepared into 5mm x 5mm sections and placed into wells containing EdU (10µm) in RPMI for 24 hours at 37°C, 5% CO_2. After 24 hours, the tissue was fixed in 3.7% formaldehyde in PBS for 15 minutes. Tissues were washed twice with 3% bovine serum albumin (BSA) in PBS. Tissue was then treated with the permealisation buffer (0.5% Triton® X-100 in PBS) at room temperature for 20 minutes and washed twice with 3% BSA in PBS. The Click-iT® reaction cocktail (Click-iT® reaction buffer, $CuSO_4$, Alexa Fluor®647 azide and reaction buffer additive) was used to treat tissue for 30 minutes, protected from light. Tissue was washed again twice with 3% BSA in PBS. Wash solution

was then replaced with PBS. The DAPI-488 (Sigma-aldrich®, Dorset, UK) stain was added 30 minutes prior to imaging with CLSM.

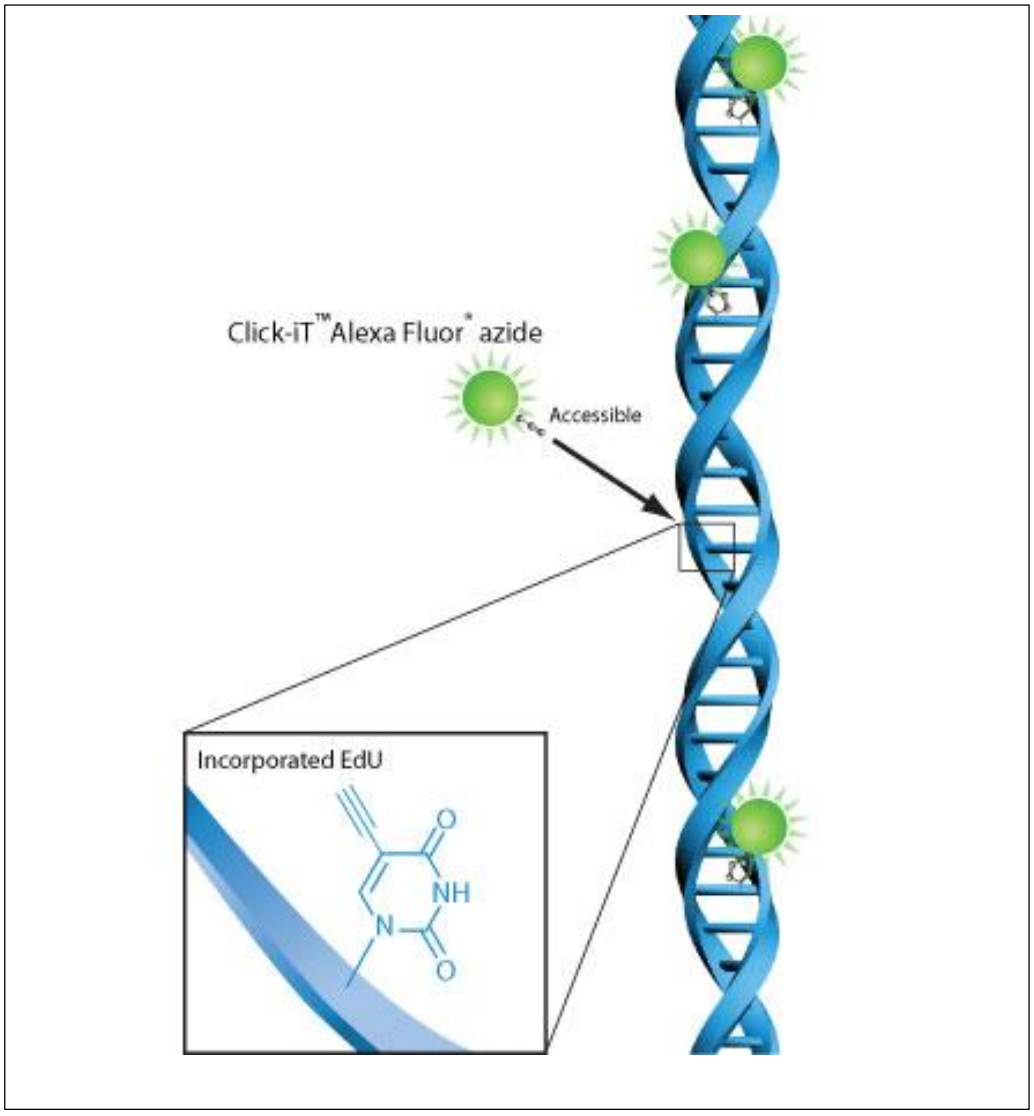

Figure 2.2 Detection of the incorporated EdU with the Alexa Fluor® 488 azide. Image from www.thermofisher.com

2.16.2 Click-iT® Edu proliferation assay in cell culture

The protocol for using the assay cell culture lines was the same as for sinonasal tissue, except after each treatment or wash step, the cells were centrifuged (11,000 G) for 10 minutes into a pellet, allowing removal or addition of buffers and solutions.

2.17 Intracellular bacteria viability assay

To test the viability of intracellular bacteria in specific host cells, a novel technique was developed by combining the Click-iT® Edu proliferation assay, primary antibodies with a fluorochrome-labelled secondary antibody and the DAPI stain.

CRS tissue was prepared into 5mm x 5mm sections and placed into wells containing 1ml of RPMI. A final concentration of 10μM of EdU was added to each well, in addition to 200μl of the specific mouse anti-human monoclonal antibody required (see Table 2.3), and then incubated for 24 hours at 37°C/ 5% CO_2. After 24 hours, the solution was removed and 200μl of donkey anti-mouse IgG H&L Alexa Fluor®568 (Abcam, Cambridge, UK) secondary antibody was added for 2 hours. The tissue was then fixed with 3.7% formaldehyde in PBS. After 15 minutes, tissues were washed three times with 0.5% Triton® X-100 in PBS, each wash lasting 30 minutes. The Click-iT® reaction cocktail (Click-iT® reaction buffer, $CuSO_4$, Alexa Fluor®647 azide and reaction buffer additive) was added to each well for 30 minutes, protected from light. Tissue was washed again twice with 0.5% Triton® X-100 in PBS, each wash lasting 30 minutes and finally replaced with PBS. Thirty minutes prior to imaging with CLSM, 20μl of the DAPI-488 (Sigma-aldrich®, Dorset, UK) stain was added to the tissue.

2.18 Explant tissue model

The *ex vivo* explant tissue model was used to test the effects of a series of exogenous agents on the host environment interface of non-polypoidal

sinonasal mucosa from patients with CRSwNP. The tissue used for the explant model was taken from the inferior turbinate.

Ex vivo tissue was divided into 6 separate 5mm x 5mm samples. One sample was immediately fixed in acetone and GMA embedded for analysis with IHC (no culture group). The remaining 5 samples were added to 5 individual wells containing RPMI and sterile penicillin/streptomycin for 30 minutes to clear exogenous bacteria on tissue surface. Tissue samples were rinsed three times in sterile PBS and then immersed in 2mls of RPMI alone. The treatment groups were setup as shown in Table 2.6. After addition of each treatment group, samples were incubated for 24 hours at 37°C, 5% CO_2. Tissue was fixed with acetone, GMA embedded and then processed for IHC.

TREATMENT GROUP	TOPICAL ANTIBIOTIC	TREATMENT
No Culture	No	Fixed immediately for IHC
Culture (control)	Yes	Cultured in RPMI alone for 24hrs
***S aureus* (live)**	Yes	Cultured with live *S aureus* for 24 hrs
IL-4	Yes	Cultured with IL-4 (20µg/ml) for 24 hrs
SEB	Yes	Cultured with SEB (10µg/ml) for 24 hrs
***S aureus* (live) & SEB**	Yes	Cultured with live *S aureus* & SEB (10µg/ml) for 24 hrs
***S aureus* (dead)**	Yes	Cultured with dead *S aureus* for 24 hrs
***S aureus* (dead) & SEB**	Yes	Cultured with dead *S aureus* & SEB for 24 hrs

Table 2.6 Treatment groups for explant model

2.18.1 *Staphylococcus aureus* (live)

S aureus (P3 isolate) was grown to the mid-log phase at 37°C in RPMI medium, centrifuged and washed with sterile PBS to remove toxins and diluted to the required concentration. Viable bacteria were determined with CFU counts after serial dilution and plating on blood-agar for 24 hours. Twenty microlitres of *S aureus* (containing 5.0 x 10^6 bacterial cells) were added to each sample.

2.18.2 Non-viable *Staphylococcus aureus*

Non-viable *S aureus* was required to investigate whether the viability of *S aureus* was essential to cause effect. The same CRS isolated *S aureus* strain P3 was used. *S aureus* was grown to the mid-log phase at 37°C in RPMI medium. The number of viable bacteria at the mid-log phase was determined after serial diluting part of the culture and plating on blood-agar. The remaining bacteria were centrifuged and immersed in 16% paraformaldehyde for 1 hour. Viability of the culture was determined after serial dilution, plating on blood-agar and incubating for 48 hours. It was confirmed there was no growth at 48 hours.

2.19 Cell culture model

2.19.1 Human mast cell line

The human mast cell (HMC-1) line was kindly donated by Dr J.H. Butterfield (Mayo Clinic, Rochester, Minn., USA). HMC-1 cells were maintained in 75cm^2 tissue culture flasks at 37°C/5% CO_2. Complete medium consists of Iscove's modified Dulbecco's medium (IMDM) (Gibco, Paisley, UK) supplemented with 25mM Hepes, sodium bicarbonate and L-glutamine, 10% calf serum and 1.2 mM alphathioglycerol (Sigma). The alpha thioglycerol and complete medium were freshly made once per week. Cell cultures were split when cell density reached 1.0-1.5x10^6 cells/ml. Following this, 2.0 x10^6 cells were seeded into a 12-well plate in 2ml of culture medium. The viability of cells was confirmed to

be 99% before the start of the stimulation. The HMC-1 culture was performed with the help of Dr Sylvia Pender and E Level laboratory staff.

2.19.2 Co-culture assay

There were 7 different treatment groups (Table 2.7) including live *S aureus* (*Section 2.18.1*) and non-viable *S aureus* (*Section 2.18.2*) at a multiplicity of infection (MOI 1:1) of 1 bacterium per HMC-1 cell, for two hours before lysostaphin (20 µg/ml) was added. Lysostaphin was added to eradicate extracellular bacteria after 2 hours, leaving only viable intracellular reservoirs.

TREATMENT GROUP	LYSOSTAPHIN	TREATMENT
Control	Yes	Cultured in RPMI alone for 24hrs
***S aureus* (live)**	Yes	Cultured with live *S aureus* for 24 hrs
***S aureus* (dead)**	Yes	Cultured with dead *S aureus* for 24 hrs
SEB	Yes	Cultured with SEB (10µg/ml) for 24 hrs
***S aureus* (live) & SEB**	Yes	Cultured with live *S aureus* & SEB for 24 hrs
***S aureus* (dead) & SEB**	Yes	Cultured with dead *S aureus* & SEB (10µg/ml) for 24 hrs
Lysostaphin	Yes	Cultured with Lysostaphin (10µg/ml) alone

Table 2.7 Treatment groups for HMC-1 cell co-culture assay

The first seven treatment groups were incubated (37.5°C, 5% CO_2) for a further 22 hours (24 hours total) and then fixed and processed with the Click-iT® EdU proliferation kit (*Section 2.19.2*.1). The other three 9-well plates were fixed for TEM at 2, 4 and 24hrs, respectively. Details of fixing and processing for TEM can be seen in Chapter 2, *Section 2.19.2.2*

2.19.2.1 Proliferation assay

The treatment groups were incubated at 37°C, 5% CO_2 for 24 hours. After incubation, each treatment group was centrifuged (11,000G) to separate the cells from the supernatant. The supernatant from each group was removed and stored at -20°C for future analysis. The remaining cells were fixed using the Click-iT® EdU proliferation kit. The Click-iT® EdU proliferation Kit directly measures DNA synthesis and therefore provides an accurate method of assessing cell proliferation. The Click-iT® EdU proliferation kit was used according to the instructions recommended by the manufacturer, as described in Chapter 2, *Section 2.19.2.1*. One million HMC-1 cells were added to each well and were incubated with EdU for 24 hours at 37°C 5% CO_2, before being fixed in 3.7% formaldehyde in PBS for fifteen minutes. After being rinsed twice with 3% bovine serum albumin (BSA) in PBS, 0.5% Triton® X-100 (permeabilisation buffer), PBS was added to the cells in each well and incubated at room temperature for 20 minutes. After further rinsing with 3% BSA in PBS the Click-iT® reaction cocktail (Click-iT® reaction buffer, CuSO4, Alexa Fluor®647 azide and reaction buffer additive) was added to each well for 30 minutes. After further rinsing the DAPI-488 (Sigma-aldrich®, Dorset, UK) stain was added to each well and the cells were imaged with confocal laser scanning microscopy (CLSM) after 30 minutes.

The total number of mast cells was counted using CLSM. Proliferation rates were calculated as a percentage of total number of cells (see equation below).

$$\textbf{Proliferation rate (\%)} = \frac{\textbf{Number of proliferating mast cells}}{\textbf{Total number of mast cells counted}} \textbf{ x 100}$$

2.19.2.2 *S aureus*$^{+ve}$ mast cell measurements

S aureus^{+ve} mast cells were identified using the CLSM on HMC-1 cells stained with the Click-iT® EdU proliferation kit and DAPI-488, as described above. Intracellular *S aureus* were easily identified within the HMC-1 cells. Five thousand cells were manually counted from each well and the proportion of *S aureus*$^{+ve}$ mast cells was presented as a percentage of the total number of cells (see below).

$$\text{Proportion of } \textit{S aureus}^{+ve} \text{ MC (\%)} = \frac{\text{Number of MC containing } \textit{S aureus} \text{ counted}}{\text{Total number of MC counted (5000)}} \times 100$$

2.19.2.3 Mast cell measurements

The diameter of 5000 HMC-1 cells was manually measured from each treatment group. One thousand cells were measured and assessed for intracellular *S aureus* from 5 separate randomly selected fields (totalling 5000). Analysis and measurements were undertaken using CLSM and the Leica Application Suite (LAS) AF software.

2.19.2.4 Transmission electron microscopy

The same treatment groups were replicated, but cells were fixed at 2, 4 and 24 hours with 3% glutaraldehyde and 4% formaldehyde in 0.1M PIPES for TEM. Processing and imaging for TEM was as described earlier.

2.19.3 Live *Staphylococcus aureus* for co-culture

S aureus (P3 strain) was grown in RPMI medium to a mid-log phase. Regular culture samples were taken, serially diluted and plated on blood agar. Regular optical density (OD) measurements were taken and plotted again CFU counts

(**Figure 2.3**). Using the linear regression graph, the number of bacteria was calculated per OD. The bacteria were centrifuged (11,200G for 5 minutes), washed with sterile PBS and diluted to the required concentration. The final concentration required was 1.0 x 10^6 bacteria per 20µl. This was added to 1.0 x10^6 HMC-1 cells per well (MOI 1:1).

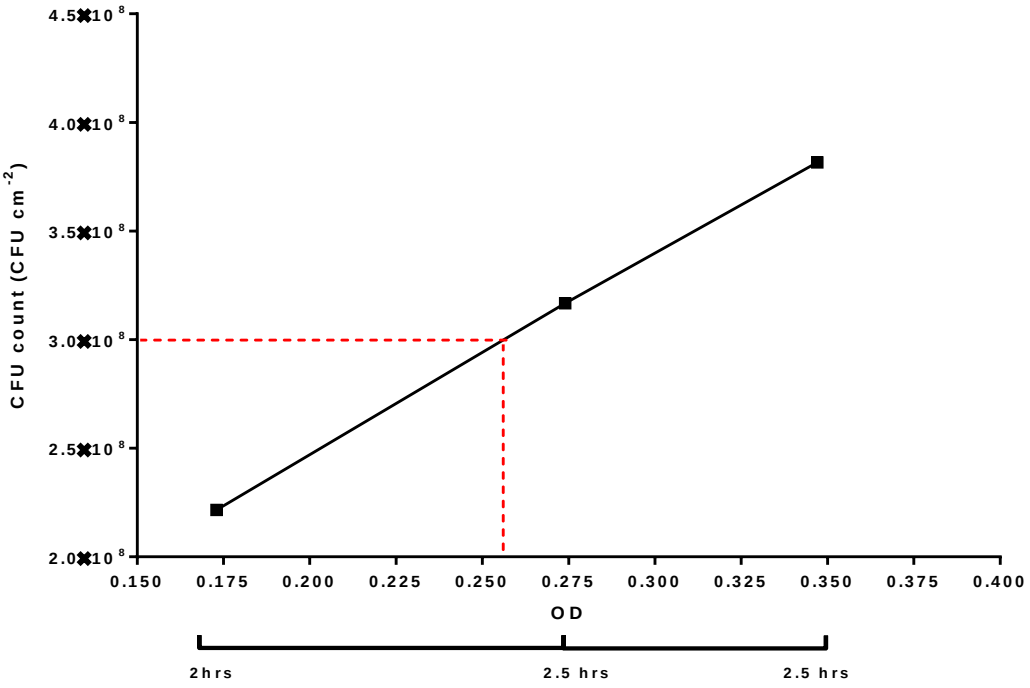

Figure 2.3 Linear regression for the CRS *S aureus* isolate P3

2.20 Statistical analysis

Statistical analysis was performed using Graph Pad Prism 6.0 software (Graph Pad Software Inc., San Diego, CA). Comparisons between clinical groups were made using either a one-sample *t*-test (when control means were zero) or a paired *t*-test (two-tailed) (when control means were not zero). The level of significance was accepted as a *p* value of less than 0.05. Statistical significance was represented on graphs using the star rating: NS = not significant, *p < 0.05, **p <0.001,***p <0.000.

3 Characterisation of bacterial biofilms in chronic rhinosinusitis

3.1 Introduction

Recent evidence has implicated surface-related bacterial biofilms in playing an active role in perpetuating the ongoing inflammatory process associated with chronic rhinosinusitis (CRS) (211). Biofilms are described as highly structured and antibiotic-resistant bacterial aggregates, consisting of highly organised communities of bacteria encased within an extracellular matrix (9, 198). Biofilms form as a result of aggregating planktonic bacteria which coalesce to surfaces within the human host as a strategy of survival within environments less than optimal for growth. These regions are often areas of high environmental stress and altered oxygen tension, such as the sinonasal cavities, where biofilms can protect bacteria from host defences and antimicrobial therapies. Intermittent dispersal of planktonic bacteria from the biofilms allows migration and re-colonisation and is thought to contribute to recurrent infective exacerbations in CRS (210, 212, 308).

Using a range of different microbial detection methods (212, 233, 240-242, 244, 308-309) bacterial biofilms have been demonstrated on the sinonasal mucosa from both CRS patients with and without nasal polyps (NP) (CRSwNP and CRSsNP, respectively). These include *S aureus, H influenzae, P aeruginosa,* and *M catarrhalis* (211, 242, 310-312). Biofilms on CRS sinonasal mucosa formed by *S aureus* and *P aeruginosa* are associated with more unfavourable post-operative course following functional endoscopic sinus surgery (FESS) (241, 244). *S aureus* biofilms have also been shown to foster a T_H2 cytokine immune response and also drive eosinophilia, both associated with NP formation (141).

Despite these associations, there remains little hard evidence that bacterial biofilms are directly or indirectly involved in initiating or driving the ongoing chronic inflammatory process that defines CRS, or whether they represent a harmless bacterial survival strategy, providing symbiotic benefits to both the host and the pathogen.

This chapter, therefore, aims to clarify these associations through further characterisation of CRS surface-related bacterial biofilms. This involves evaluating the presence, species and biology of CRS bacterial biofilms using the most advanced methods of microbial detection and analysis.

3.2 Methods

3.2.1 Subjects

Sixteen consecutive patients with CRS (CRS 1-16) and 5 control patients (CT 1-5) were recruited into the study as described in *Section 2.2*.

3.2.2 Tissue sampling

CRS and control tissue was obtained as described in *Section 2.4.*

3.2.3 Tissue analysis

- Thirteen CRS samples (n=13) were processed using the nucleic acid stain SYTO 9 (LIVE/DEAD® BacLight™ viability kit (*Section 2.5)* and imaged with confocal laser scanning microscopy (CLSM) (*Section 2.10*).
- Nine samples (n=9) were processed for scanning electron microscopy (SEM) (*Section 2.12*).
- Ten samples (n=10) were stained using fluorescent *in situ* hybridisation (FISH) (*Section 2.10*) and imaged with CLSM.
- Five control sinonasal mucosa samples (n=5) were processed for all of the above techniques.

3.2.4 Surface-related biofilm detection rate

The calculations to determine the Surface-related biofilm detection rate (SBDR) were described in full in Chapter 2, *Section 2.7.1*.

3.3 Results

3.3.1 Characteristics of datasets

A total of sixteen patients with CRSwNP and CRSsNP were included in the study cohort. This cohort was divided into three datasets, where tissue from each dataset was analysed using three different techniques. CRS sinonasal mucosa from thirteen patients (n=13) was processed using SYTO 9 and imaged with CLSM. The demographic data for this group (dataset 1) is shown in Table 3.1. CRS sinonasal mucosa from nine patients (n=9) was processed for SEM and the demographic data for this group (dataset 2) is shown in Table 3.2. CRS sinonasal mucosa from ten patients (n=10) was processed using FISH and imaged with CLSM. The demographic data for this group (dataset 3) is shown in Table 3.3.

A total of five control patients were included within the study and tissue from this group was processed for all of the above techniques. The demographic data for the control group are shown in Tables 3.1-3.3.

3.3.2 Patient demographics

The male to female ratio across datasets was evenly distributed. Within the literature, the prevalence of CRSwNP is higher in males and the prevalence of CRSsNP is higher in females. As this cohort is a mixture of patients with CRSwNP and CRSsNP, an equal distribution between the two sexes is a good reflection of the CRS population (313). The mean ages across datasets ranged from 40-45 years, which closely represents the true value from the CRS population (3). The prevalence of asthma ranged from 11% to 20% across datasets which was slightly less than the reported prevalence of 26% (314). Skin prick testing (SPT) was positive in between 11% and 20%, which was slightly higher than the reported prevalence of allergy in CRS of 10% (315). The prevalence of current smokers ranged from 23% to 40%, which is relatively high compared to the reported prevalence in the literature of 15% (316). This may represent the prevalence of smoking in the local area of recruitment. Patient with aspirin sensitivity were excluded from the study. The mean Lund-Mackay

Score (LMS) ranged from 15 to 16, indicating severe disease. As these patients were undergoing surgery due to failure of medical treatment, the high LMS were not surprising as they represent CRS patients with a more severe disease.

3.3.2.1 Control group

A total of five control patients were included in the study cohort. There was a mean age of 59 years, which was slightly higher than that seen in the CRS group. There were slightly more male than females, but with a ratio of three males to two females this was as close to the true population as possible with a sample number of five. The proportion of smokers was 20%, which closely represents the current UK population prevalence of 18.6% (317). No control patients suffered with asthma, had aspirin sensitivity or were positive for allergy on skin prick testing.

Characteristics	CRS	Control
Subject no.	13	5
Mean age (range)	45 (20-73)	59 (45-76)
Sex	7M/6F	3 M / 2F
CRSwNP	8	0
CRSsNP	5	0
Current smokers	3	1
Aspirin sensitivity	0	0
Asthma	2	0
Positive SPT	2*	0
Mean LMS (range)	16 (9-22)	0

Table 3.1 Demographics for patient dataset 1 (SYTO 9 (LIVE/DEAD® BacLight™ viability kit with CLSM). *Patient 1: tree, HDM; Patient 2: Indoor mould, HDM, cat & dog dander.

Characteristics	CRS	Control
Subject no.	9	5
Mean age (range)	41 (20-73)	59 (45-76)
Sex	5M/4F	3 M / 2F
CRSwNP	6	0
CRSsNP	3	0
Current smokers	3	1
Aspirin sensitivity	0	0
Asthma	1	0
Positive SPT	1*	0
Mean LM Score (range)	16 (10-22)	0

Table 3.2 Demographics for patient dataset 2 (SEM). *Patient 1: tree, HDM.

Characteristics	CRS	Control
Subject no.	10	5
Mean age (range)	40 (20-73)	59 (45-76)
Sex	5M/5F	3 M / 2F
CRSwNP	9	0
CRSsNP	1	0
Current smokers	4	1
Aspirin sensitivity	0	0
Asthma	1	0
Positive SPT	2	0
Mean LM Score (range)	15 (9-22)	0

Table 3.3 Demographics for patient dataset 3 (FISH with CLSM). *Patient 1: tree, HDM; Patient 2: Indoor mould, HDM, cat & dog dander.

3.3.3 Surface-related bacterial biofilms analysis

3.3.3.1 SYTO 9 with confocal laser scanning microscopy

Using the SYTO 9 nucleic acid stain combined with CLSM, bacterial biofilms were identified attached to the epithelial surface of the sinonasal mucosa in all thirteen CRS patients (100%) (Figure 3.1A-B). No bacteria biofilms were identified in any of the five control patients (Figure 3.1C).

3.3.3.1.1 Surface-related biofilm detection rate using SYTO 9 with confocal laser scanning microscopy

The mean SBDR for the CRS group was 0.89 and for the control group was 0 (p=0.0001, Table 3.4). Higher SBDRs were associated with a worse LMS as patients with a SBDR of 1.0 had significantly higher LMS than those patients with a SBDR <1.0. (p=0.003).

3.3.3.1.2 Limitations of SYTO 9 with confocal laser scanning microscopy

Using the nucleic acid stain SYTO 9 on unfixed, fresh tissue samples followed by imaging with CLSM has been very successful in identifying the presence of surface-related bacterial biofilms in CRS sinonasal mucosa (SBDR 0.89). However, this technique is limited in its ability to provide any morphological information to help characterise these bacterial biofilms and these limitations are well documented within the literature (9).

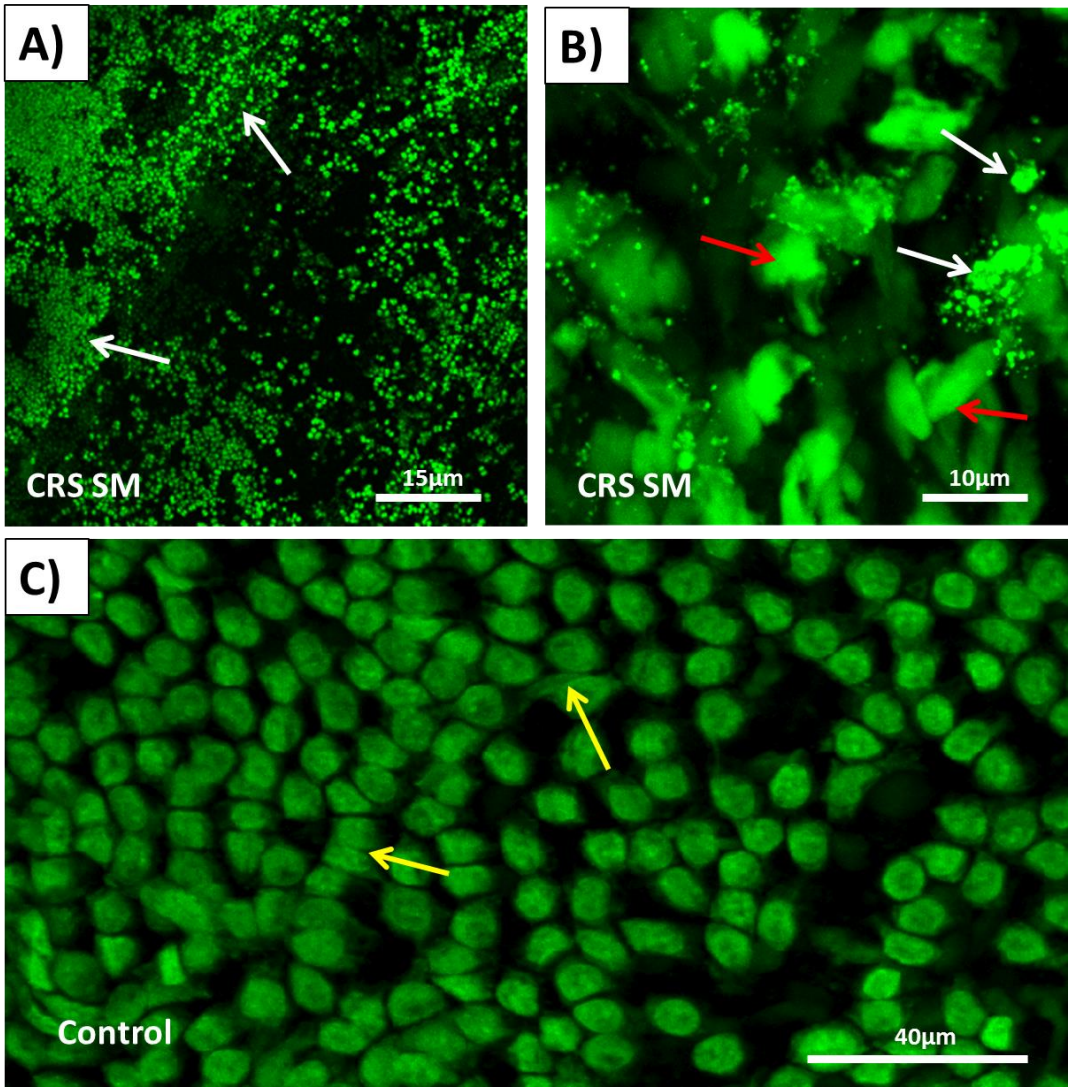

Figure 3.1 Surface-related bacterial biofilms on CRS sinonasal mucosa and control tissue. (A & B) Representative CLSM images of CRS sinonasal mucosa showing viable aggregates of bacteria (biofilms) (white arrows) attached to the underlying surface epithelium (red arrows). (C) Representative CLSM images of control sinonasal mucosa showing epithelial cells (yellow arrows) with no evidence of any associated bacterial biofilms.

Study no.	CRS Group			Lund-Mackay Score (LMS)
	SBDRs			
CRS 1	1.0			22
CRS 2	1.0			19
CRS 3	1.0			18
CRS 4	0.8			15
CRS 5	0.8			12
CRS 6	1.0			19
CRS 7	0.8			17
CRS 8	0.6			9
CRS 9	1.0			15
CRS 10	0.8			15
CRS 11	1.0			16
CRS 12	1.0			18
CRS 13	0.8			13
Total (%)	**100%**			
Mean	**0.89**			**16.7**
***p*-value**	**0.0001**			
CI	**0.81 to 0.97**			
	Control Group			
CT 1	0.0			0
CT 2	0.0			0
CT 3	0.0			0
CT 4	0.0			0
CT 5	0.0			0
Mean	0.0			**0**

Table 3.4 Surface-related biofilm detection **rates** (SBDRs) for chronic rhinosinusitis sinonasal mucosa and control tissue using SYTO 9 with confocal microscopy. (*p*-value represents chronic rhinosinusitis group compared to controls)

3.3.4 Scanning electron microscopy

Using SEM, surface-related bacteria biofilms were identified on the sinonasal mucosa in all nine CRS patients (100%) (Figure 3.2A-B). No bacterial biofilms were identified on any of the five control patients (Figure 3.2C). The morphology of the bacteria forming biofilms was assessed and classified into either *cocci* or *bacilli*-shaped microbes. Biofilms composed of *cocci*-shaped bacteria were identified attached to 89% of the CRS samples (Table 3.5). Biofilms composed of *bacilli*-shaped bacteria were identified attached to 33% of the CRS samples. In 22% of the samples, biofilms were composed of both *cocci* and *bacilli*-shaped bacteria, representing polymicrobial biofilms.

3.3.4.1 Surface biofilm detection rate using scanning electron microscopy

The mean SBDR for the CRS group was 0.47 and for the control group was 0. A significant difference between these groups was observed (p=0.004, Table 3.5).

Study no.	CRS Group			Control Group
	SBDR	*Cocci*	*Bacilli*	BDR
CRS 3	0.6	+	-	0
CRS 5	0.6	+	-	0
CRS 6	0.6	-	+	0
CRS 7	0.4	+	-	0
CRS 9	0.2	+	+	0
CRS 10	0.6	+	-	
CRS 13	0.2	+	+	
CRS 14	0.6	+	-	
CRS 15	0.4	+	_	
Total (%)	**100%**	**8 (89%)**	**3 (33%)**	**0**
Mean	**0.47**			**0**
***p*-value**	**0.004**			
CI	**0.15 to 0.69**			

Table 3.5 SBDR for CRS sinonasal mucosa and control tissue using SEM. (p-value represents CRS group compared to controls)

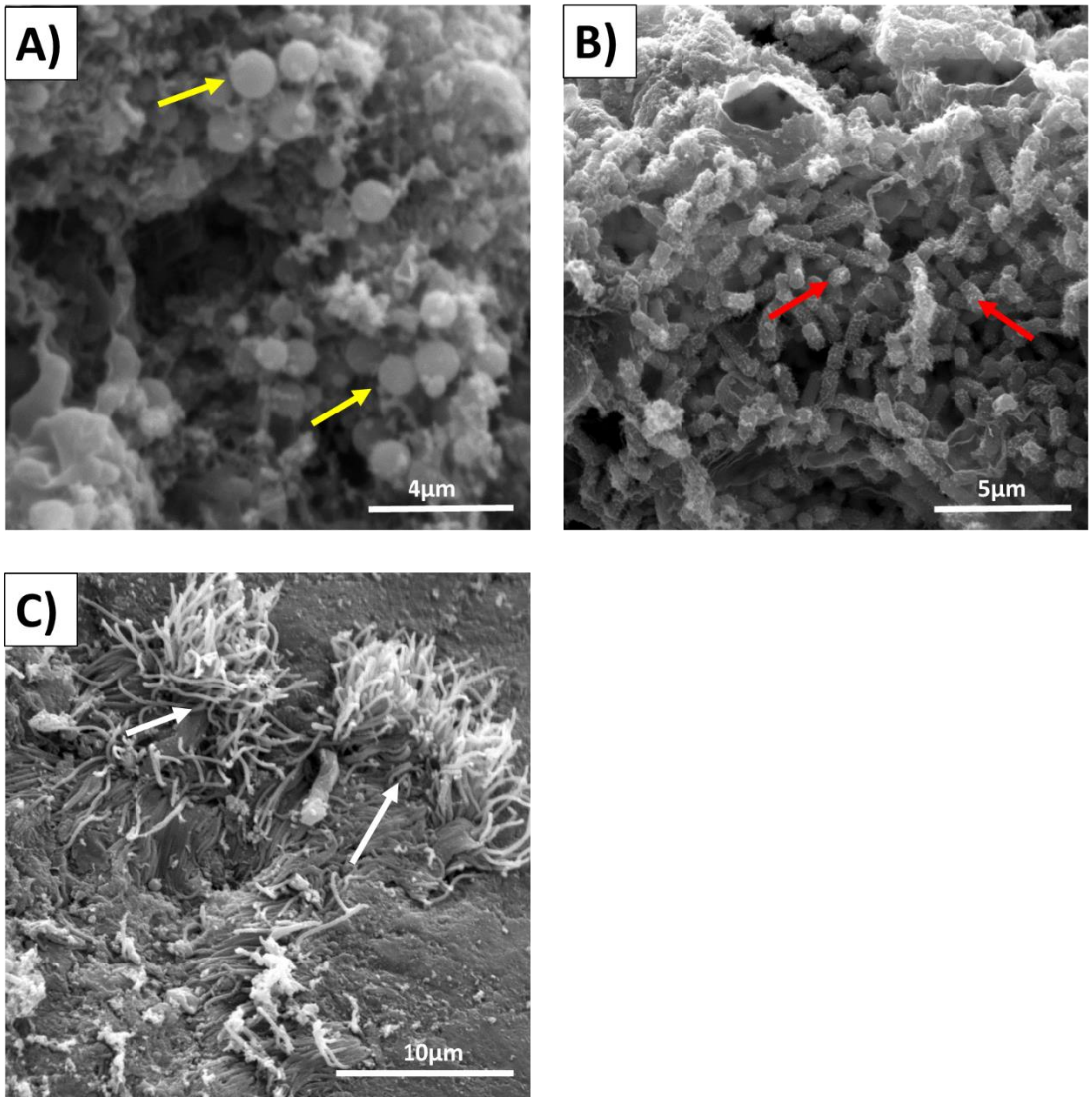

Figure 3.2 Scanning electron microscopy (SEM) images of sinonasal mucosa. *(*A) Representative SEM image of CRS sinonasal mucosa showing aggregates of cocci bacteria as biofilms (yellow arrows) attached to the epithelial surface. (B) Representative SEM image of CRS sinonasal mucosa showing aggregates of bacilli bacteria as biofilms (red arrows) attached to the epithelial surface. (C) Representative SEM image of control sinonasal mucosa showing normal surface mucosa with cilia (white arrows) and no evidence of any bacterial biofilms.

3.3.5 Fluorescence *in situ* hybridisation with confocal laser scanning microscopy

After hybridisation with 16S rRNA FISH probes and imaging with CLSM, surface-related bacterial biofilms were identified in all ten CRS samples (100%) (Table 3.6, Figure 3.3). No bacterial biofilms were observed in any of the five control patients (Table 3.6, Figure 3.3).

3.3.5.1 The surface-related biofilm detection rate

S aureus was identified as the commonest biofilm-forming microbe (Table 3.6). Surface-related biofilms composed of *S aureus* were identified on 70% of CRS sinonasal mucosa with a mean SBDR of 0.42 (p=0.007, Table 3.6). *P aeruginosa* and *H influenzae* biofilms were both identified in 30% of CRS patients. *P aeruginosa* had a mean SBDR of 0.14 and *H influenzae* had a mean SBDR of 0.16, both of which showed no significant difference from the control group (p=0.042 and p=0.057, respectively). Higher *S aureus* SBDR correlated with higher LMS. A *S aureus* SBDR above 0.8 had a mean LMS of 19.6, whereas a SBDR less than 0.8 had a LMS of 13.6. Due to the small number of samples, this was not shown to be statistically significant. Nevertheless, there was an observed trend suggesting the more extensive the biofilms, the worse the LMS. Polymicrobial biofilms when *S aureus* was present appeared to have the worst SBDR and LMS.

Patient no.	*S aureus*	*P aeruginosa*	*H influenzae*	LMS
CRS Group	**SBDR**	**SBDR**	**SBDR**	
CRS 7	0.2	0.0	0.0	15
CRS 8	0.6	0.0	0.0	17
CRS 9	0.0	0.4	0.2	10
CRS 10	0.6	0.0	0.0	15
CRS 11	0.0	0.4	0.6	12
CRS 12	0.2	0.0	0.0	13
CRS 13	0.8	0.0	0.0	18
CRS 14	1.0	0.6	0.8	22
CRS 15	0.0	0.0	0.0	9
CRS 16	0.8	0.0	0.0	19
Total (%)	**70%**	**30%**	**30%**	
Mean	**0.42**	**0.14**	**0.16**	**15**
***p*=value**	**0.007***	**0.088**	**0.121**	
95% CI	**0.15 to 0.69**	**-0.03 to 0.31**	**-0.05 to 0.37**	
Control Group				
CT 1	0.0	0.0	0.0	0
CT 2	0.0	0.0	0.0	0
CT 3	0.0	0.0	0.0	0
CT 4	0.0	0.0	0.0	0
CT 5	0.0	0.0	0.0	0
Mean	**0.0**	**0.0**	**0.0**	**0**

Table 3.6 Surface-related biofilm detection rate (SBDR) for each bacteria-forming microbial species identified using FISH and CLSM. *Statistical significance of $p<0.05$.

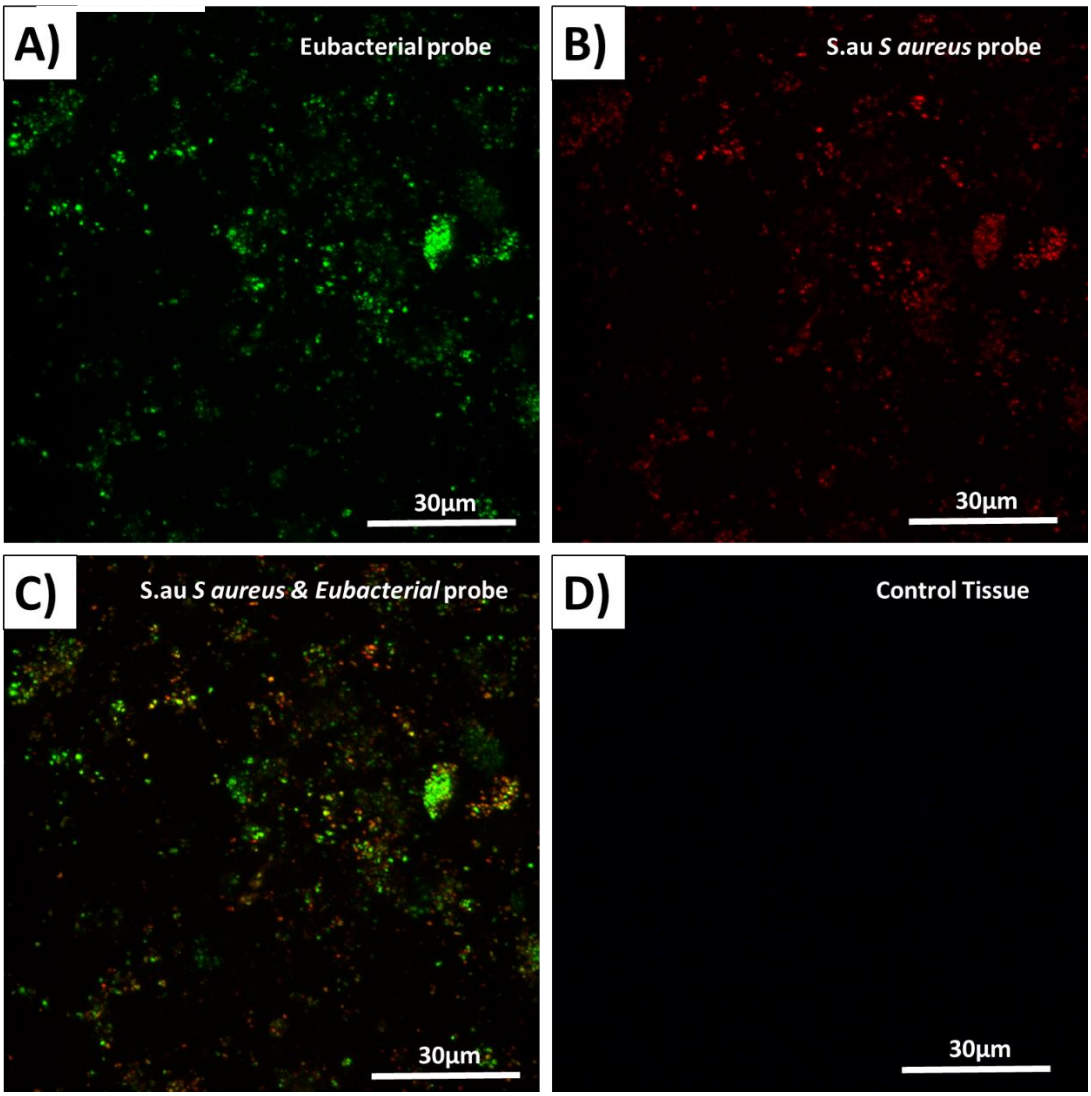

Figure 3.3 Surface-related bacterial biofilms on chronic rhinosinusitis sinonasal mucosa. Representative confocal microscopy images of chronic rhinosinusitis sinus mucosa and control tissue hybridised with 16S rRNA Eubacterial (E338) (A) and *S aureus* (S.au) (B) probes. (C) Combined S.au and Eub338 16S rRNA probes showing *S aureus* (yellow & light green) attached to the surface epithelium. (D) Control tissue stained with S.au and Eub338 16S rRNA probes showing no bacteria.

3.4 Discussion

Using the most up to date biofilm detection methods (9, 215), the current findings confirm the existence of surface-related bacterial biofilms attached to the epithelial surface of CRS sinonasal mucosa in both CRSwNP and CRSsNP. This is consistent with other studies within the literature (211, 239, 240, 242, 248, 318-319).

The use of the nucleic acid stain SYTO 9 combined with CLSM was a simple and highly effective technique for detecting bacterial biofilms, but was limited in providing adequate morphological detail. Tissue analysis using SEM validated the SYTO 9 findings and provided more detailed information on biofilm and epithelial morphology, enabling characterisation of the aggregated bacteria into *cocci* and *bacilli* groups. The dominant bacteria identified forming the biofilms were *cocci* which was consistent with the literature (249, 320).

FISH with CLSM further validated the SYTO 9 and SEM findings and identified *S aureus* as the most commonly identified biofilm-forming microbe, in keeping with other studies (249-250). *S aureus* colonises the sinonasal cavities in 27% of patients with CRSsNP and 60% of patients with CRSwNP (36). *S aureus* biofilm-formation within the sinonasal cavity is thought to be facilitated by defects within the immune barrier (158). The 'immune barrier hypothesis' proposes that coordinated defects in the physical barrier as well as a manipulated innate immune system at the host-environment interface, leads to a weakened and altered epithelial layer, allowing *S aureus* biofilms to adhere and reside (320). The release of superantigens (SAgs) from *S aureus* biofilms leads to further manipulation of the innate immune system through direct and indirect activation of host cells (97, 98). The net effect represents a *S aureus* survival strategy adapted to evade both host defences and antibacterial therapies to prolong survival.

FISH with CLSM also identified biofilms formed by *H influenzae* and *P aeruginosa*. also consistent with the literature (211, 242, 310-312). Although identified in 33% of samples, no statistical significance was found when compared to controls due to a low SBDR. With a larger sample population this is likely to become significant. This was, however, beyond the scope of this study but should be considered for future work.

Interestingly, a correlation between LMS and the SBDR was demonstrated. The higher the rate of detected biofilms, the higher the LMS. This is in keeping with recent studies that have demonstrated significantly higher LMS in biofilm-positive patients compared to biofilm-negative patients (244, 246, 254). This was particularly relevant to *S aureus* biofilms, which were also demonstrated to have more unfavourable post-operative outcomes and persistent disease compared to non-*S aureus* biofilm mediated disease (244). LMS represents a radiological severity score and is an objective assessment of severity. More extensive biofilms would suggest multi-sinus cavity involvement and therefore, worse radiological findings. A polymicrobial biofilm, including *S aureus*, *H influenzae* and *P aeruginosa,* was associated with the worst LM score in the CRS group.

All 3 techniques were consistent in identifying the absence of bacterial biofilms in any of the control samples. This is in keeping with the literature (212, 233, 240, 244, 248, 252, 253). It is well established that the sinonasal cavity in a normal individual contains an extensive microbial network of normal nasal flora. However, all tissue samples were rinsed prior to processing to remove all planktonic bacteria and weakly adhered biofilms. This would explain the lack of bacteria observed in any of the control groups. This also confirms that the biofilms detected on CRS sinonasal mucosa were strongly adherent and would therefore be resistant to treatments, such as nasal douching. The abundance of bacterial biofilms detected on the CRS sinonasal mucosa, in comparison with the lack of bacterial biofilms seen on control tissue, suggests their existence is pathogenic and likely to be contributing to the ongoing chronic inflammatory process.

Using SEM, bacterial biofilms were identified on the sinonasal mucosa of all patients with CRS. Despite this, the overall detection rate was lower than that seen previously using the technique of SYTO 9 with CLSM. This lower detection rate may be due to biofilm erosion as a consequence of the extensive processing method required for SEM processing, or difficulties with biofilm detection, which is clearer using fluorescence. However, SEM allowed detailed morphological analysis of these surface-related biofilms, enabling characterisation into *cocci* or *bacilli*.

The combination of FISH with CLSM allows identification of species-specific biofilms on sinonasal mucosa, making it the gold standard technique in biofilm detection in CRS tissue (215). FISH probes are 100% sensitive and 100% specific. However, the limitation of this technique lies in its inability to identify multiple strains of bacteria on the same tissue sample at the same time. Three specific 16S rRNA FISH probes were utilised to specifically detect *S aureus*, *H influenzae* and *P aeruginosa* as they represent the most frequently identified pathogens in CRS tissue, as reported within the literature. However, the non-specific *Staphylococcus* genus probe identified a few bacterial colonies that did not hybridise with the *S aureus* probe and may therefore represent another *Staphylococcus* species, most likely Coagulase negative *Staphylococcus*. Therefore, the use of a limited number of 16S rRNA FISH probes limits the range of bacterial species detection. Nevertheless, the species sampled in this study are the most commonly reported in association with CRS and are therefore likely to be most relevant to the disease process.

The role of polymicrobial biofilms remains unclear. Within this study 22% of samples imaged with SEM showed a mixture of bacilli and cocci species. Using FISH, 30% of samples contained polymicrobial biofilms. The polymicrobial biofilm containing *S aureus* was taken from a patient with the highest LM score, consistent with the literature. *H influenzae* was only present in a polymicrobial biofilm and was always identified together with *P aeruginosa*, which goes against other studies. Due to small numbers of polymicrobial biofilms identified within this study, it is difficult to make any clear conclusions regarding their relevance. More studies are required to further characterise these polymicrobial biofilms and explore the interspecies relationships.

3.5 Conclusion

Using a range of advanced microbial detection techniques, surface-related bacterial biofilms were observed on the sinonasal mucosa of patients suffering with CRS, as compared to controls. The biofilm load correlates with the radiological severity scores, suggesting that biofilms are involved in the disease process. *S aureus* appears to be the commonest biofilm forming microbe. Its ability to manipulate the host immune system through the release of toxins as a survival strategy requires further investigation.

4 Investigation of the effect of low dose nitric oxide on chronic rhinosinusitis - related bacterial biofilms

4.1 Introduction

Evidence of surface-related bacterial biofilms in chronic rhinosinusitis (CRS) patients has been provided. These sinonasal bacterial biofilms are associated with a poor post-operative outcome (244). Bacteria within a biofilm state represent a significant challenge to the medical profession due to their resistance to medical treatment and host defences. In contrast, bacteria in a free-floating planktonic state appear to be much more vulnerable to antimicrobial therapy. It is in the final stage of the biofilm cycle that biofilms disperse into planktonic bacteria, in an attempt to form new colonies and spread. Therefore, the development of novel therapies with the ability to induce biofilm dispersal could serve as an adjunct to antimicrobial treatment, with the aim of eradicating these biofilms.

One such proposed novel therapy is nitric oxide (NO). NO is an endogenously produced neurotransmitter that has been demonstrated to disperse *P aeruginosa* biofilms at nanomolar, non-toxic concentrations *in vitro* (297) through interaction with phosphodiesterase, thus decreasing intracellular cyclic di-GMP levels and triggering cellular dispersal (300). Gene expression studies have also demonstrated upregulation of genes associated with motility and downregulation of adhesin-associated genes (300). Current work within the University of Southampton Biofilm Group has focused on *in vitro* and *ex vivo* laboratory evaluation of NO in *P aeruginosa* biofilms from patients with cystic fibrosis (CF). The group demonstrated that low-dose NO disperses *P aeruginosa* biofilms into planktonic bacteria increasing its sensitivity to antibacterial therapy (322).

The commonest biofilm-forming species in CRS are *S aureus*, *H influenzae* and *P aeruginosa* (212). Our results are in agreement and suggest the commonest biofilm-forming bacteria are *S aureus* (70%), followed by *H influenzae* (30%) and *P aeruginosa* (30%). A study characterising the microbial diversity in CRS using Terminal Restriction Fragment Length Polymorphism (T-RFLP) profiling found that *P aeruginosa* was the most commonly detected species (90). Although the effects of NO on *S aureus* and *H influenzae* are unknown, evidence suggests a strong effect on *P aeruginosa* and therefore NO may have potential as a novel biofilm-targeted

therapy as a means of dispersing biofilms and increasing their susceptibility to antimicrobial therapy.

4.2 Methods

4.2.1 Pilot study

To test the study feasibility and to optimise the protocol for surface-related bacterial biofilm dispersal using NO, a pilot study was performed using CRS sinonasal mucosa obtained intraoperatively from two patients (CRS17-18) (n=2) undergoing functional endoscopic sinus surgery (FESS). Tissue was obtained from the middle meatus and transferred immediately on ice to the Wellcome Trust Clinical Research Facility for processing. A full description of the method is described in Chapter 2, *Section 2.14*.

4.2.1.1 Pilot study results

The results for the four treatment groups are displayed in Table 4.1. The results from this pilot study demonstrated very low CFU counts after 48 hours' incubation. These counts were too low to make any conclusions regarding the capabilities of NO to disperse CRS biofilms. These findings may be due to tissue sampling errors and difficulties with biofilm growth. To address this, the following was undertaken:

1. Multiple biopsies were obtained from different regions within the sinonasal cavity and CFU counts assessed after 48 hours.
2. Amplification of the surface-related bacterial biofilms through a pre-treatment culture.

	Group	CRS 17 CFU count (cm^2)	CRS 18 CFU count (cm^2)
1	Control	25	10
2	Antibiotic	10	10
3	Sodium Nitroprusside (SNP)	0	0
4	Antibiotic + SNP	0	0

Table 4.1 Pilot study CFU counts

4.2.1.2 Tissue sampling

Perioperative tissue samples were taken from the uncinate process, middle meatus and ethmoid bulla (Figure 1.3, Chapter 1) from two patients with CRS undergoing FESS (CRS 19-20) (n=2). Each tissue specimen was divided into 20g sections and each placed in Roswell Park Memorial Institution (RPMI) or Brain Heart Infusion (BHI) broth and incubated at 37°C/5% CO_2 for eighteen hours. After eighteen hours, the tissue was removed from the culture mediums and rinsed three times to remove any planktonic bacteria. The specimens were then homogenised, serially diluted and plated on blood, chocolate and CFC *Pseudomonas*-specific agar plates and incubated at 37°C (5% CO_2) for a further forty-eight hours.

4.2.1.2.1 Tissue sampling results

Inspection of the tissue culture mediums after incubation for eighteen hours showed the uncinate process to produce the most turbid broth, suggesting high bacterial concentrations. This finding was similar in both CRS patients. CFU counts were higher on blood agar plates compared to chocolate agar plates. Blood agar CFU counts for each tissue and culture medium are displayed in Table 4.2**.** No bacteria grew on the CFC *P aeruginosa*-specific agar plates after 48 hours.

These results suggest that the uncinate process and the ethmoid bulla contain the most consistent and highest concentration of bacteria in biofilms when compared to the middle meatal mucosa. This is consistent with recent literature (255). There was little difference in CFU counts between RPMI and BHI.

	BHI CFU counts (cm^2)		**RPMI CFU counts (cm^2)**	
CRS Tissue	**CRS 19**	**CRS 20**	**CRS 19**	**CRS 20**
Middle meatus	1×10^3	1×10^2	1×10^3	1×10^2
Uncinate process	1×10^6	7×10^6	2×10^7	4×10^7
Ethmoid bulla	4×10^4	6×10^4	4×10^4	1×10^4

Table 4.2 CFU counts for each tissue type and culture medium

4.2.1.3 Biofilm amplification

There was a significant increase in the size of the surface-related bacterial biofilms before and after culture with RPMI. Figure 4.1 shows sinonasal mucosa imaged before and after treatment with RPMI for eighteen hours. RPMI appeared to have successfully amplified the bacterial biofilms.

4.2.1.4 Tissue viability

The viability of the CRS mucosa before and after treatment with RPMI and BHI was assessed as described in *Section 2.5*. Analysis revealed minimal change in the epithelial cell viability after eighteen hours' culture with RPMI (Figure 4.2A). An increase in non-viable epithelial cells was demonstrated after eighteen hours' culture with BHI (Figure 4.2B).

4.2.1.5 Bacterial identification

The identification of bacterial isolates is described in *Section 2.14.3.1*

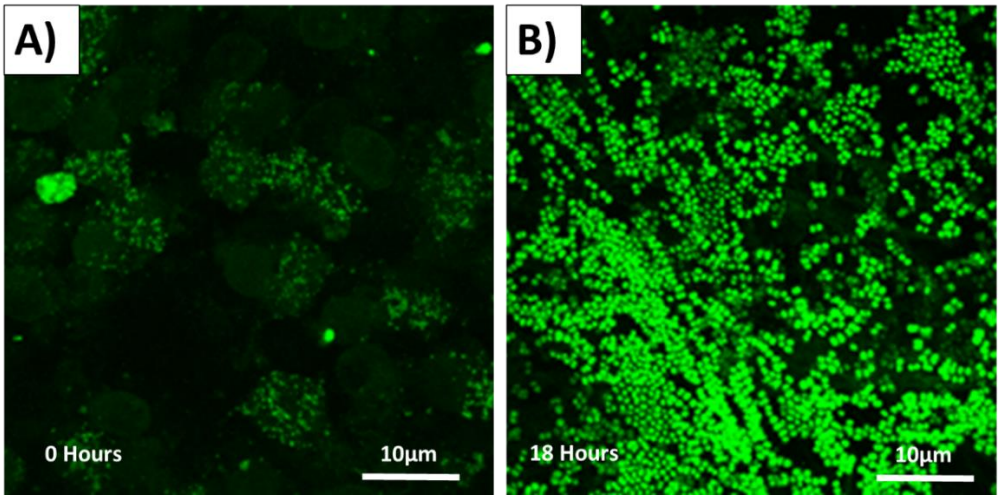

Figure 4.1 Surface-related bacteria biofilm amplification using RPMI. Representative CLSM image of CRS sinonasal mucosa, stained with SYTO 9 / propidium iodide nucleic acids, and imaged at 0 hours (A) and at eighteen hours (B) in RPMI culture medium. The green fluorescent stain shows viable

bacteria aggregated together within a biofilm. These images show that RPMI significantly amplifies the biofilm size after eighteen hours.

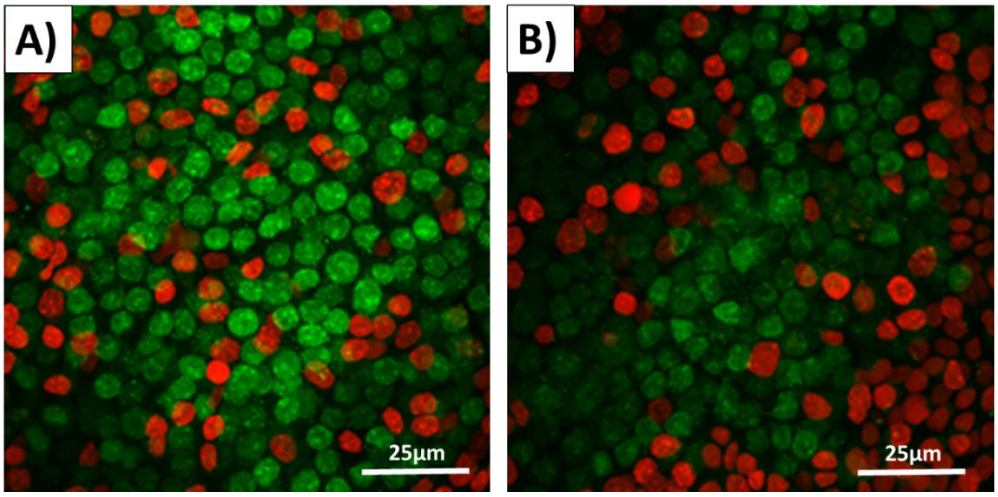

Figure 4.2 CRS epithelial cell viability after RPMI and BHI culture. Representative CLSM images of CRS sinonasal mucosa after an eighteen hour culture with (A) RPMI and (B) BHI. Tissues have been processed with a LIVE/DEAD® BacLight™ viability kit. The nucleic acid SYTO 9 stains all viable cells green and propidium iodide stains non-viable or damaged cells red. There is an increased number of non-viable cells (red) after eighteen hours of treatment with BHI compared with RPMI.

4.2.2 Optimisation of pilot study protocol

These experiments demonstrated that the bacterial biofilms are more consistent and in higher concentrations on uncinate process mucosa compared to other regions within the sinonasal cavity. RPMI was demonstrated to amplify existing bacterial biofilms over eighteen hours without affecting the viability of the host epithelial cells. The original pilot study method could now be repeated with the modifications of using uncinate process mucosa and culturing the tissue in RPMI for eighteen hours, before adding the assigned treatments.

4.3 Results

4.3.1 Characteristics of datasets

A total of four patients with CRS (CRS 21-24) and one control patient (CN 6) undergoing trans-sphenoidal pituitary surgery at UHSFT were included in the study cohort.

4.3.2 Patient demographics

Patient demographics are presented in Table 4.3. Despite the small sample numbers, which will create a high variance, the demographics of this group closely represent the published sample values. Only one control sample was obtained for comparison.

Characteristics	CRS (21-24)	Control (CN 6)
Subject no.	4	1
Mean age (range)	47 (41-52)	47
Sex	2M/2F	M
CRSwNP	2	0
CRSsNP	2	0
Current smokers	0	0
Aspirin sensitivity	0	0
Asthma	2	0
Positive SPT	0	0
Mean LM Score (range)	19.3 (15-24)	0

Table 4.3 Demographic data for the study population

4.3.3 Surface-related bacterial biofilm dispersal using the nitric oxide donor sodium nitroprusside

The CFU counts for each patient are displayed in Table 4.4. *S aureus* was cultured from all the CRS samples (n=4). The *S aureus* results are displayed in Figure 4.3. There was no significant reduction in *S aureus* CFU counts between the control group and the three other treatment groups (p=0.852, p=0.646, p=0.701, respectively, Figure 4.3).

Coagulase-negative *Staphylococcus*, *P aeruginosa* and *H influenzae* were cultured in 25% of samples. However, due to only being detected once, statistical analysis on these microbes was not possible. These results are displayed in Figures 4.4-4.6. The results for *P aeruginosa* appeared to show a reduced CFU count with antibiotics and SNP treatment (Figure 4.6), but this needs further confirmation with a larger sample size.

Polymicrobial biofilms were identified in 50% of samples and always included *S aureus*. No bacteria were cultured from the control tissue. The CFU counts for each patient are displayed in Table 4.4.

	Bacteria detected	CFU Count for each treatment group (CFU cm^2)			
		Control	Antibiotic	SNP	SNP & Antibiotic
CRS Group		**1**	**2**	**3**	**4**
CRS 21	*S aureus*	1.0×10^7	1.0×10^7	2.0×10^7	1.0×10^7
	H influenzae	3.0×10^7	3.0×10^7	3.0×10^7	1.0×10^7
	P aeruginosa	1.0×10^7	1.0×10^7	2.0×10^5	8.0×10^3
CRS 22	*S aureus*	1.2×10^6	3.1×10^5	2.0×10^6	1.05×10^6
CRS 23	*S aureus*	1.0×10^6	1.5×10^5	1.0×10^6	5.0×10^5
	Coagulase-negative *Staphylococcus*	8.0×10^5	1.2×10^5	8.0×10^5	1.3×10^5
CRS 24	*S aureus*	9.0×10^5	5.0×10^4	2.3×10^5	1.7×10^5
Control Group					
CN6	-	0	0	0	0

Table 4.4 CFU count profile in CRS and control groups after 48 hours culture. (CFU, Colony forming units: SNP, sodium nitroprusside)

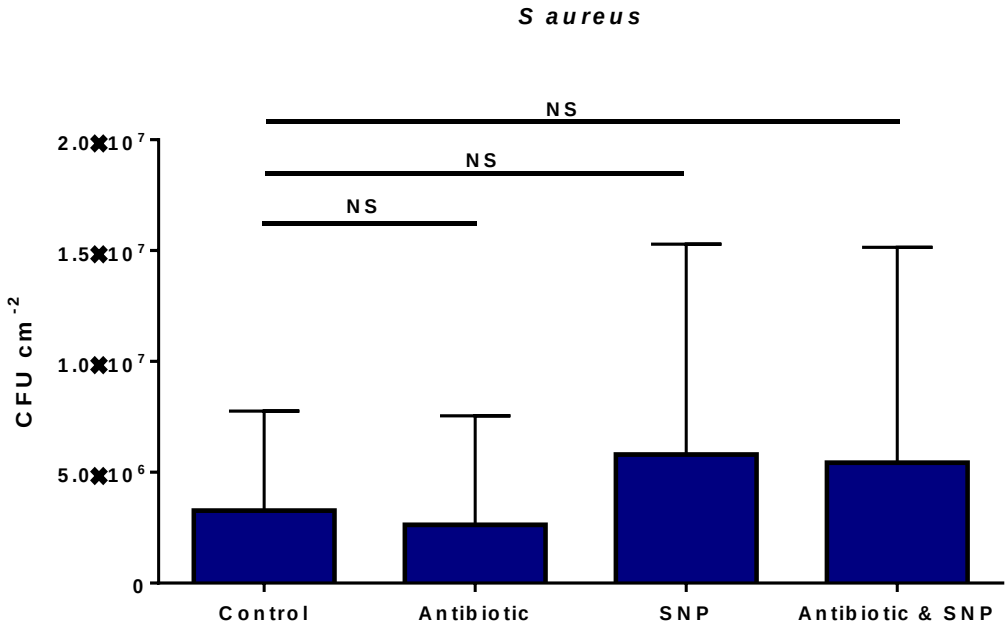

Figure 4.3 *S aureus* treatment groups (n=4) group. The CFU count for *S aureus* for each treatment group. No statistical significance was identified between any of the treatment groups when compared to the control group. Results are pooled data from 4 independent experiments (n=4). Error bars represent the means + 1SD. NS not significant. CFU, Colony forming units: SNP, sodium nitroprusside.

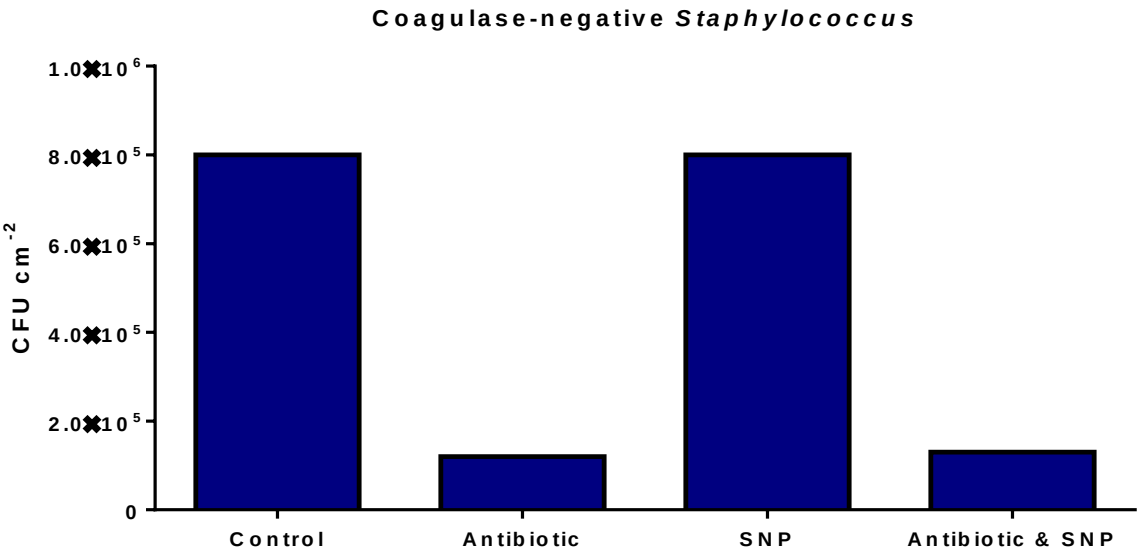

Figure 4.4 Coagulase negative *Staphylococcus* treatment group (n=1). CFU, Colony forming units: SNP, sodium nitroprusside.

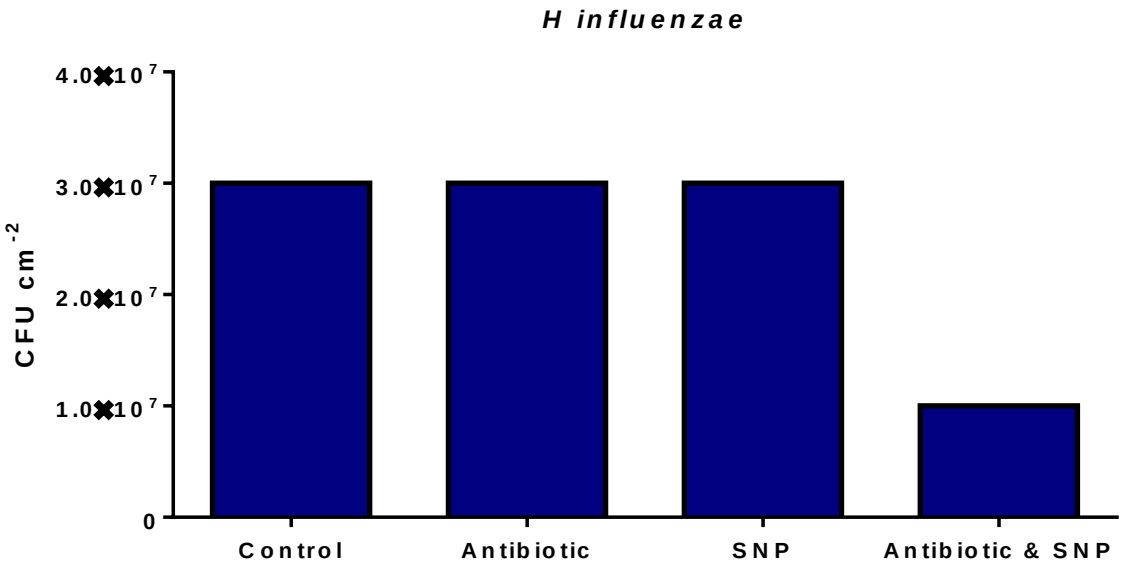

Figure 4.5 *H influenzae* treatment group (n=1). CFU, Colony forming units: SNP, sodium nitroprusside.

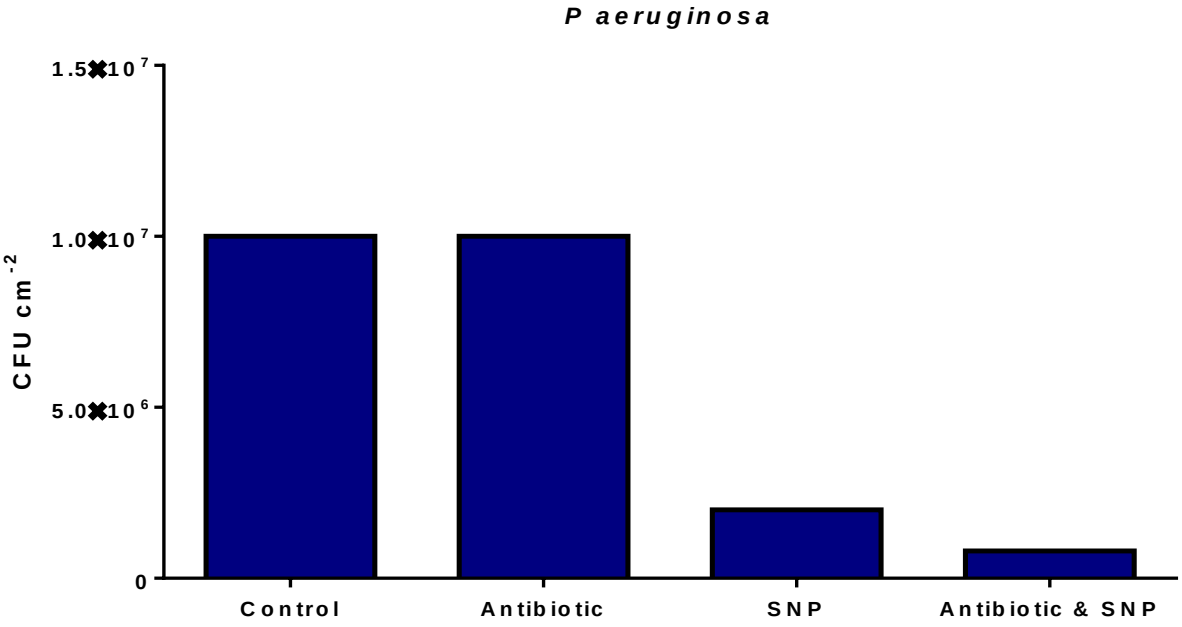

Figure 4.6 *P aeruginosa* treatment group (n=1). A reduction in CFU counts was observed for the SNP group and the antibiotics & SNP group compared to the control group. However, as *P aeruginosa* was only present in one sample, statistical analysis was not possible. CFU, Colony forming units: SNP, sodium nitroprusside.

4.4 Discussion

Studies have demonstrated *in vitro* the ability of the NO donor, SNP, to disperse *P aeruginosa* biofilms into free-floating planktonic bacteria (297, 299). Losing the protective mechanisms provided by the biofilm and extracellular matrix, planktonic bacteria become vulnerable to antibacterial therapy and host defences.

As this was the first study to use SNP on *ex vivo* CRS tissue samples, a pilot study was performed to assess study feasibility and to test the protocol. Initial pilot results demonstrated very low CFU counts in all treatment groups, too low to show any significant treatment effect. This may be explained by the difficulty in culturing bacterial biofilms, a well-documented biofilm characteristic. Modifications were made to the protocol, including improvements in tissue sampling and amplification of surface-related bacterial biofilms prior to treatment. Sampling analysis identified the uncinate process as possessing the most extensive surface-related bacterial biofilms and a pre-treatment culture of samples in RPMI resulted in biofilm amplification without changes to epithelial viability.

S aureus was the commonest microbe identified, having been cultured from all CRS samples studied. SNP did not appear to induce significant disruption of *S aureus* biofilm. In fact, the opposite effect was observed with a small non-significant increase in biofilm mass. This is consistent with a recent study, which demonstrated enhanced formation of CRS-related *S aureus* biofilms using low-dose concentrations of NO, similar to the levels used in this study (308). Reductions in the biomass of *S aureus* biofilms were only observed when using high, toxic concentrations of NO (323).

P aeruginosa, H influenzae and coagulase-negative *Staphylococcus* were identified in only 25% of samples, similar to the results in Chapter 3. However, in the one sample where *P aeruginosa* was isolated and cultured, CFU counts were reduced in the combined SNP and antibiotic group, suggesting a treatment effect. This effect was not unexpected as dispersal of *P aeruginosa* biofilms has been demonstrated previously *in vitro* (297) and in the lungs of

patients with cystic fibrosis (CF) (322). However, the effect of SNP on *P aeruginosa* biofilms on CRS sinonasal mucosa has not been previously documented. Unfortunately, due to the low sample number, statistical analysis was not possible. With larger sample sizes, this result may have been statistically significant. *P aeruginosa* biofilms have a high prevalence in CF-related CRS. Investigating the dispersal of CRS sinonasal *P aeruginosa* biofilms in the CF population would be an interesting future study to investigate the potential for SNP to be developed as an adjuvant biofilm-targeted therapy alongside antibiotics in the treatment of CF-related CRS.

4.5 Conclusion

Despite the limitations of a small sample size, the results suggest that SNP has no significant dispersal effect on CRS-related *S aureus* biofilms. On the basis of this preliminary data, it was decided not to proceed any further and to focus efforts on more detailed characterisation of the bacterial profiles of relevance to the disease process in CRS.

5 Investigation of the role of bacteria in the pathogenesis of nasal polyps

5.1 Introduction

In the UK, approximately 20% of patients suffering with chronic rhinosinusitis (CRS) develop nasal polyps (NP) (3). Despite many proposed mechanisms (3, 97, 98, 110, 140, 188, 324), the cause of NP remains poorly understood. Theories describe NP as a consequence of chronic inflammation, resulting in the formation of stromal oedema and changes in inflammatory cell profiles (325). Proposed aetiological factors associated with NP include allergy (98), asthma (3), eosinophilic mediators (38, 97, 196, 326, 327), aspirin sensitivity (3, 39, 328, 329) genetic factors (35, 330), fungal biofilms (331, 332) and *Staphylococcal* superantigens (36, 108, 140, 333, 334). However, whilst many of these associations have been well documented, the initiating cause remains unknown.

Recent EPOS guidelines propose the classification of CRSwNP and CRSsNP into two distinct pathological entities primarily based on differences in inflammatory cytokine profiles (3). A CRSwNP T-helper 2 (T_H2)-mediated profile is characterised as eosinophilic with elevated IL-5, immunoglobulin E, RANTES and eotaxin, whilst CRSsNP T-helper 1 (T_H1)-mediated profile is characterised as neutrophilic with elevated TNF-α, IL-8 and IFN-γ (3). These biochemical profiles are likely to be manifestations of various pathological processes occurring at the host-environment interface.

One of the proposed pathological aetiologies in CRS is biofilm formation within the sinonasal cavity (3). *S aureus* has been identified as the commonest biofilm-forming pathogen in CRS, colonising the sinonasal cavities in 27% of patients with CRSsNP and 60% of patients with CRSwNP (36). *S aureus* biofilms have also been associated with more severe preoperative disease, persistence of ongoing mucosal inflammation and poor postsurgical outcomes (244).

Our results have clearly demonstrated the presence of surface-related bacterial biofilms on the sinonasal mucosa in patients with both CRSwNP and CRSsNP. *S aureus* was confirmed as the commonest biofilm-forming microbe (244). We wished to extend these findings by investigating bacterial profiles in NP as little is known in this area.

5.2 Methods

5.2.1 Subjects

Twenty four patients with CRSwNP (CRS 7-8, 10-16, 25-39) and 5 control patients (CN 7-13) were recruited into the study as described in *Section 2.2*.

5.2.2 Tissue sampling

From each individual patient with CRSwNP, biopsies were taken from NP and non-polypoidal mucosa. The non-polypoidal mucosa was taken from the middle meatus, adjacent to the NP (Figure 5.1). Control tissue was obtained as described in *Section 2.4*.

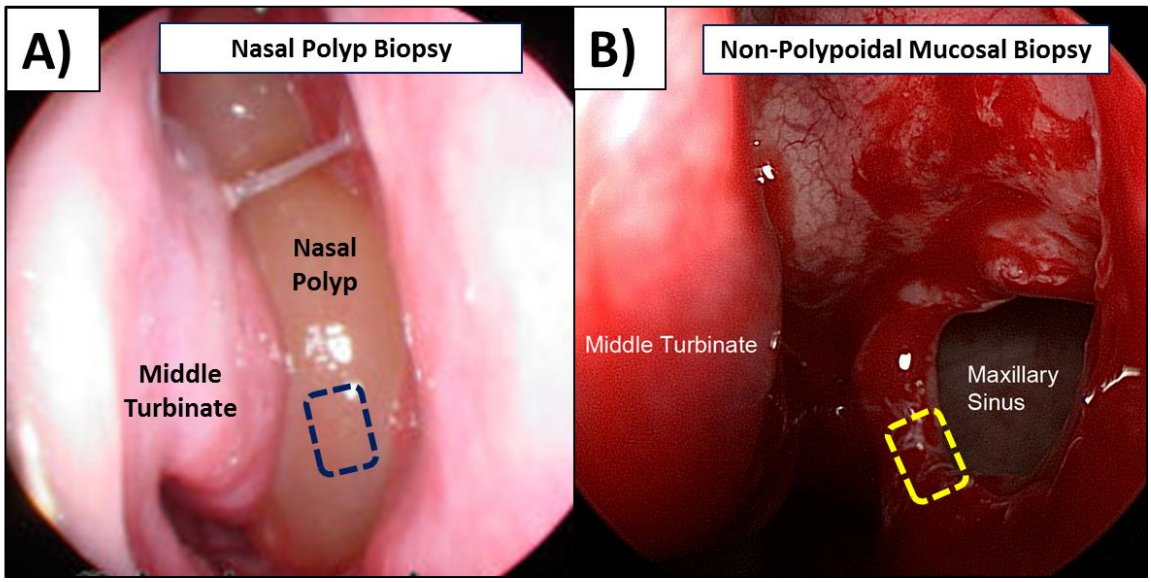

Figure 5.1 Nasal polyp and non-polypoidal mucosal biopsies. Endoscopic images of left sinonasal cavity from patient with CRSwNP. (A) First biopsy taken from NP (blue dashed line). (B) Once NP removed, a second biopsy of non-polypoidal mucosa obtained from middle meatus (yellow dashed line) from the same patient.

5.2.3 Tissue analysis

Tissue was analysed as described in **Table 5.1**.

ANALYSIS	SAMPLE STUDY NUMBERS	NP	NON-POLYPOIDAL SINONASAL MUCOSAL	CONTROL
SEM *Section 2.12*	CRS 7-8, CRS10-16, CNT 7-13	9	9	7
FISH with CLSM *Section 2.10, 2.11*	CRS 7-8, CRS10-16, CNT 7-13	9	9	7
IHC *Section 2.15*	CRS 25-34, CNT 7-13	10	10	7
TEM *Section 2.13*	CRS 30-34, CNT 7-13	5	5	7
LIVE/DEAD *Section 2.5*	CRS 35-39	5	5	0
VIABILITY *Section 2.17*	CRS35-39	5	5	0

Table 5.1 Tissue analysis for Chapter 5 including specific Sample Study Numbers and tissue type.

5.2.4 Calculations and measurements

Calculations for both the surface-related biofilm detection rate (SBDR) and the intracellular bacteria detection rate (IBDR) (Tables 2 & 3) and severity scales are described in *Sections 2.7 & 2.8*. Host cell rate calculations are described in full in *Section 2.15.4*. Cell accumulation measurements are described in *Section 2.15.5*

5.2.5 Combination of fluorescence *in situ* hybridisation, confocal laser scanning microscopy and DAPI Staining

This is a technique developed and validated for this project. In addition to the FISH protocol, described in *Section 2.11*, 30 minutes prior to imaging with CLSM, 20µl of the nucleic acid stain 4', 6-diamidino-2-phenylindole (DAPI) was added to each tissue sample. By binding to double stranded DNA, DAPI clearly identifies cell nuclei when observed under CLSM.

5.3 Results

5.3.1 Patient demographics

5.3.1.1 Chronic rhinosinusitis with nasal polyps group

A total of 24 patients with CRSwNP were included in the study cohort. Patient demographics are demonstrated in Table 5.1. Despite the small sample numbers, which will create a high variance, the demographics of this group closely represent the published sample values.

5.3.1.2 Control group

A total of seven control patients were included in the study cohort. Patient demographics for this group are demonstrated in Table 1.

Characteristics	CRSwNP	Control
Group population	24	7
Mean age (range)	47 (20-76)	54 (34-82)
Sex	15M : 9F	4M : 3F
Current smokers	7	1
Aspirin sensitivity	0	0
Asthma	4	0
Positive SPT	4*	1**
Mean LM Score (range)	16.7 (11-24)	0

Table 5.2 Patient characteristics. *SPT Results: CRSwNP patient 1 (grass), patient 2 (Indoor mould/cat), patient 3 (house dust mite/ dog); patient 4 (house dust mite); **Control patient 1 (house dust mite)

5.3.2 Scanning electron microscopy

There were clear differences in surface morphology observed between the NP, the adjacent sinonasal mucosa and control samples. The surface of the NP appeared irregular with large epithelial defects and disorganised, uneven and metaplastic-appearing squamous epithelial cells (Figure 5.2A). There was no evidence of any bacterial biofilms attached to the surface epithelium of the NP in any of the samples. In contrast, the CRS sinonasal mucosa appeared to have a regular, smooth surface, with well organised epithelium and no visible defects. Attached to the epithelial surface were aggregations of bacteria in biofilms (Figures 5.2B). These surface-related biofilms were identified in all CRS sinonasal mucosa samples. The control tissue demonstrated normal surface mucosa with cilia and no evidence of any surface-related bacterial biofilms in any of the samples (Figure 5.2C).

5.3.3 Fluorescence *in situ* hybridisation

5.3.3.1 Tissue comparison

In keeping with the results obtained from SEM, FISH detected surface-related bacterial biofilms on all sinonasal mucosal samples (n=9) (Figure 5.3A), but no surface-related biofilms were observed on any NP tissue. However, on imaging the sub-epithelial region of the NP using CLSM, bacteria were observed within the loose stroma, tightly packed into the cytoplasm of unknown host cells (Figure 5.3B). No bacterial biofilms or intracellular bacteria were observed on any of the control samples (n=5) (Figure 5.3C).

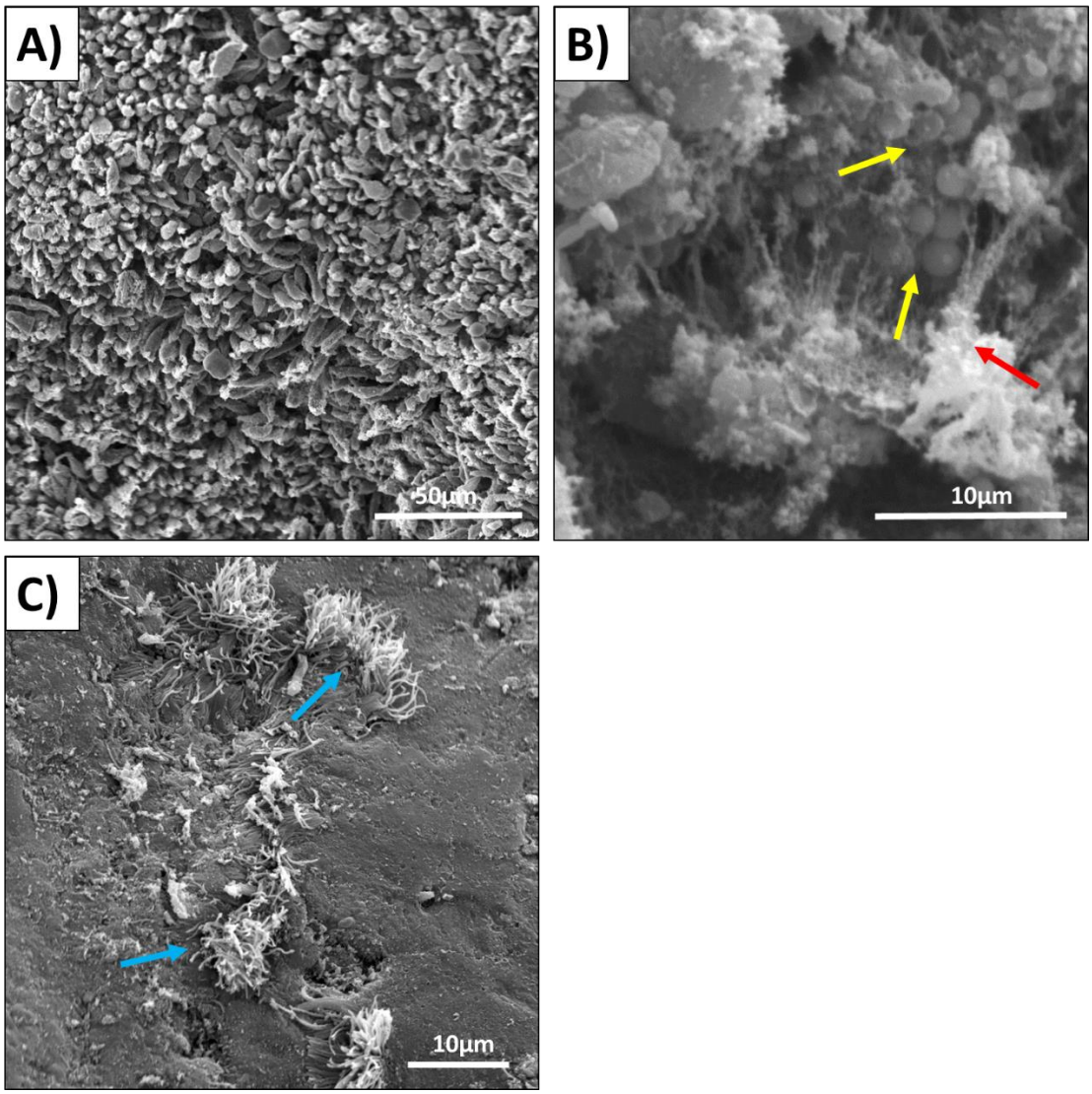

Figure 5.2 Tissue surface morphology with SEM. (A) Representative SEM image of the surface of a NP. No evidence of any bacterial biofilms can be seen on the epithelial surface. The NP surface is composed of metaplastic squamous epithelial cells, producing a 'rough' and 'rugged' appearance. (B) Representative SEM image of CRS sinonasal mucosa demonstrating aggregations of *Staphylococcus* bacteria in biofilms (yellow arrows) within an extracellular matrix (red arrow) attached to the epithelial surface. (C) Representative SEM image of control tissue showing normal surface mucosa with cilia (blue arrows) and no evidence of any bacterial biofilms.

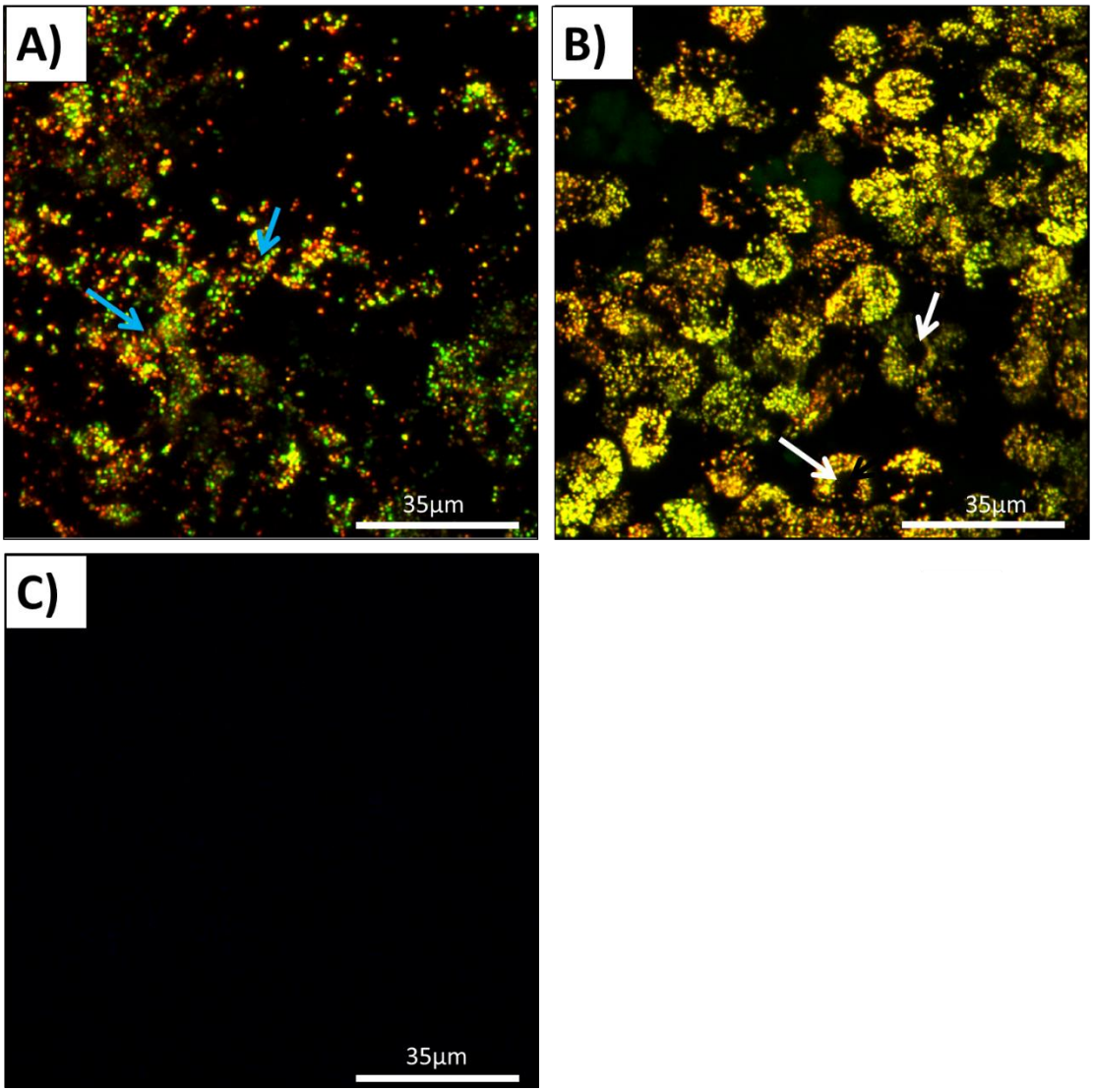

Figure 5.3 FISH analysis of CRS sinonasal mucosa, NP and control tissue. Representative CLSM images of CRS sinus mucosa (A), NP tissue (B) and control tissue (C) hybridised with 16S rRNA probes (S.au/Sta/Eub338) showing *S aureus* (yellow) biofilms. (A) Aggregations of *S aureus* bacteria (biofilms) can be seen attached to the epithelial surface of the sinus mucosa (blue arrows). (B) Aggregations of *S aureus* (yellow) seen, each spherical with central black spaces (white arrows). (C) No bacterial biofilms seen on the control tissue.

5.3.3.2 Sub-epithelial bacteria in nasal polyps

To confirm the location of intracellular bacteria below the epithelial layer (sub-epithelial), NP were stained with a combination of DAPI and FISH and imaged with the CLSM Z-axis view. This allowed the intracellular bacteria to be plotted in relation to the epithelial layer, clearly demonstrating the intracellular microbial reservoirs to be sub-epithelial (Figure 5.4 A-B).

5.3.3.3 Intracellular bacteria in nasal polyps

To confirm the observed intracellular residency of bacteria in the NP samples, the nucleic acid stain 4', 6-diamidino-2-phenylindole (DAPI) was combined with FISH and imaged with high-resolution microscopy (n=9). This technique clearly demonstrated host nuclei surrounded by tightly-packed bacteria within the cytoplasm of unknown host cells, confirming intracellular residency of bacteria in all NP samples (Figure 5.4 C-D).

5.3.3.4 Bacterial profiles

Interestingly, the bacterial profile observed in the sinonasal mucosa and NP tissue were very similar. *S aureus* was the most frequent biofilm-forming microbe found attached to the surface of the CRS sinonasal mucosa (78%). It was also the most frequently identified intracellular microbe within NP tissue (78%) (Tables 5.2-5.3). The SBDR of *S aureus* on the CRS sinonasal mucosa was 0.47 (p=0.006, compared to controls) and the IBDR in NP was 0.49 (p=0.002, compared to controls). *P aeruginosa* and *H influenzae* were also identified as biofilm-forming microbes on CRS sinonasal mucosa and as intracellular entities in NP, detected in 33% of samples (Tables 5.2-5.3). On the CRS sinonasal mucosa, the *P aeruginosa* and *H influenzae* SBDR were 0.16 and 0.18, respectively. Neither bacteria demonstrated statistical significance when compared to the control group (p=0.088 and p=0.121, respectively, Table 5.2). Similarly, in the NP tissue the IBDR for *P aeruginosa* and *H influenzae* was 0.18 and 0.11, respectively. Again, no statistical significance was observed between

either of these bacteria when compared to the control group (p=0.086 and p=0.139, respectively, Table 5.3).

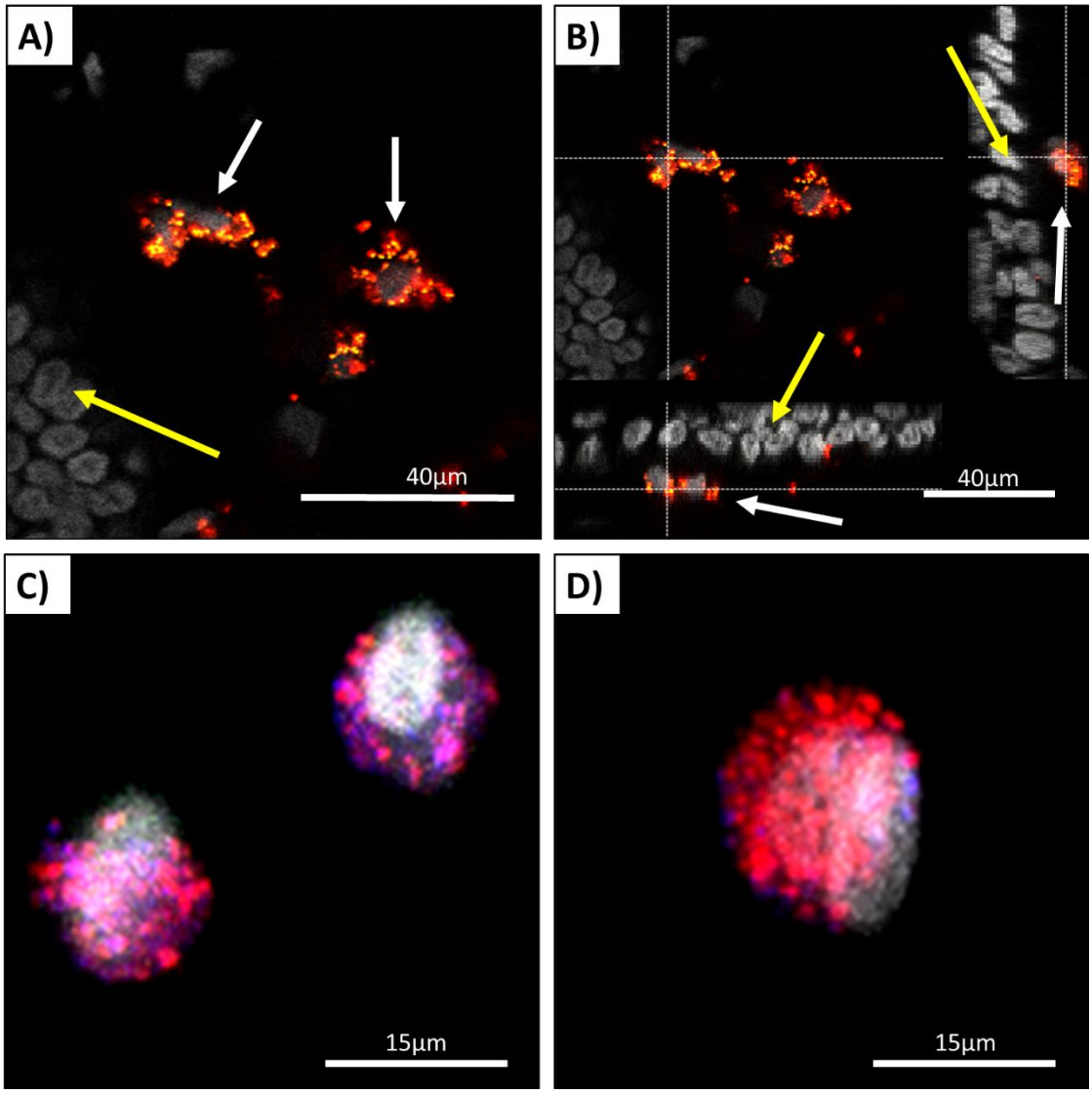

Figure 5.4 Intracellular *S aureus* in ex vivo NP tissue. (A & B) Representative high resolution CLSM images of NP tissue hybridised with 16S rRNA FISH probes (S.au/Sta) showing intracellular *S aureus* reservoirs (pink) co-localised with DAPI-stained host nuclei (grey). (C) Intracellular *S aureus* aggregates (white arrows) beneath the epithelial surface (yellow arrows). (D) XYZ view: lower magnification image clearly demonstrating intracellular *S aureus* aggregates (white arrows) beneath the epithelial surface (yellow arrows).

Study no.	*S aureus*	*P aeruginosa*	*H Influenzae*	Intracellular bacteria
	SBDR			IBDR
CRS Group				
CRS 7	0.2	0.0	0.0	0.0
CRS 8	0.6	0.0	0.0	0.0
CRS10	0.0	0.4	0.2	0.0
CRS 11	0.6	0.0	0.0	0.0
CRS 12	0.0	0.4	0.6	0.0
CRS 13	0.2	0.0	0.0	0.0
CRS 14	0.8	0.0	0.0	0.0
CRS 15	1.0	0.6	0.8	0.0
CRS 16	0.8	0.0	0.0	0.0
Total (%)	**7/9 (78%)**	**3/9 (33%)**	**3/9 (33%)**	**0**
Mean SBDR	**0.47**	**0.16**	**0.18**	**0**
***p*=value**	**0.006**	**0.088**	**0.121**	**0**
95% CI	**0.18 to 0.75**	**-0.03 to 0.34**	**-0.06 to 0.41**	**0**
Control Group				
CT 7	0.0	0.0	0.0	0.0
CT 8	0.0	0.0	0.0	0.0
CT 9	0.0	0.0	0.0	0.0
CT 10	0.0	0.0	0.0	0.0
CT 11	0.0	0.0	0.0	0.0
CT 12	0.0	0.0	0.0	0.0
CT 13	0.0	0.0	0.0	0.0
Mean	0.0	0.0	0.0	0.0

Table 5.3 Surface-related biofilm and intracellular bacteria detection rates in CRS sinonasal mucosa and control tissue.

Study no.	Surface Biofilms	*S aureus*	*P aeruginosa*	*H Influenzae*
	SBDR	**IBDR**		
CRS Group				
CRS 7	0.0	0.6	0.0	0.0
CRS 8	0.0	0.6	0.0	0.0
CRS10	0.0	0.0	0.6	0.2
CRS 11	0.0	0.8	0.0	0.0
CRS 12	0.0	1.0	0.4	0.2
CRS 13	0.0	0.4	0.0	0.0
CRS 14	0.0	0.0	0.6	0.6
CRS 15	0.0	0.4	0.0	0.0
CRS 16	0.0	0.6	0.0	0.0
Total **Mean**	**0** **0.0**	**7/9(78%)** **0.49**	**3/9 (33%)** **0.18**	**3/9 (33%)** **0.11**
***p*=value**	**0.0**	**0.002**	**0.086**	**0.139**
95% CI	**0.0**	**0.23 to 0.76**	**-0.03 to 0.34**	**-0.04 to 0.27**

Table 5.4 Surface-related biofilm detection rates (SBDR) and intracellular bacteria detection rates (IBDR) in NP detected by FISH with CLSM.

5.3.4 Detection of *Staphylococcus aureus*$^{+ve}$ host cells using immunohistochemistry

Immunohistochemistry (IHC) was utilised to validate the FISH & CLSM findings of sub-epithelial intracellular *S aureus* in NP and to assess host cell profiles within different tissue types. To help facilitate this, a mouse anti-*S aureus* monoclonal primary antibody was optimised (as described in Chapter 2, *Section 2.15.3*) and used to stain GMA sections on CRS sinonasal mucosa (n=10), NP (n=10) and control tissue (n=7).

5.3.4.1 Host cell profiling in nasal polyps and chronic rhinosinusitis sinonasal mucosa

To evaluate any histological differences in host cell profiles between NP, adjacent non-polypoidal CRS sinonasal mucosa and control tissue, a host cell count was performed for each tissue type. The results of the cell counts are presented in Figure 5.5. There was a significantly higher rate of mast cells, T-cells and eosinophils (p=0.0003, p=0.011, p=0.0004, respectively) in the loose stroma of NP compared with adjacent CRS sinonasal mucosa and control tissue. This is consistent with the cytokine profile described in patients suffering with CRSwNP. Within the sub-epithelial layer of the adjacent non-polypoidal CRS sinonasal mucosa there were significantly higher rates of neutrophils (p=0.0042, Figure 5.4) compared to NP. This is consistent with the cytokine profile seen in patients suffering with CRSsNP. Interestingly, both the NP and CRS sinonasal mucosa were taken from the same ten patients suffering with CRSwNP. The rate of *S aureus*$^{+ve}$ host cells was significantly higher in NP than CRS sinonasal mucosa and control tissue (p=0.0065, Figure 5.4).

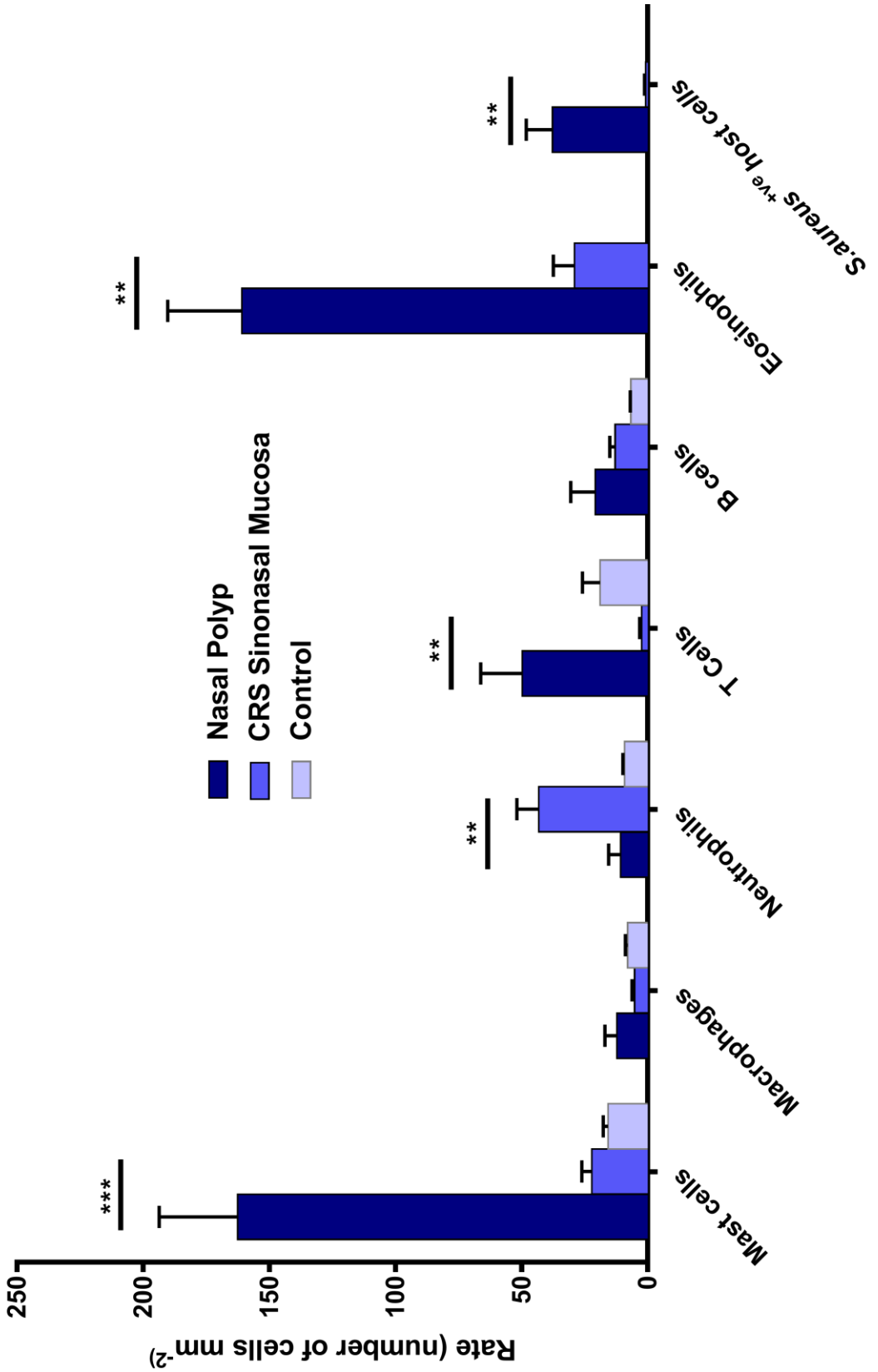

Figure 5.5 Host cell profiling in NP, CRS sinonasal mucosa and control tissue

NP & adjacent CRS sinonasal mucosa (n=10), Controls (n=7).Only significant p-values shown; error bars represent mean + 1SD. ** $p < 0.001$, *** $p < 0.0001$.

5.3.4.2 Intracellular *Staphylococcus aureus*

5.3.4.2.1 Chronic rhinosinusitis sinonasal mucosa

S aureus^{+ve} host cells were detected in 30% of CRS sinonasal mucosa samples when analysed with IHC (n=10) (Table 5.4). Within these samples, intracellular *S aureus* was identified in both the epithelial and sub-epithelial layer (Table 5.4). However, the actual number of host cells containing *S aureus* within each of these sections was extremely low (1.09 cells mm^{-1} within the epithelial layer and 0.82 cells mm^{-2} in the sub-epithelial layer) and showed no significant difference when compared with the control group (p=0.5 and p=0.5 respectively, Figure 5.6).

5.3.4.2.2 Nasal polyp tissue

S aureus^{+ve} host cells were detected in 90% of NP samples analysed with IHC (n=10). There was a significantly higher rate of *S aureus*$^{+ve}$ host cells in the NP sub-epithelial layer compared to the NP epithelial layer (p=0.0057). Within the epithelial layer, the *S aureus*$^{+ve}$ host cell rate was 4.53 cells mm^{-1} and within the sub-epithelial layer the rate was 37.73 cells mm^{-2} (Table 5.5). A significantly higher rate of *S aureus*$^{+ve}$ host cells was observed in both the NP epithelial and sub-epithelial layers when compared to the respective CRS sinonasal mucosa (p=0.0226 and p=0.0065 respectively, Table 5.4 & Figure 5.7). *S aureus*$^{+ve}$ host cells detected by IHC are demonstrated in Figure 5.8.

5.3.4.2.3 Controls

No intracellular bacterial were observed in any of the control tissue samples.

Sample no.	Epithelial Layer		Sub-epithelial Layer	
	CRS SM (cells mm^{-1})	NP (cells mm^{-1})	CRS SM (cells mm^{-2})	NP (cells mm^{-2})
CRS 25	0.00	0.94	0.00	3.65
CRS 26	3.53	5.38	3.35	23.00
CRS 27	0.00	0.56	0.00	94.97
CRS 28	0.00	4.83	0.00	82.61
CRS 29	0.00	0.00	0.00	10.40
CRS 30	5.61	19.02	1.17	66.83
CRS 31	1.71	5.10	3.66	32.21
CRS 32	0.00	0.00	0.00	0.00
CRS 33	0.00	2.86	0.00	29.36
CRS 34	0.00	6.59	0.00	34.29
Total (%)	**30%**	**80%**	**30%**	**90%**
Mean	**1.09**	**4.53**	**0.82**	**37.73**
***p* value**	**0.0266**		**0.0065**	
95% CI	**0.50 to 0.639**		**13.20 to 60.63**	

Table 5.5 *S aureus*$^{+ve}$ host cell rate within the epithelial and sub-epithelial layers of the NP and adjacent CRS sinonasal mucosa (SM) samples

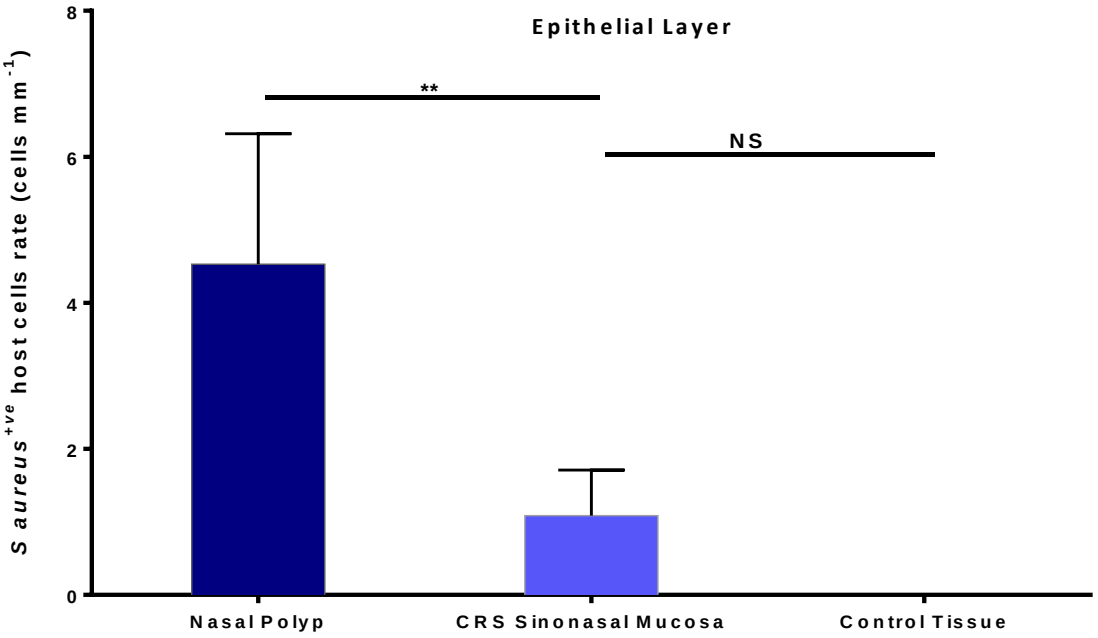

Figure 5.6 *S aureus*$^{+ve}$ host cell rate within the epithelial layer of NP, CRS sinonasal mucosa and control tissue. The rate of epithelial *S aureus*$^{+ve}$ host cells within NP, adjacent CRS sinonasal mucosa and control tissue, analysed using a mouse anti-*S aureus* monoclonal antibody on GMA embedded tissue sections. Cell count was performed as described in Chapter 2. Significantly more *S aureus*$^{+ve}$ host cells were demonstrated in the epithelial layer in NP compared to adjacent CRS sinonasal mucosa. Results are pooled data from ten independent experiments (n=10). Error bars represent the means + 1SD. $^{**}p<0.001$, NS not significant.

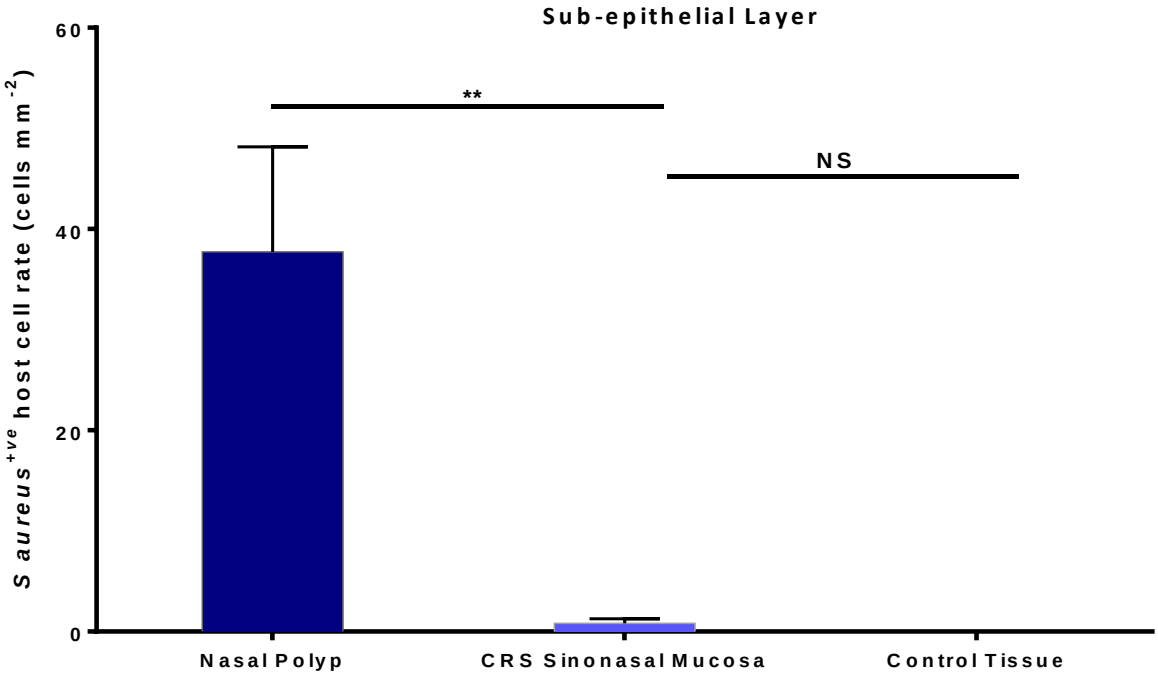

Figure 5.7 *S aureus*$^{+ve}$ host cell rate within the sub-epithelial layer of NP, CRS sinonasal mucosa and control tissue. The rate of sub-epithelial *S aureus*$^{+ve}$ host cells within NP, adjacent CRS sinonasal mucosa and control tissue, analysed using a mouse anti-*S aureus* monoclonal antibody on GMA embedded tissue sections. Cell count was performed as described in Chapter 2. Significantly more *S aureus*$^{+ve}$ host cells were demonstrated in the sub-epithelial layer in NP compared to adjacent CRS sinonasal mucosa. Results are pooled data from ten independent experiments (n=10). Error bars represent the means + 1SD. **p<0.001, NS not significant.

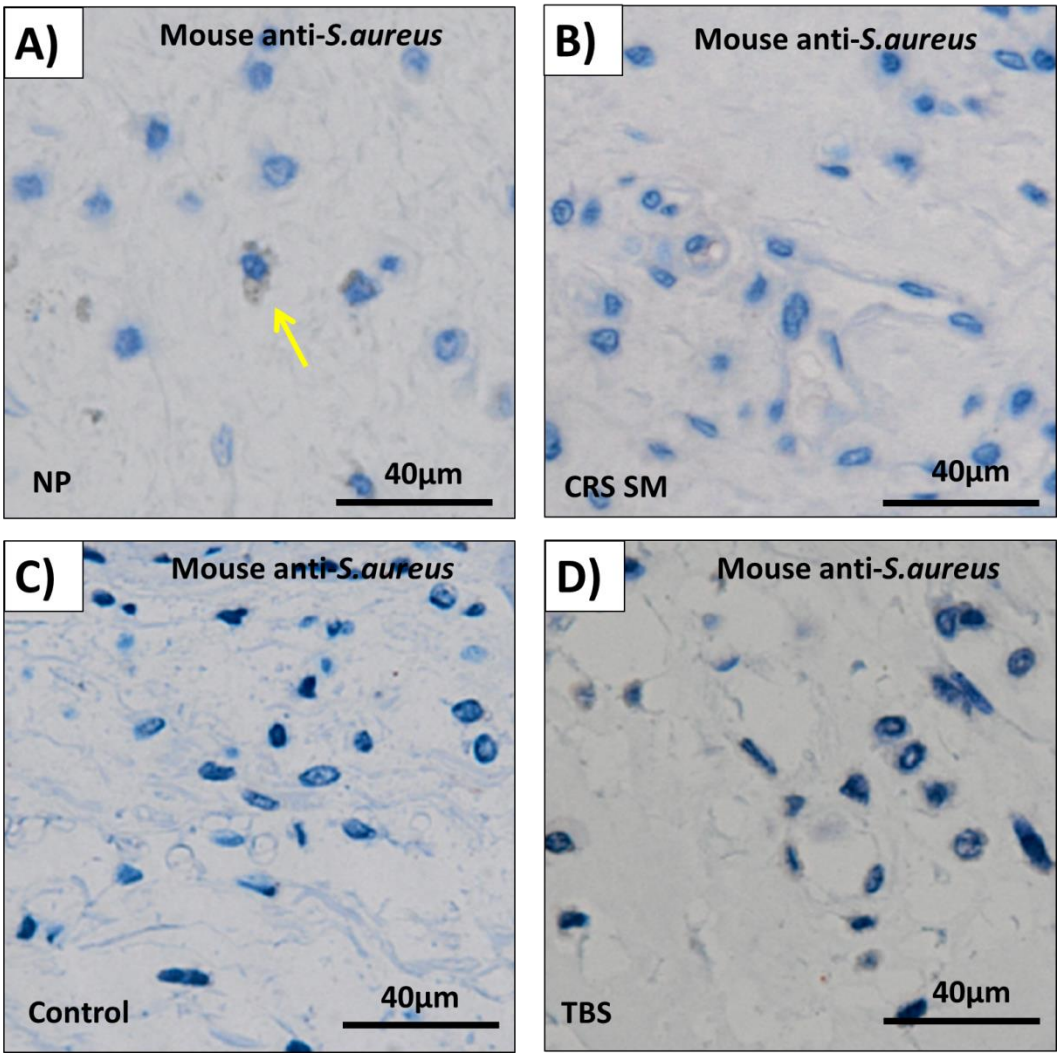

Figure 5.8 Immunohistochemical detection of *S aureus*$^{+ve}$ host cell in nasal polyps. GMA embedded NP, adjacent CRS sinonasal mucosa and control tissue, immunohistochemically stained with a monoclonal mouse anti-*S aureus* primary antibody and DAB substrate. Representative IHC photomicrographs (x40 magnification)., demonstrating the presence of *S aureus*$^{+ve}$ host cells (yellow arrow) within NP tissue (A) and the absence of *S aureus*$^{+ve}$ host cell in CRS sinonasal mucosa (B) and control tissue (C). (D) NP section stained with Tris-buffered saline (TBS) as a control.

5.3.4.3 Detection of the identity of the *S aureus*$^{+ve}$ host cell

Within NP tissue, intracellular *S aureus* has been demonstrated to reside within the cytoplasm of an unknown host cell. In order to investigate the underlying mechanism of microbial migration from a surface-related bacterial biofilm into an intracellular entity, it is essential to clarify the identity of this *S aureus*$^{+ve}$ host cell.

5.3.4.3.1 Immunohistochemistry co-localisation

Co-localisation was performed using serial 2µm thick sections, on CRS sinonasal mucosa (n=3) and NP (n=10) (CRS 25-32). The monoclonal mouse anti-*S aureus* primary antibody was used to identify intracellular *S aureus*. Sequential sections were each stained with the monoclonal anti-human primary antibodies listed in Chapter 2, *Section 2.15.2*. These primary antibodies were selected as they closely represented the range of host cells located within these tissues. Sections demonstrating *S aureus*$^{+ve}$ host cells were then directly compared with sequential sections stained with different host cells.

5.3.4.3.2 CRS non-polypoidal mucosa immunohistochemistry co-localisation

Within the 3 CRS sinonasal mucosa samples that demonstrated *S aureus*$^{+ve}$ host cells, the cells harbouring bacteria were identified as epithelial cells in the epithelial layer and macrophages in the sub-epithelial layer (Table 5.5). It must be noted that the *S aureus*$^{+ve}$ host cell rates identified in both the epithelial layer and sub-epithelial layer in the CRS non-polypoidal mucosa were extremely small and demonstrated no significant different from the rate of cells observed within the control tissue (see earlier *Section 5.5.4.2.1*).

5.3.4.3.3 Nasal polyp immunohistochemistry co-localisation

Within the nine NP samples that demonstrated *S aureus*$^{+ve}$ host cells, the cells were identified as both epithelial and mast cells (2:1 ratio) within the epithelial layer. However, in the sub-epithelial layer, 100% of the *S aureus*$^{+ve}$ host cells were identified as mast cells (*S aureus*$^{+ve}$ mast cells) (Table 5.5 & Figure 5.9).

5.3.5 Transmission electron microscopy

To further validate the findings of *S aureus*$^{+ve}$ mast cells, NP tissue was processed and imaged with TEM. Five NP samples used for IHC were processed for TEM (CRS 30-34). Five samples (n=5) previously shown to contain *S aureus*$^{+ve}$ host cells by IHC were selected for imaging. Mast cells were easily identified on TEM imaging based on their morphology of large secretory granules, absence of polarity, nucleus containing significant amounts of euchromatin and size (~12-18 μm in length). Each mast cell was examined for intracellular bacteria. Intracellular *Staphylococci* within the cytoplasm of mast cells (Figure 5.9) were observed in all five samples.

Study No.	Epithelial Layer		Sub-epithelial Layer	
	CRS SM	NP	CRS SM	NP
CRS 25	-	EC	-	MC
CRS 26	EC	EC & MC	MP	MC
CRS 27	-	EC & MC	-	MC
CRS 28	-	EC	-	MC
CRS 29	-	-	-	MC
CRS 30	EC	EC & MC	MP	MC
CRS 31	EC	EC & MC	MP	MC
CRS 32	-	-	-	-
CRS 33	-	EC	-	MC
CRS 34	-	EC	-	MC

Table 5.6 The identification of *S aureus*$^{+ve}$ host cells in the epithelial and sub-epithelial layers within CRS sinonasal mucosa (SM) and NP. Results of IHC co-localisation in NP and adjacent CRS sinonasal mucosa. EC, epithelial cells; MC, mast cells; MP, macrophages; (-), not detected.

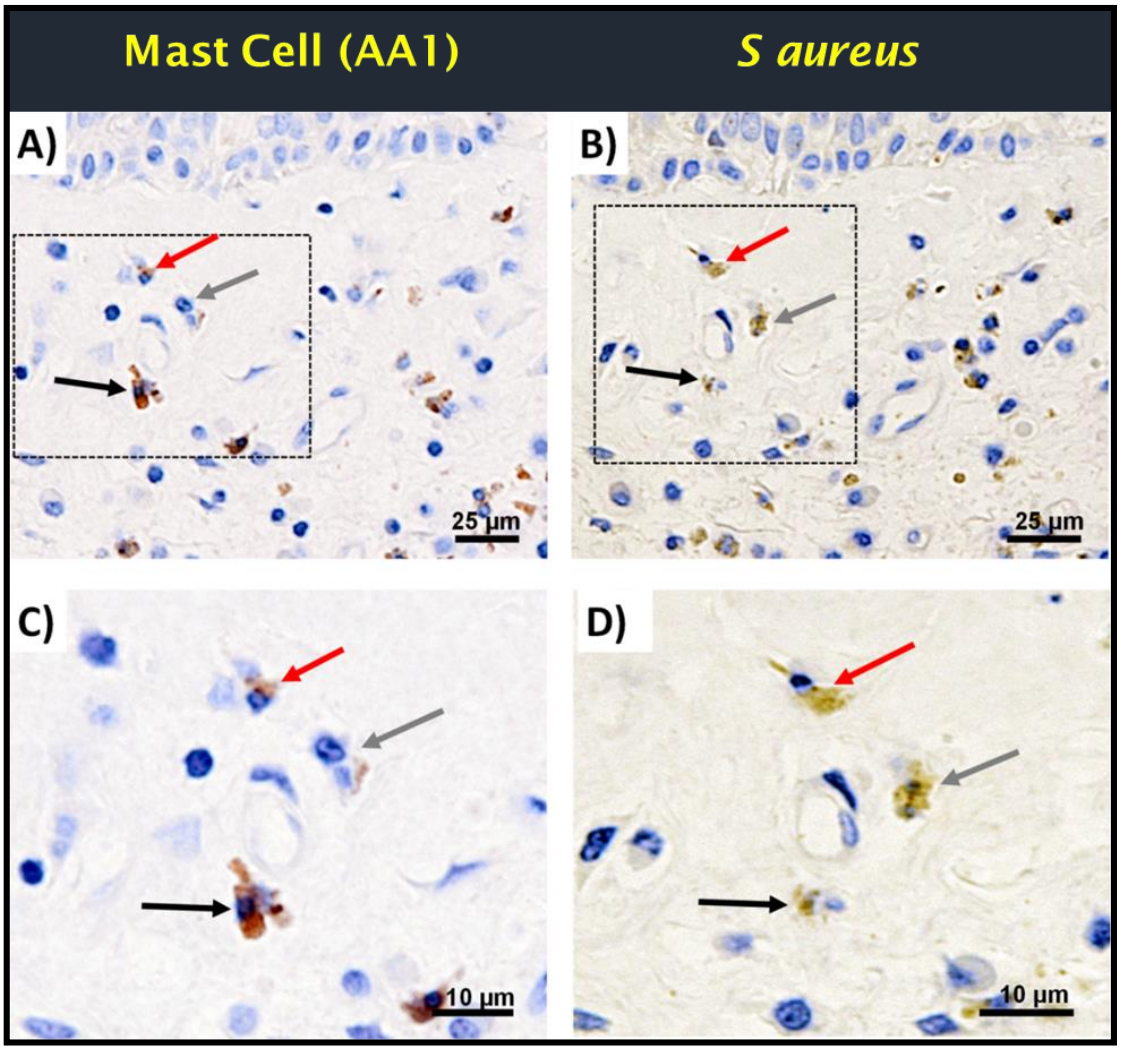

Figure 5.9 Immunohistochemical co-localisation. Photomicrographs of sequential 2µm sections of NP tissue stained with monoclonal anti-mast cell tryptase (A) and mouse monoclonal anti-*S aureus* (B) demonstrating sub-epithelial intracellular *S aureus* within mast cells (arrows) (x20 magnification). Both images are shown at higher magnification (C & D x40 magnification).

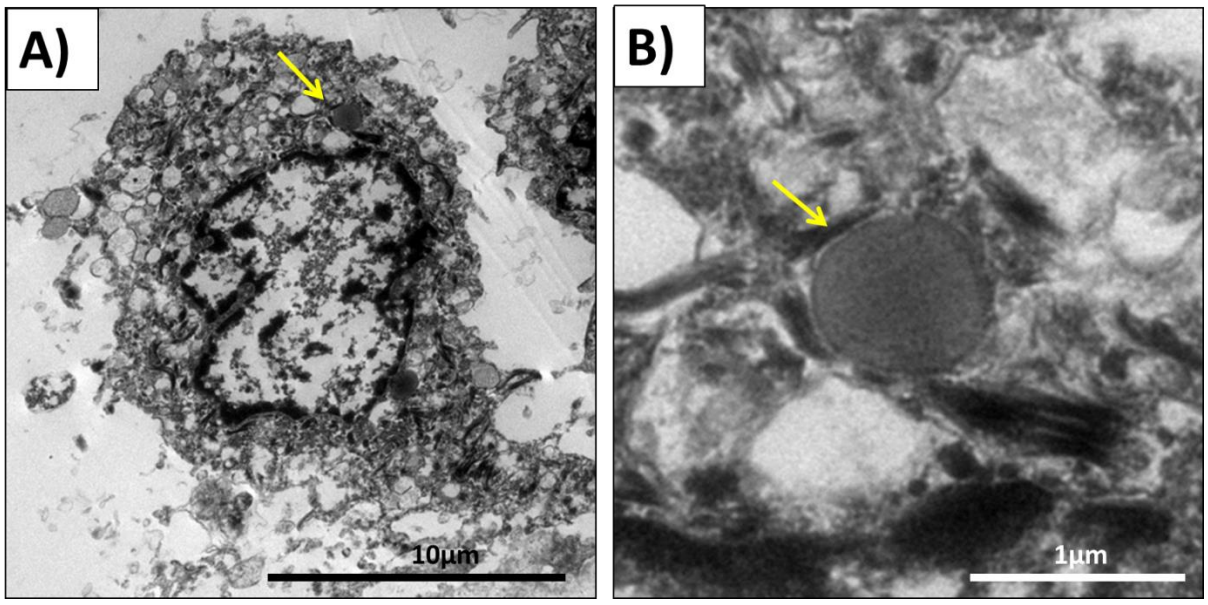

Figure 5.10 TEM image of a *S aureus*$^{+ve}$ mast cell within the loose stroma of a NP. Representative TEM images demonstrating a *S aureus*$^{+ve}$ mast cell within the loose stroma of an *ex vivo* NP (A). An individual *S aureus* microbe is demonstrated (yellow arrow) within the mast cell cytosol. (B) Higher magnification image of intracellular *S aureus.*

5.3.6 Viability of intracellular *S aureus*

5.3.6.1 Investigating the viability of intracellular bacteria in nasal polyps

Having successfully identified *S aureus* residing within the cytosol of mast cells in NP, the next step was to ascertain the viability of these intracellular bacterial reservoirs. Therefore, the LIVE/DEAD® BacLight™ Viability Kit was utilised on fresh, unfixed nasal polyp tissue (n=5) (CRS 35-39) and imaged with CLSM. In all samples examined, the intracellular bacteria identified within the cytosol of host cells were demonstrated to be viable (Figure 5.11A).

5.3.6.2 Identification of host cells with viable intracellular bacteria

In order to investigate whether intracellular *S aureus* was viable within mast cells in NP, an intracellular viability assay was developed and is described in Chapter 2, *Section 2.17*. A total of five NP samples (CRS 35-39) were processed with this novel assay and imaged with CLSM. After analysis, proliferating and therefore viable bacteria were observed within the cytosol of mast cells (Figure 5.11B). No intracellular bacteria were observed within any other NP host cell analysed with this method.

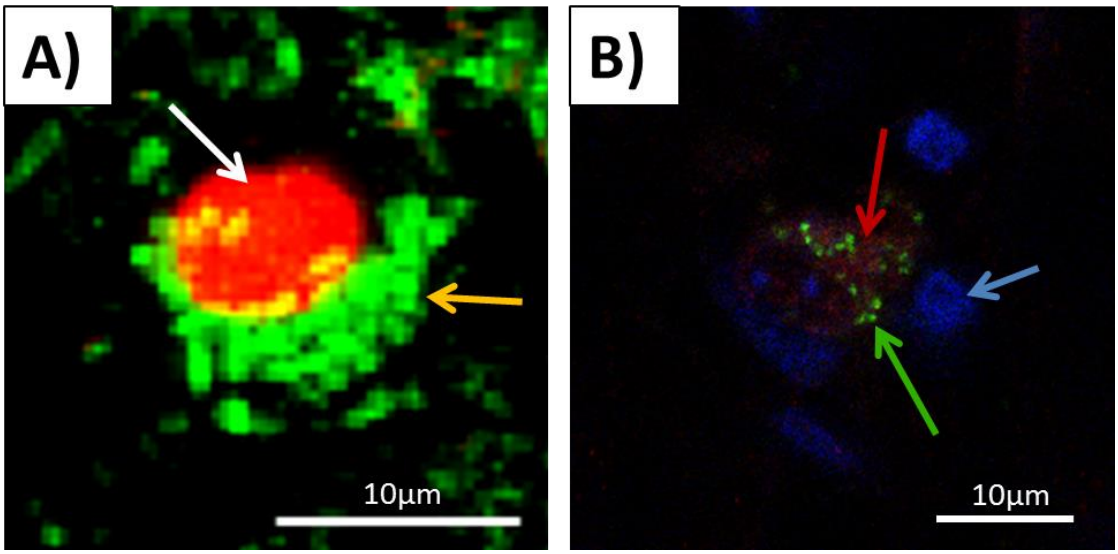

Figure 5.11 Viable bacteria within host cells. (A) Fresh NP tissue stained with a LIVE/DEAD® BacLight™ Viability Kit and imaged with CLSM. SYTO 9 stains nucleic acid green indicating viable cells with intact membranes. Propidium iodide stains nucleic acid red indicating damaged cells. Image demonstrates viable bacterial (yellow arrow) within the cytosol of damaged cell (white arrow). (B) NP tissue stained with the intracellular viability assay (described in Chapter 2) demonstrating viable intracellular bacteria within a mast cell. The mast cell nucleus is stained with DAPI (blue arrow), the cytosol is stained with the monoclonal mouse anti-mast cell tryptase primary antibody (red arrow) and the proliferating and viable bacteria are stained with the Click-iT ® Edu proliferation assay (green arrow).

5.3.7 Sub-epithelial mast cell accumulation

During IHC analysis, an observation was made of mast cell accumulation in the sub-epithelial layer. To investigate this further, a grid was used on NP IHC sections in order to calculate the mast cell density at different depths from the basement membrane into the NP loose stroma. The mast cell density was calculated as a rate for each area per 100µm depth intervals (technique described in *Section 5.4.7*). The measuring grid is illustrated in Figure 5.12.

The results for mast cell density are displayed in Figure 5.13 and Table 5.6. The results from this study strongly indicate that mast cells, within NP, accumulate closely beneath the epithelial basement membrane. Within the first 100µm below the basement membrane the mast cell rate was at its highest density of 852 cells mm^{-2}, which represented 37.63% of all mast cells within the measured section (to a depth of 700µm). As the depth increases into the loose stroma at 100µm intervals, the mast cell rate reduces significantly (p=0.0005, p=0.002, p=0.0089, p=0.0071, Figure 5.13, Table 5.6) until 500µm where the rate stabilised to approximately 100 cells mm^{-2}.

Further analysis was performed to investigate the rate of *S aureus*$^{+ve}$ mast cells in the same IHC NP sections using the same 100µm depth intervals. Results can be seen in Figure 5.14 and Table 5.7. As expected, the results from this analysis appear to mirror the mast cell accumulation findings in Figure 5.13. The *S aureus*$^{+ve}$ mast cells appear to accumulate immediately below the epithelial basement membrane. Within the first 100µm below the basement membrane, the *S aureus*$^{+ve}$ mast cell rate was 466.7 cells mm^{-2}, accounting for 49.76% of all mast cells containing *S aureus* within the measured section (to a depth of 700µm). As the depth increased into the loose stroma, the *S aureus*$^{+ve}$ mast cell rate reduced significantly (p=0.0095 and p=0.0101, Figure 5.13 and Table 5.7) to a depth of 300µm where the rate stabilised to between 20-40 cells mm^{-2}.

Figure 5.15 shows the proportion of *S aureus*$^{+ve}$ mast cells compared to mast cell rates. Within the first 100µm below the basement membrane, 54.77% of

mast cells contained intracellular *S aureus*. This number reduced to 19-32% by 700µm.

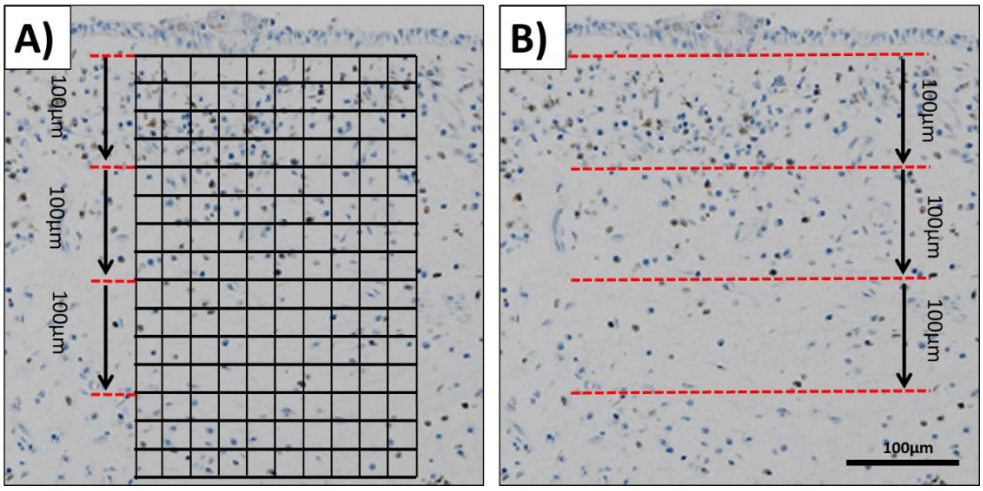

Figure 5.12 Immunohistochemical photomicrographs of nasal polyp tissue stained with AA1 mast cell tryptase primary antibody with representative grid (A) and without grid (B)

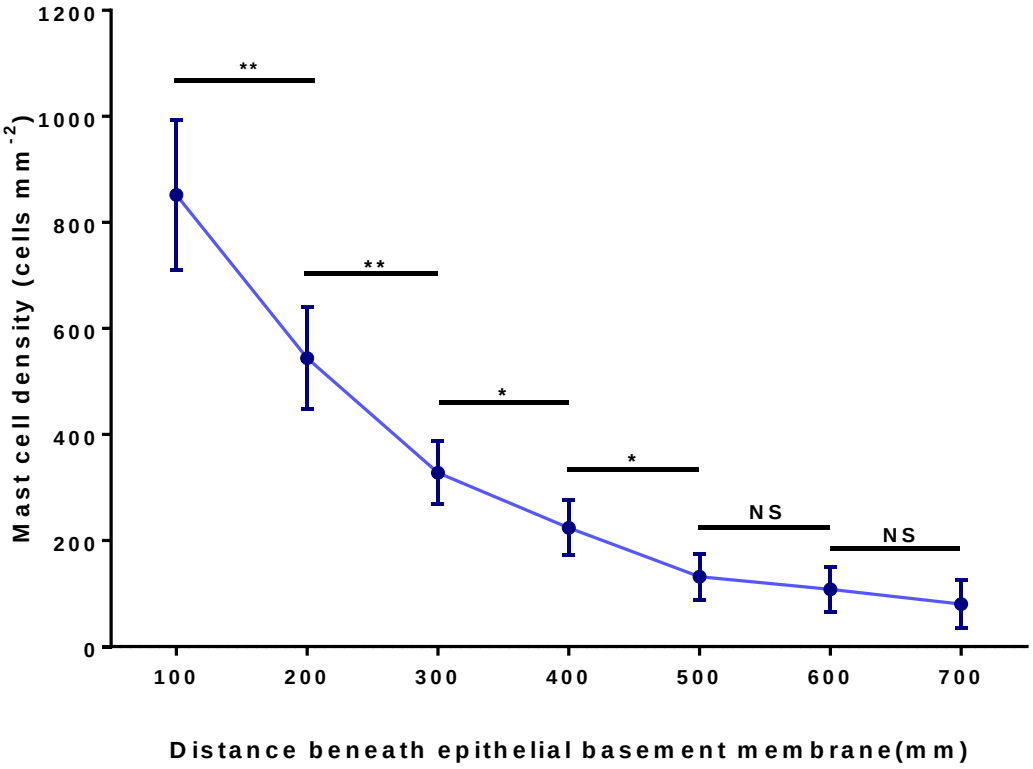

Figure 5.13 Mast cell localisation in nasal polyps. The mast cell density reduced significantly with distance from the basement membrane. Results are pooled data from nine independent experiments (n=9). Error bars represent the means +/- 1SD. *p<0.05, **p<0.001, NS not significant.

Depth	Mast cell rate/mm^2	Percent (%)	Accumulation (%)	*p-value*
0-100	852	37.63	37.63	**0.0005**
100-200	544	24.03	61.66	**0.0002**
200- 300	324	14.31	75.97	**0.0089**
300-400	224	9.89	85.87	**0.0071**
400-500	132	5.83	91.7	0.4249
500-600	108	4.77	96.47	0.3618
600-700	80	3.53	100	

Table 5.7 Mast cell localisation in nasal polyps.

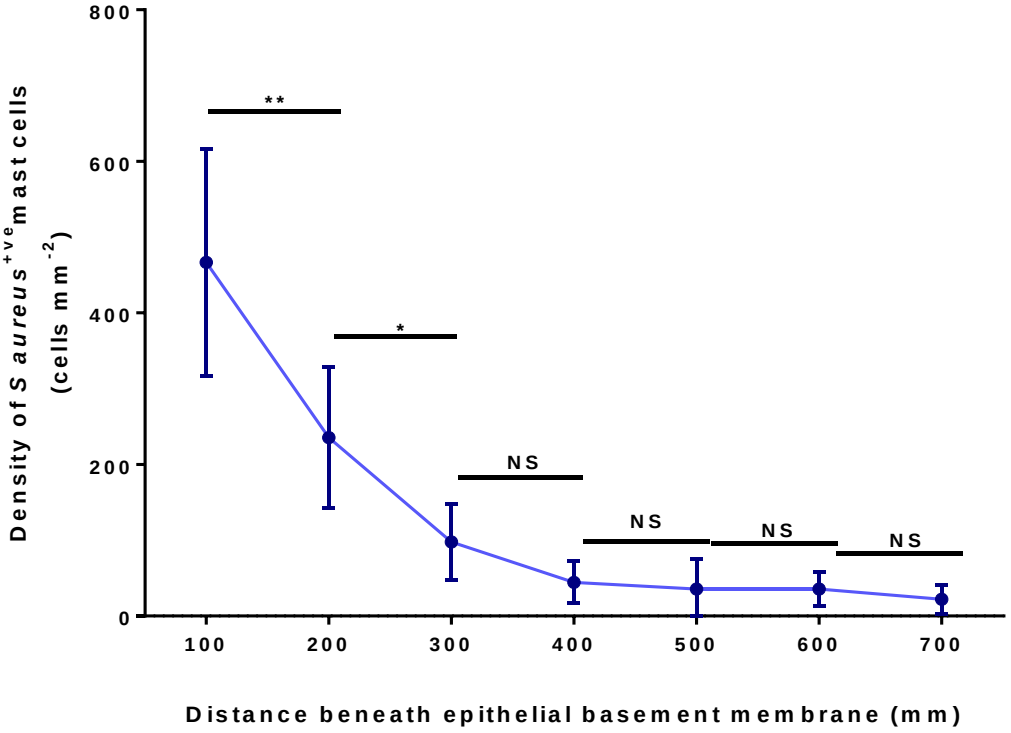

Figure 5.14 *S aureus*$^{+ve}$ mast cell localisation in nasal polyps. The *S aureus*$^{+ve}$ mast cell density reduced significantly with tissue depth. Results are pooled data from 9 independent experiments (n=9). Error bars represent the means +/- 1SD. *p<0.05, **p<0.001, NS not significant.

Depth (µm)	Mast cell rate/mm^2	Percent (%)	Accumulation (%)	*p-value*
0-100	466.67	49.76	49.76	**0.0095**
100-200	235.56	25.12	74.88	**0.0101**
200- 300	97.778	10.43	85.31	0.0648
300-400	44.44	4.74	90.05	0.7072
400-500	35.56	3.79	93.84	0.999
500-600	35.56	3.79	97.63	0.3651
600-700	22.22	2.37	100.00	

Table 5.8 *S aureus*$^{+ve}$ mast cell localisation in nasal polyps.

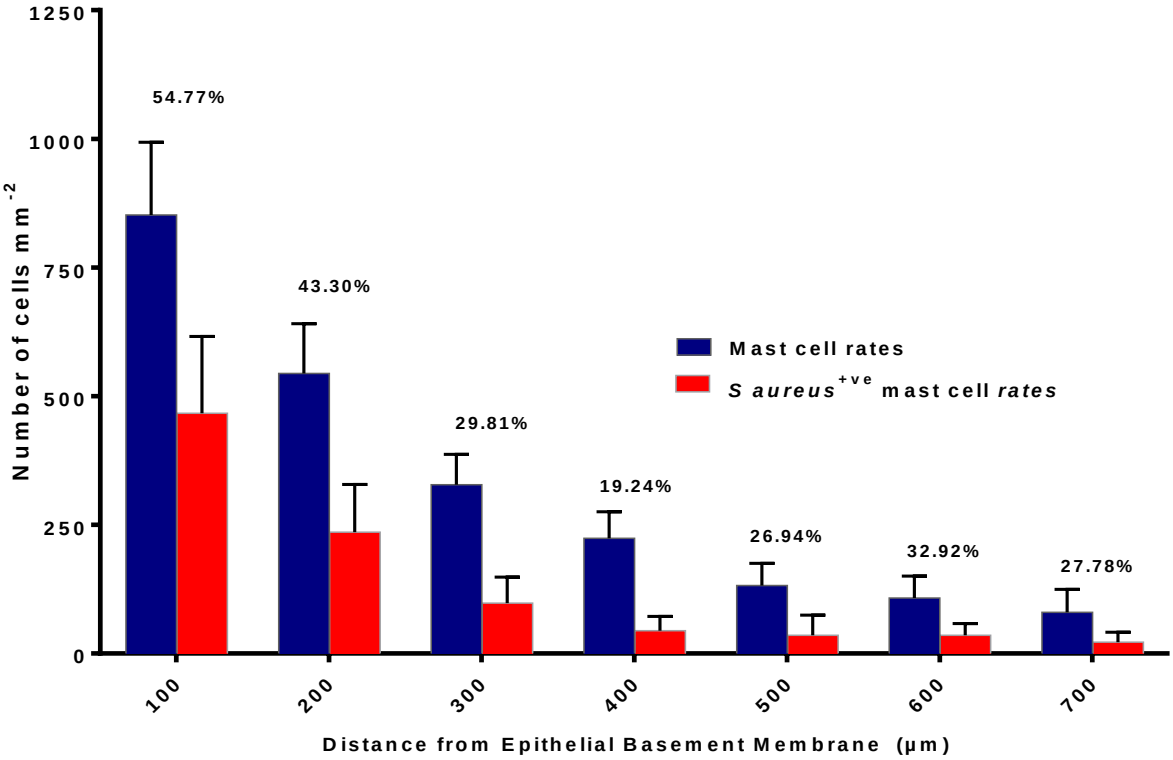

Figure 5.15 Density of mast cells and *S aureus*$^{+ve}$ mast cells in relation to tissue depth. Percentages above bars represents the proportion of mast cells containing *S aureus* per 100µm tissue depth from the epithelial basement membrane. Results are pooled data from 9 independent experiments (n=9). Error bars represent the mean + 1SD.

5.4 Discussion

Despite many proposed theories of pathogenesis, the exact cause of nasal polyps remains elusive. Recent evidence suggests that the underlying chronic inflammation which defines CRS results from a dysfunction and imbalance in host-environment interactions involving various exogenous agents and stresses, leading to changes in the sinonasal mucosal architecture. Despite evidence of surface-related bacterial biofilms on CRS sinonasal mucosa, the role bacteria play in NP pathogenesis remains unclear. In an attempt to address this question, we aimed to characterise bacterial profiles in NP and compare them to non-polypoidal mucosa harvested from the same patient, thus controlling for host genetics.

5.4.1 Surface morphology

Direct comparison of the surface morphology of the different tissues using SEM revealed an absence of surface-related bacterial biofilms in NP compared to the adjacent CRS sinonasal mucosa. The NP epithelial surface appeared rugged and irregular with large epithelial defects, which differed morphologically from the regular, smooth epithelium with associated surface-related biofilms seen in the adjacent CRS sinonasal mucosa. This is in keeping with other studies, where the NP surface has been described as having a 'cobblestone' appearance with areas deficient in epithelial cells, leaving the basement membrane exposed (335-336). The appearances of epithelial defects on NP is well supported in the literature and forms the basis of the 'immune barrier theory', which proposes that defects in the epithelial barrier lead to disruptions in adaptive and innate immunity (83-84). The epithelial layer functions as a mediator and regulator of innate and adaptive immunity as well as acting as a defensive barrier against environmental allergens and pathogens (83). Recent studies have shown that a reduction in tight junction proteins and an increase in the pro-inflammatory cytokines IFN-γ and IL-4 in NP may suggest a disruption in epithelial integrity with subsequent epithelial remodelling and formation of surface defects (84). A defective epithelial layer

could provide the opportunity for surface-related bacterial biofilms to disperse and penetrate into the NP loose stroma as a bacterial survival strategy and may help to explain the absence of any observed surface-related bacterial biofilms with SEM.

5.4.2 Bacterial profiling

Using a combination of FISH with CLSM allowed direct comparison of bacterial profiles between NP, adjacent CRS sinonasal mucosa and control tissue. Surface-related bacterial biofilms were identified attached to the epithelium of all CRS sinonasal mucosa samples, in keeping with the literature. However, no surface-related bacterial biofilms were identified on the epithelial surface of the NP. Using the CLSM Z-axis (orthogonal) view combined with the nucleic acid stain DAPI, sub-epithelial and intracellular bacteria were observed in the cytoplasm of host cells in all NP samples.

The use of FISH enabled species-specific identification of the microbes responsible for both the surface-related biofilms and the intracellular bacterial reservoirs. Despite morphological differences in the bacterial behaviour between the NP and non-polypoidal CRS sinonasal mucosa, the bacterial species identified were identical, suggesting that the appearances observed between the two tissues types may represent different survival strategies of the same bacteria. In both NP and adjacent non-polypoidal CRS sinonasal mucosa, *S aureus* was identified as the commonest microbe present (78%). This is consistent with the literature.

Intracellular *S aureus* reservoirs have been previously described in non-polypoidal CRS sinonasal mucosa, but not in NP tissue. They were first described using a combination of IHC and CLSM (91). More recently they have been identified using PNA-FISH with epifluorescence microscopy (92) and with propidium iodide and CLSM (93, 337). Intracellular bacteria were not identified within the CRS sinonasal mucosa using FISH with CLSM, but using IHC a few epithelial cells (1.09 cells mm^{-1}) and macrophages (0.82 cells mm^{-1}) were identified containing intracellular *S aureus*. However, it is worth noting that

the majority of intracellular *S aureus* reservoirs identified in the above studies were from patients suffering with AERD (the most severe form of CRS), which were excluded from our study. This may help to explain the small numbers of intracellular bacteria observed within the CRS sinonasal mucosa. Whilst intracellular *S aureus* within the sinonasal mucosa of CRS patients is not a novel finding per se, this is the first study to demonstrate intracellular localisation of bacteria in NP.

5.4.3 Intracellular localisation of *Staphylococcus aureus* within mast cells in nasal polyps

Having identified sub-epithelial intracellular *S aureus* reservoirs within the cytoplasm of host cells, the next step was to establish the identity of this bacteria-harbouring cell.

Initially, the bacteria-harbouring host cells were presumed to be mononuclear phagocytes. Part of the innate immunity defence system of the mucosal barrier in NP includes macrophages (phagocytic cells). Macrophages are classified into pro-inflammatory M1 cells associated with the T_H1 response or immunosuppressive M2 cells, which are associated with the T_H2 pathway and have been shown to have reduced phagocytic properties (182, 183). A recent study in 2010, using flow cytometry and immunohistochemistry in 28 NP samples showed impaired phagocytosis in M2 macrophages when exposed to *S aureus,* allowing the bacteria to survive intracellularly (186).

IHC co-localisation on sequential sections identified mast cells as the *S aureus*-harbouring host cell. This was further validated with TEM. This constitutes a novel finding in NP. Mast cells appear to play an important role in promoting innate immunity against microbial pathogens (201). Through activation of $CD8^+$ T cells, mast cells possess the ability to regulate both the T_H1 and T_H2 cytokine pathways, and can therefore adopt both immunosuppressive and immune-stimulatory properties (201). Recently, mast cells have been shown to exert phagocytosis-independent antimicrobial activity against *S aureus*, mediated through extracellular traps and the release of antibacterial enzymes

(203). *S aureus* has been shown to subvert these extracellular antimicrobial mechanisms by internalising within mast cells (194). Once within the mast cell, *S aureus* appears to access the nutrient-rich cytosol and up-regulate cell wall synthesis, allowing persistent and viable intracellular *S aureus* reservoirs to be established (203). The viability of the intracellular *S aureus* reservoirs within mast cells was assessed and shown to be both viable and proliferating.

The mast cell in the context of chronic *S aureus* infection may well act as a double-edged sword (203). Whilst promoting innate immunity against microbial pathogens, the mast cell may also be providing a safe haven for *S aureus* by providing protection from extracellular antimicrobial compounds. This not only avoids clearance, but also facilitates the establishment of an intracellular microbial reservoir that could lead to persistence and chronic carriage. This may explain the high levels of resistance to systemic antibacterial therapies in chronic conditions such as CRS.

5.4.4 Mast cell accumulation

As 'sentinel cells', mast cells are often the first defensive host cell against pathogens breaching the epithelial basement membrane. Mast cells are alerted to pathogenic invasion through both indirect and direct mechanisms. Epithelial cells, dendritic cells and endothelial cells all possess the ability to recruit mast cells through pattern recognition receptors (PRRs) such as Toll-like receptors (TLRs), which are activated in response to pathogen-associated molecular patterns (PAMPs). Mast cells can also directly detect pathogens through the expression of surface receptors, such as Fc receptors (FcRs), which bind pathogen-specific antibodies. Mast cells appear to express different surface receptors in response to specific pathogens, leading to the stimulation and release of different combinations of cytokines.

Our findings clearly demonstrate significant sub-epithelial accumulation of mast cells in response to *S aureus.* Within the first 100µm from the basement membrane, the mast cell rate was ten times higher than the rate between 600µm-700µm. These findings provide evidence that mast cells play an

important defensive role in response to *S aureus* in NP. Furthermore, the accumulation of mast cells potentially provides a reservoir of host cells for *S aureus* to internalise within.

The bacteria's ability to attract distant mast cells is crucial for the long-term survival. It is unknown how long a mast cell can survive containing intracellular bacteria. Intracellular *S aureus* may have the ability to lie dormant within the cell until the mast cell naturally expires, which can be up to 300 days. Accumulated mast cells may provide new vectors for the now extracellular *S aureus* and the process may continue. As in biofilm disease, there may be periodic times of bacterial amplification, which may result in clinical deterioration or recurrent disease. This may help to explain the patient who suffers with life-long recalcitrant NP who develops recurrent disease every 2-5 years.

5.4.5 Host cell profiling

Recent guidelines have proposed the classification of CRSwNP and CRSsNP into two distinct pathological entities primarily based on differences in inflammatory cytokine profiles (3). Interestingly, the results from this study demonstrated a difference in the composition of inflammatory host cells between NP and adjacent non-polypoidal CRS sinonasal mucosa, from the same patients. Profiling of the host cells in NP revealed an eosinophilic profile associated with a Th-2 skewed cytokine pathway, consistent with the above classification (3). However, the adjacent non-polypoidal CRS sinonasal mucosa from the same patients with CRSwNP demonstrated a neutrophilic composition associated with a Th-1 skewed cytokine pathway, inconsistent with the above classification (3). As this study is the first to directly compare NP with non-polypoidal sinonasal mucosa from the same patients, these findings would suggest that the inflammatory profile is not uniform and may be tissue-specific (NP versus non-polypoidal mucosa).

5.5 Conclusion

The mast cell in the context of chronic *S aureus* infection may well act as a double-edged sword. Although promoting innate immunity against microbial pathogens, the mast cells may be providing a safe haven for *S aureus* by protecting it from extracellular antimicrobial compounds. This not only avoids clearance but also facilitates the establishment of an intracellular microbial reservoir that could lead to persistence and chronic carriage. This may explain the high levels of resistance to systemic antibacterial therapies in chronic conditions such as CRS. Crucially, these intracellular *S aureus* reservoirs may constitute potential future therapeutic targets for the development of novel bacterial eradication strategies, aimed at reducing systemic antimicrobial usage and in turn, the associated risk of antimicrobial drug resistance.

6 Investigation of mechanism of internalisation of *Staphylococcus aureus* into mast cells in nasal polyps

6.1 Introduction

The findings thus far suggest that the internalisation of *S aureus* into mast cells might be of relevance to nasal polyp (NP) formation (338). We have demonstrated an eosinophilic T_H-2-skewed cytokine profile in NP and a neutrophilic T-helper 1 (T_H-1) - skewed profile in the adjacent sinonasal mucosa in patients with chronic rhinosinusitis with NP (CRSwNP). These findings are contradictory to the recent EPOS guidelines which proposes the classification of CRS into CRSwNP and CRS without NP (CRSsNP) based on different cytokine profiles (T-helper 2 (T_H-2) and T_H-1, respectively) (3). NP and adjacent sinonasal mucosa appear to differ at a microscopic, macroscopic, microbiological and cytokine level. This suggests that alterations within the architecture of sinonasal mucosa, leading to the formation of NP, may result from dysfunction in the innate immunity at specific locations contributed to by exogenous agents.

One of the possible exogenous agents is bacteria, with evidence of *S aureus* as the most commonly detected microbe in CRS (97). Within the CRS sinonasal cavities, *S aureus* has been detected as free-floating planktonic microbes within surface-related biofilms (212) and as intracellular reservoirs (337--338) and its presence has been associated with poorer post-surgical outcomes (244). However, *S aureus* has also been identified as a non-pathogenic commensal that colonises the anterior nares in 20% of the population (95). What remains unknown is how a seemingly non-pathogenic commensal in an asymptomatic patient can turn into a pathogenic microbe capable of invading and occupying host cells.

The *S aureus* superantigen theory proposes that toxins released by certain *S aureus* phenotypes have an effect on multiple cell types, manipulating the local innate immunity with the net effect of creating a T_H2 skewed cytokine profile, recruiting eosinophils and mast cells leading to local tissue damage and remodelling (3, 97, 140, 333). It is also proposed that *S aureus* uses these toxins as a survival strategy to evade the host immune response.

6.2 Methods

6.2.1 Subjects

Seven consecutive patients with CRSwNP (CRS 40-46) were recruited into the study as described in *Section 2.2*.

6.2.2 Tissue sampling

For the explant tissue model, non-polypoidal tissue was obtained from the inferior turbinate of patients with CRSwNP (Figure 6.1).

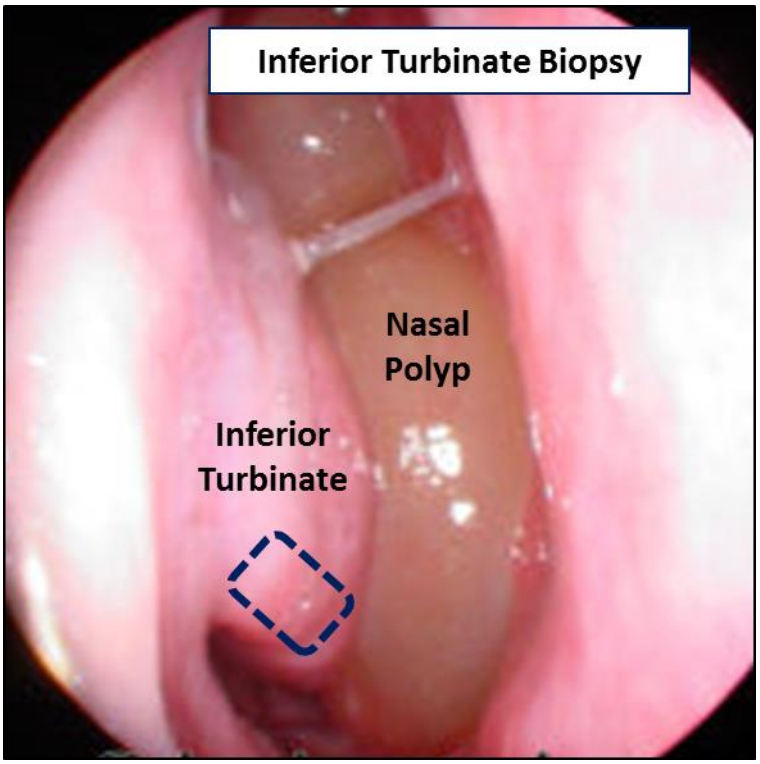

Figure 6.1 Non-polypoidal mucosal biopsy (blue dashed line) of inferior turbinate mucosa in patients with CRSwNP

6.2.3 Explant tissue model

The protocol for the explant tissue model is described in Chapter 2, *Section 2.18*. The initial treatment groups used are displayed in Table 6.1 (n=4). To investigate the effects of live and dead *S aureus* on the explant model, the treatment groups were modified for the final three samples (n=3) and are displayed in Table 6.2.

TREATMENT GROUP	TOPICAL ANTIBIOTIC	TREATMENT
Untreated	No	Fixed immediately for IHC
Culture	Yes	Cultured in RPMI for 24hrs
***S aureus* (live)**	Yes	Cultured with live *S aureus* ($1x10^6$ cells/ml) for 24 hrs
IL-4	Yes	Cultured with IL-4 (20µg/ml) for 24 hrs
SEB	Yes	Cultured with SEB (10µg/ml) for 24 hrs
***S aureus* (live) & SEB**	Yes	Cultured with live *S aureus* ($1x10^6$ cells/ml) & SEB (10µg/ml) for 24 hrs

Table 6.1 Initial groups with associated treatment regimens (n=4). IHC (immunohistochemistry); RPMI (Roswell Park Memorial Institute medium); IL-4 (Interleukin-4); SEB (Staphylococcus enterotoxin B)

TREATMENT GROUP	TOPICAL ANTIBIOTIC	TREATMENT
Control	Yes	Cultured in RPMI for 24hrs
***S aureus* (live)**	Yes	Cultured in live *S aureus* ($1x10^6$ cells/ml) for 24 hrs
***S aureus* (dead)**	Yes	Cultured in dead *S aureus* ($1x10^6$ cells/ml) for 24 hrs
SEB	Yes	Cultured in SEB (10µg/ml) for 24 hrs
***S aureus* (live) & SEB**	Yes	Cultured in live *S aureus* ($1x10^6$ cells/ml) & SEB (10µg/ml) for 24 hrs
***S aureus* (dead) & SEB**	Yes	Cultured in dead *S aureus* ($1x10^6$ cells/ml) & SEB (10µg/ml) for 24 hrs

Table 6.2 Modified groups with associated treatment groups (n=3). RPMI (Roswell Park Memorial Institute medium); SEB (*Staphylococcus* enterotoxin B)

6.2.4 Tissue analysis

Tissue was embedded in GMA for immunohistochemistry (IHC) and processed as described in *Section 2.15*.

6.2.5 Cell count

Cells were counted manually for each tissue section. The epithelial length and sub-epithelial areas were measured with the assistance of computerised image analysis (KS400 software with a Zeiss Axioskop 2 microscope and Axiocam, Zeiss, Bicester, UK). Calculations for cell counts are described in *Section 2.15.4*.

6.3 Results

6.3.1 Patient demographics

Patient demographics are demonstrated in Table 6.1.

Characteristics	CRSwNP
Subject no.	7
Mean age (range)	52 (33-78)
Sex	4M 3F
Current smokers	0
Aspirin sensitivity	0
Asthma	2
Positive skin prick testing	3*
Mean Lund-Mackay Score (range)	16.4 (11-21)

Table 6.3 Patient demographics. *(Patient 1: tree, grass, house dust mite (HDM), cat & dog dander; Patient 2: feathers, HDM, cat & dog dander; Patient 3: tree, grass & HDM)

6.3.2 Effects of Interleukin-4, *S aureus,* and *Staphylococcus* enterotoxin B on the explant tissue model

6.3.2.1 Untreated group

Biopsies designated to the untreated group were fixed within 20 minutes of being removed from the sinonasal cavity. This group was included to examine the morphology of *in situ* inferior turbinate mucosa. Interestingly, within the epithelial layer, there were significantly more *S aureus*$^{+ve}$ host cells (3.80 cell mm^{-1}) in the untreated group compared to the culture group (1.25 cells mm^{-1})

(p=0.0037, Figure 6.2, Table 6.4). However, this significant difference was not replicated in the sub-epithelial layer (Figure 6.3, Table 6.5), possibly suggesting an efficient and robust host immunity effectively dealing with the exogenous pathogens at the epithelial barrier.

Although not statistically significant, there was a trend for an increase in the number of mast cells within the epithelial layer of the untreated group, compared to the culture group (Figure 6.4, Table 6.6). In the sub-epithelial layer, the mast cell rate increased, becoming significantly higher than that of the culture group (p=0.0467, Figure 6.5, Table 6.7). This finding may be due to surface-related bacterial-biofilms on the turbinate mucosa, causing mast cell stimulation and recruitment into the epithelial and sub-epithelial layers.

This also demonstrates that within the explant tissue model, there were differences between the untreated and culture groups. As such, the culture group was used as the control in subsequent experiments.

6.3.2.2 Interleukin-4

IL-4 forms part of the T_H-2 cytokine milieu associated with NP and was utilised as an exogenous agent to observe its effect on intracellular *S aureus* and mast cells in the epithelial and sub-epithelial layers. Within the epithelial layer there was a significant increase in the number of both *S aureus*$^{+ve}$ host cells and in the mast cell rate (cells mm^{-1}) compared to the control group (p=0.0302 and p=0.0109, respectively, Figure 6.2 & 6.4, Tables 6.4 & 6.6). However, IL-4 appeared to have little or no effect on either the number of *S aureus*$^{+ve}$ host cells or mast cells in the sub-epithelial layer (Figures 6.3 & 6.5, Table 6.5 & 6.7).

6.3.2.3 *Staphylococcus aureus* and *Staphylococcus* enterotoxin B

Using live *S aureus* as an exogenous agent significantly increased both the number of *S aureus*$^{+ve}$ host cells (p=0.0011, Figure 6.2, Table 6.4) and the number of mast cells (p=0.0382, Figure 6.4, Table 6.6) within the epithelial layer, compared to the control group. The number of *S aureus*$^{+ve}$ host cells was

higher than the number of mast cells in the epithelial layer as most host cells invaded by *S aureus* were epithelial cells. Invasion of the epithelial layer by exogenous *S aureus* can be seen in Figure 6.6. However, within the sub-epithelial layer, no significant increase in the number of *S aureus*$^{+ve}$ host cells or mast cells was seen (Figure 6.3 &-6.5, Table 6.5 & 6.7).

Treating the tissue with SEB alone showed no significant effect on either the rate of *S aureus*$^{+ve}$ host cells or mast cells in the epithelial layer (Figures 6.2 & 6.4, Table 6.4 & 6.6). There was also no effect observed within the sub-epithelial layer (Figures 6.3 & 6.5, Table 6.5 & 6.7).

6.3.2.3.1 *Staphylococcus aureus* and *Staphylococcus* enterotoxin B within the epithelial layer

Interestingly, there was a remarkably enhanced effect seen when *S aureus* was combined with SEB. Within the epithelial layer, an eighteen-fold increase in *S aureus*$^{+ve}$ host cells and a 6.5-fold increase in the mast cell rate was observed compared to the control group (p=0.0001 & p=0.0001 respectively, Figures 6.2 & 6.4, Table 6.4 & 6.6). Also, the addition of SEB to *S aureus* demonstrated a 5.5-fold increase in the *S aureus*$^{+ve}$ host cells and a three-fold increase in mast cell rate, when compared with adding *S aureus* alone (p=0.0001 & p=0.0004 respectively, Figures 6.2 & 6.4, Table 6.4 & 6.6). A 22.5-fold increase in the *S aureus*$^{+ve}$ host cell rate and a 4-fold increase in mast cell rate was seen, when compared with SEB alone (p=0.0001 & p=0.0006 respectively, Figures 6.2 & 6.4, Table 6.4 & 6.6). The *S aureus*$^{+ve}$ host cell rate was twice that of the mast cell rate when directly compared. This is due to the majority of *S aureus*$^{+ve}$ host cells within the epithelial layer being identified as epithelial cells.

6.3.2.3.2 *Staphylococcus aureus* and *Staphylococcus* enterotoxin B within the sub-epithelial layer

The combination of *S aureus* and SEB showed a similar effect in the sub-epithelial layer. A 7-fold increase in *S aureus*$^{+ve}$ host cells and an 8-fold increase in the mast cell rate was observed compared to the control group (p=0.0001 & p=0.0001 respectively, Figures 6.3 & 6.5, Table 6.5 & 6.7). Figure 6.7

demonstrates mast cell recruitment under the epithelial basement membrane after treatment with *S aureus* and SEB. The addition of SEB to *S aureus* resulted in a three-fold increase in the number of *S aureus*$^{+ve}$ host cells and a 4-fold increase in the mast cell rate, when compared with adding *S aureus* alone (p=0.0013 & p=0.0001 respectively, Figures 6.3 & 6.5, Table 6.5 & 6.7). An 8-fold increase in the number of *S aureus*$^{+ve}$ host cells and a twelve-fold increase in mast cell rate was seen, when compared with SEB alone (p=0.0001 & p=0.0006 respectively, Figures 6.3 & 6.5, Table 6.5 & 6.7).

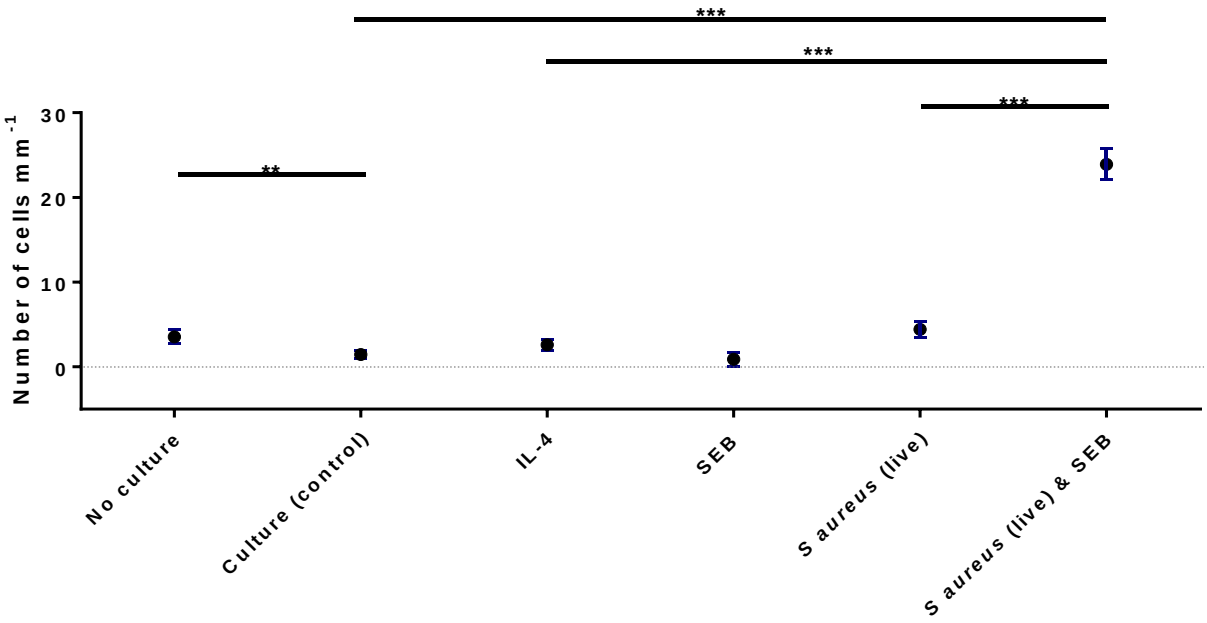

Figure 6.2 Effect of different treatments on the uptake of *S aureus* into epithelial host cells. Number of epithelial *S aureus*$^{+ve}$ host cells following 24-hour exposure to each treatment group, analysed using a mouse anti-*S aureus* monoclonal antibody in GMA embedded tissue sections. The combination of live *S aureus* with SEB significantly increased the number of *S aureus*$^{+ve}$ epithelial host cells within the epithelial layer compared to all other groups. Results are pooled data from 4 independent experiments (n=4). Error bars represent the means +/- 1SD. $^{**}p < 0.001$, $^{***}p < 0.0001$.

EPITHELIAL LAYER	Number of *S aureus*$^{+ve}$ host cells (cells mm^{-1})		
Treatment Groups	**Mean**	**95% confidence Interval**	***p*-value**
Untreated	3.80	0.9788,3.206	**0.0037**
Control	1.25	-	-
IL-4	2.86	0.1528,2.137	0.0302
SEB	1.03	-1.693, 0.538	0.2520
***S aureus* (live)**	4.19	1.718, 4.212	**0.0011**
***S aureus* (live) & SEB**	23.25	20.16, 24.74	**0.0001**

Table 6.4 Number of *S aureus*$^{+ve}$ epithelial cells (n=4).

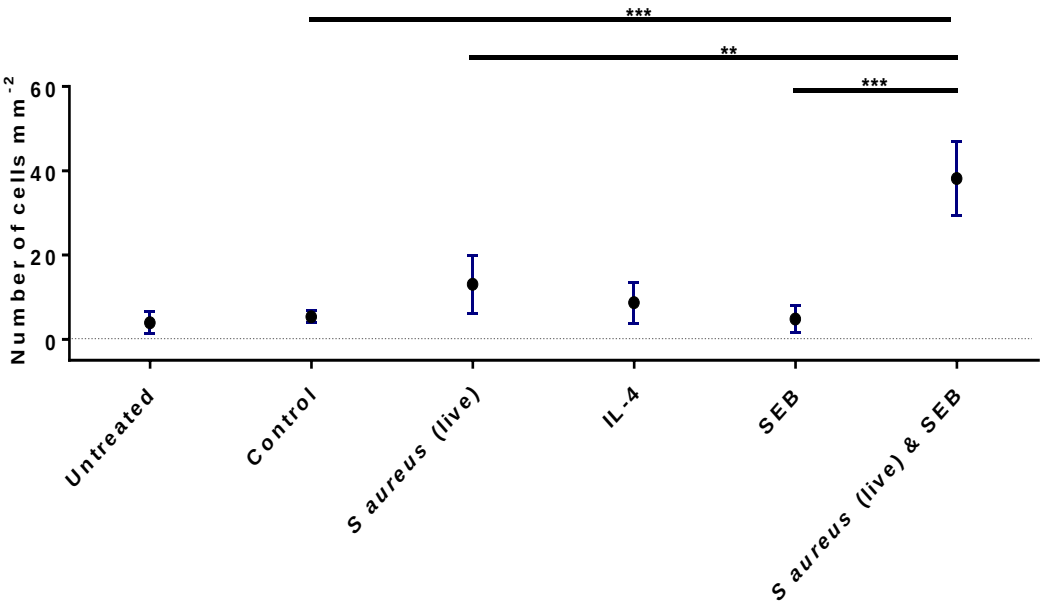

Figure 6.3 Effect of different treatments on the uptake of *S aureus* into sub-epithelial host cells. Number of *S aureus*$^{+ve}$ host cells within the sub-epithelial layer following 24-hour exposure to each treatment group, analysed using a mouse anti-*S aureus* monoclonal antibody in GMA embedded tissue sections. The combination of live *S aureus* with SEB significantly increased the number of sub-epithelial *S aureus*$^{+ve}$ host cells compared to all other groups. Results are pooled data from 4 independent experiments (n=4). Error bars represent the means +/- 1SD. ***p*<0.001, ****p*<0.0001.

SUB-EPITHELIAL LAYER	Number of *S aureus*$^{+ve}$ host cells (cells mm^{-1})		
Treatment Groups	**Mean**	**95% confidence interval**	***p*-value**
Untreated	3.91	-3.75, 0.87	0.1770
Control	5.34		
IL-4	8.67	-0.57, 7.22	0.0816
SEB	4.82	-3.18, 2.13	0.6441
***S aureus* (live)**	13.06	-7.80, 16.21	0.0680
***S aureus* (live) & SEB**	38.17	26.01, 39.64	**0.0001**

Table 6.5 Number of *S aureus*$^{+ve}$ sub-epithelial cells (n=4).

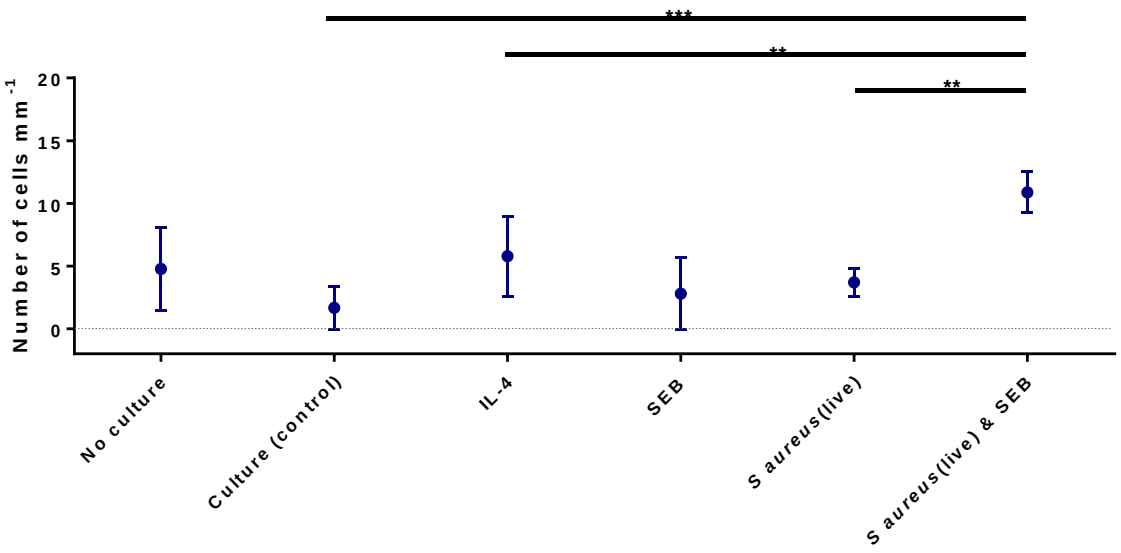

Figure 6.4 Effect of different treatments on the recruitment of mast cells into the epithelial layer. The number of mast cells (cells mm^{-1}) within the epithelial layer identified following 24-hour exposure to each treatment group, analysed using the AA1 anti-mast cell tryptase monoclonal antibody in GMA embedded tissue sections. The combination of live S aureus with SEB significantly increased the number of mast cells within the epithelial layer compared to all other groups. Results are pooled data from 4 independent experiments (n=4). Error bars represent the means +/- 1SD. **p < 0.001, ***p <0.0001.

EPITHELIAL LAYER	Number of mast cells (cells mm^{-1})		
Treatment Groups	**Mean**	**95% confidence interval**	***p*-value**
Untreated	4.77	-1.121, 7.326	0.1223
Control	1.67	-	-
IL-4	5.785	1.346, 6.884	**0.0109**
SEB	2.795	-1.450, 3.700	0.3262
***S aureus* (live)**	3.71	0.1505, 3.923	**0.0382**
***S aureus* (live) & SEB**	10.89	6.820, 11.62	**0.0001**

Table 6.6 Number of epithelial mast cell (n=4).

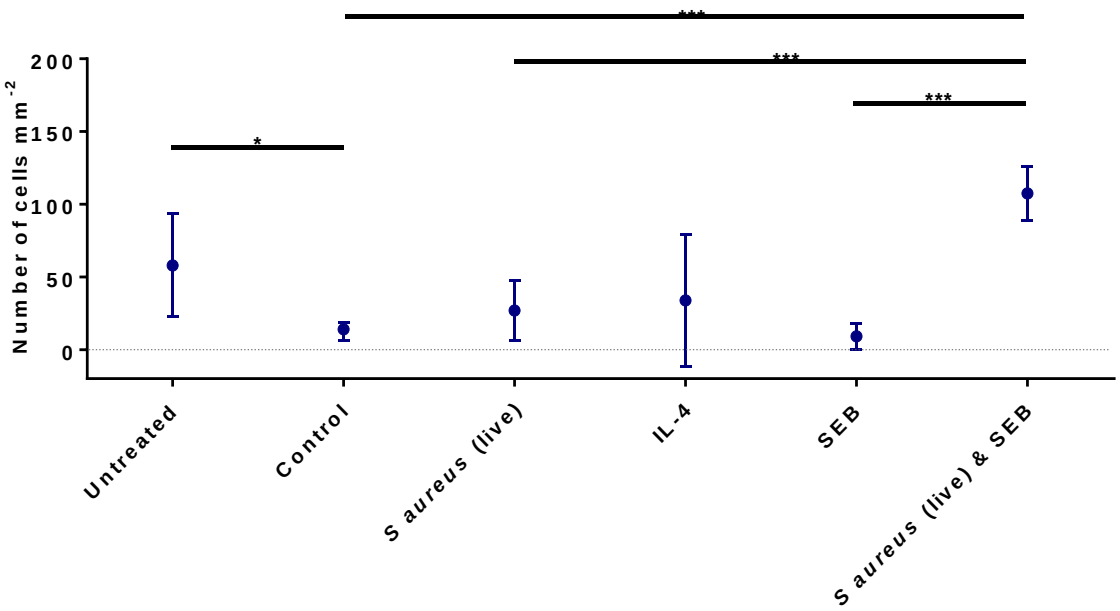

Figure 6.5 Effect of different treatments on the recruitment of mast cells into the sub-epithelial layer. Number of mast cells within the sub-epithelial layer following 24-hour exposure to each treatment group, analysed using an AA1 anti-mast cell tryptase monoclonal antibody in GMA embedded tissue sections. The combination of live *S aureus* with SEB significantly increased the number of mast cells within the sub-epithelial layer compared to all other groups. Results are pooled data from 4 independent experiments (n=4). Error bars represent the means +/- 1SD. *p<0.05, ***p<0.0001.

SUB-EPITHELIAL LAYER	Number of mast cells (cells mm^{-2})		
Treatment Groups	**Mean**	**95% confidence interval**	***p*-value**
Untreated	57.96	0.91, 0.05	0.0467
Control	13.08		
IL-4	33.81	-15.02, 56.49	0.2057
SEB	9.06	-14.29, 6.24	0.3747
***S aureus* (live)**	26.85	-3.87, 31.40	0.1047
***S aureus* (live) & SEB**	107.50	78.21, 110.50	**0.0001**

Table 6.7 Number of sub-epithelial mast cells (n=4).

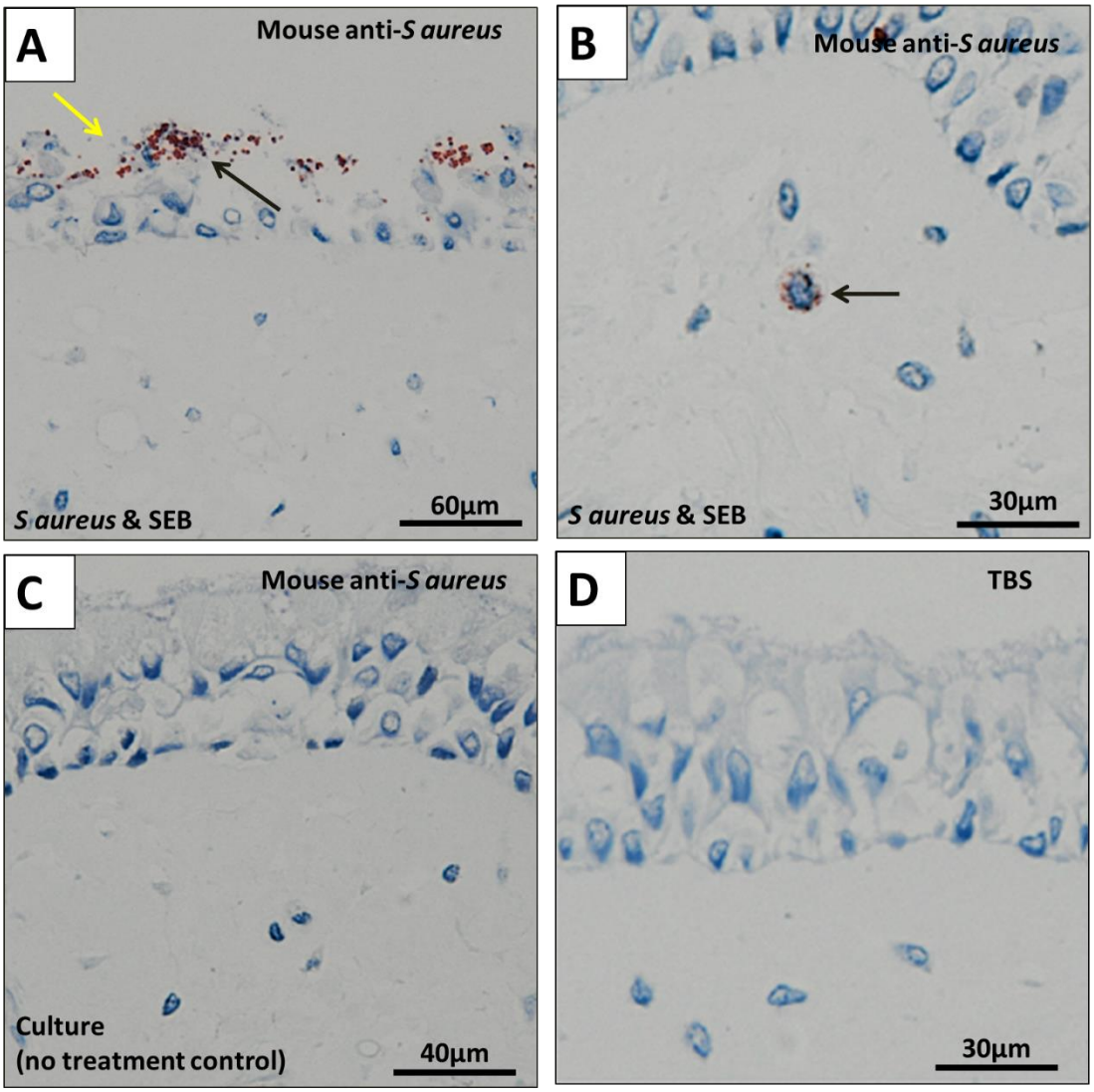

Figure 6.6 Immunostaining of *S aureus* invasion of the epithelial and sub-epithelial layers. Photomicrographs of GMA embedded inferior turbinate tissue stained with mouse anti-*S aureus* monoclonal antibody and AEC substrate (n=7). (A & B) are tissue sections treated with *S aureus* and SEB. (C) Control sample treated with culture medium only. (D) TBS non-primary antibody control sample. Image (A) demonstrates *S aureus* bacterial biofilm (yellow arrow) invading the epithelial cells (black arrow). Image (B) demonstrates intracellular *S aureus* within a mast cell in the sub-epithelial layer. (C & D) Demonstrate no intracellular *S aureus*.

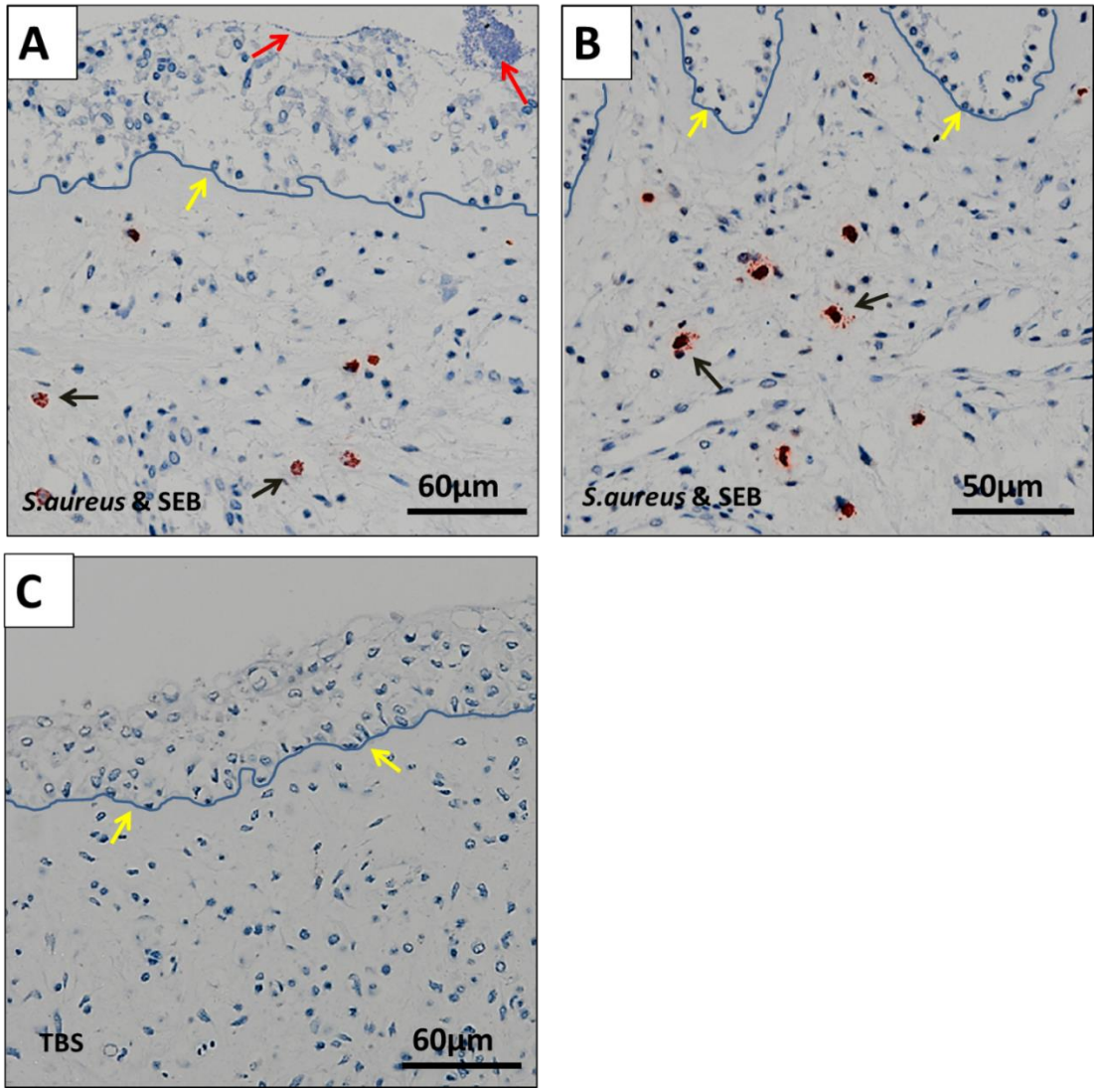

Figure 6.7 Mast cell accumulation after treatment with *S aureus* & *Staphylococcus* enterotoxin B (n=7). Photomicrographs of GMA embedded inferior turbinate tissue stained with AA1 anti-mast cell tryptase monoclonal antibody with AEC substrate. (A & B) Demonstrates mast cell recruitment (black arrow) below the epithelial basement membrane (yellow arrow) stimulated by the combination of a surface-related *S aureus* biofilm (red arrow) and SEB. (C) Shows the TSB control.

6.3.3 Effect of the *Staphylococcus aureus* viability in the explant tissue model

The initial findings from the explant tissue model demonstrate that the addition of SEB to *S aureus* stimulates mast cell recruitment and intracellular localisation of *S aureus* within host cells in both the epithelial and sub-epithelial layers. Little or no effect was observed using IL-4. To investigate how the viability of *S aureus* influences these effects, additional experiments were carried out using non-viable *S aureus* (See Chapter 2, *Section 2.18.2*).

6.3.3.1 Epithelial layer

Within the epithelial layer, in both the *S aureus* (live) and *S aureus* (live) with SEB groups, a significant increase was demonstrated in the number of *S aureus*$^{+ve}$ host cells (p=0.0314 & p=0.0065, respectively, Figure 6.8, Table 6.8). However, only *S aureus* (live) with SEB showed a significant increase in the mast cell rate (p=0.0422, Figure 6.10, Table 6.10). *S aureus* (live) demonstrated significantly higher numbers of *S aureus*$^{+ve}$ host cells and mast cell rates within the epithelial layer, compared to *S aureus* (dead) (p=0.0255 & p=0.0237 respectively, Figures 6.8 & 6.10, Tables 6.8 & 6.10). Significantly higher numbers of *S aureus*$^{+ve}$ host cells and mast cell rates were also demonstrated when the *S aureus* (live) with SEB group was directly compared to *S aureus* (dead) with SEB group (p=0.0068 & p=0.0568 respectively, Figures 6.8 & 6.10, Tables 6.8 & 6.10). These results indicate that in the epithelial layer, *S aureus* must be viable to initiate and exert any effect on intracellular localisation and/or mast cell recruitment.

6.3.3.2 *Sub-epithelial layer*

Within the sub-epithelial layer, the findings were similar to those seen within the epithelial layer (Figures 6.9 & 6.11, Tables 6.9 & 6.11. These results indicate the essential need for *S aureus* to be viable in order to exert any effect on both intracellular invasion and mast cell recruitment in the sub-epithelial layer.

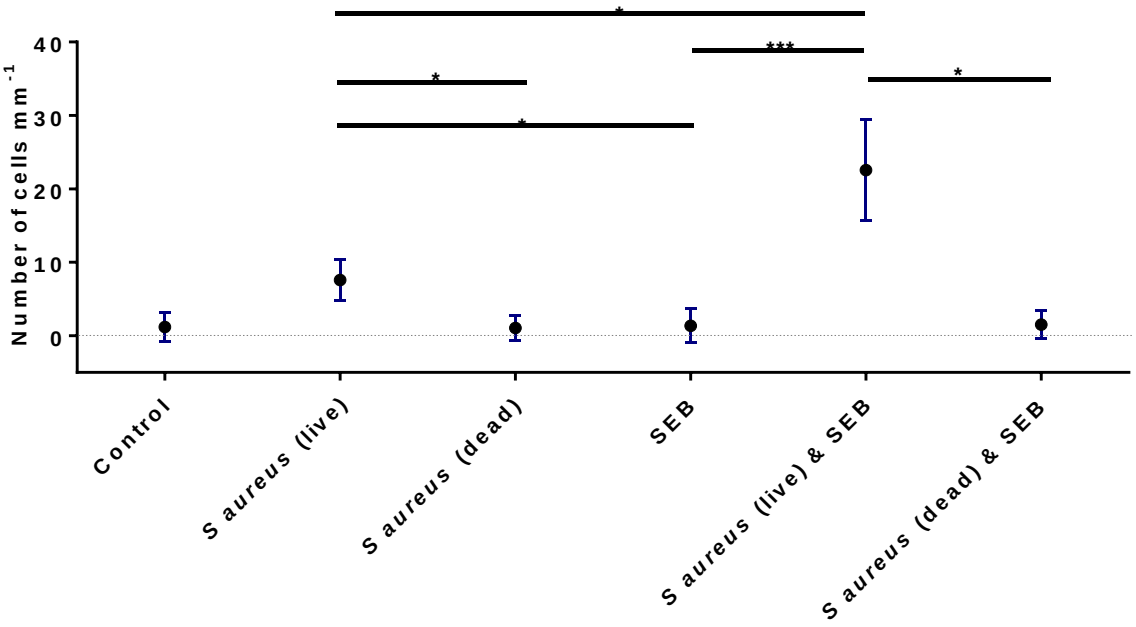

Figure 6.8 Effect of live & dead *S aureus* on intracellular invasion of *S aureus* in the epithelial layer. Both the *S aureus* (live) and *S aureus* (live) with SEB groups demonstrated significantly increased numbers of *S aureus*$^{+ve}$ host cells compared to their respective groups containing non-viable *S aureus* (dead). The addition of SEB to *S aureus* (live) demonstrated significantly more *S aureus*$^{+ve}$ host cells compared to *S aureus* (live) alone. Results are pooled data from three independent experiments (n=3). Error bars represent the means +/- 1SD. *p<0.05, ***p<0.0001.

EPITHELIAL LAYER	Number of *S aureus*$^{+ve}$ host cells (cells mm^{-1})		
Treatment Groups	**Mean**	**95% confidence interval**	***p*-value**
Culture (control)	1.19	-	-
***S aureus* (live)**	7.58	0.93, 11.85	**0.0314**
***S aureus* (dead)**	1.06	-4.23, 3.96	0.9323
SEB	1.36	-4.72, 5.05	0.9291
***S aureus* (live) & SEB**	22.55	9.95, 32.77	**0.0065**
***S aureus* (dead) & SEB**	4.84	-8.98, 16.28	0.4672

Table 6.8 Numbers of *S aureus*$^{+ve}$ host cells within the epithelial layer

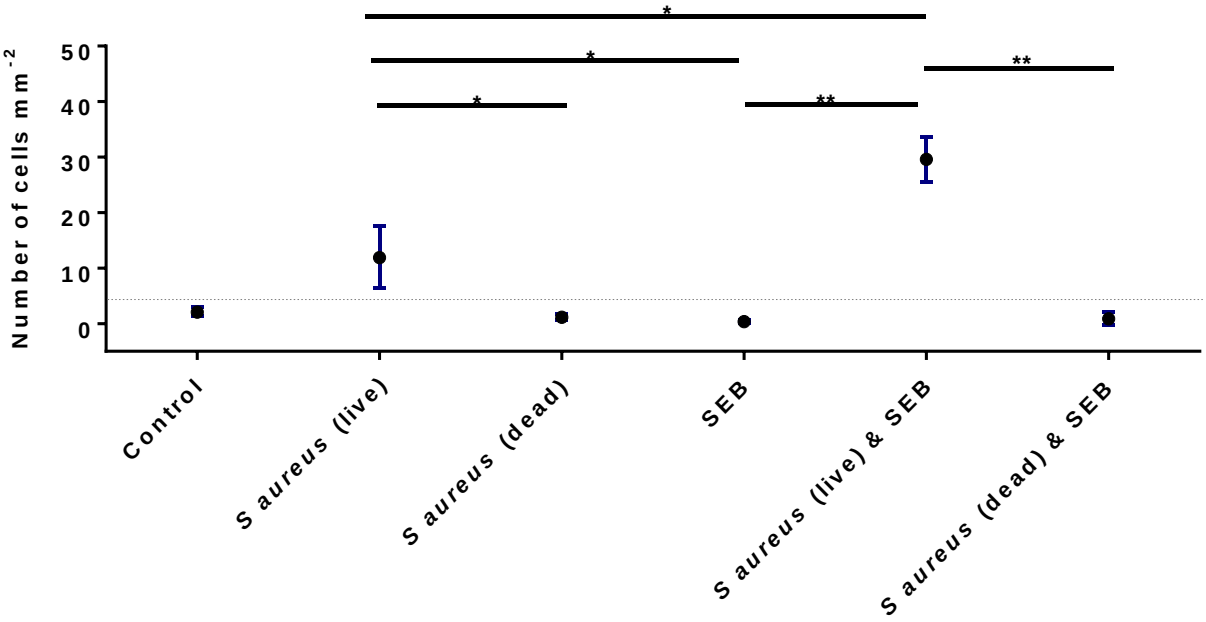

Figure 6.9 Effect of live & dead *S aureus* on the uptake of *S aureus* within host cells within the sub-epithelial layer. The number of *S aureus*$^{+ve}$ host cells within the sub-epithelial layer after 24-hour exposure to each treatment group, analysed using a mouse anti-*S aureus* monoclonal antibody on GMA embedded tissue sections. The *S aureus* (live) and *S aureus* (live) with SEB group demonstrated significantly increased numbers of *S aureus*$^{+ve}$ host cells compared to controls, groups containing non-viable *S aureus* (dead) and the SEB only group. The addition of SEB to *S aureus* (live) significantly increased the rate of *S aureus*$^{+ve}$ host cells compared to *S aureus* (live) alone. Results are pooled data from three independent experiments (n=3). Error bars represent the means +/- 1SD. *p<0.05, **p<0.001.

SUB-EPITHELIAL LAYER	Number of *S aureus*$^{+ve}$ host cells (cells mm^{-2})		
Treatment Groups	**Mean**	**95% confidence intervals**	***p*-value**
Control	2.08		
***S aureus* (live)**	11.91	0.76, 18.89	**0.0396**
***S aureus* (dead)**	1.14	-2.50, 0.60	0.1647
SEB	0.33	-0.36, 3.15	0.0651
***S aureus* (live) & SEB**	29.57	20.90, 34.07	**0.0003**
***S aureus* (dead) & SEB**	0.86	-3.54, 1.09	0.2165

Table 6.9 Number of sub-epithelial *S aureus*$^{+ve}$ host cell

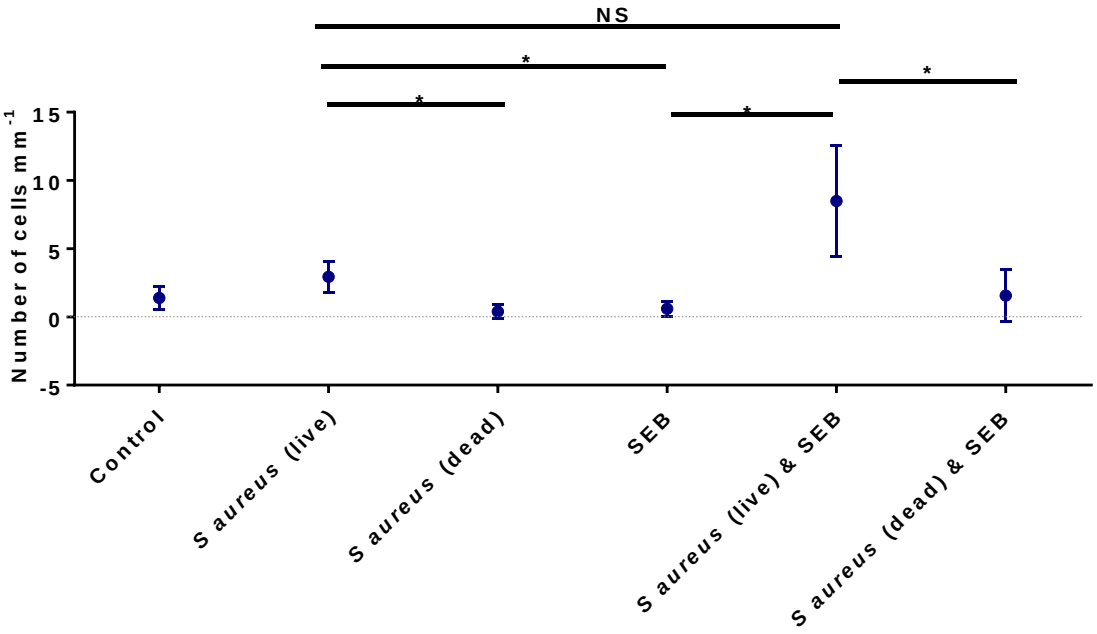

Figure 6.10 Effect of live & dead *S aureus* on mast cells within the epithelial layer. The rate of mast cells within the epithelial layer following 24-hour exposure to each treatment group, analysed using an AA1 anti-mast cell tryptase monoclonal antibody on GMA embedded tissue sections. The *S aureus* (live) with SEB group demonstrated significantly increased numbers of mast cells compared to controls, groups containing non-viable *S aureus* (dead) and the SEB only group. Results are pooled data from three independent experiments (n=3). Error bars represent the means +/- 1SD. *p<0.05, NS not significant.

EPITHELIAL LAYER	Number of mast cells (cells mm^{-1})		
Treatment Groups	**Mean**	**95% confidence interval**	***p*-value**
Culture (control)	4.71	-	
***S aureus* (live)**	2.93	-0.70, 3.80	0.1285
***S aureus* (dead)**	0.40	-0.99-10.58	0.1617
SEB	0.60	-0.78, 0.58	0.2485
***S aureus* (live) & SEB**	8.49	0.40, 13.80	**0.0422**
***S aureus* (dead) & SEB**	1.57	-3.17, 3.54	0.8868

Table 6.10 Number of epithelial mast cells

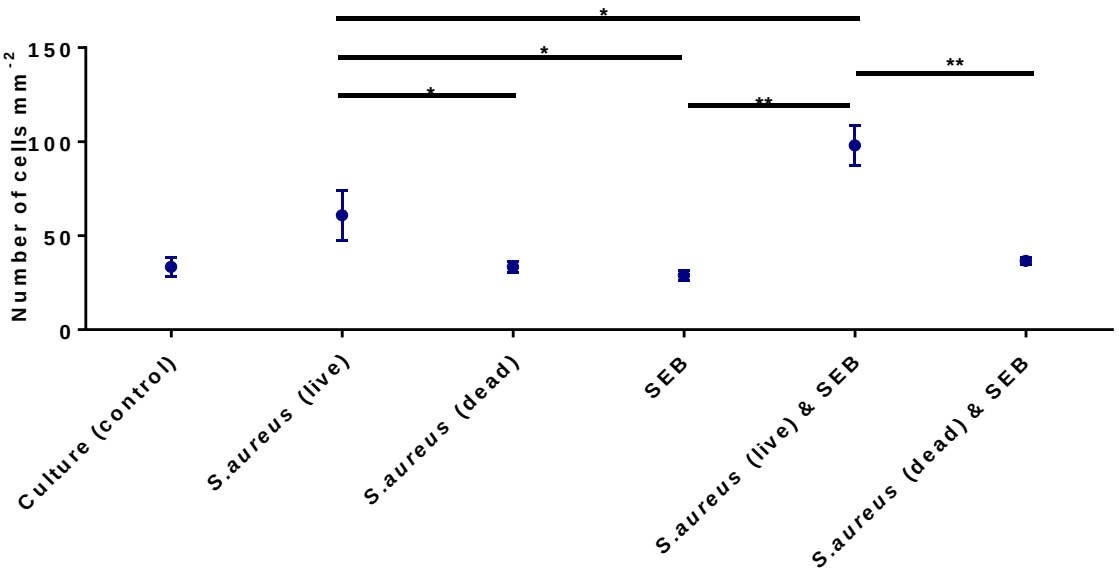

Figure 6.11 Effect of live & dead *S aureus* on mast cells. The number of mast cells within the sub-epithelial layer following 24-hour exposure to each treatment group, analysed using an AA1 anti-mast cell tryptase monoclonal antibody in GMA embedded tissue sections. The *S aureus* (live) and *S aureus* (live) with SEB group demonstrated significantly increased numbers of *S aureus*$^{+ve}$ host cells compared to controls, groups containing non-viable *S aureus* (dead) and the SEB only group. The addition of SEB to *S aureus* (live) significantly increased the rate of *S aureus*$^{+ve}$ host cells compared to *S aureus* (live) alone. Results are pooled data from three independent experiments (n=3). Error bars represent the means +/- 1SD. *p<0.05, **p<0.001.

SUB-EPITHELIAL LAYER	Number of mast cells (cells mm^{-2})		
Treatment Groups	**Mean**	**95% confidence intervals**	***p*-value**
Control	33.38		
***S aureus* (live)**	60.87	4.96, 50.03	**0.0276**
***S aureus* (dead)**	33.43	-9.07, 9.18	0.9878
SEB	28.92	-13.23, 4.30	0.2305
***S aureus* (live) & SEB**	97.96	45.97, 83.20	**0.0006**
***S aureus* (dead) & SEB**	36.65	-5.10, 11.63	0.3391

Table 6.11 Sub-epithelial *S aureus*$^{+ve}$ host cells

6.3.4 Epithelial proliferation

The Ki67 monoclonal antibody was used to investigate epithelial proliferation in different treatment groups (Figure 6.12). Live *S aureus* appears to have little effect on epithelial proliferation, but this is significantly increased when combined with SEB (p=0.0001, Figure 6.13). *S aureus* (live) combined with SEB demonstrated a significant increase in epithelial cell proliferation compared to *S aureus* (dead) with SEB and SEB alone (p=0.0001 & p=0.0001 respectively, Figure 6.13).

6.3.5 Mast cell degranulation

Mast cell degranulation was assessed on IHC sections, stained with AA1 anti-mast cell tryptase monoclonal antibody. Degranulating mast cells were identified as mast cell tryptase 'blushes' and granule dissemination. The different stages in mast cell degranulation are shown in Figure 6.14. *S aureus* (live) alone showed no significant increase in mast cell degranulation compared to the control group. However, in combination with exogenous SEB, *S aureus* (live) induced a significant increase in mast cell degranulation compared to control, *S aureus* (live) alone, SEB and *S aureus* (dead) with SEB (p=0.0002, p=0.0050, p=0.0003, p=0.0025 respectively, Figure 6.15).

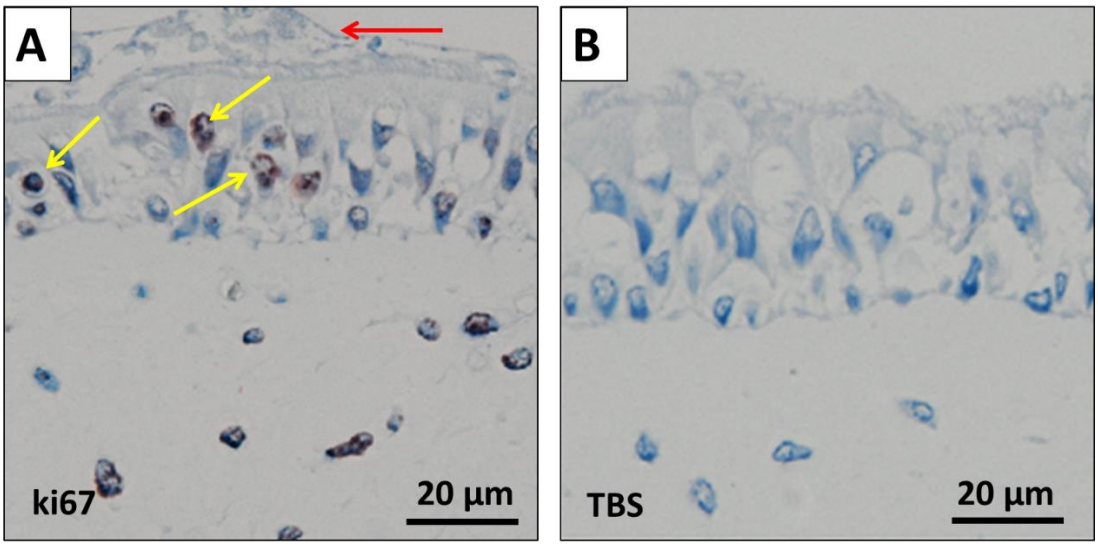

Figure 6.12 Investigating epithelial proliferation using immunohistochemical staining. Photomicrographs of GMA embedded inferior turbinate tissue stained with Ki67. A) Photomicrograph shows epithelial proliferation (yellow arrows) in tissue treated with *S aureus* & SEB. A *S aureus* biofilm can be seen attached to the epithelial surface (red arrow). B) Shows the TSB control.

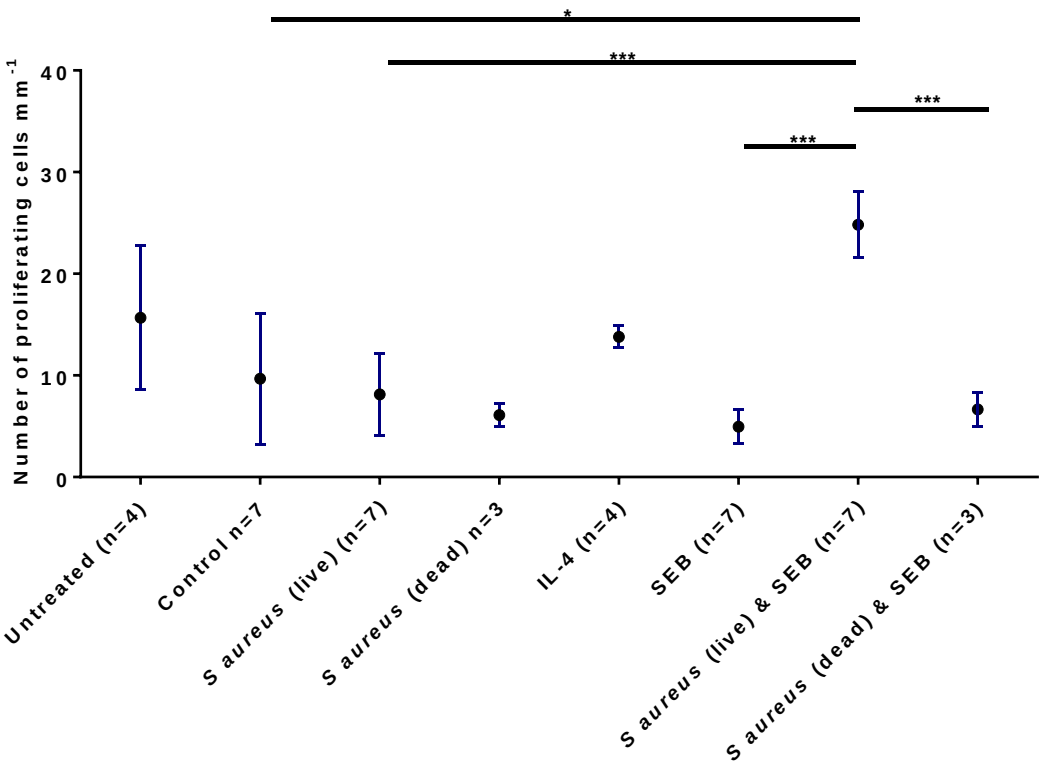

Figure 6.13 Epithelial cell proliferation in various treatment groups (n=7). The *S aureus* (live) with SEB group demonstrated a significant increase in epithelial proliferation compared to other groups. Error bars represent the means +/- 1SD. *p<0.05, ***p<0.0001.

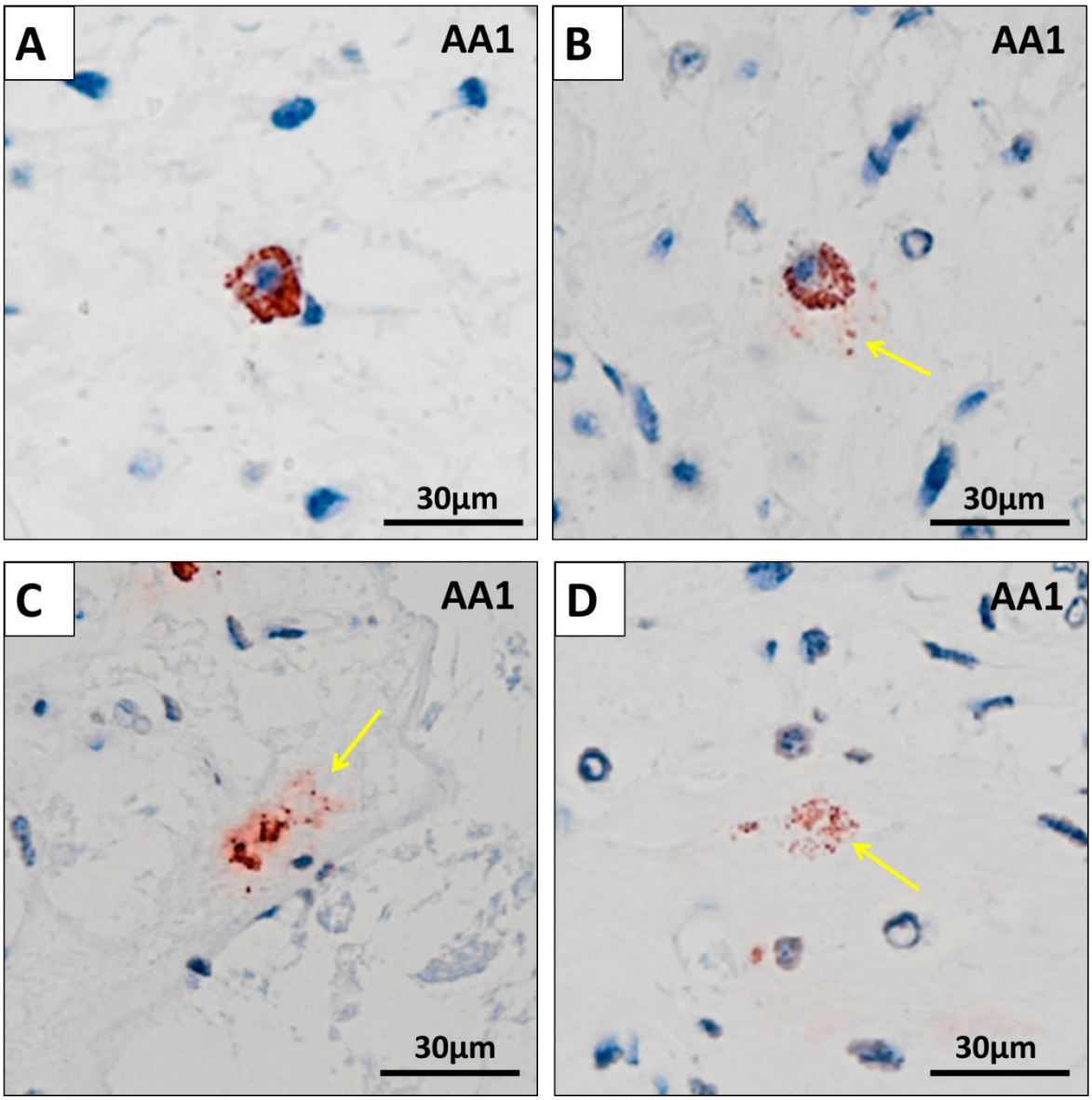

Figure 6.14 Stages of mast cell degranulation. Photomicrographs of GMA embedded inferior turbinate after 24-hour exposure to *S aureus* (live) and SEB and stained with AA1 anti-mast cell tryptase with AEC substrate. (A) Demonstrates a normal mast cell with intact granules (red) surrounding the cell nucleus (blue). (B) Demonstrates early mast cell degranulation with a mild mast cell tryptase 'blush' and disseminating granules (yellow arrow). (C & D) Demonstrate complete mast cell degranulation with a strong mast cell tryptase blush and fully disseminated granules (yellow arrows).

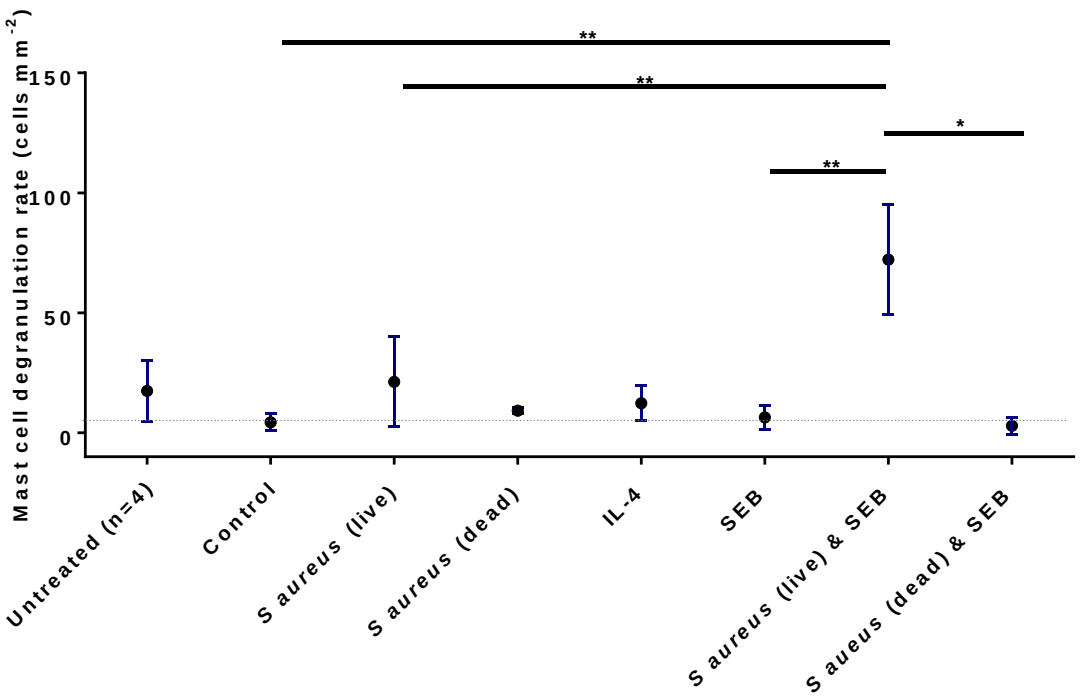

Figure 6.15 Mast cell degranulation rates in various treatment groups (n=7). The rate of mast cell degranulation following 24-hour exposure to each treatment. The *S aureus* (live) with SEB group demonstrated a significant increase in mast cell degranulation rates compared to other groups. Error bars represent the means +/- 1SD. *p<0.05, **p<0.001.

6.4 Discussion

The *Staphylococcal* superantigen (SAg) theory proposes that the exotoxins released from *S aureus* manipulate the local immunity within the sinonasal mucosa, leading to increased tissue damage and remodelling with the downstream result of NP formation (3, 100, 140, 333). SAgs have been demonstrated to exert effects on both host cells and the cytokines associated with local innate immunity (97). Host cells stimulated by the secretion of SAgs include epithelial cells, B and T cells, eosinophils, fibroblasts and mast cells (99-100). SAgs also cause up-regulation of IL-4 and IL-5 and down-regulation of TGF-β and IL-10 (101-102). Other effects reported include manipulation of eicosanoid metabolism (104-105), granulocyte augmentation (106), and the induction of glucocorticoid insufficiency (107). The net effect results in the conversion of a T_H1 cytokine profile in sinonasal mucosa into a T_H2 skewed cytokine profile, as seen in NP. This manipulation of the local innate immune system appears to be the result of a *S aureus* survival strategy.

The results presented here provide further evidence of the crucial role that SAgs play in the pathogenesis of NP formation. The explant tissue models provided a CRS mucosal template to analyse changes at the host-environment interface when different exogenous agents were applied. SEB has been shown to be associated with CRS and as such this was used in our experiment as the exogenous agent (3). The addition of SEB appeared to amplify the effects that *S aureus* had on the host innate immune system. *S aureus* with SEB demonstrated a significant increase in epithelial proliferation compared to other treatment groups. Epithelial cells play a crucial role in host defence, inflammation and mediation of the innate immune response as well as representing the first barrier for *S aureus* (83, 159). The epithelial cells are capable of neutralising microorganisms through the production of antimicrobial agents, including enzymes, permeabilising peptides, collectins and protease inhibitors (83). Epithelial cells express membrane bound and cytoplasmic pattern recognition receptors (PRRs) that recognise pathogen associated molecular patters (PAMPs) found in viruses and bacteria (3). Recognition through PRRs by the epithelial cells results in the release of chemokines and cytokines which recruit innate cellular defences (3). This results in upregulation of antigen-specific T and B cells through the release of

cell subtype-specific chemokines and the expression of soluble and cell surface-expressed molecules (83). Manipulation of these proteins by *S aureus* and SEB could alter the innate immune reaction leading to a change in the cytokine pathway.

Epithelial cells also express proteins called damage-associated molecular patterns (DAMPs), which allow detection of epithelial damage (161, 165). It is possible that these proteins are also manipulated by *S aureus* and SEB, leading to the proliferation of epithelial cells and a state of disordered repair of the epithelial barrier. Epithelial cells can survive for up to 10 days, but this will be significantly reduced in an aggressive bacterial invasion. Increased epithelial cell death will lead to increased proliferation of the remaining healthy epithelial cells.

In this study, SEB combined with *S aureus* resulted in a significant increase in epithelial cell proliferation. This proliferation most likely represented epithelial remodelling resulting from excessive release of cytokines, enzymes and mediators from damaged epithelial cells, rather than as a result of tissue preparation errors. A damaged epithelial layer leads to weakness in the tight-junction proteins and instability of the epithelial layer, allowing more bacteria to invade the sub-epithelial layer. In this study, the addition of SEB to *S aureus* significantly increased the recruitment of mast cells into the epithelial layer. This is a novel finding. Mast cells are often described as sentinel cells in the defence against pathogenic agents. With the intention of neutralising pathogens infiltrating the epithelial layer, mast cells appear to be unwittingly recruited into the epithelium, either directly or indirectly by *S aureus* in combination with SEB. Once within the epithelial layer, some of the mast cells appear to be infiltrated by the *S aureus*, followed by migration into the sub-epithelial layer laden with intracellular *S aureus* and potentially forming reservoirs which can constantly seed bacteria.

SEB combined with *S aureus* demonstrated a significant increase in the number of sub-epithelial *S aureus*$^{+ve}$ mast cells. *S aureus* was shown to be resident within up to 35.5% of sub-epithelial mast cells within this group. Initially, the *S aureus*$^{+ve}$ mast cells may be migrating into the sub-epithelial layer with seeding into the stroma through induction of mast cell degranulation, and uptake into newly recruited mast cells. A significant increase in mast cell

degranulation within the sub-epithelial layer was observed within the *S aureus* with SEB treatment group, adding strength to this proposed mechanism. Previous studies have demonstrated a significantly higher number of degranulating mast cells in nasal polyps, compared to inferior turbinate mucosa and non-CRS mucosa (339). Having reproduced these findings in our explant tissue model, it is likely that this synergistic effect of combined SEB and *S aureus* is important in NP pathogenesis.

A limitation of the study was the small sample number. Despite this, the results were reproducible. A further factor was the limited number of exogenous agents tested. However, the selection of these exogenous agents was evidence-based and in keeping with similar research carried out in this area.

6.5 Conclusion

Evidence has been provided of the ability of SEB to significantly enhance the ability of *S aureus* to influence the local innate immune response. The resultant internalisation of the bacteria into the mast cell could represent an immune-evasion strategy as well as a mechanism of ongoing seeding of the bacteria, contributing to the persistence of the inflammatory reaction and development of chronicity. In order to further investigate the mechanistic processes responsible for these observations, a cell culture model was used.

7 Investigation of *Staphylococcus aureus* internalisation using a co-culture model

7.1 Introduction

Mast cells are multifunctional sentinels that lie within the epithelial and sub-epithelial layers and form key elements of the innate immune surveillance and are active at the host-environmental interface where exogenous antigens are most often encountered (203, 340). The role of mast cells in allergic reactions, mediated by their high-affinity IgE receptors, is well documented (341). However, their role as host defence cells against invading pathogens is less well known. It is currently recognised that mast cells have the ability to recognise specific pathogens, due to antibody-dependent activation and can secrete a selective range of cytokines and inflammatory mediators specific to the invading organism, resulting in enhanced effector cell recruitment (342). They are also able to interact directly with pathogens, exerting a range of antimicrobial activities (343). These include secretion of extracellular antimicrobial compounds, such as antimicrobial peptides and reactive oxygen species (344), opsonin-mediated phagocytosis (345) and through the use of extracellular DNA traps (346).

Our analysis of bacterial profiles in nasal polyps (NP) has shown that *S aureus* is able to internalise within mast cells potentially compromising their antimicrobial activity (338). Furthermore, investigation of the host-environment interface using an inferior turbinate explant tissue model found that *Staphylococcus* Enterotoxin B (SEB) appeared to play a crucial role in this process, with significant enhancement of both local mast cell recruitment and intracellular residency of *S aureus*. The end result was an increase in mast cell degranulation, either as a mechanism of the mast cell to eradicate the intracellular microbes or as a bacterial survival strategy. Importantly though, mast cell degranulation also leads to increased levels of cytokines, chemokines, lipid mediators, histamine, leukotrienes proteases and TNF release or synthesis within the extracellular compartment, resulting in localised oedema and increased vascular permeability. This in turn may drive the formation of NP (342).

In order to further understand the mechanisms involved, interactions between *S aureus* and a human mast cell line (HMC-1) were studied using a co-culture assay model.

7.2 Methods

7.2.1 Bacterial strain

The *S aureus* strain used in this study was previously isolated from a patient with chronic rhinosinusitis with NP (CRSwNP) and was the same strain used in previous experiments. The isolation technique is described in *Section 2.6*. The preparation of live and dead S aureus is described in *Section 2.18.1 and 2.18.2.*

7.2.2 Human mast cell line co-culture conditions

The human mast cell line HMC-1 was harvested and prepared for the co-culture assay as described in Chapter 2, *Section 2.19*.

7.2.3 Co-culture assay

The co-culture assay experiments are described in full in *Section 2.19.2*

7.2.4 Mast cell proliferation

Mast cell proliferation, measurements and calculations are described in Sections *2.19.2.1 to 2.19.2.4*

7.3 Results

7.3.1 *Staphylococcus aureus*$^{+ve}$ mast cells

The Click-iT® EdU Edu kit assay, combined with DAPI and imaged with CLSM, demonstrated intracellular *S aureus*$^{+}$ within mast cells (*S aureus*$^{+ve}$ mast cells) at 24 hours, within both the *S aureus* (live) and *S aureus* & SEB treatment groups (Figure 7.1). Within the mast cells, *S aureus* was shown to be proliferating, confirming viability (Figure 7.1D). No intracellular *S aureus* was demonstrated in any of the other 5 treatment groups.

7.3.2 Mast cell proliferation

The proliferation rates are shown in Figure 7.2. Within the control group, 52% of mast cells proliferated over 24 hours. There was no significant difference in proliferation rates between the control group and the SEB, *S aureus* (dead), *S aureus* (dead) with SEB, or lysostaphin treatment groups. The exogenous agents within these groups appeared to have no effect on mast cell proliferation. However, proliferation of mast cells was significantly reduced to 5% (p=0.0045) and 3% (p=0.0021, Figure 7.2), within the *S aureus* (live) and *S aureus* (live) with SEB treatment groups, respectively. It appeared that SEB had little effect on mast cell proliferation when combined with *S aureus* (live) compared with *S aureus* (live) alone (p=0.6349).

7.3.3 Mast cell size

Mast cell size appeared to vary between different treatment groups (Figure 7.3). The diameter of each mast cell in each treatment group was measured. When directly comparing the mean diameters of each treatment group, both the *S aureus* (live) and the *S aureus* (live) with SEB groups contained significantly larger mast cells than the control group (p=0.0001 and p=0.0001, respectively, Figure 7.3 & Table 7.2). The mean diameter of mast cells within the control group was 10.95µm compared to 15.28µm in the *S aureus* (live)

group and 15.37μm in the *S aureus* with SEB group. Initially, no statistical significance was observed between the two treatment groups containing live *S aureus*. (p=0.8459, Figure 7.4). Within both these groups, *S aureus*$^{+ve}$ mast cells were separated from those without any intracellular *S aureus* and these cell diameters were directly compared (Figure 7.5). Within both the *S aureus* (live) and *S aureus* (live) with SEB treatment groups, *S aureus*$^{+ve}$ mast cells were significantly larger than those without intracellular bacteria (p=0.0001 and p=0.0001, respectively, Figure 7.5). When the mean diameters of the *S aureus*$^{+ve}$ mast cells were compared between the two groups, *S aureus* with SEB demonstrated significantly larger mast cells than the *S aureus* (live) group alone (p=0.0018, Figure 7.6).

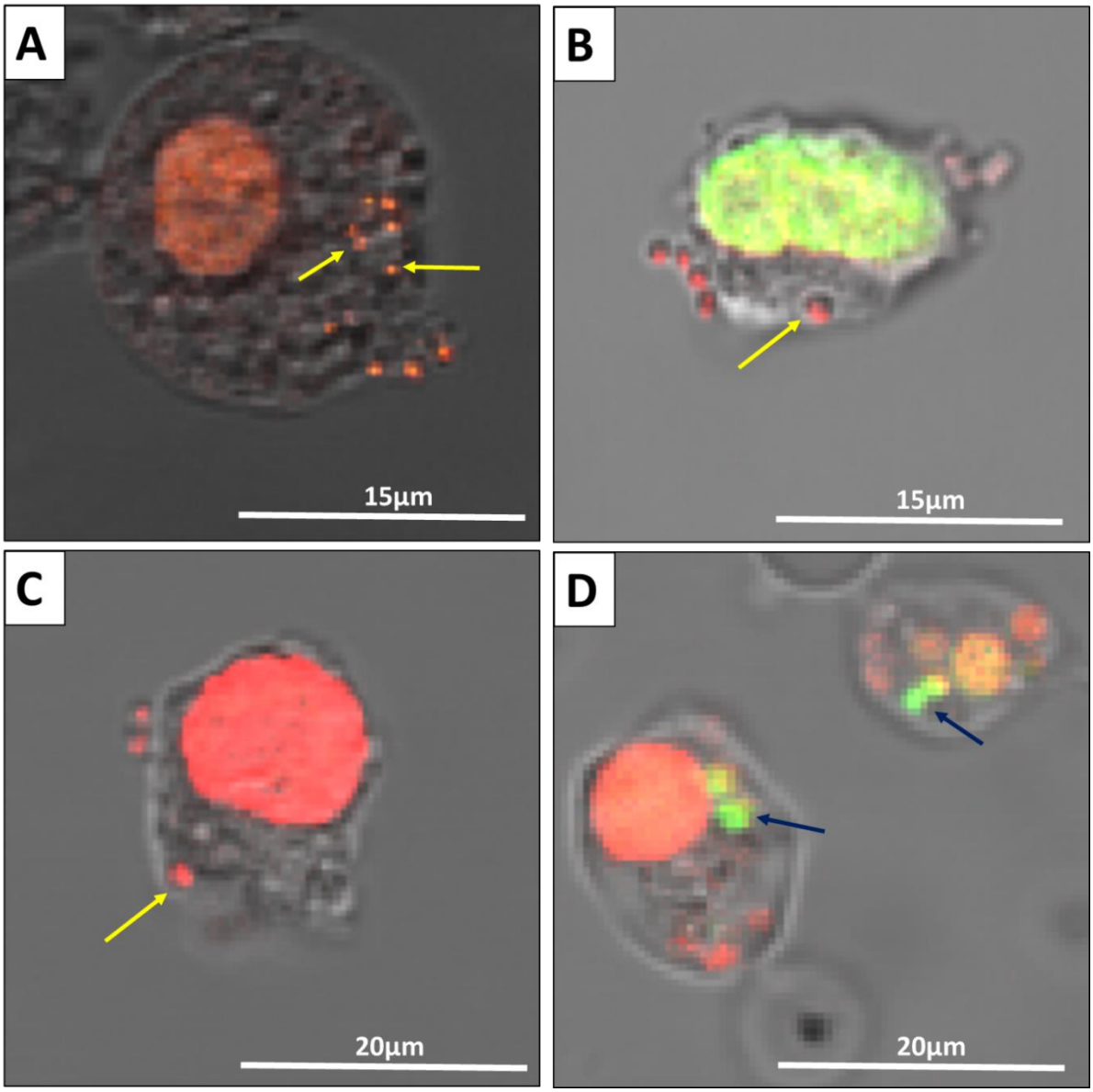

Figure 7.1 *S aureus*$^{+ve}$ HMC-1 mast cells. Representative CLSM images of mast cells (HMC-1) co-cultured with a CRS *S aureus* isolate combined with SEB and stained with a combination of the Click-iT® Edu proliferation kit and DAPI. Images (A & C) demonstrate intracellular residency of *S aureus* within the mast cell's cytosol (yellow arrows). (B) One of only a few proliferating mast cells (green nucleus) containing intracellular *S aureus* (yellow arrow) (D) Proliferating intracellular bacteria (green) within the cytosol of multiple mast cells (blue arrows).

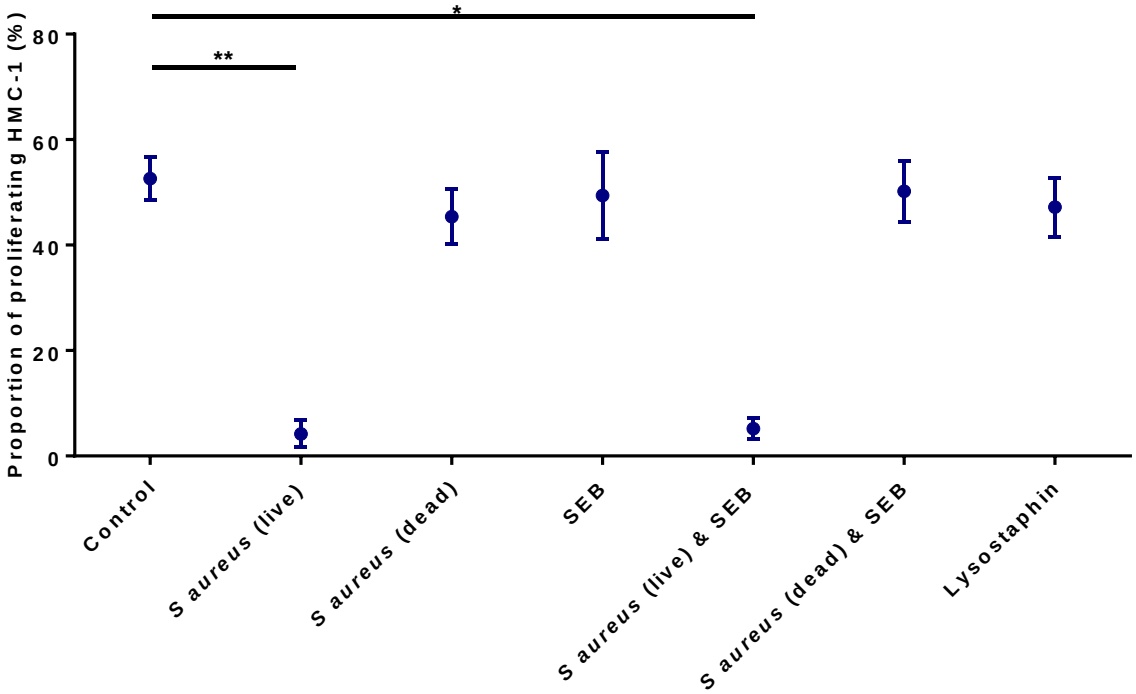

Figure 7.2 Proportion of proliferating mast cells for each treatment group. Percentage of HMC-1 cells proliferating after 24-hour exposure to each treatment group, analysed with the Click-iT® Edu proliferation kit and imaged with CLSM. Treatment groups containing live *S aureus* significantly reduced the proliferation of HMC-1 cells compared to controls. Results are pooled data from two independent experiments. Error bars represent the means +/- 1SD. *$p < 0.05$, **p <0.001.

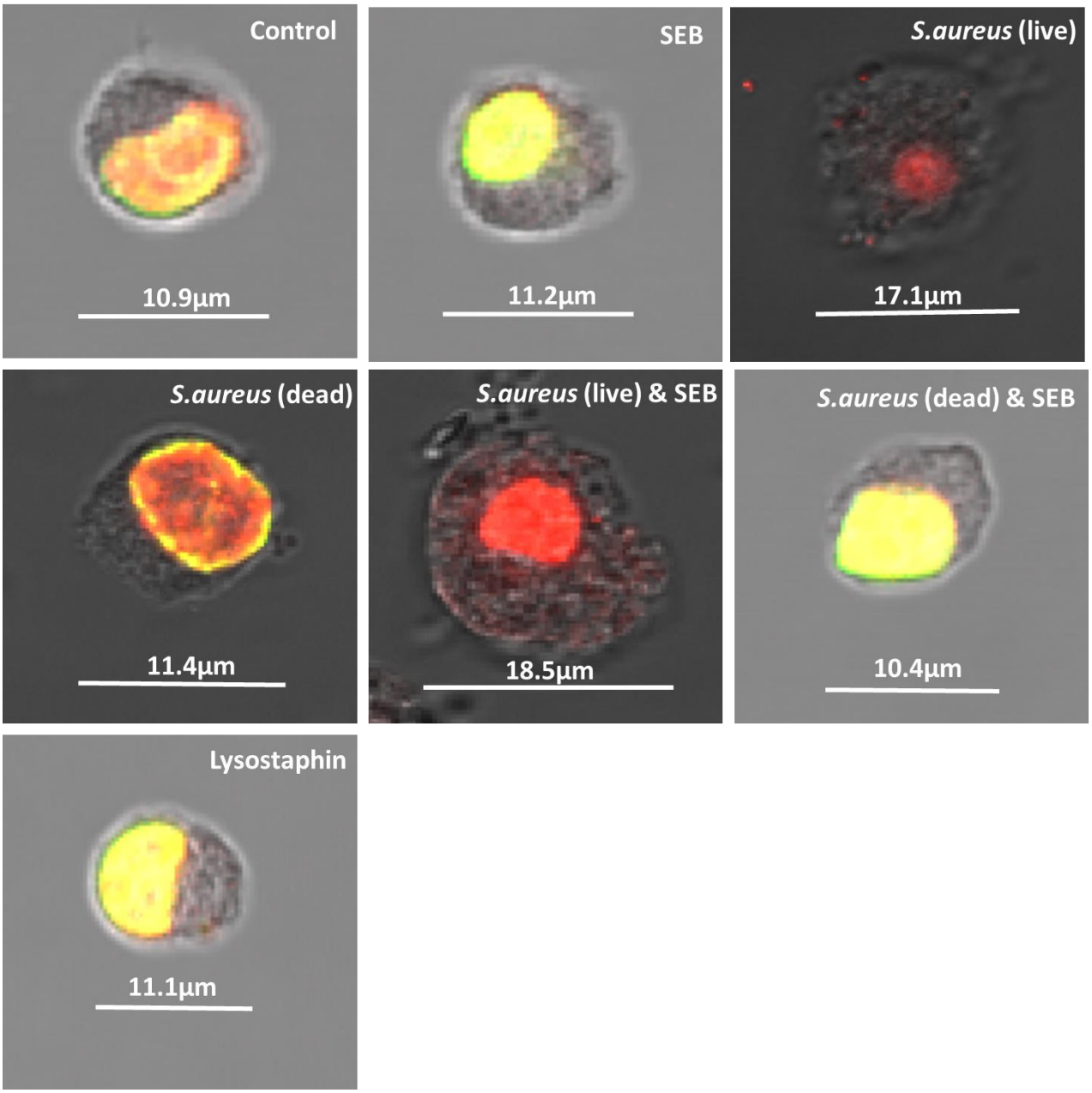

Figure 7.3 Morphological characteristics of mast cells within treatment groups. Representative CLSM images of mast cells (HMC-1 cell line) from each treatment group, after staining with Click-iT® EdU proliferation assay and DAPI. Red nuclei indicate non-proliferating cells and yellow/green nuclei represent proliferating cells. Treatment groups containing live *S aureus* had significantly larger mast cells than treatment groups without live *S aureus*.

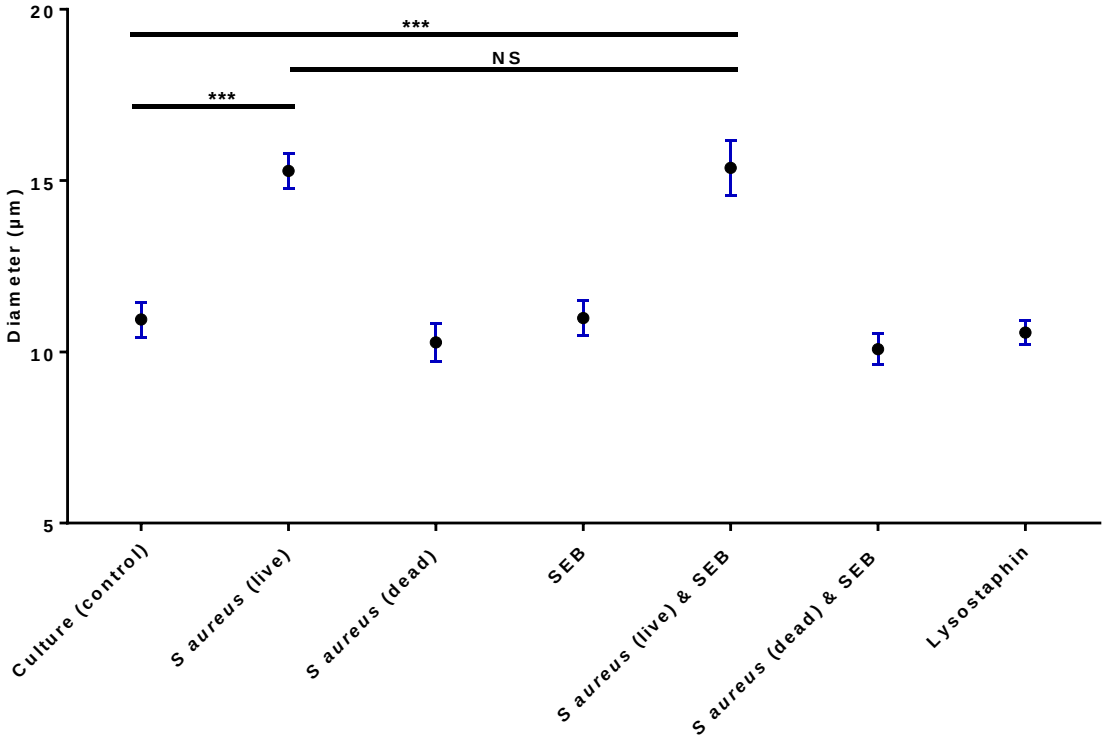

Figure 7.4 Comparison of mast cell size within the treatment groups. Mean diameter (µm) of HMC-1 cells after 24-hour exposure to each treatment group, stained with DAPI and measured using the CLSM LAS AF software. Treatment groups with live *S aureus* contained significantly larger HMC-1 cells compared to controls. Results are pooled data from two independent experiments. Error bars represent the means +/- 1SD. ****p*<0.0001. *NS*, Not significant.

	Mast cell diameter		
Treatment Group	**Mean (µm)**	**95% CI**	***p* value**
Control	10.95		
***S aureus* (live)**	**15.28**	**3.5, 5.1**	**0.0001**
***S aureus* (dead)**	10.27	-1.40, 0.06	0.0715
SEB	10.99	-0.67, 0.75	0.9080
***S aureus* (live) & SEB**	**15.37**	**3.30, 5.55**	**0.0001**
***S aureus* (dead) & SEB**	10.08	-1.53, 0.20	0.1170
Lysostaphin	10.56	-0.98, 0.22	0.2076

Table 7.1 Mast cell size in each treatment group compared to the control size. *P* values of 0.05 or smaller are considered significant and are shown in boldface

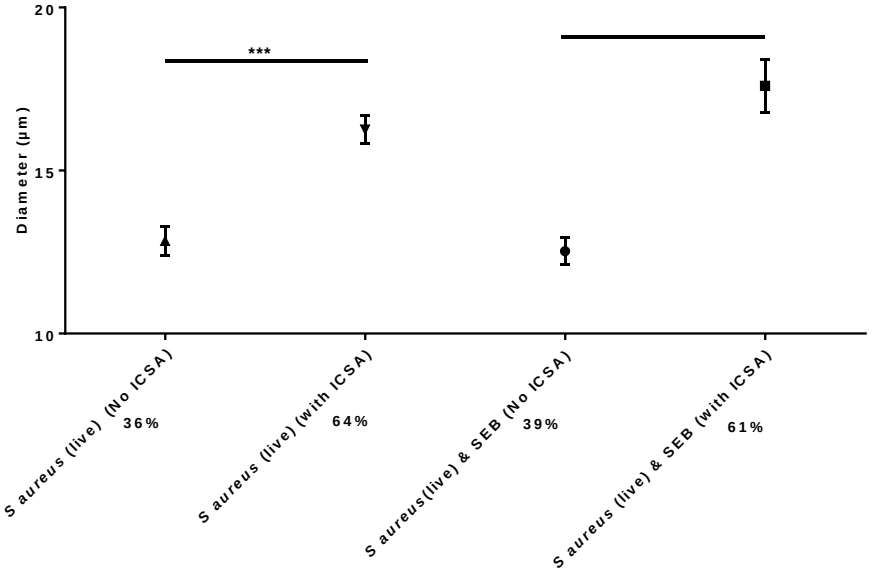

Figure 7.5 Mast cell size in HMC-1 cells with and without intracellular *S aureus*. Mean diameter (µm) of HMC-1 cells after 24-hour exposure to live *S aureus* with and without SEB, stained with DAPI and measured using the CLSM LAS AF software. Treatment groups were further subdivided into HMC-1 cells containing intracellular *S aureus* (ICSA) and HMC-1 cells not containing ICSA. HMC-1 cells with ICSA were significantly larger than HMC-1 cells without ICSA. Results are pooled data from two independent experiments. Error bars represent the means +/- 1SD. ****p*<0.0001.

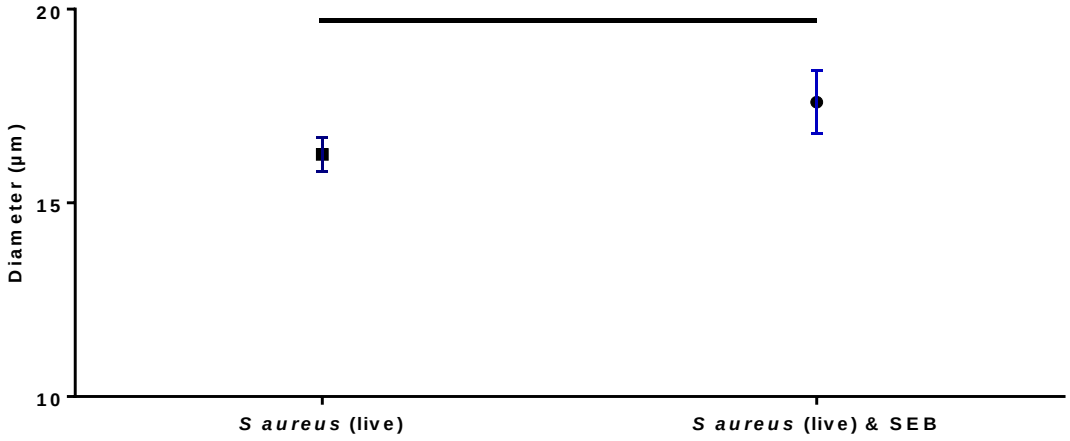

Figure 7.6 Comparison of mast cell sizes in *S aureus*$^{+ve}$ mast cells (n=2). Mean diameter (µm) of HMC-1 cells containing ICSA after 24-hour exposure to live *S aureus* with and without SEB, stained with DAPI and measured using the CLSM LAS AF software. The presence of SEB significantly increased the size of HMC-1 cells with ICSA. Error bars represent the means +/- 1SD. *p<0.05.

7.3.4 *Staphylococcus aureus*$^{+ve}$ mast cells

Intracellular residency of *S aureus* within mast cells was assessed using CLSM with the DAPI stain and TEM. CLSM with the DAPI stain identified 64% of HMC-1 cells containing bacteria within the *S aureus* (live) group (Figure 7.5) and 61% within the *S aureus* (live) with SEB group after 24 hours. Using TEM, 16% of HMC-1 were identified containing intracellular bacteria in the *S aureus* (live) group and 15% in the *S aureus* (live) with SEB group after two hours. The number of *S aureus*$^{+ve}$ mast cells in both groups increased significantly after 24 hours to 76% (p<0.0001*)* and 66% (p<0.0001), respectively.

7.3.5 *Staphylococcus aureus* internalisation within mast cells

To investigate the internalisation mechanisms of *S aureus* into mast cells, *S aureus*, SEB, and HMC-1 (MOI 1:1) were co-cultured and fixed for TEM at 2, 4

and 24 hours. TEM images demonstrating the internalisation of *S aureus* into mast cells are shown in Figure 7.7. *S aureus* appears to initially adhere to the mast cells surface, before being engulfed in a phagocytic manner within 4 hours. Once within the mast cell, *S aureus* continues to proliferate and by 24 hours the bacteria have divided multiple times within the cell. At 24 hours, the mast cells were filled with viable *S aureus* and had increased in size with evidence of degranulation and damage to the nuclei.

7.3.6 Extracellular traps

Another antimicrobial property of mast cells is the use of extracellular traps to catch and internalise extracellular pathogens in order to degrade them. Using TEM, mast cell extracellular traps were demonstrated pulling lines of extracellular *S aureus* into their intracellular cytosol (Figure 7.8A-B). This was also demonstrated using the Click-iT® Edu proliferation kit with CLSM (Figure 7.8D) and also on IHC staining of GMA-embedded NP samples (Figure 7.8D).

7.3.7 Mast cell degranulation and cell destruction

The intracellular residency of viable *S aureus* appears to cause mast cell degranulation. However, it was also demonstrated that mast cells appear to eventually rupture, seeding viable *S aureus* into the extracellular environment with potential for further invasion of newly recruited mast cells (Figure 7.9). This observation was supported by the fact that despite initial treatment of the extracellular *S aureus* with antimicrobial therapy at two hours to eliminate these bacteria, at 24 hours the extracellular compartment contained an abundance of viable *S aureus*. This suggests an ongoing process of bacterial seeding into the extracellular compartment due to mast cell degradation and rupture.

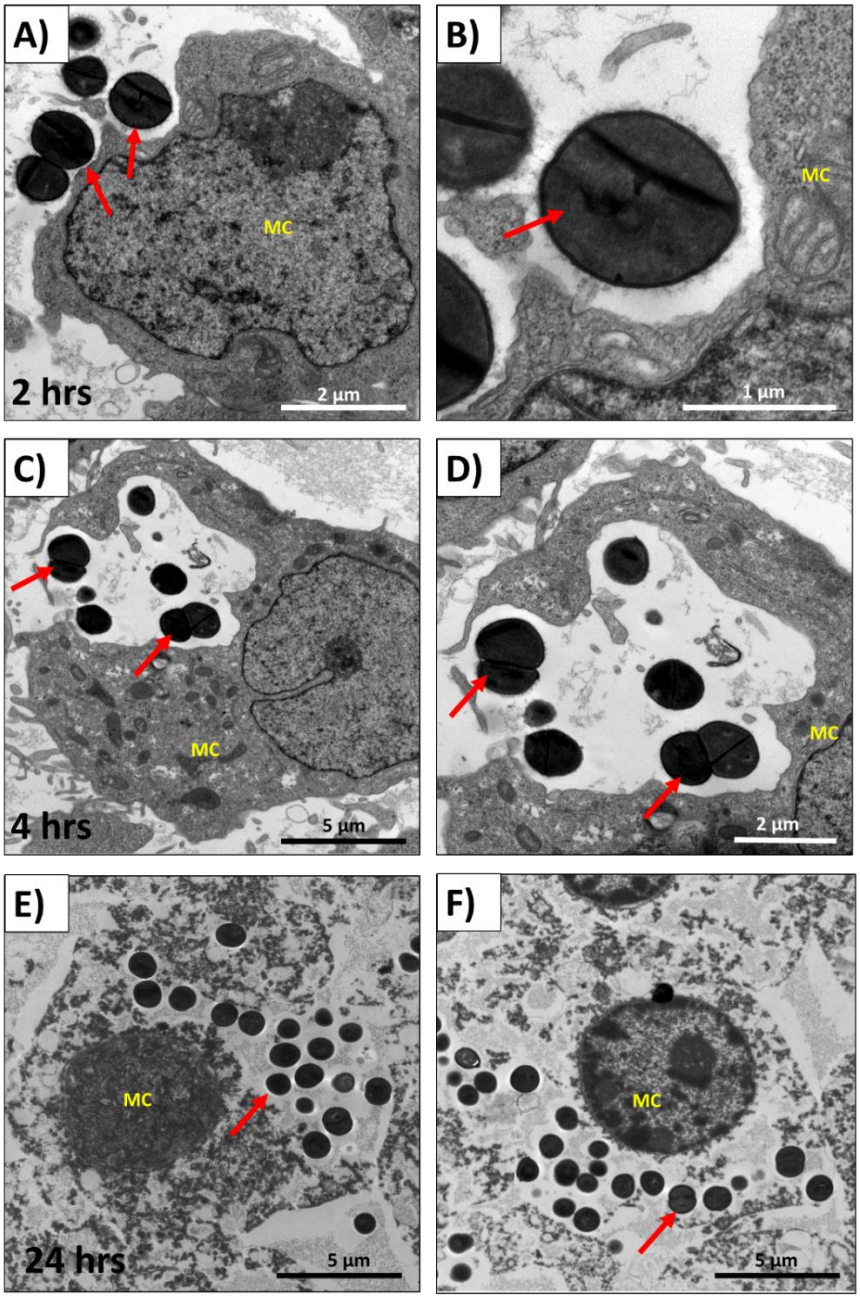

Figure 7.7 *S aureus* internalisation within mast cells. TEM images showing *S aureus* internalising within HMC-1. (A) By two hours *S aureus* (red arrows) had adhered to the mast cell wall. (B) Higher magnification image of *S aureus* attaching to the mast cell wall and demonstrating expression of surface proteins. (C) By 4 hours, *S aureus* (red arrows) were engulfed and internalised. (D) Higher magnification image demonstrating proliferating (viable) internalised *S aureus*. (E) & (F) By 24 hours, *S aureus* were well established within the HMC-1.

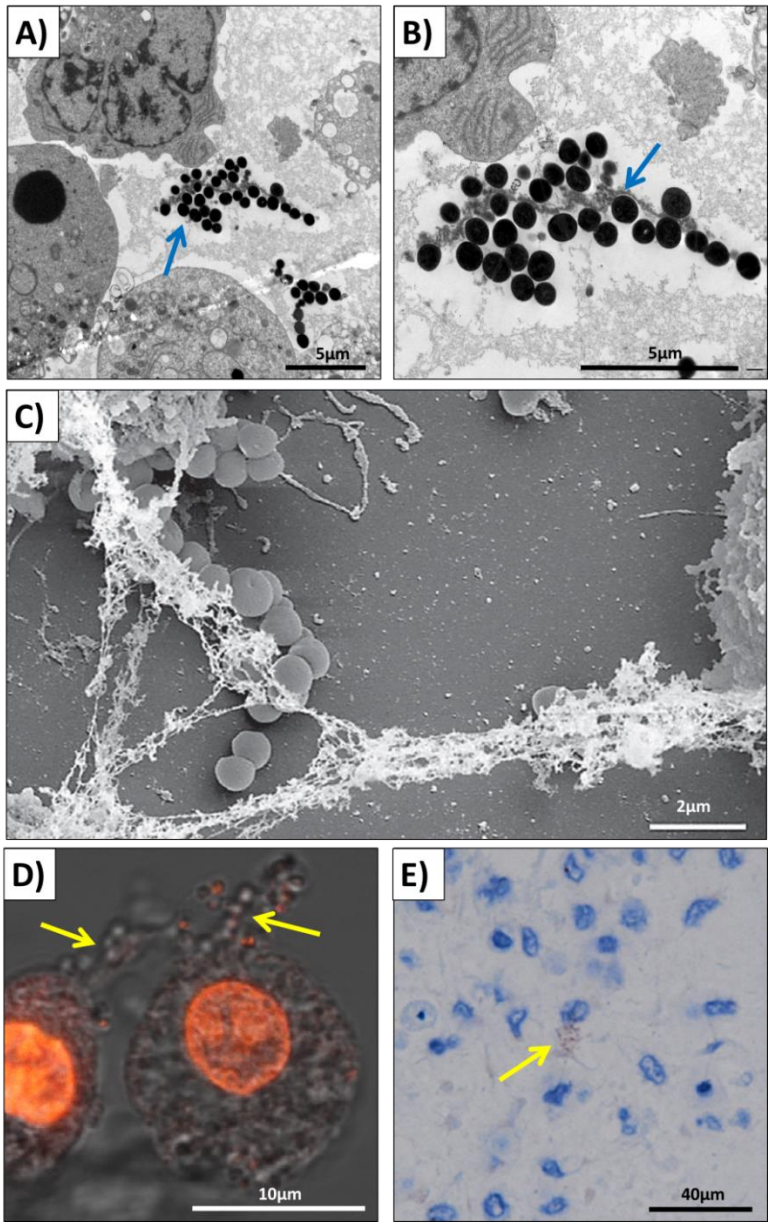

Figure 7.8 Mast cell extracellular traps. (A) Representative TEM image showing clusters of *S aureus* attached to an HMC-1 DNA extracellular trap (blue arrow). (B) Higher magnification of HMC-1 extracellular trap. (C) SEM image of *S aureus* caught in an HMC-1 extracellular trap (Image from Abel et al, 2011 (194)). (D) Representative CLSM image of co-culture HMC-1 with *S aureus* (live) and stained with the Click-iT® EdU proliferation kit and DAPI. *S aureus* (yellow arrows) are shown within extracellular traps entering the mast cell cytosol. (E) Photomicrographs of GMA-embedded NP showing *S aureus* (yellow arrow) entering a mast cell attached to an extracellular trap, within the NP loose stroma.

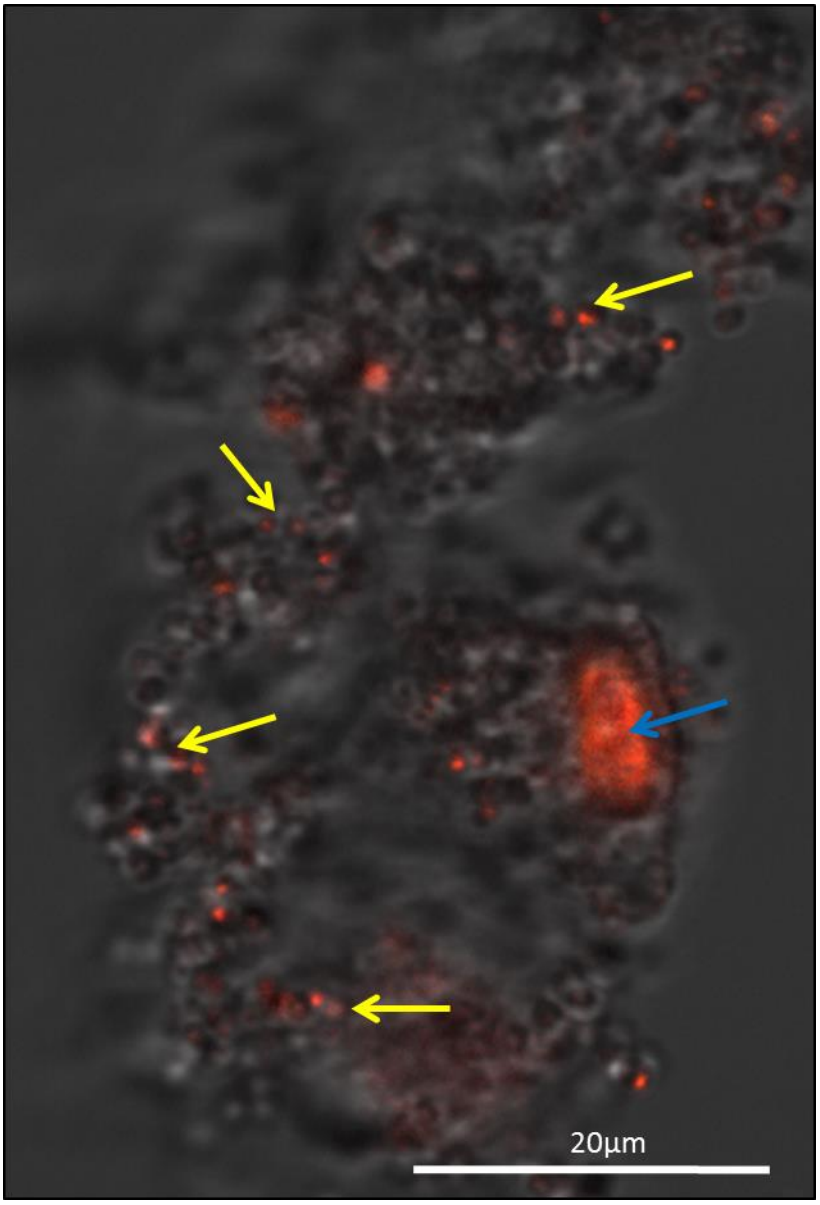

Figure 7.9 Rupture of mast cell with seeding of intracellular *S aureus* into the extracellular space. Representative CLSM image of co-culture HMC-1 with *S aureus* and SEB after 24 hours. CLSM image demonstrates rupture of a mast cell leading to seeding of the intracellular *S aureus* (yellow arrows) and release of mast cell granules into the extracellular compartment. Mast cell nucleus (blue arrow). The same effect was also observed in the *S aureus* without SEB group.

7.4 Discussion

In addition to their well-established role in allergic inflammation, it is becoming more evident that mast cells play a crucial role in the innate response to pathogenic infections. Described as sentinel cells, mast cells appear to play an important role in the initial defence against pathogenic invasion. Following invasion by environmental pathogens, mast cells initially respond by secreting a range of pro-inflammatory mediators, including histamine, IgE, IL-6, chemokines and TNF-α, resulting in the recruitment of further inflammatory cells, such as neutrophils, dendritic cells and additional mast cells to the site of infection. Furthermore, mast cells also appear to exert a direct effect on pathogens, through the secretion of preformed and *de novo* synthesised mediators, secretion of extracellular antimicrobial compounds, phagocytosis and through the use of DNA extracellular traps. The degree of mast cell reaction appears to be microbial-specific, probably through the recognition of PAMPs by the cells PRRs, facilitating a tailored innate response based on stored information from previous encounters (3).

Through the activation of $CD8^+$ T cells, mast cells have the ability to regulate both the T_H1 and T_H2 cytokine pathways and can therefore adopt both immunosuppressive and immunostimulatory properties (201). Exposure to viable *S aureus* appears to cause mast cells to terminally differentiate and stop proliferating. This would suggest that within sinonasal mucosa, the presence of *S aureus* together with SEB increases mast cell numbers through recruitment from distant sites, rather than from local proliferation.

Direct interaction of mast cells with bacteria has been analysed through several *in vitro* studies. It is well established that one of the antimicrobial mechanisms of bacterial internalisation includes phagocytosis and this was demonstrated clearly within this study. Within two hours of *in vitro* co-culture of *S aureus* with HMC-1, bacteria began to bind and adhere to different surface-receptors on the mast cells. By 4 hours, the mast cells had engulfed the *S aureus* within nascent phagosomes derived from the cell membrane. At this stage, other *in vitro* studies have described the eventual incorporation of this phagosome into the mast cell endocytic pathway, fusing lysosomes with the net result of bacterial digestion (343). In our study, this same observation was seen within the first 4 hours of co-culture. However, alongside phagosomes digesting *S*

aureus were also healthy, proliferating, viable bacteria. After 24 hours, the numbers of individual viable *S aureus*$^{+ve}$ mast cells, had significantly increased. The intracellular bacteria were viable and there was no evidence of phagosomes digesting bacteria. This suggests that the CRS *S aureus* isolate used within this co-culture assay contained bacteria with several different phenotypes. Within the co-culture assay, the *S aureus* phenotype with the ability to internalise and thrive within mast cells, proliferated and gradually replaced the other *S aureus* phenotypes being degraded which is a basic natural selection survival mechanism. This may suggest that the ability of *S aureus* to survive within mast cells may be dependent on whether the invading pathogen is of a specific phenotype and may help explain why intracellular internalisation is not a feature in all *S aureus*-related infections.

These findings are consistent with another *in vitro* study that demonstrated *S aureus* within HMC-1 cells, which remained viable for up to 5 days (203). After two hours, 20% of mast cells contained viable intracellular *S aureus* (203). At two hours, our co-culture model demonstrated similar proportions of intracellular *S aureus* in HMC-1 cells and this increased significantly to 76% at 24 hours.

Despite eradicating all extracellular bacteria at 2 hours with antibacterial therapy, by 24 hours the extracellular space was full of viable *S aureus*. Furthermore, the mast cells containing live, viable *S aureus* at this time point were significantly larger than cells with no intracellular bacteria and the addition of SEB further increased cell size significantly. This may represent expansion of the mast cells secondary to the exponential growth of the proliferating intracellular bacteria. As the mast cells reach maximal capacity, the cell wall appears to rupture with expulsion of its contents into the extracellular space. Through this mechanism, viable *S aureus* can leave the mast cells and enter into the extracellular space with further internalisation into newly recruited mast cells.

Extracellular traps have been previously described as an antimicrobial mechanism adopted by mast cells to trap and ensnare extracellular bacteria (203, 344). These traps are composed of DNA and granule proteins and have been demonstrated *in vitro* to trap *S aureus*, before reeling the bacteria into the cell for degradation (203). Our study clearly demonstrated mast cell

extracellular traps using TEM, CLSM and IHC. Described as an antimicrobial mechanism, it is an active route into the mast cell cytosol and manipulation of this mechanism by *S aureus* could lead to a 'Trojan Horse' invasion of the mast cell.

Another anti-pathogenic mast cell defence mechanism includes the initial release of extracellular antimicrobial compounds, such as cathelicidin-related antimicrobial peptide, stored within the cell granules (345). These granules are released through degranulation on exposure to certain pathogens. Studies, including ours, have demonstrated mast cell degranulation on exposure to *S aureus* (346). The internalisation of *S aureus* within mast cells may be a survival strategy to escape these extracellular compounds. The type of degranulation occurring on exposure to *S aureus* is a slow process and differs from the rapid secretory events seen in anaphylactic reactions (346). As well as antimicrobial compounds, mast cells granules released into the extracellular space also contain tryptase, chymase, lysozymes, histamine, heparin, proteases, β-hexosamines and positives charged proteins, such as TNF-α (203, 343). Slow mast cell degranulation, together with cell rupture due to proliferating intracellular *S aureus,* could result in a localised increase in the levels of extracellular pro-inflammatory cytokines and mediators, manifesting as oedema within the lamina propria and potentially contributing to the formation of NP.

A potential limitation of this study was the use of a mast cell line rather than primary mast cells. The HMC-1 cell line is derived from a patient suffering with mast cell leukaemia (347). These mast cells are therefore malignant mast cells and are found in approximately 1 in 20 million humans and therefore do not accurately represent the true tissue mast cells present at the host-environmental interface in the sinuses of patients suffering with CRSwNP. Despite this, the HMC-1 cell line is the only established continually growing human mast cell line exhibiting a phenotype similar to that of human tissue mast cells. They are widely used to research mast cell biology due to their similarities to human tissue mast cells, such as the expression of histamine, tryptase, heparin and cell surface antigens. Malignant mast cells can increase in size *in vitro* due to maturation or delayed mitosis. However, within this study only HMC-1 cells that contained intracellular bacteria significantly increased in size. The HMC-1 cells containing no intracellular bacteria did not enlarge. This

suggests that the increase in mast cell size was a result of the intracellular *S aureus* rather than from using a malignant mast cell line. A primary mast cell line would of course be the gold standard, but unfortunately the isolation of the mast cells from NP proved challenging and as such the use of the HMC-1 cell line was the only viable alternative. For future work, we plan to re-attempt the isolation of mast cells from NP and will repeat the same studies using a primary cell line to validate our results.

7.5 Conclusion

Through successfully developing a working co-culture model to investigate the *S aureus*-mast cell interactions, valuable information was gained regarding the underlying mechanisms responsible for the internalisation of *S aureus* within mast cells. It is evident that *S aureus* and its associated toxins, have developed the ability to manipulate the host's innate immune system to ensure survival. *S aureus* actively internalises within the mast cell cytosol through phagocytosis and via extracellular traps. Specific *S aureus* phenotypes appear to be immune to the mast cell degradation methods. These bacterial phenotypes thrive and increase the cell size leading eventually to cell rupture, seeding the intracellular *S aureus* into the extracellular space and repeat of this cycle. The end result of this process is a build-up of pro-inflammatory cytokines and mediators within the lamina propria leading to localised stromal oedema potentially contributing to the formation of NP.

8 Summary

8.1 Summary of findings

Chronic rhinosinusitis (CRS) is a complex condition with as yet unclear pathophysiology, thus making the development of novel therapies challenging (9). Many aetiological factors have been proposed as playing a role in the ongoing inflammatory process, but strong evidence for a single responsible aetiological agent is lacking. In fact, it is becoming more evident that the pathogenesis of CRS is multifactorial, involving interactions between the environment and genetic profile (3).

Bacteria were previously considered to merely play a role in acute infective rhinosinusitis with little relevance to development of CRS. However, with the advancement of molecular detection techniques, such as scanning electron microscopy (SEM) fluorescent *in situ* hybridisation (FISH), and confocal laser microscopy (CLSM), a clearer understanding of the role and importance of bacteria in CRS is starting to emerge (9).

8.1.1 Bacterial biofilms in chronic rhinosinusitis

The existence of bacteria as biofilms in CRS appears to be a survival strategy to resist antibacterial therapy and evade host immune defences. Their presence appears to be clinically significant, suggesting a possible role in the pathogenesis of CRS. These biofilms appear to be resistant to conventional antibiotics used in the medical treatment of CRS (3). Therefore, improved understanding of the role of these biofilms in mediating the disease process is needed in order deliver novel biofilm-targeted therapies for this chronic and expensive condition.

8.1.2 Dispersal of surface-related bacterial biofilms

A novel biofilm-targeted therapy, used successfully within our Research Group on *P aeruginosa* biofilms in the lungs of patients with cystic fibrosis (CF) is the nitric oxide (NO) donor, sodium nitroprusside (SNP). Through the interaction

with phosphodiesterases, SNP reduces intracellular cyclic di-GMP levels, causing the biofilm to disperse into the more vulnerable planktonic bacteria (297). SNP used as an adjuvant treatment to antibacterial therapy was used on *ex vivo* tissue samples. Although a small trend in biofilm reduction was seen in *P aeruginosa* biofilms, no effect was demonstrated in the dominant *S aureus* biofilms. This small reduction in *P aeruginosa* biofilms may become statistically significant with an increased sample size. This may be relevant in CF-related CRS and will be the subject of future studies. However, as *S aureus* was repeatedly demonstrated to be the most common biofilm-forming microbe in CRS, it was concluded that SNP was not as effective a biofilm-dispersing agent in non-CF related CRS.

8.1.3 Intracellular *Staphylococcus aureus* in nasal polyps

The recent classification of CRS with and without nasal polyps (CRSwNP and CRSsNP) into two distinct pathological entities based primarily on differences in the inflammatory cytokine profiles (3), poses the question of whether these variations could be the result of differences in bacterial profiles. Surface-related bacterial biofilms were identified on the CRS sinonasal mucosa of patients with both CRSwNP and CRSsNP and no observed difference was detected between them. However, in the initial study, bacterial profiles were not characterised specifically in NP tissue. Therefore, using the same advanced molecular detection methods, bacterial profiles were analysed in NP tissue and directly compared to adjacent non-polypoidal mucosa from the same patients with CRSwNP.

Surface-related biofilms were detected on non-polypoidal CRS sinonasal mucosa samples, but not on the epithelial surface of NP. However, sub-epithelial and intracellular bacteria were observed in the cytoplasm of host cells in all NP samples. *S aureus* was again the dominant pathogen detected. These findings were confirmed using immunohistochemistry (IHC) and TEM. IHC co-localisation identified the *S aureus*$^{+ve}$ host cells as mast cells and the development of a novel intracellular viability assay demonstrated the intracellular *S aureus* to be viable.

8.1.4 Host cell profiling

Immunohistochemistry profiling of inflammatory cells in NP and CRS sinonasal mucosa demonstrated an eosinophilic T_H2 profile in NP tissue and a neutrophilic T_H1 profile in CRS sinonasal mucosa from the same patients with CRSwNP. This is an interesting finding as it challenges the classification of CRSwNP and CRSsNP based purely on cytokine profiles (3). These findings suggest that the difference in cytokine profiles may exist within different parts of the sinonasal cavity in the same patient resulting in different pathological manifestations or progression from one disease state to another. These differing profiles could be a manifestation of bacteria-related effects.

8.1.5 Role of *Staphylococcus* enterotoxin B

An explant tissue model was successfully developed and validated to investigate the effects of *S aureus* at the host-environment interface. The addition of SEB to viable *S aureus* enhanced mast cell recruitment and increased numbers of *S aureus*$^{+ve}$ mast cells within both the epithelial and sub-epithelial layers. The addition of SEB to viable *S aureus* also demonstrated increased epithelial proliferation and mast cell degranulation. These findings suggest that SEB is a pre-requisite for the intracellular localisation of *S aureus*.

8.1.6 The *Staphylococcus aureus*-mast cell interaction

Using the human mast cell-1 line (HMC-1), the interaction between *S aureus* and mast cells was studied. In the presence of *S aureus,* terminally-differentiated mast cells appear to stop proliferating. This suggests that, in the explant tissue model, mast cells are recruited from distant sites by *S aureus* and SEB, rather than through local proliferation. *S aureus* is internalised into the mast cell through phagocytosis and extracellular traps. Some *S aureus* appear to survive and proliferate within the mast cell, whereas others were denatured, suggesting that some bacteria possess the ability to reside and multiply within mast cells. The number of viable intracellular *S aureus* appears

to significantly increase over time, swelling the mast cell to approximately twice its normal size, before rupturing and releasing both the granules and viable bacteria into the extracellular space. Bacteria can then internalise into newly recruited mast cells, thus repeating the cycle. This intracellular reservoir of *S aureus* can continuously seed bacteria resulting in the persistence of the inflammatory reaction and development of chronicity and disease recalcitrance. Targeting surface bacteria may literally be 'scratching the surface' as these bacteria are merely the tip of the iceberg and the real problem lies within the intracellular compartment. This concept has important implications in relation to development of future therapies for CRS as these will need to target the intracellular bacterial reservoir rather than just the surface bacteria.

8.2 Proposed mechanism for the pathogenesis of nasal polyps

The pathogenesis of NP is undoubtedly complex and cannot be explained by a single aetiological factor or simple pathway. Nevertheless, we have used the findings from this study alongside well-established evidence, including the superantigen and immune barrier hypotheses, to propose a potential mechanism for the pathogenesis of NP.

Mast cells are recruited into the epithelial layer by SEB, where non-motile *S aureus* are internalised within these mast cells through phagocytosis and extracellular traps and to the sub-epithelial layer for degrading. Some of the intracellular *S aureus* appear to possess the ability to remain viable and multiply within the mast cells. The combined effect of SEB and viable intracellular *S aureus* stimulates mast cell degranulation, releasing pro-inflammatory mediators and cytokines into the extracellular space. This process of degranulation empties the mast cell granules, creating more space for proliferating *S aureus* which fill the cell cytosol.

Intracellular *S aureus* proliferates within the mast cells, significantly increasing the cell size. Eventually, the mast cells rupture, emptying their pro-inflammatory cytokines, mediators and viable *S aureus* into the extracellular space. SEB released from *S aureus* causes damage to the epithelial cells, leading to epithelial proliferation and remodelling, resulting in a disorganised and defective epithelial barrier.

The end result of these processes is a build-up of pro-inflammatory cytokines and mediators within the lamina propria on a background of a defective epithelial barrier, leading to localised stromal oedema and downstream promoting the formation and growth of NP. This proposed mechanism is illustrated in Figure 8.1.

Evidently, substantiation of this proposed mechanism will require further research which is discussed in the ‘Future Work’ section on page 241.

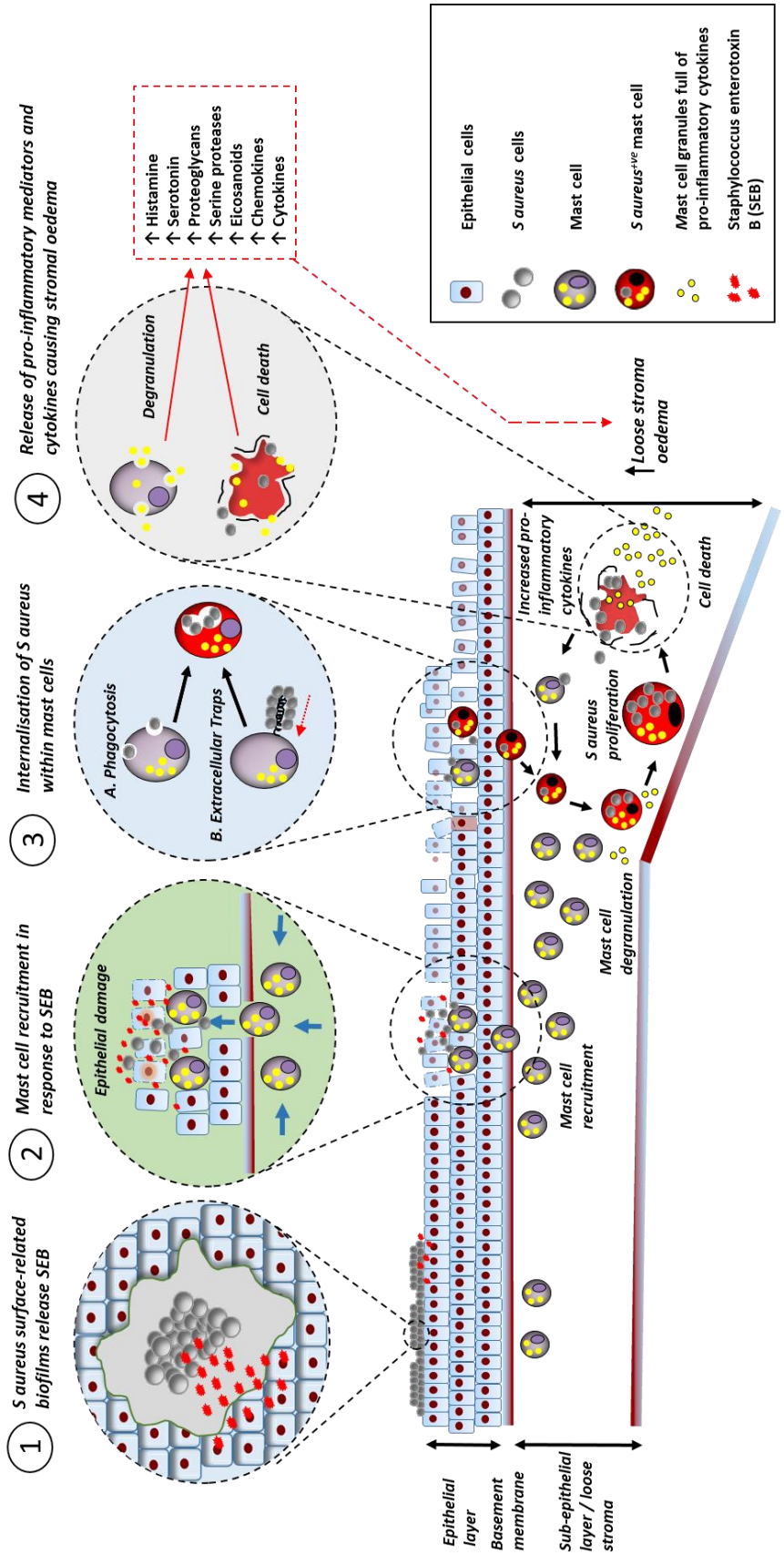

Figure 8.1 Proposed mechanism for nasal polyp formation

8.3 Limitations of Study

Every biofilm detection method used in this project had its own individual limitations. This was partly overcome by the use of as many techniques as possible in order to validate the findings. This included the gold standard CRS biofilm detection method of FISH combined with CLSM, as described within the literature (214).

Sample numbers were relatively small for some parts of the study due to the inconsistent availability of control tissue, the extensive time for processing and the constrained use of expensive imaging equipment due to limited funds. Larger sample sizes would have allowed for more accurate statistical analysis. Despite this, most of the observed trends were shown to be statistically significant.

All patients within these studies were selected from the same geographical region of the United Kingdom. It is therefore, not possible to assess the effects of geography, ethnicity or genetics on these findings. For example, the pathogenesis and pathophysiology of NP have been shown to differ between Western and Far Eastern populations. The findings from this study may therefore not be universally applicable.

Due to the difficulty in culturing primary mast cells from NP, the HMC-1 line was used. The behaviour of the HMC-1 line will differ from primary mast cells. As such, we plan to re-attempt the isolating of mast cells from NP with the aim of repeating this study to validate our findings.

8.4 Future Work

Potential future work is summarised and illustrated in Figure 8.2. The proposed mechanism of NP formation, based on findings from this project, centres around increasing levels of pro-inflammatory cytokines and mediators within the sub-epithelial layer released from degranulating and ruptured mast cells as a result of *S aureus* internalisation. The next stage of this project would be to investigate intracellular *S aureus* survival mechanisms and the effects of mast cell degranulation on the sub-epithelial layer.

Phenotyping and the genetic profiling of isolated intracellular *S aureus* could help explain why some of the bacteria are able to compromise the antimicrobial defences of the mast cell, whilst others are phagocytosed and degraded. Proteomics may help to identify surface proteins responsible for intracellular survival and shed light on the underlying mechanisms. Isolation of a primary NP mast cell line would allow a more valid assessment of the true *S aureus*-mast cell interaction. It would also enable evaluation of the contents and nature of the mast cell-related granules and validation of the HMC-1 cell line findings.

Assessment of pro-inflammatory cytokines and mediators released into the extracellular space as a result of mast cell degranulation may clarify whether mast cell degranulation is responsible for the switch from a T_H1 to the T_H2 cytokine profile seen in NP tissue.

As oedema increases within the loose stroma, a point of weakness within the epithelium is required for the mucosa to prolapse, forming a NP. Therefore, further investigation of epithelial integrity is warranted. This would involve evaluation of epithelial cytokines in response to SEB, which may help clarify how *S aureus* survives by evading the host's innate immune system.

Investigation into the association between epithelial integrity and surface-related bacterial biofilms may help clarify the lack of surface biofilms on NP tissue. It is feasible that a point may be reached whereby a surface-biofilm is no longer a safe haven for bacteria resulting in a switch in survival strategy with intracellular localisation of bacteria. Pre-empting or preventing this switch could negate the downstream sequelae and may reduce the likelihood of NP formation.

The role that bacterial biofilms play in CRS may be explored further through using simple regression analysis. An equation could be developed using possible aetiological factors, which would build both error and uncertainty into it.

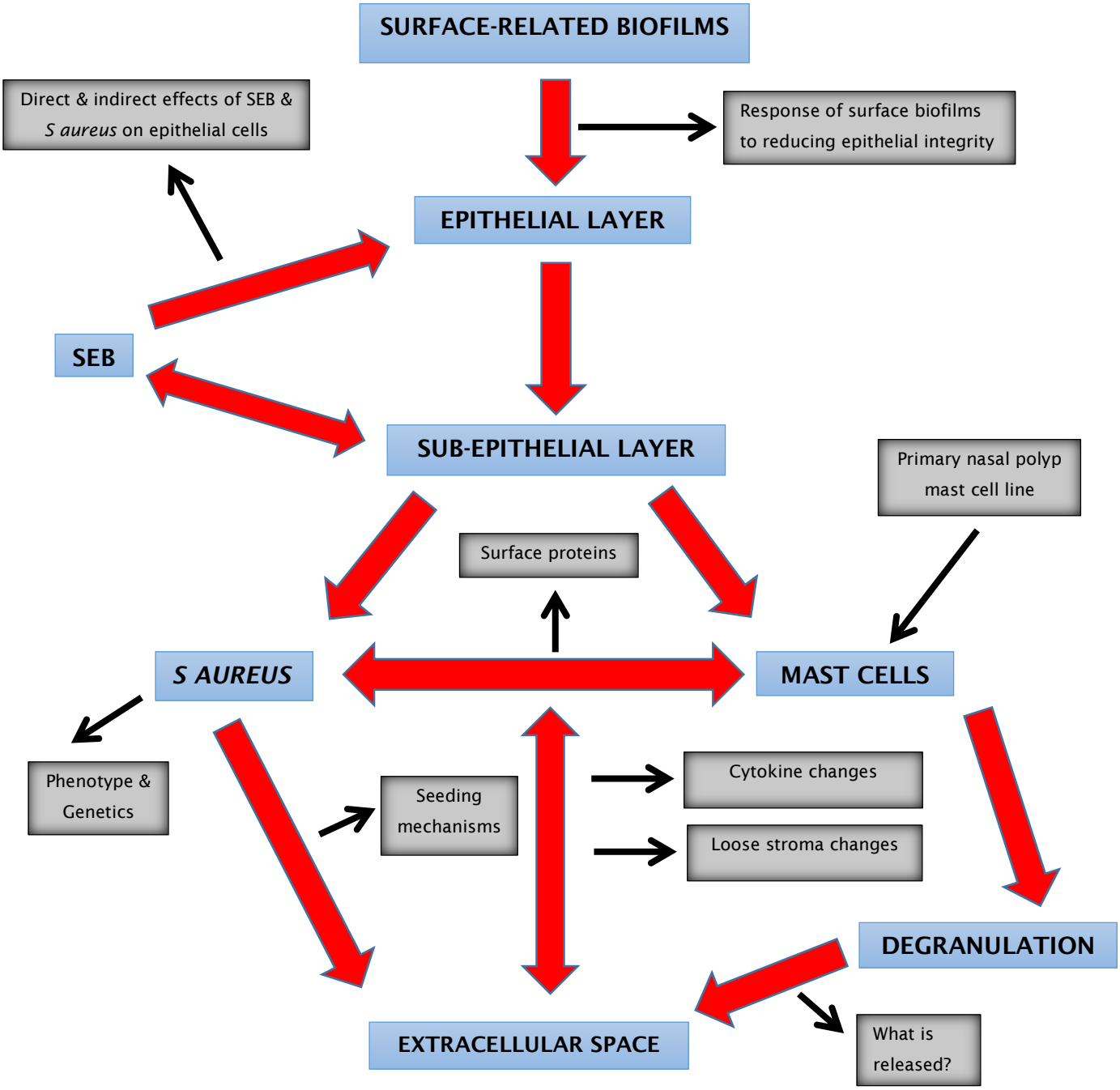

Figure 8.2 Future work. A summary and illustration of possible future work. Proposed questions requiring further investigation are displayed in the grey boxes.

Appendix I

PATIENT CONSENT FORM

PATIENT CONSENT FORM

Regulation of inflammation in the upper airways

Mr R Salib, Mr S Hayes, Mr S Nair, Dr P Howarth

Please initial box

1. I confirm that I have read and understand the information sheet dated 06/07/2010 (version 4) for the above study. I have had an opportunity to consider the information, ask questions and have had these questions answered satisfactorily. ☐ 1

2. I understand that my participation is voluntary and that I am free to withdraw at any time, without giving any reason, without my medical care or legal rights being affected. ☐ 2

3. I agree to my nasal tissue, taken as part of my surgery, being stored for the duration of this study for use in this research project into inflammatory processes. ☐ 3

4. I agree to my nasal tissue, taken as part of my surgery, to be transferred securely and anonymously to those centres to get the best information possible with respect to the assessing the presence of bacteria and fungi ☐ 4

5. I agree to genetic material being extracted from my nasal tissue to investigate genes which may be involved in inflammation. ☐ 5

_____	_____	_____
Name of Patient	Date	Signature
_____	_____	_____
Name of Person taking consent (if different from researcher)	Date	Signature
_____	_____	_____
Name of Researcher	Date	Signature

Appendix II

PATIENT INFORMATION SHEET

UNIVERSITY OF Southampton School of Medicine

Southampton NHS University Hospitals NHS Trust

Information sheet for adult patients undergoing ENT procedures

Investigation of Mechanisms of Disease in Children and Adults with Chronic Ear, Nose and Throat Disease

Adult Patient information sheet

We are conducting research into new ways of treating ear, nose and throat (ENT) conditions. You are being invited to take part in a research study because you have either been diagnosed with one of these conditions or are being cared for by the ENT service. Before you decide it is important for you to understand why the research is being done and what it will involve. Please take time to read the following information carefully and discuss it with friends, relatives and your GP if you wish. Ask us if there is anything that is not clear or if you would like more information. Take time to decide whether or not you wish to take part.

People who suffer with chronic ENT problems often require surgery to effectively treat their condition. The research we are doing looks at new ways of studying bacteria from tissue samples taken during surgery and possible ways of enhancing antibiotic treatment of infection. By investigating these things we hope to improve our understanding of the role of infection in causing ENT disease. Finding out about the processes that cause ENT diseases, or make them worse, is important for the development of new treatments. If you agree we would like to use your tissue samples for this microbiological and inflammation research.

It is up to you to decide whether or not to take part. If you decide to take part you will be asked to sign a consent form and your GP will be notified of your participation by letter. Even after you have decided to take part you are still free to withdraw from the study at any time and without giving a reason. This will not affect the standard of care you receive.

What will happen if I take part?
If you agree to take part we will retain samples of infectious material that would normally be removed during your surgery. You will not undergo <u>any</u> additional procedures as a result of your participation in this study. It is only the processing of the samples once they get to the laboratory that will change. Part of the specimen will be sent for routine processing and the rest will be used for research purposes. Some of the sample will be frozen and stored for analysis at a later date. All samples will be given a study number which cannot

be directly traced back to you. A doctor involved in the study will check your medical notes to record certain details of symptoms, history and treatment which will help in the analysis of these samples. A research study number will also be given to any documentation so that it cannot be traced back to you. Section B on the consent form asks you to give us permission to store the sample for use in future studies. The official name for such permission is linked anonymised, whereby results of future studies can be linked with your medical details but will not have access to your identity.

What are the side effects of taking part?
None.

What are the possible disadvantages and risks of taking part?
None. The extra laboratory tests will not affect you in any way.

What are the possible benefits of taking part?
The information we get from this study may help us to treat people with ENT diseases better. It will not directly benefit you now but may help you or people with similar problems in the future.

Will my taking part in this study be kept confidential?
Yes. Any information about you that leaves the hospital will have your details removed so that you cannot be identified.

What will happen to the results of the research?
The results may be published in a scientific or medical journal. They may also be presented at a scientific conference. Your confidentiality will not be broken by publication, as the information presented will not be related to named individuals.

What if something goes wrong?
Any complaint about the way you have been dealt with during the study or any possible harm you might suffer will be addressed. Please raise your concerns in the first instance with the Principal Investigator (that is the lead researcher), Dr Saul Faust – his contact details are at the end of this form. If you wish to make a more formal complaint, please contact the Patient Advice and Liaison Service (available from 9am-4.30pm Monday to Friday, out of hours there is an answer phone), PALS, C level, Centre Block, Mailpoint 81, Southampton General Hospital. Email PALS@suht.swest.nhs.uk Tel 02380 798498

What insurance provisions are in place?
In the event that something does go wrong and you are harmed during the research and this is due to someone's negligence then you may have grounds for a legal action for compensation against the sponsor, Southampton University Hospitals NHS Trust but you may have to pay your legal costs. The former National Health Service complaints mechanism will still be available to you. As the Principal Investigator is an employee of the University of Southampton, additional professional indemnity and clinical investigation insurance is in place.

Contact for further information:
If you have any questions relating to this research you will have the opportunity to discuss them with a doctor either on the ward or when you come to clinic. Otherwise you can contact Mr William Hellier or Mr Rami Salib, Consultant

Otolaryngologists, Southampton University Hospitals NHS Trust, Tremona Road, Southampton, SO16 6YD, Tel: 02380825526 / 5635

General information about participating in research in the NHS is available on the National Patient Safety Agency website at

http://www.nres.npsa.nhs.uk/public/index.htm.

Thank you for reading this

Appendix III

STAPHYLOCOCCUS AUREUS ISOLATION

S aureus isolation Protocol

S aureus is a facultatively anaerobic, Gram-positive coccus and has large, round, golden-yellow colonies, often with hemolysis, when grown on blood agar plates.
S aureus is catalase-positive (meaning that it can produce the enzyme "catalase") and able to convert hydrogen peroxide (H_2O_2) to water and oxygen, which makes the catalase test useful to distinguish staphylococci from enterococci and streptococci.
A small percentage of *S aureus* can be differentiated from most other staphylococci by the coagulase test: *S aureus* is primarily coagulase-positive (meaning that it can produce the enzyme "coagulase") that causes clot formation, whereas most other *Staphylococcus* species are coagulase-negative. However, while the majority of *S aureus* are coagulase-positive, some may be atypical in that they do not produce coagulase.

1.1. Equipment & Chemicals

- Blood agar (Oxoid)
- Baird-Parker agar (Sigma)
- Egg yolk tellurite as supplement for Baird-Parker agar (Oxoid/Sigma)
- Trypticase soy broth (Oxoid/Sigma)
- Brain Heart Infusion (Oxoid)
- Hydrogen Peroxide (Sigma)
- Hydrochloric acid (Sigma)
- DNase agar (Sigma)
- Coagulase slide test (Sigma)
- Toluidine blue (Sigma)
- Incubator set at 37 °C
- Glass slides
- Bunsen burner & lighter
- Inoculation loops
- Universal tubes

1.2. Culture and Identification of *S aureus*

1.2.1. Primary isolation media

- Inoculate DNase agar and blood agar plates and grow at 37 °C for 18-24 h.
- Examine for colonial morphology (cream or golden colour up to 3mm in diameter)

- Baird-Parker agar (Sigma), supplemented with egg yolk tellurite (Sigma) can be used to identify *S aureus* as shown in the Table 1 when incubated for 48 h at 37 °C.

Table 1.
Colonial morphology of *S aureus* on Baird-Parker agar.

Organisms	Colour of colony/comments
S aureus	Grey-black, shiny colony due to reduction of tellurite. Surrounded by a zone of clearing

1.2.2. DNase production

This test is used to determine the ability of an organism to produce DNase. The test is used primarily to distinguish pathogenic Staphylcocci which produce large quantities of extracellular DNase. It reacts with medium containing DNA with the resulting hydrolysis of the DNA. The oligonucleotides liberated by the hydrolysis are soluble in acid and in a positive reaction, the addition of HCL results in a clear zone around the inoculum. A hazy zone is produced in a negative reaction, due the precipitation of DNA by HCL. In contrast to HCL, toluidine blue produces much more delineated zones of DNase activity.
Most strains of *S aureus* hydrolyse DNA and give positive reactions in this test. However, some MRSA strains do not and some strains of coagulase-negative staphylocci may give weak reactions.

- Flood a DNase agar plate containing plated organism with Toluidine blue O solution (TBO/TBS @ 0.01-0.05 % [w/v] concentration) or 1M HCL.
- After 2 min, discard excess reagent
- TBO-positive reaction – TBO forms a complex with hydrolysed DNA to produce colonies surrounded by pink zone against a blue background
- HCL-positive reaction – colonies demonstrate a defined zone of clearing
- A negative result for both solutions equates to no zone of clearing.

1.2.3. Coagulase Production

Members of the genus Staphylococcus are differentiated by the ability to clot plasma by the action of the enzyme coagulase.
Coagulase exists in two forms: “bound coagulase” (or clumping factor) which is bound to the cell wall and “free coagulase” which is liberated by the cell wall.

Bound coagulase is detected by the slide coagulase test, whereas free coagulase is detected by the tube coagulase test.

Bound coagulase adcorbs fibrinogen from the plasma and alters it so it precipitates on the Staphylococci causing them to clump resulting in cell agglutination. The tube coagulase test detects both bound and free coagulase. Free coagulase reacts with a substance in plasma to form a fibrin clot.

1.2.3.1. Slide Coagulase test

- Place a drop of distilled water on a slide
- Emulsify the test strain to obtain and homogenous thick suspension. False negative reactions will occur if the bacterial suspension is not heavy enough
- Observe for auto-agglutination
- Dip a loop in the plasma and mix gently with the homogenous suspension
- A positive result, will produce clumping within 10 seconds. Conversely, an negative control produces no visible clumping.
- Ensure you perform an autoagglutination negative control test
-

1.2.3.2. Tube Coagulase Test

- Place approx. 1 ml of commercially available plasma suitable for tube coagulase in a sterile eppendorf
- Emulsify test colonies in the plasma and incubate for 4 h at 37 °C
- Examine for a clot which gels the whole contents of the tube or forms a loose web of fibrin
- If negative, incubate overnight at 22-25 °C and re examine at 24 h.
- A positive result will produce a formation of a clot at 4 h following 37 °C incubation or following overnight incubation at 22-25 °C. A negative result will produce no clot at either time point.

Table 2.
Tube and Slide Coagulase test results for *S aureus*

Species	Tube Coagulase test	Slide Coagulase test
Staphylococcus aureus Subspecies aureus	+	+
Staphylococcus aureus Subspecies anerobius	+	-

(+) = delayed reaction

1.2.4. Catalase Test

This test is to detect the catalase enzyme present in most cytochrome-containing aerobic and facultatively anaerobic bacteria. Streptococcus and Enterococcus sp. are exceptions.

The catalase test is used to detect the presence of catalase enzymes by the decomposition of hydrogen peroxide to release oxygen and water. Hydrogen peroxide is formed by some bacteria as an oxidative end product of the aerobic breakdown of sugars. If allowed to accumulate it is highly toxic to bacteria and can result in cell death. Catalase either decomposes hydrogen peroxide or oxidises secondary substrates, but it has no effect on other peroxides.

Media containing whole red blood cells will contain catalase and could give a false positive. Colonies taken from chocolate agar may be tested. Hydrogen peroxide is unstable and should be stored in a spark proof fridge. Avoid undue exposure to light. Cultures of anaerobic bacteria should be exposed to air for 30 min prior to testing.

- Place approx. 0.2 ml of hydrogen peroxide solution in a test tube
- Carefully pick a colony and rub the colony on the inside wall of the test tube above the surface of the hydrogen peroxide solution
- Cap the tube or bottle and tilt it to allow the hydrogen peroxide solution to cover the colony.
- Look for vigorous bubbling occurring within 10 sec.

Table 3.
FINAL *S aureus* CONFORMATION RESULTS

Test	Result
Culture	Grows on DNase and blood agar plates to produce cream/golden colonies Baird-Parker agar produces grey-black, shiny colonies surrounded by zone of clearing
DNase test	Positive reaction (identified by zone of clearing)
Coagulase test	Positive reaction (identified by agglutination)
Catalase test	Positive (identified by bubbling around colony)
Further test suggested: PCR	

1.3. *S aureus* Biofilm Growth

S aureus biofilms can be grown *in vitro* using brain heart infusion, Mueller-Hinton broth medium[3] or Trypticase Soy broth for 24 h at 37 °C.

Appendix IV

LYSOZYME CONCENTRATION CALCULATIONS

Lysozyme Concentration Calculations

10mg Lysozyme:

- **Need a solution of 10mg/ml Lysozyme in 0.1M TrisHCL and 0.05M EDTA**
  - Perform 1 in 5 dilution of 1M TrisHCL to get 0.2M with dH_2O
  - Perform 1 in 5 dilution of 0.5M EDTA to get 0.1M with dH_2O
  - Dissolve 20mg Lysozyme powder in 1ml of 0.2M TrisHCL to give 20mg/ml Lysozyme
  - Perform 1 in 2 dilution of Lysozyme / TrisHCL solution with 0.1M EDTA and store in 1ml aliquots to give a final concentration of 10mg/ml Lysozyme in 0.1M TrisHCL and 0.05M EDTA

5mg Lysozyme:

- **Need a solution of 5mg/ml Lysozyme in 0.1M TrisHCL and 0.05M EDTA**
  - Perform 1 in 5 dilution of 1M TrisHCL to get 0.2M with dH_2O
  - Perform 1 in 5 dilution of 0.5M EDTA to get 0.1M with dH_2O
  - Dissolve 10mg Lysozyme powder in 1ml of 0.2M TrisHCL to give 10mg/ml Lysozyme
  - Perform 1 in 2 dilution of Lysozyme / TrisHCL solution with 0.1M EDTA and store in 1ml aliquots to give a final concentration of 5mg/ml Lysozyme in 0.1M TrisHCL and 0.05M EDTA

2.5mg Lysozyme:

- **Need a solution of 2.5mg/ml Lysozyme in 0.1M TrisHCL and 0.05M EDTA**
  - Perform 1 in 5 dilution of 1M TrisHCL to get 0.2M with dH_2O
  - Perform 1 in 5 dilution of 0.5M EDTA to get 0.1M with dH_2O
  - Dissolve 5mg Lysozyme powder in 1ml of 0.2M TrisHCL to give 5mg/ml Lysozyme
  - Perform 1 in 2 dilution of Lysozyme / TrisHCL solution with 0.1M EDTA and store in 1ml aliquots to give a final concentration of 2.5mg/ml Lysozyme in 0.1M TrisHCL and 0.05M EDTA

1mg Lysozyme:

- **Need a solution of 1mg/ml Lysozyme in 0.1M TrisHCL and 0.05M EDTA**
  - Perform 1 in 5 dilution of 1M TrisHCL to get 0.2M with dH_2O
  - Perform 1 in 5 dilution of 0.5M EDTA to get 0.1M with dH_2O
  - Dissolve 2mg Lysozyme powder in 1ml of 0.2M TrisHCL to give 2mg/ml Lysozyme
  - Perform 1 in 2 dilution of Lysozyme / TrisHCL solution with 0.1M EDTA and store in 1ml aliquots to give a final concentration of 1mg/ml Lysozyme in 0.1M TrisHCL and 0.05M EDTA

0.5mg Lysozyme:

- **Need a solution of 0.5mg/ml Lysozyme in 0.1M TrisHCL and 0.05M EDTA**
  - Perform 1 in 5 dilution of 1M TrisHCL to get 0.2M with dH_2O
  - Perform 1 in 5 dilution of 0.5M EDTA to get 0.1M with dH_2O
  - Dissolve 1mg Lysozyme powder in 1ml of 0.2M TrisHCL to give 1mg/ml Lysozyme
  - Perform 1 in 2 dilution of Lysozyme / TrisHCL solution with 0.1M EDTA and store in 1ml aliquots to give a final concentration of 0.5mg/ml Lysozyme in 0.1M TrisHCL and 0.05M EDTA

0.25mg Lysozyme:

- **Need a solution of 0.25mg/ml Lysozyme in 0.1M TrisHCL and 0.05M EDTA**
  - Perform 1 in 5 dilution of 1M TrisHCL to get 0.2M with dH_2O
  - Perform 1 in 5 dilution of 0.5M EDTA to get 0.1M with dH_2O
  - Dissolve 0.5mg Lysozyme powder in 1ml of 0.2M TrisHCL to give 0.5mg/ml Lysozyme
  - Perform 1 in 2 dilution of Lysozyme / TrisHCL solution with 0.1M EDTA and store in 1ml aliquots to give a final concentration of 0.25mg/ml Lysozyme in 0.1M TrisHCL and 0.05M EDTA

Appendix V

PUBLISHED PAPER

Intracellular residency of Staphylococcus aureus within mast cells in nasal polyps: A novel observation

To the Editor:

Chronic rhinosinusitis (CRS) with or without nasal polyps (NPs) (CRSwNP and CRSsNP, respectively) is one of the most commonconditionsencounteredinmedicine.[1] CRS is a disease of the mucosa lining the sinonasal cavity characterized by recurrent episodes of inflammation resulting in chronic symptoms such as nasal obstruction, facial pain, rhinorrhea, and reduction in sense of smell.[1] CRS affects up to 15% of the general population in Europe and the United States, ranking it second in prevalence among chronic conditions,[1] and significantly affecting quality of life and health care resources.[2] Despite the massive expenditure on medical and surgical therapies for this condition, a subset of patients remains resistant to all established treatments.[2] Identification of either a host or an environmental cause has been unsuccessful. Proposed mechanisms of CRS pathophysiology include the role of superantigens, abnormal cell-mediated immune responses, changes in the inflammatory cytokine cascade, epithelial defects, osteitis of the sinus walls, and viral, bacterial, and fungal factors.[1] Recent guidelines propose the classification of CRSwNP and CRSsNP into 2 distinct pathological entities primarily based on differences in inflammatory cytokine profiles.[1] A CRSwNP T_H2-mediated profile is characterized as eosinophilic with elevated IL-5, IgE, RANTES, and eotaxin,[1] and a CRSsNP $T_H1$mediated profile is characterized as neutrophilic with elevated TNF-a, IL-8, and IFN-g.[1]

Emerging evidence implicates bacterial biofilms as mediators of the inflammatory reaction in CRS.[1] Several studies provide strong evidence that bacterial biofilms perpetuate inflammation in CRS and are associated with more severe preoperative disease, persistence of ongoing mucosal inflammation, and poor postsurgical outcomes.[3] Staphylococcus aureus has been identified as the commonest biofilm-forming microbe in CRS and colonizes the sinonasal cavities in 27% of the patients with CRSsNP and in 60% of the patients with CRSwNP.[4]

Around 20% of the patients with CRS develop NPs,[1] and although studies have clearly identified bacterial biofilms on the sinonasal mucosa of patients with CRS, little data pertain to the bacterial profiles specifically in NPs. We conducted a preliminary study characterizing bacterial profiles in NPs, comparing them with those on nonpolypoidal sinonasal mucosa from the same patients and with non-CRS sinonasal mucosa as control tissue.

A prospectivestudy with full ethical approval was conducted in 9 patients with CRSwNP undergoing functional endoscopic sinus surgery and 5 control patients undergoing transsphenoidal pituitary surgery. Nonpolypoidal sinonasal mucosa and NPs were collected from each patient with CRSwNP and sinonasal mucosa from controls. The bacterial profiles were assessed using fluorescence in situ hybridization with confocal laser scanning microscopy (CLSM) and immunohistochemistry. Hybridization conditions were optimized for CRS tissue using appropriate controls (see the Methods section in this article's Online Repository at www.jacionline.org).

CLSM demonstrated surface-related bacterial biofilms on the nonpolypoidal sinonasal mucosa of all 9 CRS samples (Fig 1, A), but not on the epithelial surface of NPs. However, subepithelial and intracellular bacteria were observed in the cytoplasm of host cells in all 9 NP samples (Fig 1, B). The CLSM Z-axis view indicated that intracellular bacteria were subepithelial in all cases (Fig 1, C). Bacteria were confirmed within host cells using 49,6-diamidino-2-phenylindole, a nucleic acid stain that resolves the host cell nucleus, surrounded by densely packed bacteria filling the cytoplasm (Fig 1, D). Biofilms were not observed in any control samples. Species-specific fluorescence in situ hybridization identified brightly fluorescent bacteria in CRS samples including S aureus in 78%, Haemophilus influenza in 33%, and Pseudomonas aeruginosa in 33% of the patients (see Table E1 in this article's Online Repository at www. jacionline.org). Immunohistochemistry confirmed our finding of subepithelial intracellular S aureus, using an S aureus mAb (Fig 1, E). Immunohistochemical colocalization on sequential sections identified the S aureus–harboring host cells as mast cells (MCs) (Fig 2, A-D).

Our study directly compared nonpolypoidal sinonasal mucosa with NPs from the same patient (thus controlling for host genetics) and is the first to observe both subepithelial bacteria in ex vivo NP tissue and intracellular localization of S aureus within MCs. This contrasts with recent studies that have shown intracellular S aureus in nonpolypoidal CRS sinonasal mucosa.[5]

Sachse et al[6] demonstrated intracellular S aureus replication in vitro in NP epithelial cells by introducing an S aureus strain to a cell culture model. The mechanism of bacterial migration from surface-related biofilms to intracellular reservoirs remains unclear. However, growing evidence suggests that alterations in the epithelial layer compromise its function as a defensive barrier against environmental allergens and pathogens, as well as a mediator and regulator of innate and adaptive immunity.[7] A reduction in tight junction proteins and increased proinflammatory cytokines IFN-g and IL-4 within NPs lead to a disruption in epithelial integrity, induction of epithelial remodeling, and the formation of surface defects.[7] A defective epithelial layer may provide an opportunity for surface-related bacterial biofilms, already present in CRS, to disperse and penetrate into the tissue. This may explain the absence of surface-related biofilms observed on NP tissue in our study compared with those seen on sinonasal mucosa.

Initially, the bacteria-harboring host cells were presumed to be mononuclear phagocytes, but our immunohistochemical findings rather unexpectedly confirmed them to be MCs. This constitutes a novel finding in NPs. MCs appear to play an important role in promoting innate immunity against microbial pathogens.[8] Through activation of CD8¹T cells, MCs possess the ability to regulate both the T_H1 and T_H2 cytokine pathways, and can therefore adopt both immunosuppressive and immune-stimulatory properties.[8]

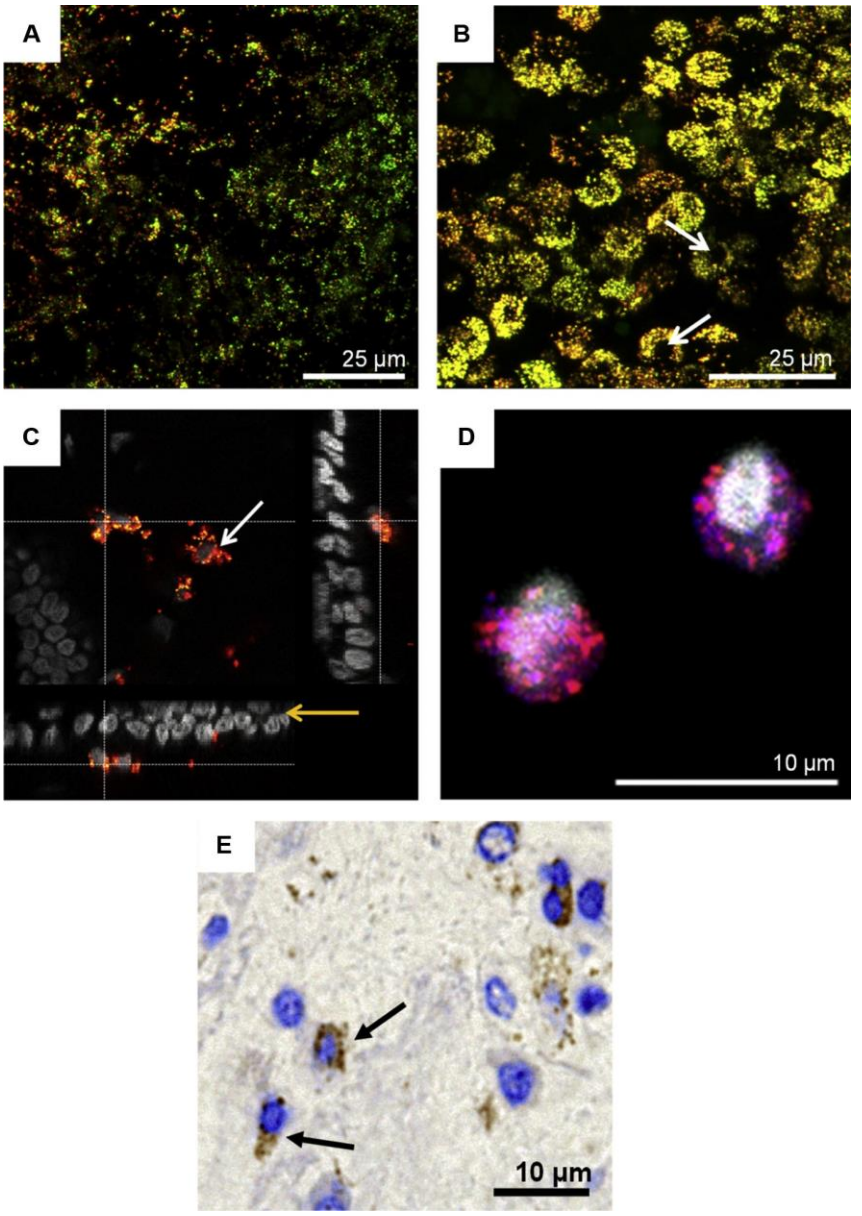

FIG 1. Intracellular S aureus in ex vivo NPs. Representative CLSM images of sinus mucosa and NP tissue following FISH showing Staphylococcus aureus (yellow), Staphylococcus genus biofilms (red), and bacteria hybridized only with a eubacterial probe (green). A, Aggregated bacteria are widely distributed over the epithelial surface of sinus mucosa. B, In contrast, bacterial reservoirs surround host cell nuclei in NP biopsies (white arrows). C, XYZ view: staphylococcal aggregates (white arrow) clearly visible beneath the epithelial surface (yellow arrow). D, Intracellular S aureus reservoirs (pink) colocalized with DAPI-stained host nuclei (gray). E, Immunohistochemistry staining with mouse anti–S aureus (brown) in an NP biopsy section demonstrating S aureus within the cytoplasm of host cells (black arrows) (340 magnification).
DAPI, 49-6-Diamidino-2-phenylindole, dihydrochloride; FISH, fluorescence in situ hybridization.

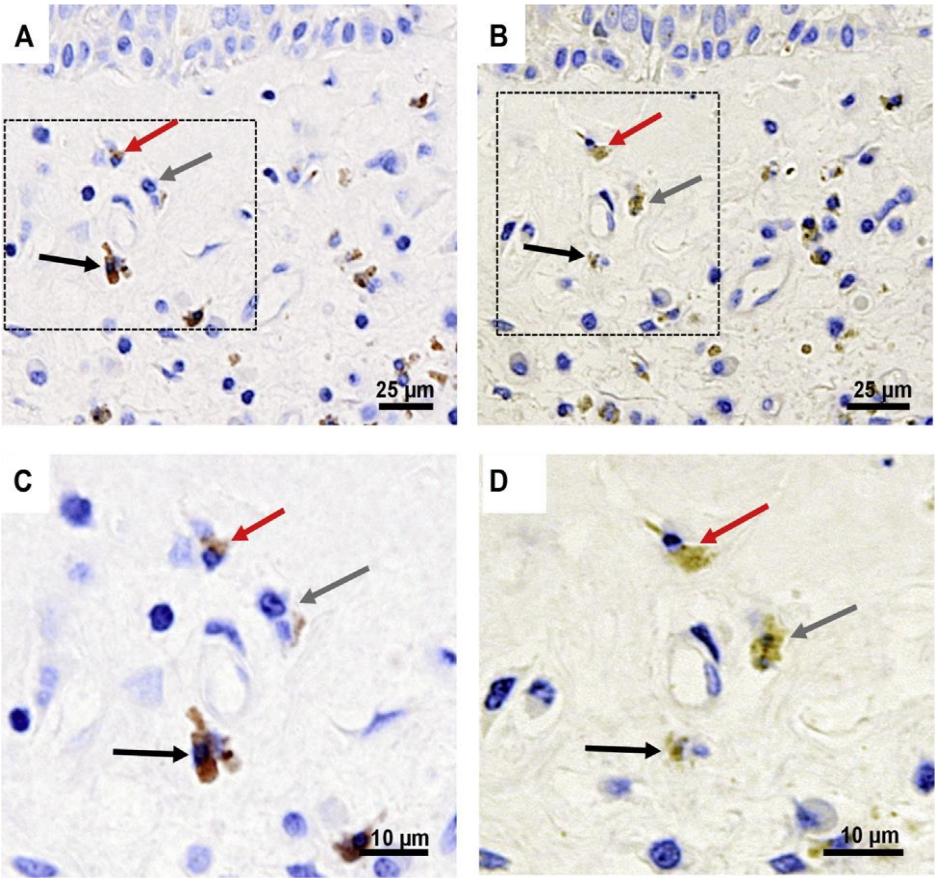

FIG 2. Immunohistochemical colocalization. Photomicrographs of sequential 2-mm sections of NP tissue stained with anti-AA1 MC tryptase (A) and mouse anti–S aureus (B) demonstrating subepithelial intracellular S aureus within MCs (arrows) (320 magnification). Both images are shown at higher magnification. (C and D 340 magnification).

Recently, MCs have been demonstrated to exert phagocytosis-independent antimicrobial activity against S aureus, mediated through extracellular traps and the release of antibacterial enzymes.[9] S aureus has been shown in vitro to subvert these extracellular antimicrobial mechanisms by internalizing within MCs.[9] Once within the MCs, S aureus appears to access the nutrient-rich cytosol and upregulate cell wall synthesis, allowing persistent and viable intracellular SA reservoirs to be established.[9]

The MC in the context of chronic S aureus infection may well act as a double-edged sword.[9] Although promoting innate immunity against microbial pathogens, the MC may be providing a safe haven for S aureus by protecting it from extracellular antimicrobial compounds. This not only avoids clearance but also facilitates the establishment of an intracellular microbial reservoir that could lead to persistence and chronic carriage. This may explain the high levels of resistance to systemic antibacterial therapies in chronic conditions such as CRS. Crucially, these intracellular S aureus reservoirs may constitute potential future therapeutic targets for the development of novel bacterial eradication strategies, aimed at reducing systemic antimicrobial usage, and in turn, the associated risk of antimicrobial drug resistance. To clarify mechanisms underlying survival of S aureus, mechanistic studies using invitro MC culture models are currently being planned.

We are indebted to all the study participants. We are grateful for the assistance received from staff of the Histochemistry Research and

Biomedical Imaging Units. We also thank Nijaguna Mathad (Consultant Neurosurgeon, University Hospital Southampton NHS Foundation Trust [UHSNFT]) and Ashok Rokade (Consultant Rhinologist and Anterior Skull Base Surgeon, UHSNFT) for providing us with the control tissue.

Stephen M. Hayes, MRCS[a,b,c,d]
Robert Howlin, PhD[a,b,c,e]
David A. Johnston, PhD[f]
Jeremy S. Webb, PhD[a,b,d,e,g]
Stuart C. Clarke, FRCPath, FFPH[a,b,c,d,g,h]
Paul Stoodley, PhD[a,b,d,g,i,j]
Philip G. Harries, FRCS (ORL-HNS)[b]
Susan J. Wilson, PhD[a,b,c,d,k]
Sylvia L. F. Pender, PhD[a,b,c,d]
Saul N. Faust, PhD, FRCPCH[a,b,c,d,g,l]
Luanne Hall-Stoodley, PhD[a,b,c,d,g,j,l]
Rami J. Salib, PhD, FRCS (ORL-HNS)[a,b,c,d,g,l]

From [a]the Southampton NIHR Respiratory Biomedical Research Unit, University of Southampton and University Hospital Southampton NHS Foundation Trust, [b]the Academic Unit of Clinical and Experimental Sciences, Faculty of Medicine, [c]University Hospital Southampton NHS Foundation Trust, [d]University of Southampton, [e]Centre for Biological Sciences, Faculty of Natural and Environmental Sciences, [f]the Biomedical Imaging Unit, [g]the Institute for Life Sciences, [h]Public Health England, and [i]the National Centre for Advanced Tribology, Faculty of Engineering, Southampton, United Kingdom; [j]the Centre for Microbial Interface Biology, The Ohio State University, Columbus, Ohio; and [k]the Histochemistry Research Unit and [l]Southampton NIHR Wellcome Trust Clinical Research Facility, Southampton, United Kingdom. E-mail: R.J.Salib@soton.ac.uk.

This work was supported by a surgical research fellowship grant from the Royal College of Surgeons of England (to S.M.H.) and a pump priming grant from the Royal College of Surgeons of England (to R.J.S.). S.M.H., R.H., J.S.W., S.C.C., S.J.W., S.L.F.P., S.N.F., L.H.-S., and R.J.S. were supported in part by the Southampton National Institute of Health Research (NIHR) Respiratory Biomedical Research Unit and NIHR Wellcome Trust Clinical Research Facility.

Disclosure of potential conflict of interest: J. S. Webb has received research support from the Biotechnology and Biological Sciences Research Council (David Phillips Fellowship award). S. C. Clarke has received research support from the National Institute for Health Research, GlaxoSmithKline, Pfizer, and Novartis. S. J. Wilson and R. J. Salib have received research support from the Royal College of Surgeons of England. S. N. Faust has received research support from the National Institute for Health Research (NIHR) Wellcome Trust Clinical Research Facility and NIHR Respiratory Biomedical Research Unit, Pfizer, Sanofi, GlaxoSmithKline, Novartis, and Cubist; has consultant arrangements with Novartis, Pfizer, and Sanofi; and has received travel support from GlaxoSmithKline. The rest of the authors declare that they have no relevant conflicts of interest.

REFERENCES

1. Fokkens WJ, Lund VJ, Mullol J, Bachert C, Alobid I, Baroody F, et al. European position paper on rhinosinusitis and nasal polyps 2012. Rhinology 2012; 23:1-298.
2. Cohen M, Kofonow J, Nayak JV, Palmer JN, Chiu AG, Leid JG, et al. Biofilms in chronic rhinosinusitis: a review. Am J Rhinol Allergy 2009;23:255-60.
3. Singhal D, Psaltis AJ, Foreman A, Wormald PJ. The impact of biofilms on outcomes after endoscopic sinus surgery. Am J Rhinol Allergy 2010;24:169-74.
4. Bachert C, van Zele T, Gevaert P, de Schrijver L, Van Cauwenberge P. Superantigens and nasal polyps. Curr Allergy Asthma Rep 2003;3:523-31.
5. Tan NC, Foreman A, Jardeleza C, Douglas R, Tran H, Wormald PJ. The multiplicity of Staphylococcus aureus in chronic rhinosinusitis: correlating surface biofilm and intracellular residence. Laryngoscope 2012;122:1655-60.
6. Sachse F, Becker K, von Eiff C, Metze D, Rudack C. Staphylococcus aureus invades the epithelium in nasal polyposis and induces IL-6 in nasal epithelial cells in vitro. Allergy 2010;65:1430-7.
7. Soyka MB, Wawrzyniak P, Eiwegger T, Holzmann D, Treis A, Wanke K, et al. Defective epithelial barrier in chronic rhinosinusitis: the regulation of tight junctions by IFN- and IL-4. J Allergy Clin Immunol 2012;130:1087-96.
8. Stelekati E, Bahri R, D'Orlando O, Orinska Z, Mittrucker HW, Langenhaun R, et al. Mast cell-mediated antigen presentation regulates CD8[1] T cell effector functions. Immunity 2009;31:665-76.
9. Abel J, Goldmann O, Ziegler C, Holtje C, Smeltzer MS, Cheung AL, et al. Staphylococcus aureus evades the extracellular antimicrobial activity of mast cells by promoting its own uptake. J Innate Immun 2011;3:495-507.

Available online February 11, 2015. http://dx.doi.org/10.1016/j.jaci.2014.12.1929

References

1. ENT-USA. Nasal photos (Internet). 1999 (Updated 2014 Oct). Accessed on: http://www.entusa.com/nose_photos.htm

2. Getbodysmart. 2000 (Updated 2016). Accessed on: www.getbodysmart.com.

3. Fokkens WJ, Lund VJ, Mullol J, Bachert C, Alobid I, Baroody F, et al. European Position Paper on Rhinosinusitis and Nasal Polyps 2012. Rhinology - Supplement. 2012(23):3 p preceding table of contents, 1-298.

4. Hastan D, Fokkens WJ, Bachert C, Newson RB, Bislimovska J, Bockelbrink A, et al. Chronic rhinosinusitis in Europe an underestimated disease. A GA2LEN study. Allergy. 2011;66(9):1216-23.

5. Blackwell DL, Collins JG, Coles R. Summary health statistics for U.S. adults: National Health Interview Survey, 1997. Vital & Health Statistics - Series 10: Data From the National Health Survey. 2002;(205):1-109.

6. Fokkens W, Lund V, Mullol J. European Position Paper on Rhinosinusitis and Nasal Polyps group. Rhinol Suppl. 2007;(20):1-136.

7. Schulzke JD, Ploeger S, Amasheh M, Fromm A, Zeissig S, Troeger H, et al. Epithelial tight junctions in intestinal inflammation. Ann N Y Acad Sci. 2009;(1165):294-300.

8. Collins JG. Prevalence of selected chronic conditions: United States, 1990-1992. Vital & Health Statistics - Series 10: Data From the National Health Survey. 1997(194):1-89.

9. Cohen M, Kofonow J, Nayak JV, Palmer JN, Chiu AG, Leid JG, et al. Biofilms in chronic rhinosinusitis: a review. Am J of Rhinol Allergy. 2009;23(3):255-60.

10. Gliklich RE, Metson R. The health impact of chronic sinusitis in patients seeking otolaryngologic care. Otolaryngol Head Neck Surg. 1995;113(1):104-9.

11. Stankiewicz J, Tami T, Truitt T, Atkins J, Winegar B, Cink P, et al. Impact of chronic rhinosinusitis on work productivity through one-year follow-up after

balloon dilation of the ethmoid infundibulum. Int Forum Allergy & Rhinol. 2011;1(1):38-45.

12. Bhattacharyya N, LJ K. Assessment of trends in antimicrobial resistance in chronic rhinosinusitis. Ann otol rhinol laryngol. 2008;117(6):448-52.

13. Antimicrobial resistance. Global Report on surveillance World Health Organisation. 2014;1-256.

14. Meltzer EO, Hamilos DL, Hadley JA, Lanza DC, Marple BF, Nicklas RA, et al. Rhinosinusitis: Establishing definitions for clinical research and patient care. Otolaryngol Head Neck Surg. 2004;131(6):S1-62.

15. Meltzer EO, Hamilos DL, Hadley JA, Lanza DC, Marple BF, Nicklas RA, et al. Rhinosinusitis: developing guidance for clinical trials. J Allergy Clin Immunol. 2006;118(5):S17-61.

16. Scadding GK, Durham SR, Mirakian R, Jones NS, Drake-Lee AB, Ryan D, et al. BSACI guidelines for the management of rhinosinusitis and nasal polyposis. Clin Exp Allergy. 2008;38(2):260-75.

17. Banerji A, Piccirillo JF, Thawley SE, Levitt RG, Schechtman KB, Kramper MA, et al. Chronic rhinosinusitis patients with polyps or polypoid mucosa have a greater burden of illness. Am J Rhinol. 2007;21(1):19-26.

18. Litvack JR, Fong K, Mace J, James KE, Smith TL. Predictors of olfactory dysfunction in patients with chronic rhinosinusitis. Laryngoscope. 2008;118(12):2225-30.

19. Tomassen P, Newson RB, Hoffmans R, Lötvall J, Cardell LO, Gunnbjörnsdóttir M, et al. Reliability of EP3OS symptom criteria and nasal endoscopy in the assessment of chronic rhinosinusitis a GA2LEN study. Allergy. 2011;66(4):556-61.

20. Shashy G, Moore J, Weaver A. Prevalence of the chronic sinusitis diagnosis in Olmsted County, Minnesota. Arch Otolaryngol Head Neck Surg. 2004;130(3):320-3.

21. Greisner WA, Settipane GA. Hereditary factor for nasal polyps. Allergy Asthma Proc. 1996;17(5):283-6.

22. Pilan RR, Pinna FR, Bezerra TF, Mori RL, Padua FG, Bento RF, et al. Prevalence of chronic rhinosinusitis in Sao Paulo. Rhinology. 2012;50(2):129-38.

23. Gordts F, Clement PA. Epidemiology and prevalence of aspecific chronic sinusitis. Acta Otorhinolaryngol Belg. 1997;51(4):205-8.

24. Ahsan SF, Jumans S, Nunez DA. Chronic rhinosinusitis: a comparative study of disease occurrence in North of Scotland and Southern Caribbean otolaryngology outpatient clinics over a two month period. Scot Med J. 2004;49(4):130-3.

25. Chen Y, Dales R, Lin M. The epidemiology of chronic rhinosinusitis in Canadians. Laryngoscope. 2003;113(7):1199-205.

26. Johansson L, Akerlund A, Holmberg K, Melen I, Bende M. Prevalence of nasal polyps in adults: the Skovde population-based study. Annals of Otology, Rhinology & Laryngology. 2003;112(7):625-9.

27. Kim YS, Kim NH, Seong SY, Kim KR, Lee G-B, Kim K-S. Prevalence and risk factors of chronic rhinosinusitis in Korea. Am J Rhinol Allergy. 2011;25(3):117-21.

28. Hedman J, Kaprio J, Poussa T, Nieminen MM. Prevalence of asthma, aspirin intolerance, nasal polyposis and chronic obstructive pulmonary disease in a population-based study. Int J Epidemiol. 1999;28(4):717-22.

29. Klossek JM, Neukirch F, Pribil C, Jankowski R, Serrano E, Chanal I, et al. Prevalence of nasal polyposis in France: a cross-sectional, case-control study. Allergy. 2005;60(2):233-7.

30. Settipane GA. Epidemiology of nasal polyps. Allergy Asthma Proc. 1996;17(5):231-6.

31. Settipane GA, Chafee FH. Nasal polyps in asthma and rhinitis. A review of 6,037 patients. J Allergy Clin immunol. 1977;59(1):17-21.

32. Larsen K, Tos M. The estimated incidence of symptomatic nasal polyps. Acta Otolaryngol. 2002;122(2):179-82.

33. Hosemann W, Göde U, Wagner W. Epidemiology, pathophysiology of nasal polyposis, and spectrum of endonasal sinus surgery. Am J Otolaryngol. 1994;15(2):85-98.

34. Drake-Lee AB, Lowe D, Swanston A, Grace A. Clinical profile and recurrence of nasal polyps. J Laryngol Otol. 1984;98(8):783-93.

35. Larsen K, Tos M. Clinical course of patients with primary nasal polyps. Acta otolaryngol. 1994;114(5):556-9.

36. Bachert C, Van Zele T, Gevaert P, De L, Van Cauwenberge P. Superantigens and nasal polyps. Curr Allergy Asthma Rep. 2003;3(6):523-31.

37. Mygind N. Nasal polyposis. J Allergy Clin Immunol. 1990;86(6 Pt 1):827-9.

38. Mygind N, Dahl R, Bachert C. Nasal polyposis, eosinophil dominated inflammation, and allergy. Thorax. 2000;55(Suppl 2):S79-83.

39. Samter M, Beers RF. Intolerance to aspirin. Clinical studies and consideration of its pathogenesis. Ann Int Med. 1968;68(5):975-83.

40. Szczeklik A, Gryglewski RJ, Czerniawska-Mysik G. Relationship of inhibition of prostaglandin biosynthesis by analgesics to asthma attacks in aspirin-sensitive patients. BMJ. 1975;1(5949):67-9.

41. Stevenson DD, Szczeklik A. Clinical and pathologic perspectives on aspirin sensitivity and asthma. J Allergy Clin Immunol. 2006;118(4):773-86.

42. Berges-Gimeno MP, Simon RA, Stevenson DD. The natural history and clinical characteristics of aspirin-exacerbated respiratory disease. Ann of Allergy Asthma Immunol. 2002;89(5):474-8.

43. Kowalski ML, Makowska JS, Blanca M, Bavbek S, Bochenek G, Bousquet J, et al. Hypersensitivity to nonsteroidal anti-inflammatory drugs (NSAIDs) - classification, diagnosis and management: review of the EAACI/ENDA(#) and GA2LEN/HANNA*. Allergy. 2011;66(7):818-29.

44. Settipane GA, Lund VJ, Bernstein J, Tos M. Nasal polyps: epidemiology, pathogenesis and treatment. Am J Otolaryngol. 1998;19(6):417-8.

45. Bezerra TF, Padua FG, Gebrim EM, Saldiva PH, Voegels RL. Biofilms in chronic rhinosinusitis with nasal polyps. Otolaryngol Head Neck Surg. 2011;144(4):612-6.

46. Van Bruaene N, Perez-Novo CA, Basinski TM, Van Zele T, Holtappels G, De Ruyck N, et al. T-cell regulation in chronic paranasal sinus disease. J Allergy Clin Immunol. 2008;121(6):1435-41.

47. Peters AT, Kato A, Zhang N, Conley DB, Suh L, Tancowny B, et al. Evidence for altered activity of the IL-6 pathway in chronic rhinosinusitis with nasal polyps. J Allergy Clin Immunol. 2010;125(2):397-403.

48. Van Zele T, Claeys S, Gevaert P, Van G, Holtappels G, Van P, et al. Differentiation of chronic sinus diseases by measurement of inflammatory mediators. Allergy. 2006;61(11):1280-9.

49. Tomassen P, Van Zele T, Zhang N, Perez-Novo C, Van Cauwenberge N, Gevaert P, et al. Pathophysiology of chronic rhinosinusitis. Proc Am Thorac Soc. 2011;8(1):115-20.

50. Zhang N, Van Zele T, Perez-Novo C, Van Cauwenberge N, Holtappels G, DeRuyck N, et al. Different types of T-effector cells orchestrate mucosal inflammation in chronic sinus disease. J Allergy Clin Immunol. 2008;122(5):961-8.

51. Riordan JR, Rommens JM, Kerem B, Alon N, Rozmahel R, Grzelczak Z, et al. Identification of the cystic fibrosis gene: cloning and characterization of complementary DNA. Science. 1989;245:1066–73.

52 Kerem B, Rommens JM, Buchanan JA, Markiewicz D, Cox TK, Chakravarti A, et al. Identification of the cystic fibrosis gene: genetic analysis. Science. 1989;245:1073–80.

53. Koitschev A, Wolff A, Koitschev C, Preyer S, Ziebach R, Stern M. Routine otorhinolaryngological examination in patients with cystic fibrosis. HNO. 2006;54(5):361-4.

54. Mainz JG, Koitschev A. Pathogenesis and management of nasal polyposis in cystic fibrosis. Curr Allergy Asthma Rep. 2012;12(2):163-74.

55. Henriksson G, Westrin KM, Karpati F, Wikstrom AC, Stierna P, Hjelte L. Nasal polyps in cystic fibrosis: clinical endoscopic study with nasal lavage fluid analysis. Chest.

56. Cimmino M, Cavaliere M, Nardone M, Plantulli A, Orefice A, Esposito V, et al. Clinical characteristics and genotype analysis of patients with cystic fibrosis and nasal polyposis. Clin Otolaryngol Allied Sci. 2003;28:125-32

57. Ratjen F, Doring G. Cystic fibrosis. Lancet. 2003;361:681-9

58. Schraven SP, Wehrmann M, Wagner W, Blumenstock G, Koitschev A. Prevalence and histopathology of chronic polypoid sinusitis in pediatric patients with cystic fibrosis. J Cyst Fibros. 2011;10:181-6.

59. Claeys S, Van Hoecke H, Holtappels G, Gevaert P, De Belder T, Verhasselt B, et al. Nasal polyps in patients with and without cystic fibrosis: a differentiation by innate markers and inflammatory mediators. Clin Exp Allergy. 2005;35:467-72

60. Knipping S, Holzhausen HJ, Riederer A, Bloching M. Cystic fibrosis: ultrastructural changes of nasal mucosa. Eur Arch Otorhinolaryngol. 2007;264:1413-8

61. Stammberger H. Functional endoscopic sinus surgery. Philadelphia: BC Decker. 1991.

62. Beninger M. Rhinitis, sinusitis and their relationship to allergies. Am J Rhinol 1992;(6):37-43.

63. Drake-Lee AB, McLaughlan P. Clinical symptoms, free histamine and IgE in patients with nasal polyposis. Int Arch Allergy Appl Immunol. 1982;69(3):268-71.

64. Drake-Lee AB, McLoughlan P. The release of histamine from nasal polyp tissue and peripheral blood when challenged with antihuman IgE, house dust mite extract and mixed grass pollen extract and compared with positive skin tests. J Laryngol Otol. 1988;102(10):886-9.

65. Bousquet J, Van Cauwenberge P. Allergic rhinitis and its impact on asthma. J Allergy Clin Immunol. 2001;108(suppl):S147-S334.

66. Brozek L, Bousquet J, Baena-Cagnani E, Bonini S, Canonica GW, Casale B, et al. Allergic Rhinitis and its Impact on Asthma (ARIA) guidelines: 2010 revision. J Allergy Clin Immunol. 2010;126(3):466-76.

67. ISAAC. Worldwide variation in prevalence of symptoms of asthma, allergic rhinoconjunctivitis, and ectopic eczema: ISAAC. The international study of asthma and allergies in childhood (ISAAC) steering committee. Lancet. 1998;351(9111):1225-32.

68. Langdon C, Mullol J. Nasal polyps in patients with asthma: prevalence, impact, and management challenges. J Asthma Allergy. 2016; 9: 45–53

69. Kowalski ML. Aspirin-sensitive rhinosinusitis and asthma. Clin Allergy Immunol. 2007;19:147-75.

70. Picado C, Bioque G, Roca-Ferrer J, Pujols L, Mullol J, Benitez P, et al. Nuclear factor-kappaB activity is down-regulated in nasal polyps from aspirin-sensitive asthmatics. Allergy. 2003;58(2):122-6.

71. Kowalski ML, Pawliczak R, Wozniak J, Siuda K, Poniatowska M, Iwaszkiewicz J, et al. Differential metabolism of arachidonic acid in nasal polyp epithelial cells cultured from aspirin-sensitive and aspirin-tolerant patients. Am J Respir Crit Care Med. 2000;161(2 Pt 1):391-8.

72. Fischer AR, Rosenberg MA, Lilly CM, Callery JC, Rubin P, Cohn J, et al. Direct evidence for a role of the mast cell in the nasal response to aspirin in aspirin-sensitive asthma. J Allergy Clin Immunol. 1994;94(6):1046-56.

73. Hamilos DL, Leung DY, Huston DP, Kamil A, Wood R, Hamid Q. GM-CSF, IL-5 and RANTES immunoreactivity and mRNA expression in chronic hyperplastic sinusitis with nasal polyposis (NP). Clin Exp Allergy. 1998;28(9):1145-52.

74. Varga EM, Jacobson MR, Masuyama K, Rak S, Till SJ, Darby Y, et al. Inflammatory cell populations and cytokine mRNA expression in the nasal mucosa in aspirin-sensitive rhinitis. Eur Respir J. 1999;14(3):610-5.

75. Katial R, Strand M, Prasertsuntarasai T, Leung R, Zheng W, Alam R. The effect of aspirin desensitization on novel biomarkers in apirin-exacerbated respiratory diseases. J Allergy Clin Immunol. 2010;126(4):738-44.

76. Ellegard E. The etiology and management of pregnancy rhinitis. Am J Respir Med. 2003;2(6):469-75.

77. Zinreich SJ, Mattox DE, Kennedy DW, Chisholm HL, Diffley DM, Rosenbaum AE. Concha bullosa: CT evaluation. J Comput Assist Tomogr. 1988;12(5):778-84.

78. Bolger WE, Butzin CA, Parsons DS. Paranasal sinus bony anatomic variations and mucosal abnormalities: CT analysis for endoscopic sinus surgery. Laryngoscope. 1991;101(1 Pt 1):56-64.

79. Holbrook EH, Brown CL, Lyden ER, Leopold DA. Lack of significant correlation between rhinosinusitis symptoms and specific regions of sinus computer tomography scans. Am J Rhinol. 2005;19(4):382-7.

80. Lee JT, Kennedy DW, Palmer JN, Feldman M, Chiu AG. The incidence of concurrent osteitis in patients with chronic rhinosinusitis: a clinicopathological study. Am J Rhinol. 2006;20(3):278-82.

81. Braun H, Buzina W, Freudenschuss K, Beham A, Stammberger H. 'Eosinophilic fungal rhinosinusitis': a common disorder in Europe? Laryngoscope. 2003;113(2):264-9.

82. Shin SH, Ponikau JU, Sherris DA, Congdon D, Frigas E, Homburger HA, et al. Chronic rhinosinusitis: an enhanced immune response to ubiquitous airborne fungi. J Allergy Clin Immunol. 2004;114(6):1369-75.

83. Schleimer RP, Kato A, Kern R, Kuperman D, Avila PC. Epithelium: at the interface of innate and adaptive immune responses. J Allergy Clin Immunol. 2007;120(6):1279-84.

84. Soyka MB, Wawrzyniak P, Eiwegger T, Holzmann D, Treis A, Wanke K, et al. Defective epithelial barrier in chronic rhinosinusitis: the regulation of tight junctions by IFN- and IL-4. J Allergy Clin Immunol. 2012;130(5):1087-96.

85. De Benedetto A, Rafaels NM, McGirt LY, Ivanov AI, Georas SN, Cheadle C, et al. Tight junction defects in patients with atopic dermatitis. J Allergy Clin Immunol. 2011;127(3):773-86.

86. Kirschner N, Houdek P, Fromm M, Moll I, Brandner JM. Tight junctions form a barrier in human epidermis. Eur J Cell Biol. 2010;89(11):839-42.

87. Holgate ST. Epithelium dysfunction in asthma. J Allergy Clin Immunol. 2007;120(6):1233-44.

88. Richer L, Truong-Tran Q, Conley B, Carter R, Vermylen D, Grammer C, et al. Epithelial genes in chronic rhinosinusitis with and without nasal polyps. Am J Rhinol. 2008;22(3):228-34.

89. Araujo E, Palombini BC, Cantarelli V, Pereira A, Mariante A. Microbiology of middle meatus in chronic rhinosinusitis. Am J Rhinol. 2003;17(1):9-15.

90. Stressmann FA RG, Chan SW, Howarth PH, Harries PG, Bruce KD, Salib RJ. Characterisation of bacterial community diversity in chronic rhinosinusitis infections using novel culture-independent techniques. Am J Rhinol Allergy. 2011;25(4):133-40.

91. Clement S, Vaudaux P, Francois P, Schrenzel J, Huggler E, Kampf S, et al. Evidence of an intracellular reservoir in the nasal mucosa of patients with recurrent Staphylococcus aureus rhinosinusitis. J Infect Dis. 2005;192(6):1023-8.

92. Sachse F, Becker K, von Eiff C, Metze D, Rudack C. Staphylococcus aureus invades the epithelium in nasal polyposis and induces IL-6 in nasal epithelial cells in vitro. Allergy. 2010;65(11):1430-7.

93. Corriveau MN, Zhang N, Holtappels G, Van Roy N, Bachert C. Detection of Staphylococcus aureus in nasal tissue with peptide nucleic acid-fluorescence in situ hybridization. Am J Rhinol Allergy. 2009;23(5):461-5.

94. Tan NC, Foreman A, Jardeleza C, Douglas R, Tran H, Wormald PJ. The multiplicity of Staphylococcus aureus in chronic rhinosinusitis: correlating surface biofilm and intracellular residence. Laryngoscope. 2012;122(8):1655-60.

95. Kluytmans J, van A, Verbrugh H. Nasal carriage of Staphylococcus aureus: epidemiology, underlying mechanisms, and associated risks. Clin Microbiol Rev. 1997;10(3):505-20.

96. Proft T, Fraser JD. Bacterial superantigens. Clin Exp Immunol. 2003;133(3):299-306.

97. Bachert C, Gevaert P, Holtappels G, Cuvelier C, van P. Nasal polyposis: from cytokines to growth. Am J Rhinol. 2000;14(5):279-90.

98. Derycke L, Perez-Novo C, Van K, Corriveau MN, Bachert C. Staphylococcus aureus and Chronic Airway Disease. World Allergy Organ J. 2010;3(8):223-8.

99. Bachert C, Gevaert P, Holtappels G, Johansson SG, van P. Total and specific IgE in nasal polyps is related to local eosinophilic inflammation. J Allergy Clin Immunol. 2001;107(4):607-14.

100. Bachert C, Gevaert P, Zhang N, Van Zele T, Perez-Novo C. Role of staphylococcal superantigens in airway disease. Chem Immunol Allergy. 2007;93:214-36.

101. Patou J, Gevaert P, Van Zele T, Holtappels G, Van Cauwenberge P, Bachert C. Staphylococcus aureus enterotoxin B, protein A, and lipoteichoic acid stimulations in nasal polyps. J Allergy Clin Immunol. 2008;121(1):110-5.

102. Pérez Novo CA, Jedrzejczak-Czechowicz M, Lewandowska-Polak A, Claeys C, Holtappels G, Van P, et al. T cell inflammatory response, Foxp3 and TNFRS18-L regulation of peripheral blood mononuclear cells from patients with nasal polyps-asthma after staphylococcal superantigen stimulation. Clin Exp Allergy. 2010;40(9):1323-32.

103. Langier S, Landsberg R, Sade K, Kivity S. Anti-IL-5 immunomodulates the effect of Staphylococcus aureus enterotoxin on T cell response in nasal polyps. Rhinology. 2011;49(5):570-6.

104. Pérez-Novo A, Waeytens A, Claeys C, Cauwenberge PV, Bachert C. Staphylococcus aureus enterotoxin B regulates prostaglandin E2 synthesis,

growth, and migration in nasal tissue fibroblasts. J Infect Dis. 2008;197(7):1036-43.

105. Okano M, Fujiwara T, Haruna T, Kariya S, Makihara S, Higaki T, et al. Prostaglandin E(2) suppresses staphylococcal enterotoxin-induced eosinophilia-associated cellular responses dominantly through an E-prostanoid 2-mediated pathway in nasal polyps. J Allergy Clin Immunol. 2009;123(4):868-74.

106. Huvenne W, Callebaut I, Reekmans K, Hens G, Bobic S, Jorissen M, et al. Staphylococcus aureus enterotoxin B augments granulocyte migration and survival via airway epithelial cell activation. Allergy. 2010;65(8):1013-20.

107. Wang M, Shi P, Chen B, Shi G, Li H, Wang H. Superantigen-induced glucocorticoid insensitivity in the recurrence of chronic rhinosinusitis with nasal polyps. Otolaryngol Head Neck Surg. 2011;145(5):717-22.

108. Zhang N, Gevaert P, Van Zele T, Perez-Novo C, Patou J, Holtappels G, et al. An update on the impact of Staphylococcus aureus enterotoxins in chronic sinusitis with nasal polyposis. Rhinology. 2005;43(3):162-8.

109. Gevaert P, Holtappels G, Johansson SG, Cuvelier C, Cauwenberge P, Bachert C. Organization of secondary lymphoid tissue and local IgE formation to Staphylococcus aureus enterotoxins in nasal polyp tissue. Allergy. 2005;60(1):71-9.

110. Van Crombruggen K, Zhang N, Gevaert P, Tomassen P, Bachert C. Pathogenesis of chronic rhinosinusitis: inflammation. J Allergy Clin Immunol. 2011;128(4):728-32.

111. Xaubet A, Mullol J, López E, Roca-Ferrer J, Rozman M, Carrión T, et al. Comparison of the role of nasal polyp and normal nasal mucosal epithelial cells on in vitro eosinophil survival. Mediation by GM-CSF and inhibition by dexamethasone. Clin Exp Allergy. 1994;24(4):307-17.

112. Leung YM, Bloom W. Update on glucocorticoid action and resistance. J Allergy Clin Immunol. 2003;111(1):3-22.

113. Pujols L, Mullol J, Roca-Ferrer J, Torrego A, Xaubet A, Cidlowski A, et al. Expression of glucocorticoid receptor alpha- and beta-isoforms in human cells and tissues. Am J Physiol Cell Physiol. 2002;283(4):1324-31

114. Oakley RH, Sar M, Cidlowski JA. The human glucocorticoid receptor beta isoform. Expression, biochemical properties, and putative function. J Biol Chem. 1996;271(16):9550-9.

115. Pujols L, Mullol J, Benítez P, Torrego A, Xaubet A, de HJ, et al. Expression of the glucocorticoid receptor alpha and beta isoforms in human nasal mucosa and polyp epithelial cells. Respir Med. 2003;97(1):90-6.

116. Hamilos DL, Leung DY, Muro S, Kahn AM, Hamilos SS, Thawley SE, et al. GRbeta expression in nasal polyp inflammatory cells and its relationship to the anti-inflammatory effects of intranasal fluticasone. J Allergy Clin Immunol. 2001;108(1):59-68.

117. Lund J, Black H, Szabó Z, Schrewelius C, Akerlund A. Efficacy and tolerability of budesonide aqueous nasal spray in chronic rhinosinusitis patients. Rhinology. 2004;42(2):57-62.

118. Sykes DA, Wilson R, Chan KL, Mackay IS, Cole PJ. Relative importance of antibiotic and improved clearance in topical treatment of chronic mucopurulent rhinosinusitis. A controlled study. Lancet. 1986;2(8503):359-60.

119. Cuenant G, Stipon JP, Plante-Longchamp G, Baudoin C, Guerrier Y. Efficacy of endonasal neomycin-tixocortol pivalate irrigation in the treatment of chronic allergic and bacterial sinusitis. ORL; J Otorhinolaryngol Relat Spec. 1986;48(4):226-32.

120. Lavigne F, Cameron L, Renzi M, Planet JF, Christodoulopoulos P, Lamkioued B, et al. Intrasinus administration of topical budesonide to allergic patients with chronic rhinosinusitis following surgery. Laryngoscope. 2002;112(5):858-64.

121. Parikh A, Scadding GK, Darby Y, Baker RC. Topical corticosteroids in chronic rhinosinusitis: a randomized, double-blind, placebo-controlled trial

using fluticasone propionate aqueous nasal spray. Rhinology. 2001;39(2):75-9.

122. Mygind N, Pedersen CB, Prytz S, Sørensen H. Treatment of nasal polyps with intranasal beclomethasone dipropionate aerosol. Clin Allergy. 1975;5(2):159-64.

123. Vendelo L, Illum P, Kristensen S, Winther L, Vang S, Synnerstad B. The effect of budesonide (Rhinocort) in the treatment of small and medium-sized nasal polyps. Clinical otolaryngology and allied sciences. 1993;18(6):524-7.

124. Stjärne P, Blomgren K, Cayé-Thomasen P, Salo S, Søderstrøm T. The efficacy and safety of once-daily mometasone furoate nasal spray in nasal polyposis: a randomized, double-blind, placebo-controlled study. Acta Otolaryngol. 2006;126(6):606-12.

125. Aukema AC, Mulder GH, Fokkens J. Treatment of nasal polyposis and chronic rhinosinusitis with fluticasone propionate nasal drops reduces need for sinus surgery. J Allergy Clini Immunol. 2005;115(5):1017-23.

126. Lildholdt T, Rundcrantz H, Lindqvist N. Efficacy of topical corticosteroid powder for nasal polyps: a double-blind, placebo-controlled study of budesonide. Clin Otolaryngol Allied Sci. 1995;20(1):26-30.

127. Lildholdt T, Rundcrantz H, Bende M, Larsen K. Glucocorticoid treatment for nasal polyps. The use of topical budesonide powder, intramuscular betamethasone, and surgical treatment. Arch Otolaryngol Head Neck Surg. 1997;123(6):595-600.

128. Van Camp C, Clement PA. Results of oral steroid treatment in nasal polyposis. Rhinology. 1994;32(1):5-9.

129. Damm M, Jungehülsing M, Eckel HE, Schmidt M, Theissen P. Effects of systemic steroid treatment in chronic polypoid rhinosinusitis evaluated with magnetic resonance imaging. Otolaryngol Head Neck Surg. 1999;120(4):517-23.

130. Benítez P, Alobid I, de HJ, Berenguer J, Bernal-Sprekelsen M, Pujols L, et al. A short course of oral prednisone followed by intranasal budesonide is an effective treatment of severe nasal polyps. Laryngoscope. 2006;116(5):770-5.

131. Hissaria P, Smith W, Wormald J, Taylor J, Vadas M, Gillis D, et al. Short course of systemic corticosteroids in sinonasal polyposis: a double-blind, randomized, placebo-controlled trial with evaluation of outcome measures. J Allergy Clin Immunol. 2006;118(1):128.

132. Vaidyanathan S, Barnes M, Williamson P, Hopkinson P, Donnan PT, Lipworth B. Treatment of chronic rhinosinusitis with nasal polyposis with oral steroids followed by topical steroids: a randomized trial. Ann Intern Med. 2011;154(5):293-302.

133. Rupa V, Jacob M, Mathews MS, Seshadri S. A prospective, randomised, placebo-controlled trial of postoperative oral steroid in allergic fungal sinusitis. Eur Arch Otorhinolaryngol. 2010;267(2):233-8.

134. Van Zele T, Gevaert P, Holtappels G, Beule A, Wormald PJ, Mayr S, et al. Oral steroids and doxycycline: two different approaches to treat nasal polyps. J Allergy Clin Immunol. 2010;125(5):1069-76.

135. Benitez P, Alobid I, de J, Berenguer J, Bernal-Sprekelsen M, Pujols L, et al. A short course of oral prednisone followed by intranasal budesonide is an effective treatment of severe nasal polyps. Laryngoscope. 2006;116(5):770-5.

136. Namyslowski G, Misiolek M, Czecior E, Malafiej E, Orecka B, Namyslowski P, et al. Comparison of the efficacy and tolerability of amoxycillin/clavulanic acid 875 mg b.i.d. with cefuroxime 500 mg b.i.d. in the treatment of chronic and acute exacerbation of chronic sinusitis in adults. J Chemother. 2002;14(5):508.

137. Kudoh S, Uetake T, Hagiwara K, Hirayama M, Hus LH, Kimura H, et al. Clinical effects of low-dose long-term erythromycin chemotherapy on diffuse panbronchiolitis]. Nihon Kyōbu Shikkan Gakkai Zasshi. 1987;25(6):632-42.

138. Wallwork B, Coman W, Mackay-Sim A, Greiff L, Cervin A. A double-blind, randomized, placebo-controlled trial of macrolide in the treatment of chronic rhinosinusitis. Laryngoscope. 2006;116(2):189-93.

139. Suzuki H, Ikeda K, Honma R, Gotoh S, Oshima T, Furukawa M, et al. Prognostic factors of chronic rhinosinusitis under long-term low-dose macrolide therapy. ORL; journal for oto-rhino-laryngology and its related specialties. 2000;62(3):121.

140. Van Zele T, Gevaert P, Watelet J-B, Claeys G, Holtappels G, Claeys C, et al. Staphylococcus aureus colonization and IgE antibody formation to enterotoxins is increased in nasal polyposis. J Allergy Clin Immunol. 2004;114(4):981-3.

141. Foreman A, Holtappels G, Psaltis AJ, Jervis-Bardy J, Field J, Wormald PJ, et al. Adaptive immune responses in Staphylococcus aureus biofilm-associated chronic rhinosinusitis. Allergy. 2011;66(11):1449-56.

142. Schalek P, Petrás P, Klement V, Hahn A. Short-term antibiotics treatment in patients with nasal polyps and enterotoxins producing Staphylococcus aureus strains. Eur Arch Otorhinolaryngol. 2009;266(12):1909-13.

143. Yamada T, Fujieda S, Mori S, Yamamoto H, Saito H. Macrolide treatment decreased the size of nasal polyps and IL-8 levels in nasal lavage. American journal of rhinology. 2000;14(3):143.

144. Wormald PJ, Cain T, Oates L, Hawke L, Wong I. A comparative study of three methods of nasal irrigation. Laryngoscope. 2004;114(12):2224-7.

145. Pynnonen A, Mukerji S, Kim HM, Adams E, Terrell E. Nasal saline for chronic sinonasal symptoms: a randomized controlled trial. Arch Otolaryngol Head Neck Surg. 2007;133(11):1115-20.

146. Harvey R, Hannan SA, Badia L, Scadding G. Nasal saline irrigations for the symptoms of chronic rhinosinusitis. Cochrane Database Syst Rev. 2007(3).

147. Freeman SRM, Sivayoham ESG, Jepson K, de J. A preliminary randomised controlled trial evaluating the efficacy of saline douching following endoscopic sinus surgery. Clin Otolaryngol. 2008;33(5):462-5.

148. Ragab S, Parikh A, Darby YC, Scadding GK. An open audit of montelukast, a leukotriene receptor antagonist, in nasal polyposis associated with asthma. Clin Exp Allergy. 2001;31(9):1385-91.

149. Schäper C, Noga O, Koch B, Ewert R, Felix SB, Gläser S, et al. Anti-inflammatory properties of montelukast, a leukotriene receptor antagonist in patients with asthma and nasal polyposis. J Investig Allergol Clin Immunol. 2011;21(1):51-8.

150. Haye R, Aanesen JP, Burtin B, Donnelly F, Duby C. The effect of cetirizine on symptoms and signs of nasal polyposis. J laryngol Otol. 1998;112(11):1042-6.

151. Chester C, Sindwani R. Symptom outcomes in endoscopic sinus surgery: a systematic review of measurement methods. Laryngoscope. 2007;117(12):2239-43.

152. Hopkins C, Browne JP, Slack R, Lund V, Topham J, Reeves B, et al. The national comparative audit of surgery for nasal polyposis and chronic rhinosinusitis. Clin Otolaryngol. 2006;31(5):390-8.

153. Poetker M, Mendolia-Loffredo S, Smith L. Outcomes of endoscopic sinus surgery for chronic rhinosinusitis associated with sinonasal polyposis. Am J Rhinol. 2007;21(1):84-8.

154. Antunes B, Gudis A, Cohen A. Epithelium, cilia, and mucus: their importance in chronic rhinosinusitis. Immunol Allergy Clin North Am. 2009;29(4):631-43.

155. Saito M, Innes L, Pletcher D. Rheologic properties of sinonasal mucus in patients with chronic sinusitis. Am J Rhinol Allergy. 2010;24(1):1-5.

156. Zuckerman D, Lee Y, DelGaudio M, Moore E, Nava P, Nusrat A, et al. Pathophysiology of nasal polyposis: the role of desmosomal junctions. Am J Rhinol. 2008;22(6):589-97.

157. Rogers GA, Den BK, Parkos A, Nusrat A, Delgaudio M, Wise K. Epithelial tight junction alterations in nasal polyposis. Int Forum Allergy Rhinol. 2011;1(1):50-4.

158. Tieu D, Kern C, Schleimer P. Alterations in epithelial barrier function and host defense responses in chronic rhinosinusitis. J Allergy Clin Immunol. 2009;124(1):37-42.

159. Schleimer RP, Lane P, Kim J. Innate and acquired immunity and epithelial cell function in chronic rhinosinusitis. Clin Allergy Immunol. 2007;(20):51-78.

160. Vandermeer J, Sha Q, Lane P, Schleimer P. Innate immunity of the sinonasal cavity: expression of messenger RNA for complement cascade components and toll-like receptors. Archives of otolaryngology--head & neck surgery. 2004;130(12):1374.

161. Claeys S, de T, Holtappels G, Gevaert P, Verhasselt B, van P, et al. Human beta-defensins and toll-like receptors in the upper airway. Allergy. 2003;58(8):748-53.

162. Sha Q, Truong-Tran Q, Plitt R, Beck A, Schleimer P. Activation of airway epithelial cells by toll-like receptor agonists. Am J Respir Cell Mol Biol. 2004;31(3):358-64.

163. Lane P, Truong-Tran Q-A, Myers A, Bickel C, Schleimer P. Serum amyloid A, properdin, complement 3, and toll-like receptors are expressed locally in human sinonasal tissue. Am J Rhinol. 2006;20(1):117-23.

164. Lane P, Truong-Tran QA, Schleimer P. Altered expression of genes associated with innate immunity and inflammation in recalcitrant rhinosinusitis with polyps. Am J Rhinol. 2006;20(2):138-44.

165. Bianchi E, Manfredi A. Immunology. Dangers in and out. Science. 2009;323(5922):1683-4.

166. Iwasaki A, Medzhitov R. Toll-like receptor control of the adaptive immune responses. Nat Immunol. 2004;5(10):987-95.

167. Kato A, Schleimer P. Beyond inflammation: airway epithelial cells are at the interface of innate and adaptive immunity. Curr Opin Immunol. 2007;19(6):711-20.

168. Ramanathan M, Lee W-K, Dubin G, Lin S, Spannhake W, Lane P. Sinonasal epithelial cell expression of toll-like receptor 9 is decreased in chronic rhinosinusitis with polyps. Am J Rhinol. 2007;21(1):110-6.

169. Ooi EH, Psaltis AJ, Witterick IJ, Wormald PJ. Innate immunity. Otolaryngol Clin North Am. 2010;43(3):473-87.

170. Laudien M, Dressel S, Harder J, Gläser R. Differential expression pattern of antimicrobial peptides in nasal mucosa and secretion. Rhinology. 2011;49(1):107-11.

171. Seshadri S, Lin DC, Rosati M, Carter RG, Norton JE, Suh L, et al. Reduced expression of antimicrobial PLUNC proteins in nasal polyp tissues of patients with chronic rhinosinusitis. Allergy. 2012;67(7):920-8.

172. Ramanathan M, Lee W-K, Spannhake W, Lane P. Th2 cytokines associated with chronic rhinosinusitis with polyps down-regulate the antimicrobial immune function of human sinonasal epithelial cells. Am J Rhinol. 2008;22(2):115-21.

173. Wolk K, Kunz S, Witte E, Friedrich M, Asadullah K, Sabat R. IL-22 increases the innate immunity of tissues. Immunity. 2004;21(2):241-54.

174. Pickert G, Neufert C, Leppkes M, Zheng Y, Wittkopf N, Warntjen M, et al. STAT3 links IL-22 signaling in intestinal epithelial cells to mucosal wound healing. J Exp Med. 2009;206(7):1465-72.

175. Aujla J, Chan R, Zheng M, Fei M, Askew J, Pociask A, et al. IL-22 mediates mucosal host defense against Gram-negative bacterial pneumonia. Nat Med. 2008;14(3):275-81.

176. Ramanathan M, Spannhake W, Lane P. Chronic rhinosinusitis with nasal polyps is associated with decreased expression of mucosal interleukin 22 receptor. Laryngoscope. 2007;117(10):1839-43.

177. Peters T, Kato A, Zhang N, Conley B, Suh L, Tancowny B, et al. Evidence for altered activity of the IL-6 pathway in chronic rhinosinusitis with nasal polyps. J Allergy Clin Immunol. 2010;125(2):397-403.

178. Lundberg JO, Farkas-Szallasi T, Weitzberg E, Rinder J, Lidholm J, Anggaard A, et al. High nitric oxide production in human paranasal sinuses. Nat Med. 1995;1(4):370-3.

179. Colantonio D, Brouillette L, Parikh A, Scadding GK. Paradoxical low nasal nitric oxide in nasal polyposis. Clin Exp Allergy. 2002;32(5):698-701.

180. Lindberg S, Cervin A, Runer T. Nitric oxide (NO) production in the upper airways is decreased in chronic sinusitis. Act Otolaryngologica. 1997;117(1):113-7.

181. Ragab SM, Lund VJ, Saleh HA, Scadding G. Nasal nitric oxide in objective evaluation of chronic rhinosinusitis therapy. Allergy. 2006;61(6):717-24.

182. Tantilipikorn P, Bunnag C, Nan Z, Bachert C. Staphylococcus aureus superantigens and their role in eosinophilic nasal polyp disease. Asian Pac J Allergy Immunol. 2012;30(3):171-6.

183. Fairweather D, Cihakova D. Alternatively activated macrophages in infection and autoimmunity. J Autoimmun. 2009;33(3-4):222-30.

184. Martinez O, Helming L, Gordon S. Alternative activation of macrophages: an immunologic functional perspective. Ann Rev Immunol. 2009;27:451-81.

185. Krysko O, Holtappels G, Zhang N, Kubica M, Deswarte K, Derycke L, et al. Alternatively activated macrophages and impaired phagocytosis of S. aureus in chronic rhinosinusitis. Allergy. 2011;66(3):396-403.

186. Krysko O, Vandenabeele P, Krysko DV, Bachert C. Impairment of phagocytosis of apoptotic cells and its role in chronic airway diseases. Apoptosis. 2010;15(9):1137-46.

187. Lee JJ, Jacobsen EA, McGarry MP, Schleimer RP, Lee NA. Eosinophils in health and disease: the LIAR hypothesis. Clin Exp Allergy. 2010;40(4):563-75.

188. Ponikau JU, Sherris DA, Kern EB, Homburger HA, Frigas E, Gaffey TA, et al. The diagnosis and incidence of allergic fungal sinusitis. Mayo Clin proc. 1999;74(9):877-84.

189. Jankowski R, Bouchoua F, Coffinet L, Vignaud JM. Clinical factors influencing the eosinophil infiltration of nasal polyps. Rhinology. 2002;40(4):173-8.

190. Jankowski R, Béné MC, Moneret-Vautrin AD, Haas F, Faure G, Simon C, et al. Immunohistological characteristics of nasal polyps. A comparison with healthy mucosa and chronic sinusitis. Rhinol Suppl. 1989;8:51-8.

191. Zhang N, Holtappels G, Claeys C, Huang G, van CP, Bachert C. Pattern of inflammation and impact of Staphylococcus aureus enterotoxins in nasal polyps from southern China. Am J Rhinol. 2006;20(4):445-50.

192. Kim J-W, Hong S-L, Kim Y-K, Lee CH, Min Y-G, Rhee C-S. Histological and immunological features of non-eosinophilic nasal polyps. Otolaryngol Head Neck Surg. 2007;137(6):925-30.

193. Yao T, Kojima Y, Koyanagi A, Yokoi H, Saito T, Kawano K, et al. Eotaxin-1, -2, and -3 immunoreactivity and protein concentration in the nasal polyps of eosinophilic chronic rhinosinusitis patients. Laryngoscope. 2009;119(6):1053-9.

194. Ying S, Meng Q, Taborda-Barata L, Corrigan CJ, Barkans J, Assoufi B, et al. Human eosinophils express messenger RNA encoding RANTES and store and release biologically active RANTES protein. Eur J Immunol. 1996;26(1):70-6.

195. Cao P-P, Li H-B, Wang B-F, Wang S-B, You X-J, Cui Y-H, et al. Distinct immunopathologic characteristics of various types of chronic rhinosinusitis in adult Chinese. J Allergy Clin Immunol. 2009;124(3):478-84.

196. Bachert C, Wagenmann M, Hauser U, Rudack C. IL-5 synthesis is upregulated in human nasal polyp tissue. J Allergy Clin Immunol. 1997;99(6 Pt 1):837-42.

197. Rudack C, Steinhoff M, Mooren F, Buddenkotte J, Becker K, von C, et al. PAR-2 activation regulates IL-8 and GRO-alpha synthesis by NF-kappaB, but not RANTES, IL-6, eotaxin or TARC expression in nasal epithelium. Clin Exp Allergy. 2007;37(7):1009-22.

198. Allen JS, Eisma R, Leonard G, Lafreniere D, Kreutzer D. Interleukin-8 expression in human nasal polyps. Otolaryngol Head Neck Surg 1997;117(5):535-41.

199. Zhang N, Van Zele T, Perez-Novo C, Van BN, Holtappels G, DeRuyck N, et al. Different types of T-effector cells orchestrate mucosal inflammation in chronic sinus disease. J Allergy Clin Immunol. 2008;122(5):961-8.

200. Wedemeyer J, Galli SJ. Mast cells and basophils in acquired immunity. Br Med Bull. 2000:56(4):936-55.

201. Stelekati E, Bahri R, D'Orlando O, Orinska Z, Mittrucker HW, Langenhaun R, et al. Mast cell-mediated antigen presentation regulates CD8+ T cell effector functions. Immunity. 2009;31(4):665-76.

202. Stone D, Prussin C, Metcalfe D. IgE, mast cells, basophils, and eosinophils. J Allergy Clin Immunol. 2010;125(2):73-80.

203. Abel J, Goldmann O, Ziegler C, Holtje C, Smeltzer MS, Cheung AL, et al. Staphylococcus aureus evades the extracellular antimicrobial activity of mast cells by promoting its own uptake. J Innate Immun. 2011;3(5):495-507.

204. Balzar S, Strand M, Rhodes D, Wenzel E. IgE expression pattern in lung: relation to systemic IgE and asthma phenotypes. J Allergy Clin Immunol. 2007;119(4):855-62.

205. Pawankar R, Lee KH, Nonaka M, Takizawa R. Role of mast cells and basophils in chronic rhinosinusitis. Clin Allergy Immunol. 2007;20:93-101.

206. Xue L, Gyles L, Wettey R, Gazi L, Townsend E, Hunter G, et al. Prostaglandin D2 causes preferential induction of proinflammatory Th2 cytokine production through an action on chemoattractant receptor-like molecule expressed on Th2 cells. J immunol. 2005;175(10):6531-6.

207. Costerton JW, Stewart PS, Greenberg EP. Bacterial biofilms: a common cause of persistent infections. Science. 1999;284(5418):1318-22.

208. Bezerra TF, Padua FG, Ogawa AI, Gebrim EM, Saldiva PH, Voegels RL. Biofilm in chronic sinusitis with nasal polyps: pilot study. Revista Brasileira de Otorrinolaringologia. 2009;75(6):788-93.

209. Costerton JW, Montanaro L, Arciola CR. Biofilm in implant infections: its production and regulation. Int J Artif Organs. 2005;28(11):1062-8.

210. Palmer JN. Bacterial biofilms: do they play a role in chronic sinusitis? Otolaryngol Clin North Am. 2005;38(6):1193-201.

211. Foreman A, Psaltis AJ, Tan LW, Wormald PJ. Characterization of bacterial and fungal biofilms in chronic rhinosinusitis. Am J Rhinol Allergy. 2009;23(6):556-61.

212. Lewis K. Persister cells, dormancy and infectious disease. Nat Rev. 2007; 5(1):48-56.

213. Fux CA, Costerton JW, Stewart PS, Stoodley P. Survival strategies of infectious biofilms. Trends Microbiol. 2005;13(1):34-40.

214. Keir J, Pedelty L, Swift A. Biofilms in chronic rhinosinusitis: systematic review and suggestions for future research. J Laryngol Otol. 2011;125(4):331-7.

215. Chole RA, Faddis BT. Anatomical evidence of microbial biofilms in tonsillar tissues: a possible mechanism to explain chronicity. Arch Otolaryngol Head Neck Surg. 2003;129(6):634-6.

216. De Beer D, Stoodley P, Roe F, Lewandowski Z. Effects of biofilm structures on oxygen distribution and mass transport. Biotechnol Bioeng. 1994;43(11):1131-8.

217. Mladina R, Poje G, Vukovic K, Ristic M, Music S. Biofilm in nasal polyps. Rhinology. 2008;46(4):302-7.

218. Hypertext Bookshop. Introduction to biofilms. 2001 (updated 2010). Accessed at:http://www.hypertextbookshop.com/biofilmbook/working_version/contents/chapters/chapter001/section2/green/page.html.

219. Potera C. Forging a link between biofilms and disease. Science. 1999;283 (5409):1837-9.

220. Hall-Stoodley L, Stoodley P. Evolving concepts in biofilm infections. Cell Microbiol. 2009;11(7):1034-43.

221. Hall-Stoodley L, Hu FZ, Gieseke A, Nistico L, Nguyen D, Hayes J, et al. Direct detection of bacterial biofilms on the middle-ear mucosa of children with chronic otitis media. JAMA. 2006;296(2):202-11.

222. Singh PK, Schaefer AL, Parsek MR, Moninger TO, Welsh MJ, Greenberg EP. Quorum-sensing signals indicate that cystic fibrosis lungs are infected with bacterial biofilms. Nature. 2000;407(6805):762-4.

223. Zuliani G, Carron M, Gurrola J, Coleman C, Haupert M, Berk R, et al. Identification of adenoid biofilms in chronic rhinosinusitis. Int J Ped Otorhinolaryngol. 2006;70(9):1613-7.

224. Elwany S, El-Dine AN, El-Medany A, Omran A, Mandour Z, El-Salam AA. Relationship between bacteriology of the adenoid core and middle meatus in children with sinusitis. J Laryngol Otol. 2011;125(3):279-81.

225. Kania RE, Lamers GE, Vonk MJ, Dorpmans E, Struik J, Tran PH, et al. Characterization of mucosal biofilms on human adenoid tissues. Laryngoscope. 2008;118(1):128-34.

226. Stickler DJ. Bacterial biofilms and the encrustation of urethral catheters. Biofouling. 1998;94:293-305.

227. Chole RA, Faddis BT. Evidence for microbial biofilms in cholesteatomas. Arch Otolaryngol Head Neck Surg. 2002;128(10):1129-33.

228. Bjarnsholt T, Kirketerp-Moller K, Jensen PO, Madsen KG, Phipps R, Krogfelt K, et al. Why chronic wounds will not heal: a novel hypothesis. Wound Repair Regen. 2008;16(1):2-10.

229. Raad I. Intravascular-catheter-related infections. Lancet. 1998;351(9106):893-8.

230. Pawlowski KS, Wawro D, Roland PS. Bacterial biofilm formation on a human cochlear implant. Otol Neurotol. 2005;26(5):972-5.

231. Oxley KS, Thomas JG, Ramadan HH. Effect of ototopical medications on tympanostomy tube biofilms. Laryngoscope. 2007;117(10):1819-24.

232. Cryer J, Schipor I, Perloff JR, Palmer JN. Evidence of bacterial biofilms in human chronic sinusitis. ORL J Otorhinolaryngol Relat Spec. 2004;66(3):155-8.

233. Perloff JR, Palmer JN. Evidence of bacterial biofilms on frontal recess stents in patients with chronic rhinosinusitis. Am J Rhinol. 2004;18(6):377-80.

234. Chaaban MR1, Kejner A, Rowe SM, Woodworth BA. Cystic fibrosis chronic rhinosinusitis: a comprehensive review. Am J Rhinol Allergy. 2013:27(5):387-95.

235. Mainz JG1, Naehrlich L, Schien M, Käding M, Schiller I, Mayr S, et al. Concordant genotype of upper and lower airways P aeruginosa and S aureus isolates in cystic fibrosis. Thorax. 2009:64(6):535-40.

236. Godoy JM, Godoy AN, Ribalta G, Largo I. Bacterial pattern in chronic sinusitis and cystic fibrosis. Otolaryngol Head Neck Surg. 2011:145:673–676.

237. Walter S, Gudowius P, Bosshammer J et al. Epidemiology of chronic Pseudomonas aeruginosa infections in the airways of lung transplant recipients with cystic fibrosis. Thorax 1997;52:318–21.

238. Perloff JR, Palmer JN. Evidence of bacterial biofilms in a rabbit model of sinusitis. Am J Rhinol. 2005;19(1):1-6.

239. Ramadan HH, Sanclement JA, Thomas JG. Chronic rhinosinusitis and biofilms. Otolaryngol Head Neck Surg. 2005;132(3):414-7.

240. Sanclement JA, Webster P, Thomas J, Ramadan HH. Bacterial biofilms in surgical specimens of patients with chronic rhinosinusitis. Laryngoscope. 2005;115(4):578-82.

241. Ferguson BJ, Stolz DB. Demonstration of biofilm in human bacterial chronic rhinosinusitis. Am J Rhinol. 2005;19(5):452-7.

242. Sanderson AR, Leid JG, Hunsaker D. Bacterial biofilms on the sinus mucosa of human subjects with chronic rhinosinusitis. Laryngoscope. 2006;116(7):1121-6.

243. Healy DY, Leid JG, Sanderson AR, Hunsaker DH. Biofilms with fungi in chronic rhinosinusitis. Otolaryngol Head Neck Surg. 2008;138(5):641-7.

244. Psaltis AJ, Weitzel EK, Ha KR, Wormald PJ. The effect of bacterial biofilms on post-sinus surgical outcomes. Am J Rhinol. 2008;22(1):1-6.

245. Psaltis AJ, Wormald PJ, Ha KR, Tan LW. Reduced levels of lactoferrin in biofilm-associated chronic rhinosinusitis. Laryngoscope. 2008;118(5):895-901.

246. Singhal D, Psaltis AJ, Foreman A, Wormald PJ. The impact of biofilms on outcomes after endoscopic sinus surgery. Am J Rhinol & Allergy. 2010;24(3):169-74.

247. Foreman A, Singhal D, Psaltis AJ, Wormald PJ. Targeted imaging modality selection for bacterial biofilms in chronic rhinosinusitis. Laryngoscope. 2010;120(2):427-31.

248. Psaltis AJ, Ha KR, Beule AG, Tan LW, Wormald PJ. Confocal scanning laser microscopy evidence of biofilms in patients with chronic rhinosinusitis. Laryngoscope. 2007;117(7):1302-6.

249. Foreman A, Wormald PJ. Different biofilms, different disease? A clinical outcomes study. Laryngoscope. 2010;120(8):1701-6.

250. Bendouah Z, Barbeau J, Hamad WA, Desrosiers M. Biofilm formation by Staphylococcus aureus and Pseudomonas aeruginosa is associated with an unfavorable evolution after surgery for chronic sinusitis and nasal polyposis. Otolaryngol Head Neck Surg. 2006;134(6):991-6.

251. Chen H-H, Liu X, Ni C, Lu Y-P, Xiong G-Y, Lu Y-Y, et al. Bacterial biofilms in chronic rhinosinusitis and their relationship with inflammation severity. Auris Nasus, Larynx. 2012;39(2):169-74.

252. Sun Y, Zhou B, Wang C-s, Huang Q, Zhang Q, Han Y-h, et al. Clinical and histopathologic features of biofilm-associated chronic rhinosinusitis with nasal polyps in Chinese patients. Chin Med J. 2012;125(6):1104-9.

253. Wang X, Du J, Zhao C. Bacterial biofilms are associated with inflammatory cells infiltration and the innate immunity in chronic rhinosinusitis with or without nasal polyps. Inflammation. 2014;37(3):871-9.

254. Jung JH, Cha HE, Kang IG, Kim ST. Clinical characteristics of biofilms in patients with chronic rhinosinusitis: a prospective case-control study. Indian J Otolaryngol Head Neck Surg. 2015;67(1):1-6.

255. Arild Danielsen K, Eskeland Ø, Fridrich-Aas K, Cecilie OV, Bachmann-Harildstad G, Burum-Auensen E. Bacterial biofilms in chronic rhinosinusitis; distribution and prevalence. Acta Otolaryngol. 2016;136(1):109-12.

256. Bjarnsholt T, Moser C, Ostrup Jenson P, Hoiby N. Biofilm Infections. Springer. 201. First Edition.

257. Hai PV, Lidstone C, Wallwork B. The effect of endoscopic sinus surgery on bacterial biofilms in chronic rhinosinusitis. Otolaryngol Head Neck Surg. 2010;142(3 Suppl 1):S27-32.

258. Desrosiers M, Myntti M, James G. Methods for removing bacterial biofilms: in vitro study using clinical chronic rhinosinusitis specimens. Am J of Rhinol. 2007;21(5):527-32.

259. Maira-Litran T, Kropec A, Goldmann D, Pier GB. Biologic properties and vaccine potential of the staphylococcal poly-N-acetyl glucosamine surface polysaccharide. Vaccine. 2004;22(7):872-9.

260. Tashiro Y, Nomura N, Nakao R, Senpuku H, Kariyama R, Kumon H, et al. Opr86 is essential for viability and is a potential candidate for a protective antigen against biofilm formation by Pseudomonas aeruginosa. J Bacteriol. 2008;190(11):3969-78.

261. Aberg V, Fallman E, Axner O, Uhlin BE, Hultgren SJ, Almqvist F. Pilicides regulate pili expression in E. coli without affecting the functional properties of the pilus rod. Mol Biosyst. 2007;3(3):214-8.

262. Chopra I. The increasing use of silver-based products as antimicrobial agents: a useful development or a cause for concern? J Antimicrob Chemother. 2007;59(4):587-90.

263. Chopra I, Schofield C, Everett M, O'Neill A, Miller K, Wilcox M, et al. Treatment of health-care-associated infections caused by Gram-negative bacteria: a consensus statement. Lancet Infect Dis. 2008;8(2):133-9.

264. Allesen-Holm M, Barken KB, Yang L, Klausen M, Webb JS, Kjelleberg S, et al. A characterization of DNA release in Pseudomonas aeruginosa cultures and biofilms. Mol Microbiol. 2006;59(4):1114-28.

265. Del JLJ, Rouse MS, Patel R. Bioelectric effect and bacterial biofilms. A systematic review. Int J Artif Organs. 2008;31(9):786-95.

266. Bjarnsholt T, Givskov M. Quorum-sensing blockade as a strategy for enhancing host defences against bacterial pathogens. Philos Trans R Soc Lon B Bio Sci. 2007;362(1483):1213-22.

267. Hudson DL, Layton AN, Field TR, Bowen AJ, Wolf-Watz H, Elofsson M, et al. Inhibition of type III secretion in Salmonella enterica serovar Typhimurium by small-molecule inhibitors. Antimicrob Agents Chemother. 2007;51(7):2631-5.

268. Bartley J, Young D. Ultrasound as a treatment for chronic rhinosinusitis. Med Hypotheses. 2009;73(1):15-7.

269. Young D, Morton R, Bartley J. Therapeutic ultrasound as treatment for chronic rhinosinusitis: preliminary observations. J Laryngol Otol. 2010;124(5):495-9.

270. Valentine R, Jervis-Bardy J, Psaltis A, Tan LW, Wormald PJ. Efficacy of using a hydrodebrider and of citric acid/zwitterionic surfactant on a Staphylococcus aureus bacterial biofilm in the sheep model of rhinosinusitis. Am J Rhinol Allergy. 2011;25(5):323-6.

271. Uren B, Psaltis A, Wormald P-J. Nasal lavage with mupirocin for the treatment of surgically recalcitrant chronic rhinosinusitis. Laryngoscope. 2008;118(9):1677-80.

272. Chiu AG, Palmer JN, Woodworth BA, Doghramji L, Cohen MB, Prince A, et al. Baby shampoo nasal irrigations for the symptomatic post-functional endoscopic sinus surgery patient. Am J Rhinol. 2008;22(1):34-7.

273. Chiu AG, Antunes MB, Palmer JN, Cohen NA. Evaluation of the in vivo efficacy of topical tobramycin against Pseudomonas sinonasal biofilms. J Antimicrob Chemother. 2007;59(6):1130-4.

274. Jervis-Bardy J, Foreman A, Bray S, Tan L, Wormald PJ. Methylglyoxal-infused honey mimics the anti-Staphylococcus aureus biofilm activity of

manuka honey: potential implication in chronic rhinosinusitis. Laryngoscope. 2011;121(5):1104-7.

275. Lusby PE, Coombes AL, Wilkinson JM. Bactericidal activity of different honeys against pathogenic bacteria. Arch Med Res. 2005;36(5):464-7.

276. Kilty SJ, Duval M, Chan FT, Ferris W, Slinger R. Methylglyoxal: (active agent of manuka honey) in vitro activity against bacterial biofilms. Int Forum Allergy Rhinol. 2011;1(5):348-50.

277. Alandejani T, Marsan J, Ferris W, Slinger R, Chan F. Effectiveness of honey on Staphylococcus aureus and Pseudomonas aeruginosa biofilms. Otolaryngol Head Neck Surg. 2009;141(1):114-8.

278. Badet C, Quero F. The in vitro effect of manuka honeys on growth and adherence of oral bacteria. Anaerobe. 2011;17(1):19-22.

279. Maddocks SE, Lopez MS, Rowlands RS, Cooper RA. Manuka honey inhibits the development of Streptococcus pyogenes biofilms and causes reduced expression of two fibronectin binding proteins. Microbiology. 2012;158(Pt 3):781-90.

280. Lee JH, Park JH, Kim JA, Neupane GP, Cho MH, Lee CS, et al. Low concentrations of honey reduce biofilm formation, quorum sensing, and virulence in Escherichia coli O157:H7. Biofouling. 2011;27(10):1095-104.

281. Kilty SJ, Almutari D, Duval M, Groleau MA, De Nanassy J, Gomes MM. Manuka honey: histological effect on respiratory mucosa. Am J Rhinol Allergy. 2010;24(2):e63-6.

282. Sahin G, Klimek L, Mullol J, Hormann K, Walther LE, Pfaar O. Nitric oxide: a promising methodological approach in airway diseases. Int Arch Allergy Immunol. 2011;156(4):352-61.

283. Andersson JA, Cervin A, Lindberg S, Uddman R, Cardell LO. The paranasal sinuses as reservoirs for nitric oxide. Acta Otolaryngol. 2002;122(8):861-5.

284. Lundberg JO, Weitzberg E, Nordvall SL, Kuylenstierna R, Lundberg JM, Alving K. Primarily nasal origin of exhaled nitric oxide and absence in Kartagener's syndrome. Eur Respir J. 1994;7(8):1501-4.

285. Gustafsson LE, Leone AM, Persson MG, Wiklund NP, Moncada S. Endogenous nitric oxide is present in the exhaled air of rabbits, guinea pigs and humans. Biochem Biophys Res Commun. 1991;181(2):852-7.

286. Zhang Y, Endam LM, Filali-Mouhim A, Bosse Y, Castano R, Desrosiers M. Polymorphisms in the nitric oxide synthase 1 gene are associated with severe chronic rhinosinusitis. Am J Rhinol Allergy. 2011;25(2):e49-54.

287. Lundberg JO. Airborne nitric oxide: inflammatory marker and aerocrine messenger in man. Acta Physiol Scand Suppl. 1996;633:1-27.

288. Lindberg S, Cervin A, Runer T. Low levels of nasal nitric oxide (NO) correlate to impaired mucociliary function in the upper airways. Acta Otolaryngol. 1997;117(5):728-34.

289. Nathan CF, Hibbs JB, Jr. Role of nitric oxide synthesis in macrophage antimicrobial activity. Curr Opin Immunol. 1991;3(1):65-70.

290. Alving K, Weitzberg E, Lundberg JM. Increased amount of nitric oxide in exhaled air of asthmatics. Eur Respir J. 1993;6(9):1368-70.

291. Arnal JF, Didier A, Rami J, M'Rini C, Charlet JP, Serrano E, et al. Nasal nitric oxide is increased in allergic rhinitis. Clin Exp Allergy. 1997;27(4):358-62.

292. Kharitonov SA, Yates D, Barnes PJ. Increased nitric oxide in exhaled air of normal human subjects with upper respiratory tract infections. Eur Respir J. 1995;8(2):295-7.

293. Baraldi E, Azzolin NM, Biban P, Zacchello F. Effect of antibiotic therapy on nasal nitric oxide concentration in children with acute sinusitis. Am J Respir Crit Care Med. 1997;155(5):1680-3.

294. Marletta MA. Mammalian synthesis of nitrite, nitrate, nitric oxide, and N-nitrosating agents. Chem Res Toxicol. 1988;1(5):249-57.

295. Schlosser RJ, Spotnitz WD, Peters EJ, Fang K, Gaston B, Gross CW. Elevated nitric oxide metabolite levels in chronic sinusitis. Otolaryngol Head Neck Surg. 2000;123(4):357-62.

296. Naraghi M, Deroee AF, Ebrahimkhani M, Kiani S, Dehpour A. Nitric oxide: a new concept in chronic sinusitis pathogenesis. Am J Otolaryngol. 2007;28(5):334-7.

297. Barraud N, Hassett DJ, Hwang SH, Rice SA, Kjelleberg S, Webb JS. Involvement of nitric oxide in biofilm dispersal of Pseudomonas aeruginosa. J Bacteriol. 2006;188(21):7344-53.

298. Hall-Stoodley L, Stoodley P. Biofilm formation and dispersal and the transmission of human pathogens. Trends Microbiol. 2005;13(1):7-10.

299. Barraud N, Storey MV, Moore ZP, Webb JS, Rice SA, Kjelleberg S. Nitric oxide-mediated dispersal in single- and multi-species biofilms of clinically and industrially relevant microorganisms. Microb Biotechnol. 2009;2(3):370-8.

300. Barraud N, Schleheck D, Klebensberger J, Webb JS, Hassett DJ, Rice SA, et al. Nitric oxide signaling in Pseudomonas aeruginosa biofilms mediates phosphodiesterase activity, decreased cyclic di-GMP levels, and enhanced dispersal. J Bacteriol. 2009;191(23):7333-42.

301. Lund VJ, Mackay IS. Staging in rhinosinusitis. Rhinology. 1993;107:183–4.

302. Hopkins C, Browne JP, Slack R, Lund V, Brown P. The Lund-Mackay staging system for chronic rhinosinusitis: how is it used and what does it predict? Otolaryngol Head Neck Surg. 2007:137(4):555-61.

303. Ashraf N, Bhattacharyya N. Determination of the "incidental" Lund score for the staging of chronic rhinosinusitis. Otolaryngol Head Neck Surg. 2001:125(5):483-6.

304. Parsek MR, Singh PK. Bacterial biofilms: an emerging link to disease pathogenesis. Ann Rev Microbiol. 2003;57:677-701.

305. Nistico L, Kreft R, Gieseke A, Coticchia JM, Burrows A, Khampang P, et al. Adenoid reservoir for pathogenic biofilm bacteria. J Clin Microbiol. 2011;49(4):1411-20.

306. Erlandsen SL, Kristich CJ, Dunny GM, Wells CL. High-resolution visualization of the microbial glycocalyx with low-voltage scanning electron microscopy: dependence on cationic dyes. J Histochem Cytochem. 2004;52(11):1427-35.

307. Britten KM, Howarth PH, Roche WR. Immunohistochemistry on resin sections: a comparison of resin embedding techniques for small mucosal biopsies. Biotechnic & Histochemistry. 1993;68(5):271-80.

308. Wood K, Knabel J, Kwan W. Bacterial persister cell formation and dormancy. Appl Environ Microbiol. 2013;79(23):7116-21.

309. Ramadan HH. Chronic rhinosinusitis and bacterial biofilms. Curr Opin Otolaryngol Head Neck Surg. 2006;14(3):183-6.

310. Prince AA, Steiger JD, Khalid AN, Dogrhamji L, Reger C, Eau Claire S, et al. Prevalence of biofilm-forming bacteria in chronic rhinosinusitis. Am J Rhinol. 2008;22(3):239-45.

311. Suh JD, Ramakrishnan V, Palmer JN. Biofilms. Otolaryngol Clin North Am. 2010;43(3):521-30.

312. Suh D, Cohen A, Palmer N. Biofilms in chronic rhinosinusitis. Curr Opin Otolaryngol Head Neck Surgery. 2010;18(1):27-31.

313. Uijen JH, Bindels PJ, Schellevis G, van CJ. ENT problems in Dutch children: trends in incidence rates, antibiotic prescribing and referrals 2002-2008. Scand J Prim Health Care. 2011;29(2):75-9.

314. Downing E. Bronchial reactivity in patients with nasal polyps before and after polypectomy. J Allergy Clin Immunol. 1982;69(2):102.

315. Blumstein GI, Tuft L. Allergy treatment in recurrent nasal polyposis: its importance and value. Am J Med Sci. 1957;234(3):269-80.

316. Rugina M, Serrano E, Klossek JM, Crampette L, Stoll D, Bebear JP, et al. Epidemiological and clinical aspects of nasal polyposis in France; the ORLI group experience. Rhinology. 2002;40(2):75-9.

317. Health & Social Care Information Centre. Accessed on: www.hscic.gov.uk.

318. Coticchia J, Zuliani G, Coleman C, Carron M, Gurrola J, 2nd, Haupert M, et al. Biofilm surface area in the pediatric nasopharynx: Chronic rhinosinusitis vs obstructive sleep apnea. Arch Otolaryngol Head Neck Surg. 2007;133(2):110-4.

319. Galli J, Calo L, Ardito F, Imperiali M, Bassotti E, Passali GC, et al. Damage to ciliated epithelium in chronic rhinosinusitis: what is the role of bacterial biofilms? Annals of Otology, Rhinol Laryngol. 2008;117(12):902-8.

320. Singhal D, Foreman A, Bardy JJ, Wormald PJ. Staphylococcus aureus biofilms: Nemesis of endoscopic sinus surgery. Laryngoscope. 2011;121(7):1578-83.

321. Kern C, Conley B, Walsh W, Chandra R, Kato A, Tripathi-Peters A, et al. Perspectives on the etiology of chronic rhinosinusitis: an immune barrier hypothesis. Am J Rhinol. 2008;22(6):549-59.

322. Howlin RP, Cathie K, Hall-Stoodley L, Cornelius V, Duignan C, Allan A, et al. Low dose nitric oxide as targeted anti-biofilm adjunctive therapy to treat chronic Pseudomonas aeruginosa infection in cystic fibrosis. Mol Ther. 2017;25(9):2104-2116.

323. Jardeleza C, Foreman A, Baker L, Paramasivan S, Field J, Tan LW, et al. The effects of nitric oxide on Staphylococcus aureus biofilm growth and its implications in chronic rhinosinusitis. Int Forum Allergy Rhinol. 2011;1(6):438-44.

324. Roca-Ferrer J, Garcia-Garcia J, Pereda J, Perez-Gonzalez M, Pujols L, Alobid I, et al. Reduced expression of COXs and production of prostaglandin E(2) in patients with nasal polyps with or without aspirin-intolerant asthma. J Allergy Clinical Immunol. 2011;128(1):66-72.

325. Bateman D, Fahy C, Woolford J. Nasal polyps: still more questions than answers. J laryngol Otol. 2003;117(1):1-9.

326. Gevaert P, Bachert C, Holtappels G, Novo CP, Van JH, Fransen L, et al. Enhanced soluble interleukin-5 receptor alpha expression in nasal polyposis. Allergy. 2003;58(5):371-9.

327. Zabeau L, Gevaert P, Bachert C, Tavernier J. Interleukin-5, eosinophilic diseases and therapeutic intervention. Curr Drug Targets Inflamm Allergy. 2003;2(4):319-28.

328. Pérez-Novo A, Kowalski L, Kuna P, Ptasinska A, Holtappels G, van CP, et al. Aspirin sensitivity and IgE antibodies to Staphylococcus aureus enterotoxins in nasal polyposis: studies on the relationship. Int Arch Allergy Immunol. 2004;133(3):255-60.

329. Kowalski ML, Grzegorczyk J, Pawliczak R, Kornatowski T, Wagrowska-Danilewicz M, Danilewicz M. Decreased apoptosis and distinct profile of infiltrating cells in the nasal polyps of patients with aspirin hypersensitivity. Allergy. 2002;57(6):493-500.

330. Drake-Lee A. Nasal polyps in identical twins. J Laryngol Otol. 1992;106(12):1084-5.

331. Safirstein BH. Allergic bronchopulmonary aspergillosis with obstruction of the upper respiratory tract. Chest. 1976;70(6):788-90.

332. Cody DT, 2nd, Neel HB, 3rd, Ferreiro JA, Roberts GD. Allergic fungal sinusitis: the Mayo Clinic experience. Laryngoscope. 1994;104(9):1074-9.

333. Bachert C, Zhang N, Patou J, van T, Gevaert P. Role of staphylococcal superantigens in upper airway disease. Curr Opin Allergy Clin Immunol. 2008;8(1):34-8.

334. Tantilipikorn P, Bunnag C, Nan Z, Bachert C. Staphylococcus aureus superantigens and their role in eosinophilic nasal polyp disease. Asian Pac J Allergy Immunol. 2012;30(3):171-6.

335. Zernotti ME, Angel Villegas N, Roques Revol M, Baena-Cagnani CE, Arce Miranda JE, Paredes ME, et al. Evidence of bacterial biofilms in nasal polyposis. J Investig Allergol Clin Immunol. 2010;20(5):380-5.

336. Drake-Lee AB, Barker TH, Thurley KW. Nasal polyps. Scanning electron microscopy and artifact. J laryngol Otol. 1984;98(3):285-92.

337. Tan NC, Tran HB, Foreman A, Jardeleza C, Vreugde S, Wormald PJ. Identifying intracellular Staphylococcus aureus in chronic rhinosinusitis: a direct comparison of techniques. Am J Rhinol Allergy. 2012;26(6):444-9.

338. Hayes S, Howlin R, Johnston A, Webb S, Clarke C, Stoodley P, et al. Intracellular residency of Staphylococcus aureus within mast cells in nasal polyps: A novel observation. J Allergy Clin Immunol. 2015;135(6):1648-51.

339. Drake-Lee A, Price J. Mast cell ultrastructure in the inferior turbinate and stroma of nasal polyps. J Laryngol Otol. 1997;111(4):340-5.

340. Mekori YA, Metcalfe DD. Mast cells in innate immunity. Immunol Rev. 2000;173:131-40.

341. Kalesnikoff J, Galli J. New developments in mast cell biology. Nat Immunol. 2008;9(11):1215-23.

342. Marshall S. Mast-cell responses to pathogens. Nat Rev Immunol. 2004;4(10):787-99.

343. Abraham N, St LA. Mast cell-orchestrated immunity to pathogens. Nat Rev Immunol. 2010;10(6):440-52.

344. Von Köckritz-Blickwede M, Goldmann O, Thulin P, Heinemann K, Norrby-Teglund A, Rohde M, et al. Phagocytosis-independent antimicrobial activity of mast cells by means of extracellular trap formation. Blood. 2008;111(6):3070-80.

345. Di NA, Vitiello A, Gallo L. Cutting edge: mast cell antimicrobial activity is mediated by expression of cathelicidin antimicrobial peptide. J Immunol. 2003;170(5):2274-8.

346. McLachlan JB, Abraham SN. Studies of the multifaceted mast cell response to bacteria. Curr Opin Microbiol. 2001;4(3):260-6.

347. Butterfield JH, Weiler D, Dewald G, Gleich GJ. Establishment of an immature mast cell line from a patient with mast cell leukemia. Leuk Res. 1988;12(4):345-55.